

LA-6454

C. 2

UC-34

Issued: November 1976

Accuracy of the Conventional Lagrangian Scheme for One-Dimensional Hydrodynamics

by

Wildon Fickett



DO NOT CIRCULATE

PERMANENT RETENTION


REQUIRED BY CONTRACT



los alamos
scientific laboratory

of the University of California

LOS ALAMOS, NEW MEXICO 87545



An Affirmative Action/Equal Opportunity Employer

UNITED STATES
ENERGY RESEARCH AND DEVELOPMENT ADMINISTRATION
CONTRACT W-7405-ENG. 36

Printed in the United States of America. Available from
National Technical Information Service
U.S. Department of Commerce
5285 Port Royal Road
Springfield, VA 22161
Price: Printed Copy \$6.75 Microfiche \$3.00

This report was prepared as an account of work sponsored by the United States Government. Neither the United States nor the United States Energy Research and Development Administration, nor any of their employees, nor any of their contractors, subcontractors, or their employees, makes any warranty, express or implied, or assumes any legal liability or responsibility for the accuracy, completeness, or usefulness of any information, apparatus, product, or process disclosed, or represents that its use would not infringe privately owned rights.

Notation

Δt - time step
 $\Delta y, y = x, p, u, \text{ or } \rho$ - calculated minus exact solution at the given time at the test particle or leading shock
N - total number of computation cells
p - pressure
q - artificial viscosity
 ρ - density
t - time
u - particle velocity
U - shock velocity
x - distance
 \hat{x} - thickness
Sub-zero - initial

Glossary

Body - the body whose motion is calculated
Calculation - a calculation with the PAD code
Cell - a computation cell of the finite-difference method
Cell size - the cell width, proportional to N^{-1}
Dial - a parameter of the numerical method
Extrapolation - to $N = \infty$
HE = high explosive
Number of cells - the total number of computation cells N
Piston - a left boundary whose motion is a specified function of time
Problem - a test problem
Residual error - a non-zero extrapolated value of Δy
Shell - a section of the body consisting of a single material
Snapshot - a profile at fixed time
Standard calculation - a calculation with the standard dial settings for the particular problem
Test particle - the particle whose motion is studied

Units

The units are those of the coherent SI set based on mm, mg, and μs , which give p in GPa, ρ in Mg/m^3 , u in km/s, and e in MJ/kg.

Significant Figures and Exponents

Numerical values are rounded to three significant figures. Positive and negative exponents are indicated by P and N. Thus $3N4 = 3 \times 10^{-4}$.

LOS ALAMOS NATIONAL LABORATORY



3 9338 00375 1459

ACCURACY OF THE CONVENTIONAL LAGRANGIAN SCHEME FOR ONE-DIMENSIONAL HYDRODYNAMICS

by

Wildon Fickett

ABSTRACT

The accuracy of the conventional Lagrangian scheme for one-dimensional hydrodynamics is assessed by detailed comparison with a variety of test problems having exact solutions. The choice of test problems is made in the context of wave motions in the pressure range of detonations in condensed explosives.

For each test problem the calculation is made for 16, 32, 64, 128, and 256 computation cells. The results and the exact solution are compared along particle and shock paths by superposing a plot of the exact solution on a plot of the calculated result. Also, the integrated errors over a typical time span are plotted against the reciprocal number of cells.

The effect of changing such parameters of the computational method as the form and amount of artificial viscosity is investigated.

For these relatively simple geometries, accuracy better than that found for typical experimental geometries can be achieved with 100 or 200 cells and a CDC 7600 computer time of a minute or two.

I. INTRODUCTION

The "standard" Lagrangian numerical method for one-dimensional inviscid hydrodynamics described in 1967 by Richtmyer and Morton¹ has remained a *de facto* standard, with only minor variations, and continues to be used extensively for a variety of problems. Some tests of its accuracy have been made,² but we needed a detailed study in the field of shock and detonation waves in the pressure range associated with condensed explosives.

The first part of this work required a set of test problems that admit exact solutions, and these have been assembled.³ Here we report on the testing of the standard numerical method, as embodied in the PAD code⁴ running on the Control Data Corp. 7600 computer, against some of the test problems. Throughout this report, the unmodified word "calculation" means a calculation made with PAD.

The method uses a number of "dials" or parameters of the numerical method, such as the form and amount of artificial viscosity, the number and distribution of the computation cells, and the size of the time step. Typical "standard" dial settings are chosen for each problem

(see Sec. II) and, by varying only the number of computation cells, we can display the results of the calculation and its comparison with the exact solution. Section III contains comparisons made with different dial settings. Results are summarized in Sec. IV.

The finite-difference method places p and v at the cell center and x and u at its right boundary. (These locations become important primarily when one is looking at large-gradient regions.) The method does not treat shocks explicitly, so the leading shock is located and its state determined by a separate procedure which differs slightly from that described in the manual.⁴ This and other minor changes in the code are described in Appendix A. The code keeps a "least-active-cell" marker just ahead of the leading shock, and saves time by not calculating for the inactive cells ahead of it. Only the active cells appear in the snapshots. The left and right boundaries are represented by dummy cells, and the left dummy cell also appears in the snapshots. Its state is set equal to that of the first interior cell, except for x and u , which are calculated from the boundary prescription. The left dummy cell is not included in the count for the number of computation cells.

The calculations are set up so that the principal wave moves through the body from left to right. In most cases the wave is produced or supported by a prescribed left-boundary motion. We call this left boundary the piston, and prescribe its velocity as a function of time. If the body is of a single material, we use a uniform cell size throughout. If there are two slabs of material, or *shells*, a uniform cell size is used within each shell, but a different cell size is used between shells. Throughout the calculation, we use a fixed time step set at one-quarter to one-third of the Courant value for the cell requiring the smallest value. For each problem, the calculation is made with 16, 32, 64, 128, and 256 cells. For the standard calculations, an optimum artificial viscosity was chosen for each problem by examining the shock's anatomy and making the choice for sharpness and critical damping at a typical pressure. Results of this preliminary study are described in Appendix B. The optimum viscosities are marked with a superscript c in Table B-II.

The calculated results are given for each problem in turn. *The problem numbers are those of Ref. 3.* For each calculation, there are three types of plot: (1) snapshots—profiles at fixed time, (2) particle histories—the history of the position and state of a *test particle* (fluid element), approximated as the history of a particular computation cell, and (3) the lead-shock history—the history of the position and state of the leading shock, determined as described above. We make the comparison with the exact solution in one of two ways: (1) by superposing the exact solution as a dashed line on the plot of the calculated particle or shock history, or (2) by displaying the difference Δy between the calculated and exact solutions:

$$\Delta y = (\text{calculated solution}) - (\text{exact solution}) \quad ,$$

where y is x , p , u , or ρ , at each time of the histories. The standard scale labels of the code are used in both cases, but the difference plots are labeled by the word "difference" in the title at the top of the page (and are also distinguishable by their appearance and small range). The code chooses the scales of each plot to span the range of the data plus a small margin. This gives maximum resolution, thereby making life tolerable for the designer of the calculation, but does give a different scale for each plot. The histories show every time step and the snapshots show every cell. The points are connected by straight lines, and each point is marked with a dot where this does not make too dense a line. The slight imprecision in plotting resolution is not caused by hardware limitations but by old software, whose resolution is 1024 points per page width (four plots per page for all plots). The finite resolution can occasionally be discerned in the form of small steps in a nearly horizontal portion of a curve.

In contrast to the rough snapshots, the particle histories are always smooth, with approximately sinusoidal noise. This can be understood by regarding the set of computation cells as a system of coupled oscillators. Typically, the passage of a shock excites in each cell a small spurious ringing. Adjacent cells show similar ringing patterns, but snapshots will show a random-looking noise because the adjacent cells are caught at different phases. The ringing is well resolved in the histories because the time step is so small (about one-quarter of the space step). The shock histories show a random-looking but still periodic noise, due partly to the nature of the locating recipe. The minor period is the transit time of the shock through a cell, and the major period is the time required to approximately repeat the same phase for the time of shock entry into a cell relative to the beginning of a time step.

The results for each problem are displayed in a set of plots selected from the standard sequence given in Table I. Not all types of plots are presented for all problems. For some types of plots there may be more than one page, showing different values of N .

The particle histories are for a particular *test particle* specified for each problem. The snapshots are at a *test time* (also specified for each problem), usually the time when the test particle is about halfway through the wave. The particle history over a truncated time range is included (item 3 of Table I) because, in those problems with a leading shock, the passage of the shock over the particle generates such large errors that later errors are hard to see on the same scale. The truncation consists of removing the initial time segment containing the large shock-passage errors. The artificial viscosity q has no counterpart in the exact solutions, all of which have discontinuous shock transitions. The value of q displayed in some of the shock histories is the maximum (quadratically) interpolated value in the profile at each time.

The extrapolation plots present for each problem the mean absolute value of Δy over the pertinent time range vs N^{-1} . The truncated time range is used for the particle, and the full time range for the shock, except in problem 7, where the truncated range is used for both. The mean absolute value is

$$|\overline{\Delta y}| = n^{-1} \sum_{i=1}^n |\Delta y_i| ,$$

where i numbers the times of the calculation steps covering the truncated time range ($t_{i+1} = t_i + \Delta t$), and y_i is the value of y at time i . In most cases these plots become more or less linear as they approach $N^{-1} = 0$ and extrapolate to $|\overline{\Delta y}| = 0$ there, indicating agreement with the exact solution in the limit of zero cell size. Where this is not the case, we refer to the extrapolated value of $|\overline{\Delta y}|$ as the *residual error*.

There is probably no single measure that is suitably representative of the overall error in all cases. In most cases, the error does not change sign anywhere in the time range studied, so that the mean absolute value is identical to the arithmetic mean and is quite suitable. When the error changes sign only once or twice in the range, the absolute value is still the most appropriate, for it gives the mean size of the error, whereas the arithmetic mean could give a misleadingly small value through cancellation. When the oscillations are much larger than the mean error, the absolute value is less appropriate, for it then measures mainly the amplitude of oscillations. For some of these cases we have also supplied estimates of the arithmetic mean.

A. Results

•**Problem 1, Rarefaction.** Test problem 1, Fig. 1, is a centered, simple rarefaction wave propagating into a semi-infinite slab of aluminum, initially at rest and uniformly isothermally precompressed to $p = 30$. The left boundary is a piston initially at $x = 0$; the rarefaction is generated by instantaneously decreasing its velocity at $t = 0$ from $u = 0$ to $u \cong -1.542$, the exact value being chosen to make the final pressure exactly zero. The calculation thickness is $\hat{x} = 10$ and the coarsest calculation has $\Delta t = 0.04$. The test particle is initially at $x = 5$ (cell $N/2$).

The calculation rounds off the wave head, with motion beginning early, then lags and undershoots at the tail, producing a small spurious tension there. The artificial viscosity turns on after the minimum velocity point of the undershoot. Its peak value is approximately proportional to cell size. Typically, the pattern of differences from the exact solution is qualitatively the same, regardless of cell size. For this problem there is no shock and thus no need to truncate the time range. The cell-size extrapolation is quite smooth and nearly linear.

•**Problem 2, Shock Deceleration.** Problem 2, Fig. 2, looks at the deceleration of a shock by a following rarefaction wave. The left edge of a semi-infinite slab of aluminum is a piston initially at $x = 0$. At $t = -0.1304$, its velocity is increased instantaneously from $u = 0$ to $u = 1.743$, generating a flat-topped shock of $p = 37.3$. At $t = 0$, its velocity is instantaneously reduced to zero again, generating a centered rarefaction wave which, with the special equation of state used, brings the pressure down to exactly zero. The rarefaction head overtakes the shock at $x = 10$, $t = 1$ (the initial piston velocity and time having been chosen to give these even numbers). The calculation thickness is $\hat{x} = 20$ and the coarsest calculation has $\Delta t = 0.04$. The test particle is at $x = 10$ (cell $N/2$).

The calculated particle motion is similar to that in problem 1. Because of the finite shock width, the test particle begins to move early, first overtaking the exact trajectory, then lagging behind it in the undershoot at the tail of the rarefaction wave. The passage of the particle through the shock generates some quickly damped ringing, most easily seen in the p - u plot. The number of cycles of ringing appears to be approximately proportional to N ; the frequency is, of course, proportional to N^{-1} , as is the shock thickness.

The calculated shock is well below the true value, and the first hint of the slope discontinuity at the overtake appears at 128 cells. The magnitude of the shock-position error increases slightly with time, with the calculated position lagging behind the true value. Both extrapolations are reasonably smooth.

•**Problem 3, Free-Surface Deceleration.** Problem 3, Fig. 3, shows the deceleration of a free surface (previously accelerated by a shock) by a rarefaction wave. The left edge of an aluminum slab is a piston initially at $x = -1.5$; the right edge is a free surface at $x = 8.5$. At $t = -1$, the piston velocity is increased instantaneously from $u = 0$ to $u = 1.5$, thereby generating a flat-topped shock with $p = 29.4$. At $t = 0$ the piston reaches $x = 0$ and its velocity is instantaneously reduced to zero, generating a centered rarefaction wave. The shock reaches the free surface at $t = 0.421$, accelerating it to $u = 3.02$; the rarefaction head reaches it at $t = 1.35$, initiating the deceleration; and the rarefaction tail reaches it at $t = 2.36$, at which point its velocity has been reduced to $u = 0.0189$. The coarsest calculation has $\Delta t = 0.04$. The test particle is at the free-surface (cell N).

The particle motion is again similar to that of problem 1, with the same early motion but a less pronounced undershoot at the tail. The initial acceleration of the free surface by the shock (not shown here) leaves the density high by $\sim 1\%$. This artifact (exaggerated density

error at an edge or interface) is characteristic of the calculational method and is not reduced by decreasing the cell size, because the artificial shock width is reduced proportionately. It can have either sign, depending on the type and magnitude of the artificial viscosity. Passage of the entire rarefaction wave through the free surface leaves this edge-cell density error virtually unchanged. Note that a small artificial viscosity, approximately proportional to cell size, is present throughout the deceleration, because the interaction region of the forward-facing rarefaction wave with the free surface has a small positive velocity gradient.

•**Problem 7, Decelerating Shock from HE.** In problem 7, Fig. 4, a slab of HE is driving a shock into a magnesium slab. This problem looks at the motion of the interface between the two materials and at the deceleration of the shock by the transmitted Taylor rarefaction wave of the detonation. The left boundary of the explosive is a piston initially at $x = 0$, the explosive/magnesium interface is initially at $x = 10$, and the magnesium slab is considered to be semi-infinite. At $t = 0$ an instantaneous-reaction, steady, unsupported Chapman-Jouguet detonation is initiated at the piston, whose velocity drops instantaneously from $u = 0$ to $u = -1$, producing a Taylor wave of sufficient extent that its tail characteristic does not affect the motion in the time range of interest. The shock impedance of the magnesium is sufficiently low that the wave reflected into the explosive is a (weak) rarefaction. The calculation begins when the detonation front reaches the interface at $t = 1.18$. The complete detonation wave has been precalculated and entered as an initial condition, and the result is a pronounced initial discontinuity at the interface. The explosive thickness is $\hat{x} = 10$ and the magnesium thickness is a nominal $\hat{x} = 12$. The coarsest calculation has $\Delta t = 0.04$. Half of the computation cells are in each material, so that the magnesium cells are 1.2 times larger than the explosive cells. The test particle is at the interface (last explosive cell) on the explosive side.

The calculated particle motion shows a strongly damped oscillatory transient coming from the initial discontinuity and with a time period inversely proportional to cell size. The position error increases with time, with the calculation running ahead of the true solution. The transient peak value of q (not shown) increases slightly as the cell size decreases, presumably because the interface cell samples less of the Taylor wave. Again, the shock errors are appreciable. The early shock history is, of course, affected by the starting transient. The snapshots show some ringing behind the shock and suggestions of the typical undershoots at the tails of both the Taylor and reflected rarefaction waves. The typical interface density error, mostly in the inert, is evident in the 128-cell snapshot. The particle-density extrapolation shows what may be a small residual error. We expect some residual density error because the particle is at an interface.

•**Problem 8, Reverberation.** Problem 8, Fig. 5, examines the free-surface motion in an aluminum plate driven by a supported (flat-topped) Chapman-Jouguet detonation in a semi-infinite slab of explosive. The detonation can be assumed to initiate at the left boundary of the explosive, and is treated in the same approximation as in problem 7. In problem 8, however, the piston velocity is raised to the Chapman-Jouguet particle velocity to produce the desired flat-topped wave. The detonation drives a $p = 29.0$ shock into the plate, which accelerates by the usual sequence of reverberations.

The calculation gives the explosive a nominal thickness of $\hat{x} = 30$ (large enough that the presence of the left boundary does not affect the plate motion in the time range of interest) and places the explosive/aluminum interface initially at $x = 20$. The calculation begins at time $t = 2.50$, with the detonation front at the interface, and with the detonation wave entered as an initial condition as in problem 7. The coarsest calculation has $\Delta t = 0.04$. Half of

the computation cells are placed in each material, so that the explosive cells are three times larger than the aluminum cells. The test particle is at the plate's free surface (cell N).

The exact calculation of the complete free-surface motion is quite complicated, and we have not reproduced all of it here. Instead, we use only the second constant-state plateau, extending from $t = 7.27$ to $t = 10.12$. The full time range is $t = 6$ to 12 , including the preceding and following reverberations. The truncated time range is $t = 8.4$ to 9.4 , approximately the central third of the plateau.

As in problem 3, the calculation shows an initial high density left over from the initial shock acceleration of the free surface. At the beginning of the plateau, the pressure and density show rapidly damped ringing. The velocity overshoots, but rings less. Most of the ringing has disappeared from the truncated time range at 256 cells. In addition to the expected residual density error, both the position and velocity show small residual errors which are discussed in the next section.

•**Problem 9, Blast Wave.** Problem 9, Fig. 6, is a spherical blast wave in a $\gamma = 7$ polytropic gas. The initial pressure is zero (to achieve the required infinite shock strength) and the initial density is unity. The center is at $x = 0$. The problem is designed so that at $t = 1$ the shock passes through $x = 10$ with $p = 25$, $U = 10$, $u = 2.5$. The wave is generated by a piston programmed to follow a particle path of the exact solution. The piston is initially at $x = 14.4$. At $t = 1/4$ its velocity increases instantaneously from $u = 0$ to $u = 5.74$, generating a shock with $p = 132.0$, $U = 23.0$, $u = 5.74$. Thus there is a fivefold decrease in shock strength over the time of the calculation. The calculation extends from $x = 14.4$ to $x = 35.6$, the outer boundary being chosen so as to place the test particle at $x = 25$ on the right boundary of cell N/2. The coarsest calculation has $\Delta t = 0.01$, a small value at the observation time required by the strong initial shock.

The particle starts moving too soon and remains a nearly constant distance ahead of the exact solution. A feature not previously seen is the very slow damping of the ringing behind the shock. The 128-cell snapshot implies that the ringing terminates abruptly at $t \cong 1.75$. We have verified this by an additional calculation in which the particle history extends to time 2. The 128-cell truncated-time particle history from this calculation is included for comparison. Another instance of this sudden termination of ringing will be presented in the problem-2 variation in the next section. We are unable to explain this abrupt termination.

The shock also runs ahead of the exact solution in a similar way. The shock noise pattern differs in appearance from the previous problems because of the small time step—at the observation time the shock requires about 13 time steps to cross a cell.

•**Problem 10, Steady Detonation.** Problem 10, Fig. 7, calculates the reaction zone of a steady, supported Chapman-Jouguet detonation in Composition B represented by a polytropic gas equation of state with $\gamma = 3$. As in problem 9, the desired flow is generated by programming the piston velocity to be that of a particle passing through the steady solution. The reaction rate is a function only of λ , the degree of reaction. The velocity of the piston, initially at $x = 0$, increases instantaneously from $u = 0$ to the spike value $u = 4.25$, then decreases following the steady solution until the reaction is finished, and finally is left at the constant Chapman-Jouguet value of $u = 2.125$. The reaction-rate multiplier merely sets the time scale. It is chosen for unit reaction time. The corresponding reaction-zone length is 5.31. The calculation thickness is $\hat{x} = 20$. The test particle is initially at $x = 10$ (cell N/2). The coarsest calculation has $\Delta t = 0.025$. The simple reaction rate used makes p and u linear functions of time; this gives zero truncation error in the calculation's integration of u for the piston position, which is thus calculated exactly (excluding roundoff error).

For the smaller values of N , the gross features of the particle motion are like those of problem 9: the particle begins to move too soon and continues ahead of the exact solution, and oscillations persist through the reaction zone. With increasing N , the oscillation is essentially undamped. Its period increases with time. The undershoot at the end of the reaction zone is qualitatively similar to that at the end of a rarefaction wave, but is smaller and is masked by the oscillations. The artificial viscosity, of course, always turns on at this point. With increasing N , a nonzero q first appears within the reaction zone at $N = 128$, and decreases in size with increasing N . The position error shows a curious change at $N = 256$: for smaller N it is always positive when the particle emerges from the shock, and then it decreases. For $N = 256$, the error is initially negative, and then increases. We have not made calculations to examine in detail the final state following the reaction zone, but it appears to have positive Δx and $\Delta \rho$, a negative Δp , and a Δu whose sign is not certain. The final-state errors in p , u , and ρ are considerably smaller than the amplitude of the oscillations within the reaction zone.

The shock also shows some curious features. Trends in the errors with time first become evident at $N = 64$, with Δx increasing and Δp and Δu decreasing. At $N = 128$ and $N = 256$ (not shown), the trend in Δx is reversed, and that in Δu has become more pronounced. For all N , the (peak value of) q oscillates between 16 and 24.

III. PARAMETER VARIATIONS

In this section we consider the effects of varying the numerical computation dials. We chose problem 7 as the main testing ground for the fairly extensive and systematic set of variations listed in Table II. In addition to this set for problem 7, we have investigated the effect of omitting the energy advance in problem 1, and the effect on a shock of switching to a quadratic (only) viscosity in problem 2. We have rerun problem 8 with the quadratic viscosity to reduce as far as possible the braking effect of the artificial viscosity on the compression waves. We have rerun problem 10 with the quadratic viscosity to see if this would reduce the small residual error in the mesh-size extrapolation. To save space and make the results easier to correlate we have settled on a small standard set of plots for most of the variations. The tabular summary of the next section is also pertinent.

To check the effect of roundoff (not listed in Table II), we used the hardware option of the CDC 7600 which offers a choice of truncation or rounding in the floating-point operations. The standard option, used for all of our calculations, is truncation. We completely recompiled the code, specifying the rounding option, and then repeated the standard calculation for problem 2. The recompilation changed all arithmetical operations except those in the exponential routine, which came from the system library. The 250-cell calculation had 1.6×10^6 "points" (the advance of one cell through one time step). The differences between truncation and rounding ranged from 5 parts in 10^{14} for x to 1.4 parts in 10^{11} for u . The results for calculations with fewer cells showed that the error was roughly proportional to \sqrt{N} .

A. Results

Variations on Problem 1. In problem 1, we eliminated the energy by replacing the full equation of state

$$p(\rho, e) = \gamma a (\rho/\rho_0 - 1) + (\gamma - 1) \rho e$$

$$\gamma = 3, \quad a = 0.264, \quad \rho_0 = 2.79$$

with the corresponding isentrope function

$$p(\rho) = k \rho^\gamma, \quad k = 0.01254,$$

calculated to pass through the initial state. The exact solution is unchanged because the flow is isentropic. The calculation is different because it no longer depends on the energy advance. However, the changes were very small: the differences from the exact solution changed by less than 1% (of the differences). In the full equation of state, the first term, which depends on the density only, is dominant, being about four times the second term in the initial compressed state.

Variations on Problem 2, Fig. 8. The next variation is the quadratic viscosity $q = 0, 1.414$ for problem 2 (see Appendix B for the viscosity specification). With no linear term, damping is very slow, and the viscosity is turned on at some points behind the shock. Oscillation stops abruptly about halfway through the wave, at a time that is almost independent of N . Some of the errors are larger than for the standard case; for example, the shock position error is almost twice as large.

The results illustrate the effect of an underdamped shock produced by a quadratic q or a small linear q . For a flat-topped shock, a simple shock-state recipe like ours will have a positive residual error: the oscillations produce a peak pressure above the true value, and this maximum is picked up by the state recipe. The same will be true for sufficiently large N when a rarefaction wave follows the shock, for the effect of the fixed physical gradient over the first oscillation period decreases with N because the period goes as N^{-1} . Another interesting property may be inferred from the results: different particles have sufficiently different histories that some exceed the peak pressure of the exact solution and some do not. The particular particle displayed does not exceed the peak pressure, but the shock history shows that some do.

Variations on Problem 7

- **$q = 0.3, 0$ - Underdamped Shock, Fig. 9.** The snapshots show that the large oscillations at the front are rapidly damped; even so, the amplitude of the later oscillation is about 80% greater than for the standard case. Velocity and density errors also are appreciably larger than for the standard case.

- **$q = 0.5, 0$ - Critically Damped Shock, Fig. 10.** The behavior here is about the same as in the standard case. The oscillation amplitude and particle errors are about the same, except for an appreciably larger density error. The shock history noise is greater than in the standard case.

- **$q = 0.7, 0$ - Overdamped Shock, Fig. 11.** With overdamped shock, the oscillation amplitude is less than in the standard case, and shows some irregularity. It is curious that with this reduced amplitude of oscillation, the snapshots are rougher than those for the standard case. The particle errors are comparable to those for the standard case, with Δx a little smaller and $\Delta \rho$ a little larger. The shock history noise is about the same as for the standard case.

- $q = 0, 1.414$ - **Quadratic, Fig. 12.** As expected, the oscillation amplitude here is large—about three times larger than that for the standard—but the particle errors are comparable. An interesting feature of the pressure snapshot is the smooth portion centered on the interface. Unlike problem 2 with this q (Fig. 8) in which the oscillations stopped abruptly, they here continue; presumably the smooth portion of the snapshot indicates that all oscillations are in phase. The shock histories show the same qualitative behavior as in problem 2 with this q , and the remarks there are applicable here.

- $q = 0, 0, 2$ - **PIC Form, Fig. 13.** The main difference from the standard is the $\sim 40\%$ reduction in the oscillation amplitude. The particle errors are about the same or slightly smaller, and the shock histories are very similar. The snapshots are slightly rougher.

- **Δt Halved, Fig. 14.** Figure 4 for the standard case shows that the time resolution is good—about 20 steps per oscillation cycle. Reduction of Δt would therefore be expected to make little difference; this was found to be the case, with the particle oscillation about the same and the errors in p , u , and ρ slightly reduced.

To investigate the increased noise in the shock history, we made additional runs showing every particle at every time step over a small region. The switchover from one cell to the next in the shock finder is the main source of noise. In brief, the explanation is that the smaller time step resolves this switchover process better and larger fluctuations result. The velocity is noisiest. Its rise through the shock lags behind the pressure rise. At the switchover, the velocity of the maximum-pressure cell still has a way to go to reach the top, resulting in a large dip in the velocity history recorded by our simple recipe.

- **Δt Doubled, Fig. 15.** Surprisingly, doubling Δt produces little difference from the standard case. The oscillation amplitude is slightly reduced, and the errors are almost the same. The shock history noise is less regular and the snapshots are rougher.

- **Changed Cell-Size Ratio, Fig. 16.** Instead of having 8 cells each in the explosive and inert material, we change to 6 in the explosive and 10 in the inert, changing the inert/explosive cell-size ratio from 1.2 to 0.72. Compared to the standard, the oscillation amplitude is increased about 40%, the position error is significantly reduced, and the other errors are changed a little. The shock histories differ slightly, showing smaller errors and a more pronounced long-period oscillatory component with the changed cell-size ratio.

Variations on Problem 8, Fig. 17. The next variation is on problem 8 with the quadratic viscosity $q = 0, 1.414$. Again, the most striking feature is the characteristic lack of damping associated with removal of the linear viscosity. The oscillation amplitude is much larger—sufficiently so that the original errors in ρ and u , of fixed sign with small oscillations superimposed, are converted into errors of alternating sign. The mean velocity error here is comparable to that in the standard calculation, but the oscillation amplitude is now an order of magnitude larger than the mean error.

The residual errors are still with us: -0.0076 and -0.001 for Δx and Δu , compared with -0.0068 and -0.0018 in the standard case. These values for the present case have been arrived at not by looking at the extrapolation plots, whose main component is the large oscillations, but by extrapolating averages over the truncated time range. We had hoped to find the averages greatly reduced by the change to the quadratic viscosity, which should reduce the frictional braking effect of the viscosity on the finite-width compression waves of the reverberation. Such is not the case. We are unable to offer any other explanation of the residual errors.

Variations on Problem 10, Fig. 18. Finally, we have rerun problem 10 with the quadratic-only viscosity, $q = 0, 1.414$. The oscillations are several times larger than in the standard case, but do decay with time. The mean particle errors are appreciably larger for x and ρ , but smaller for p and u . The position error has the same form and sign for all N . The viscosity within the reaction zone is several times larger than in the standard case and regularly distributed in time. The small trends with time in the shock history are different, with Δx here increasing with time for $N = 128$, and decreasing at late times for $N = 256$. We have included the snapshots for $N = 256$ because they show an interesting pattern of "beats," presumably caused by changes in phase of the individual-cell oscillations.

The residual mean particle errors are reduced. By examining the graphs we have estimated mean errors, for x over the truncated time range, and for p , u , and ρ in the neighborhood of $t = 1.8$. The estimated residual mean errors for the standard and for the present calculation are

	<u>Standard</u>	<u>$q = 0, 1.414$</u>
Δx	-0.013	-0.009
Δp	-0.09	+0.02
$\Delta \rho$	+0.007	~ 0 .
Δu	+0.008	+0.006

Thus switching to the quadratic q reduces the residual error but does not remove it entirely. Apart from remarking on the persistence of the oscillations, we have no explanation of the residual errors or of the small trends in the shock history.

IV. SUMMARY AND CONCLUSIONS

The 128-cell errors for each calculation are given in Table III. All are the absolute mean value as defined in Sec. II. In a few cases where the oscillations are much larger than the mean error, we have added in parentheses graphical estimates of the mean error over several cycles in the middle of the time range.

In most cases, the values given are representative in the sense that the linear form inferred from them for the function $\Delta y(N^{-1})$ would be reasonably good. However, there can be appreciable curvature of either sign; in these cases the inferred linear form would be less satisfactory.

Our results can be summarized as follows:

- Ringing is caused by a shock followed by a wave that decreases the pressure. Typically, a small residual ringing persists for a long time but may vanish abruptly.
- Errors due to smearing of discontinuities have the expected sign.
- Shock errors (as defined by our recipe for locating the shock) are significantly larger than particle errors, but the difference varies from a factor to 2 to 3 in problem 9, to 10 or more in problem 2.
- Recognized sources of residual error—overheating at an interface and overshoot at a noisy shock—appear as expected and should be remembered in drawing conclusions.

- Small, but clear-cut residual errors in problems 8 and 10 remain unexplained.
- The sensitivity of the results to variations in the parameters of the finite-difference method is not as great as we had thought. The effects of such variations are sufficiently diverse that it is difficult to come up with general recommendations.

APPENDIX A

CODE CHANGES

The shock state is determined in a slightly different way than that described in Ref. 2. It is located as described there—at each time, its position is taken as that of maximum q as defined by a quadratic interpolation. But its state is taken to be that of the maximum- p cell, typically 3 or 4 cells behind that of maximum q . The value of u is that at the center of this cell, taken as the mean of the left- and right-edge values.

The code provides for centering the energy advance in time by iterative simultaneous solution of the energy advance and the equation of state. For an equation of state linear in the energy

$$p(v,e) = f(v) + g(v)e \quad ,$$

the iteration is avoided by explicit solution. The current version of the code also allows the time-saving explicit solution through local linearization of the equation of state, taking

$$f(v^+) = p - (\partial p / \partial e)_v e$$

$$g(v^+) = (\partial p / \partial e)_v \quad ,$$

with e the old energy and v^+ the new volume, and with p and $(\partial p / \partial e)_v$ evaluated at (v^+, e) . The problems affected here are problems 2 and 7, which use the Walsh equation of state. If chemical reaction is present, as in problem 10, iteration is required to center the advances of both λ and e . The standard number of passes n is 2, and we use this value. A trial calculation with $n = 4$ showed little difference.

APPENDIX B

ANATOMY OF THE SHOCK

We used three forms of the artificial viscosity: Landshoff (linear), Richtmyer-von Neumann (quadratic), and PIC (linear). Written in linear combination, these are

$$q = A\rho c(\Delta x)u_x + B^2\rho(\Delta x)^2|u_x|u_x + C\rho|u|(\Delta x)u_x \quad . \quad (B-1)$$

We specify the viscosity by the values of the coefficients A, B, and C. (If the value of C is omitted from the specification, C is zero.) For each of the three forms, we have chosen coefficients ranging from too small (underdamped) to too large (overdamped). Linear combinations of the Landshoff and Richtmyer-von Neumann forms are popular, and we have included a number of these. We obtain an infinite-strength shock for the polytropic gases ($\gamma = 3$ and $\gamma = 7$) by taking zero initial pressure. For these systems, a pure Landshoff viscosity would never produce a finite pressure because it has a sound-speed multiplier and the initial sound speed is zero. So for these two systems we have added a small quadratic term to those calculations for which we would otherwise have chosen a pure Landshoff form. The value of B used in these cases is too small to have a significant effect on the shock shape.

The calculation is a shock driven by a constant-pressure rear-boundary condition. The shock is displayed after it has traversed 50 cells. We used an arbitrary choice of $\Delta x_0 = 10$ throughout. The time steps relative to the Courant value $\Delta t^*(= c/\Delta x)$ in the shocked state are given in Table B-I. The ratios vary somewhat because we used time steps of the power of 2 next larger than $0.25 \Delta t^*$. In several cases we also tried time-step values twice as large and half as large as the standard. Cutting the time step to half the standard value usually makes no significant difference. In some cases, doubling it does make a difference, and we have included some such cases in the results.

The results are given in Figs. B-1 and B-2 and Table B-II. From them we have chosen an optimum viscosity for each material, the criterion being that the damping be critical. These optimum values are marked with a superscript c in Table B-II. The viscosity variations described in Sec. III are marked with a superscript b.

Figure B-1 shows (1) snapshots for aluminum, (2) the history of p , u , ρ , and q for the fiftieth cell as it passes through the shock, for each of the materials at the optimum viscosity, and (3) snapshots and profiles for the quadratic viscosity used in several of the variations given in Sec. III. The shock crosses a cell in about four time steps, so the histories have about four times more points through the shock than do the profiles, and are smoother and more informative. Figure B-2 shows the velocity history for each entry in Table B-I.

Table B-I gives estimates of the shock thickness δ measured in number of cells. We calculate δ from

$$\delta = (U/\Delta x_0)\tau \quad , \quad (B-2)$$

where τ is the time width of the shock as illustrated in the first velocity-history frame of Fig. B-I. We define τ as the time width of the shock determined by the straight line tangent to the point of maximum slope in the particle velocity history. (This definition of course becomes meaningless for very large or very small viscosities.) The range of the time scales throughout Fig. B-2 is set inversely proportional to the shock velocity U so that δ is proportional to τ , as

measured by a ruler laid on the page. Table B-I also gives an approximate value of the peak-to-peak particle-velocity amplitude of the first peak in units of the particle-velocity jump through the shock, for underdamped shocks which show such oscillation. This measure is recorded as zero whenever the rise is monotone or slightly bumpy.

As expected, the shocks go from under- to overdamped as the viscosity is increased, and the Landshoff form with polytropic gas shows more complex oscillations. Away from the optimum viscosity, doubling of the time step makes the history rougher and increases the oscillation. When the viscosity is large enough ($q = (5, 0.125, 0)$ for $\gamma = 7$ polytropic gas), one sees the beginning of instability.

REFERENCES

1. R. D. Richtmyer and K. W. Morton, *Difference Methods for Initial-Value Problems*, 2nd ed. (Interscience, New York, 1967), p. 295.
2. P. J. Roache, *Computational Fluid Dynamics* (Hermosa Publishers, Albuquerque, NM, 1972), p. 326.
3. W. Fickett and W. C. Rivard, "Test Problems for Hydrocodes," Los Alamos Scientific Laboratory report LA-5479 (August 1974).
4. W. Fickett, "PAD—A One-Dimensional Lagrangian Hydrocode," Los Alamos Scientific Laboratory report LA-5910-MS (April 1975).

TABLE I
DISPLAY SEQUENCE

1. Snapshots	p, u, ρ , q vs x
2. Test-Particle History	first page - x, p, u, ρ vs t second page - p-u, p- ρ , q-t
A. Exact solution superimposed on first page	
B. Δ (calculated - exact), all quantities, both pages	
C. Same as B with truncated time range	
3. Leading-Shock History	same as 2
A and B as above	
4. $\overline{\Delta y}$ vs N^{-1}	x, p, u, ρ vs N^{-1}

TABLE II
PARAMETER VARIATIONS

<u>Figure</u>	<u>Problem</u>	<u>Variation</u>
---	1	Remove energy dependence
---	2	Roundoff
8	2	q = 0, 1.414
9	7	q = 0.3, 0
10	7	q = 0.5, 0
11	7	q = 0.7, 0
12	7	q = 0, 1.414
13	7	q = 0, 0, 2
14	7	Δt halved
15	7	Δt doubled
16	7	6/10 cells
17	8	q = 0, 1.414
18	10	q = 0, 1.414

TABLE III

SUMMARY OF 128-CELL ERRORS

Problem	Variation	Path*	Δx	Δp	Δu	$\Delta \rho$
1	Standard	P	0.0031	0.24	0.013	0.062
2	"	P	0.0036	0.18	0.014	0.0043
		S	0.042	2.6	0.11	0.047
3	"	P	0.0052	0.17	0.014	0.015
7	"	P	0.012	0.12	0.0068	0.0074
		S	0.030	0.59	0.049	0.019
8	"	P	0.037	3.2N4	0.0014	0.029
9	"	P	0.040	0.202	0.011	0.0066
		S	0.15	0.353	0.023	0.0098
10	"	P	0.013	0.31 (-0.35)	0.11 (0.0025)	0.0062 (-0.0068)
		S	0.019	0.99	0.092	0.054
2	q = 0, 1.414	P	0.0024	0.45	0.012	0.012
		S	0.053	0.98	0.058	0.017
7	q = 0.3, 0	P	0.012	0.12	0.0076	0.018
		S	0.035	1.45	0.15	0.042
7	q = 0.5, 0	P	0.012	0.12	0.0069	0.014
		S	0.026	0.67	0.083	0.021
7	q = 0.7, 0	P	0.010	0.12	0.0064	0.0099
		S	0.038	0.86	0.075	0.028
7	q = 0, 1.414	P	0.012	0.12	0.0076	0.0066
		S	0.036	0.48	0.066	0.013
7	q = 0, 0, 2	P	0.011	0.12	0.0070	0.0070
		S	0.033	0.85	0.075	0.027
7	Δt halved	P	0.012	0.12	0.0049	0.0081
		S	0.032	0.45	0.062	0.014
7	Δt doubled	P	0.012	0.12	0.0068	0.0074
		S	0.030	0.59	0.049	0.019
7	6/10 cells	P	0.0090	0.17	0.0059	0.0087
		S	0.025	0.45	0.043	0.015
8	q = 0, 1.414	P	0.032	0.091 (~0)	0.0086 (-0.0019)	0.020
10	q = 0, 1.414	P	0.033	0.64 (-0.32)	0.033 (0 \pm 0.01)	0.015 (-0.014)
		S	0.081	1.2	0.12	0.032

*P = particle, S = shock

TABLE B-I
SHOCK STATES

<u>Substance</u>	<u>p</u>	<u>u, p</u>	<u>c, u</u>	<u>$\Delta t/\Delta t^*$</u>
1. Aluminum (Walsh) $\rho_o = 2.79$ $U = 5.33 + 1.34 u$	30	1.47 3.49	7.41 7.30	0.23
2. PMMA (Walsh) $\rho_o = 1.19$ $U = 2.57 + 1.54 u$	15	2.15 1.87	5.83 5.88	0.26
3. Polytropic Gas $\gamma = 7$ $p_o = 0, \rho_o = 1$	15	1.94 1.33	8.87 7.75	0.15
4. Polytropic Gas $\gamma = 3$ $p_o = 0, \rho_o = 1.6$	60	4.33 3.20	7.50 8.66	0.19

TABLE B-II

CALCULATED SHOCKS

	<u>Viscosity</u>	<u>u-Oscillation^a</u> (%)	<u>Thickness</u> (No. cells)
1. Al	0.1, 0, 0	45	1.0
	0.2, 0, 0	15	1.6
	0.3, 0, 0	0	1.9
	0.4, 0, 0	0	2.9
	^b 0, 1.414, 0	15	1.8
	0, 2, 0	6	2.6
	^c 0.3, 1, 0	0	2.6
	0, 0, 2	0	1.7
2. PMMA (Plexiglas)	^b 0.3, 0, 0	33	1.0
	^b 0.5, 0, 0	3	1.3
	^b 0.7, 0, 0	0	2.0
	^b 0, 1.414, 0	10	1.9
	^c 0.3, 1, 0	0	1.6
	0, 0, 1	27	1.0
	^b 0, 0, 2	0	1.4
	0, 0, 3	0	1.8
3. PG (Polytropic gas), $\gamma = 7$	1, 0.125, 0	67	0.6
	1.5, 0.125, 0	27	0.8
	same, $2\Delta t$	113	0.3
	3, 0.125, 0	5	0.9
	5, 0.125, 0	2	1.8
	0, 2, 0	10	1.9
	same, $2\Delta t$	7	1.9
	0.3, 1, 0	20	1.0
	0.5, 1, 0	5	1.1
	same, $2\Delta t$	19	1.0
	^c 0.2, 2, 0	2	2.0
	same, $2\Delta t$	1	2.0
	0, 0, 2	28	0.9
	0, 0, 3	5	1.1
4. PG, $\gamma = 3$	1, 0.125, 0	29	0.7
	2, 0.125, 0	0	
	4, 0.125, 0	0	2.0
	0, 2, 0	4	2.9
	^c 0.3, 1, 0	0	1.5
	0, 0, 2	0	1.5

^aPeak-to-peak amplitude (first peak to first trough) in u-oscillation, expressed as percentage of shock u.

^bVariations for effect of viscosity on accuracy (Sec. III).

^cOptimum viscosity used for most calculations.

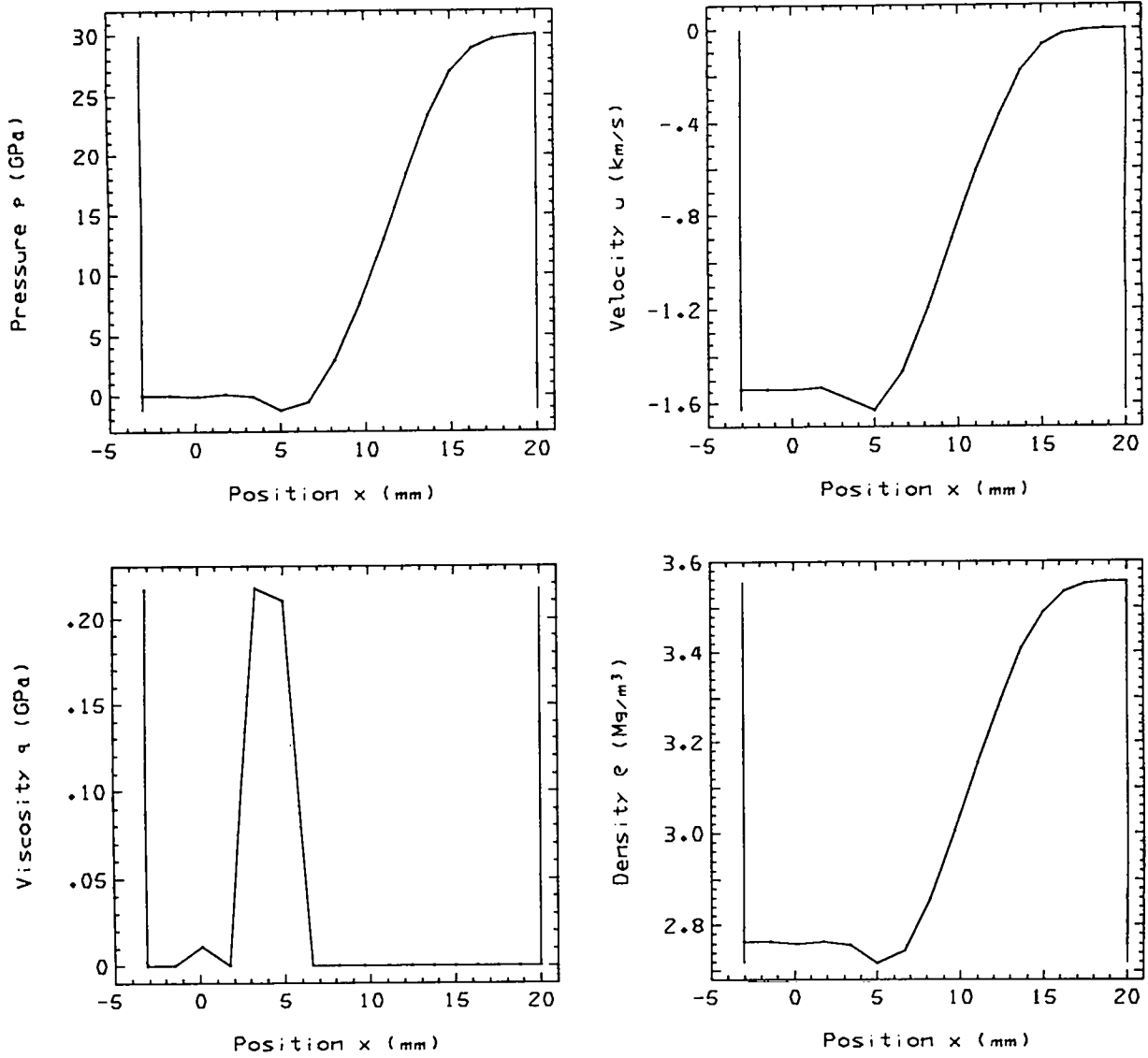


Fig. 1.
Problem 1. Rarefaction. Standard calculation.

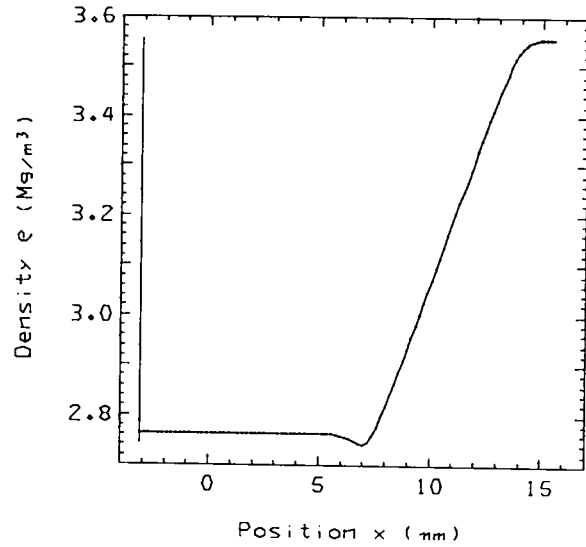
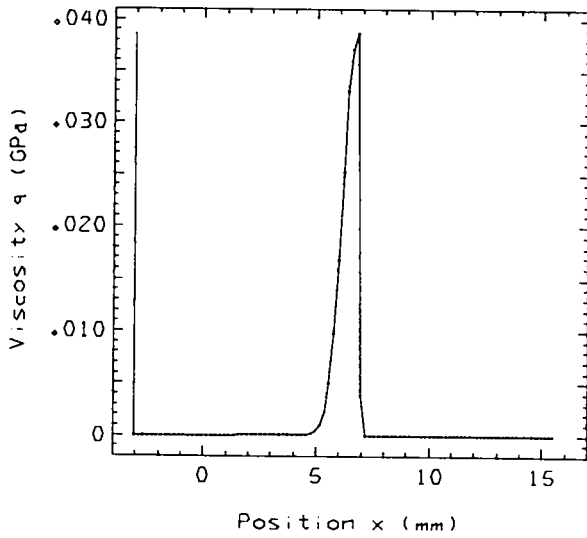
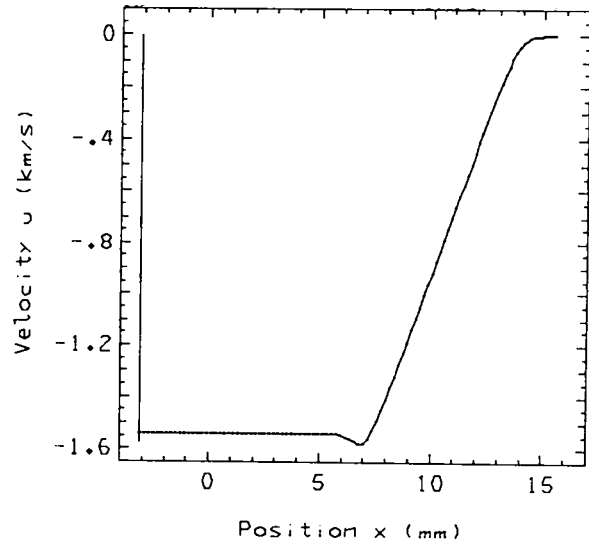
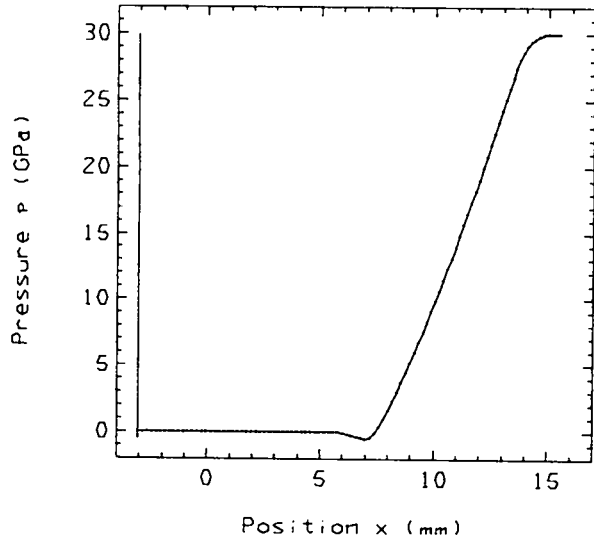


Fig. 1 (cont)

1. RARE. / PARTICLES

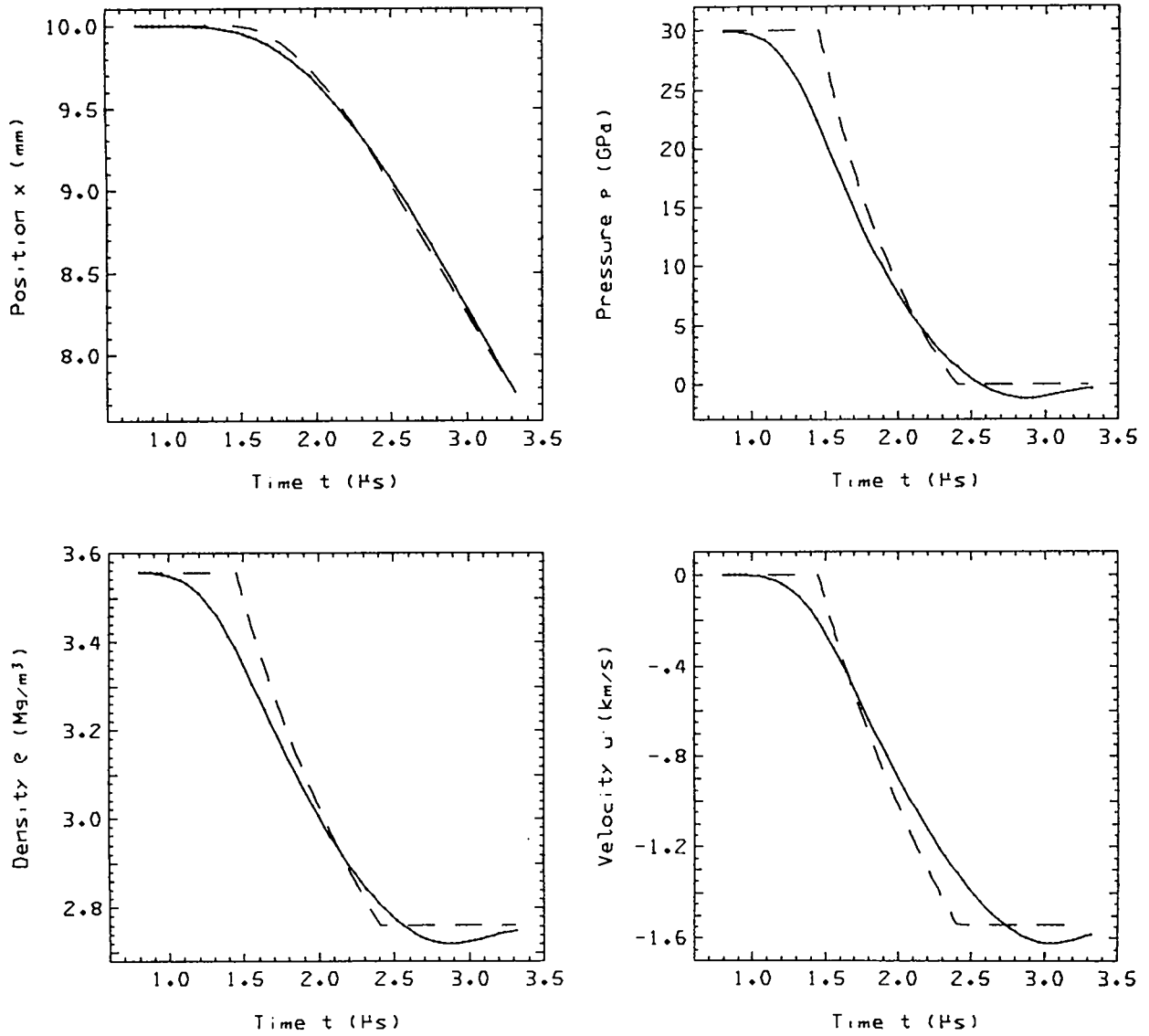


Fig. 1 (cont)

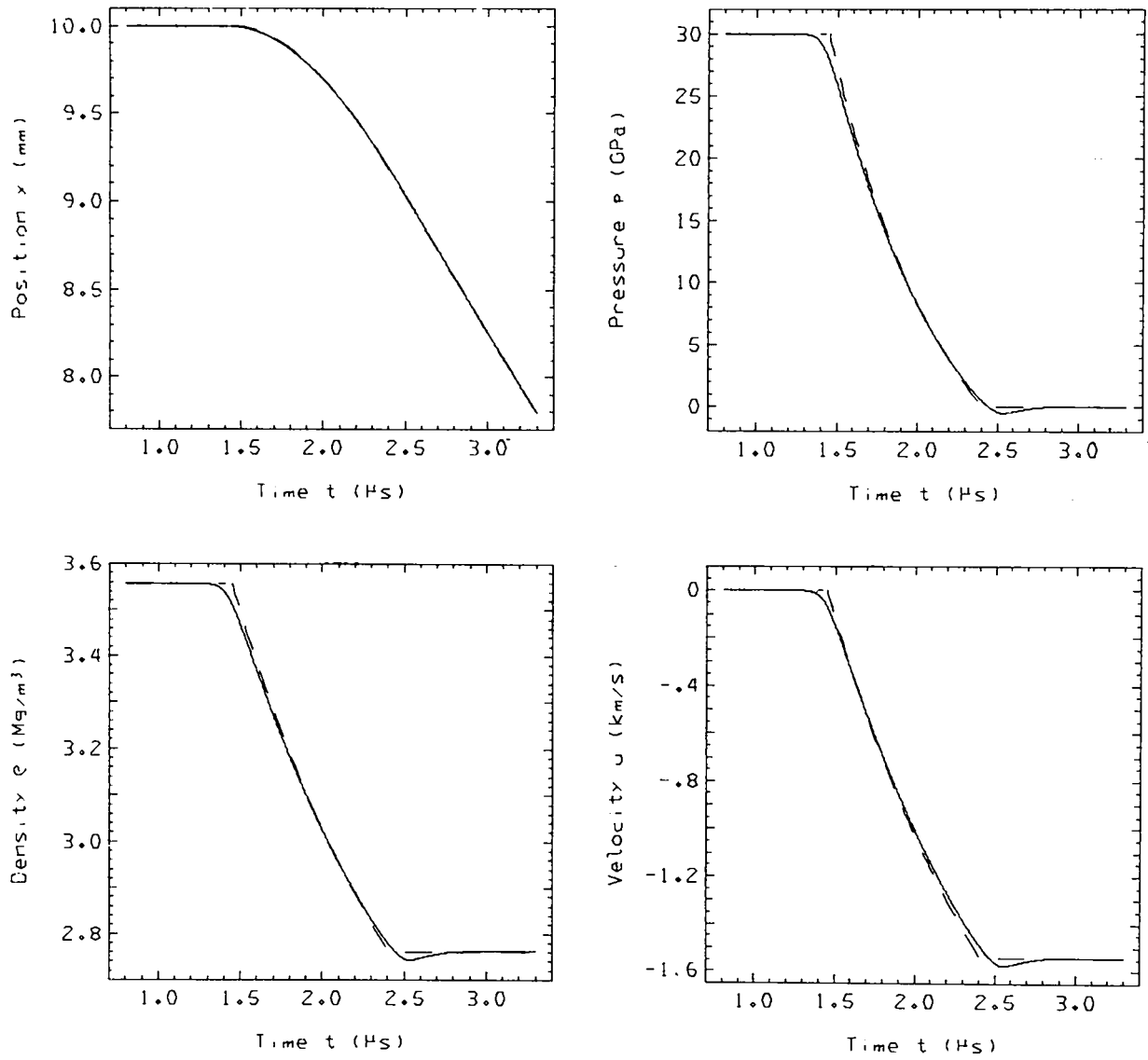
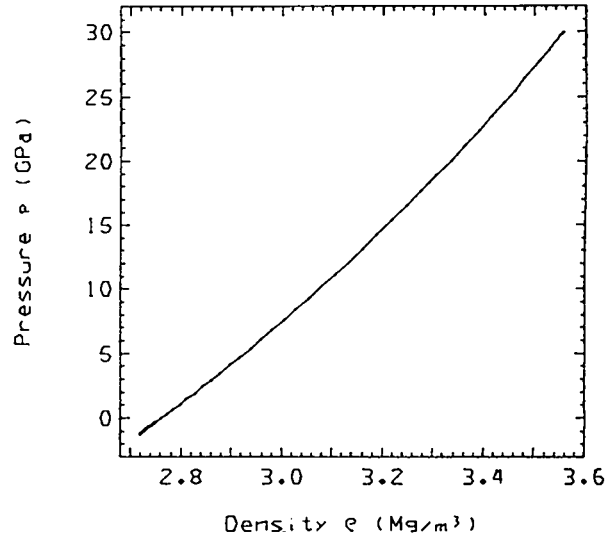
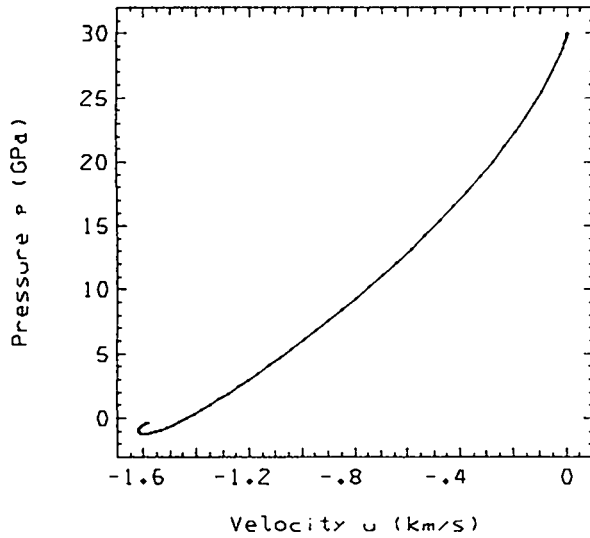


Fig. 1 (cont)

PAD3.3F6 - 75JUL14 RUN 2 LAC2A *1. RARE.*
TFICKETIGY. .528 SEC ON RUN, 2.298 SEC ON JOB

ERUN 1. 16 CELLS 07/21/75

1. RARE. / PARTICLES



PAD3.3F6 - 75JUL14 RUN 3 LAC2A *1. RARE.*
TFICKETIGY. .380 SEC ON RUN, 16.351 SEC ON JOB

ERUN 1. 16 CELLS 07/21/75

1. RARE. / DIFFERENCE / PARTICLES

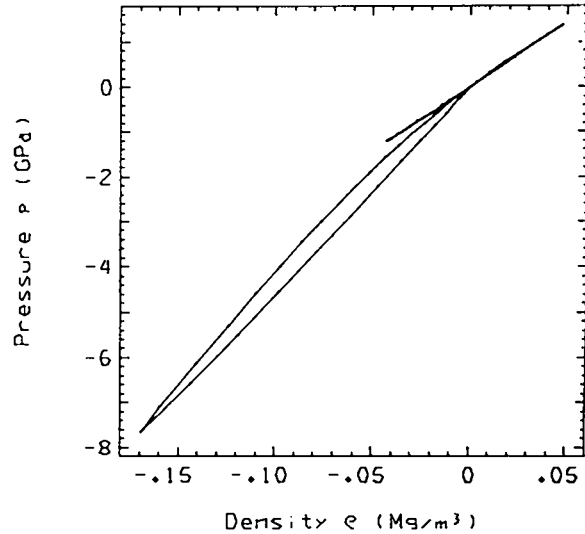
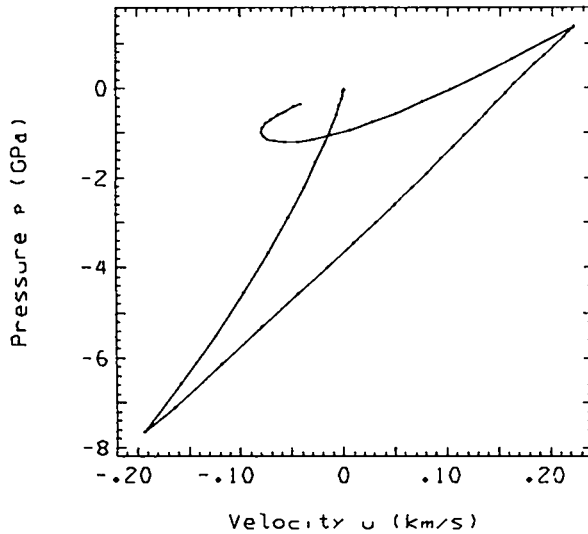


Fig. 1 (cont)

1. RARE. / DIFFERENCE / PARTICLES

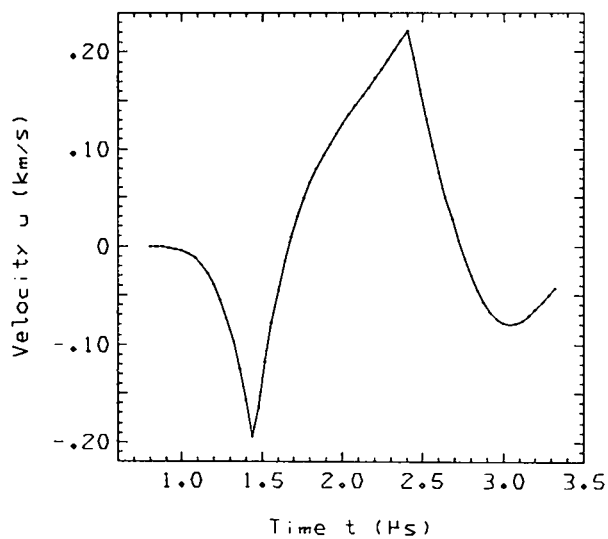
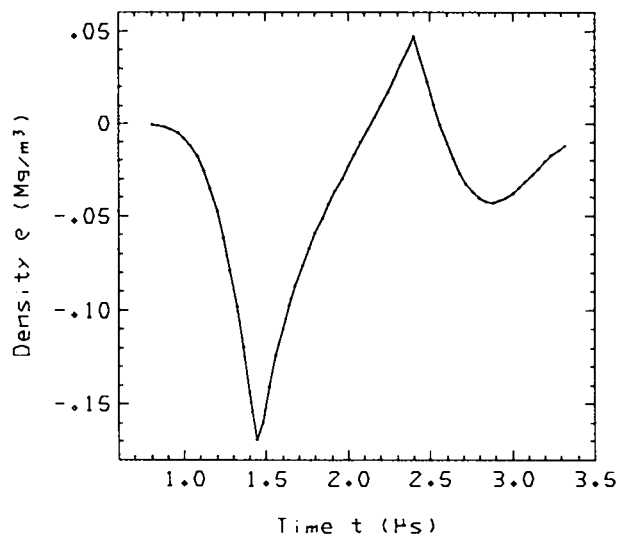
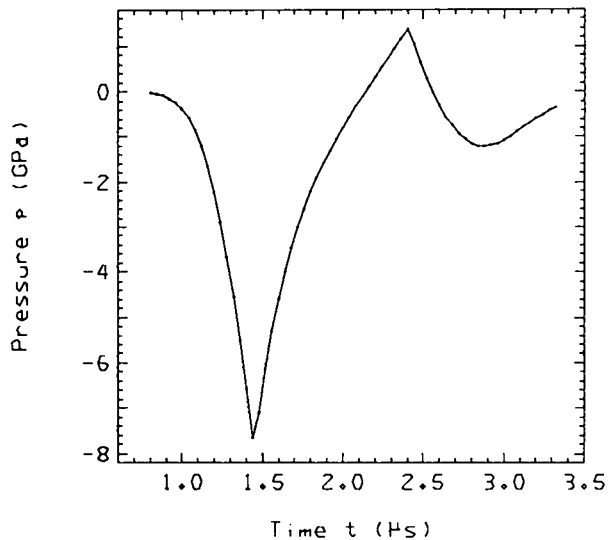
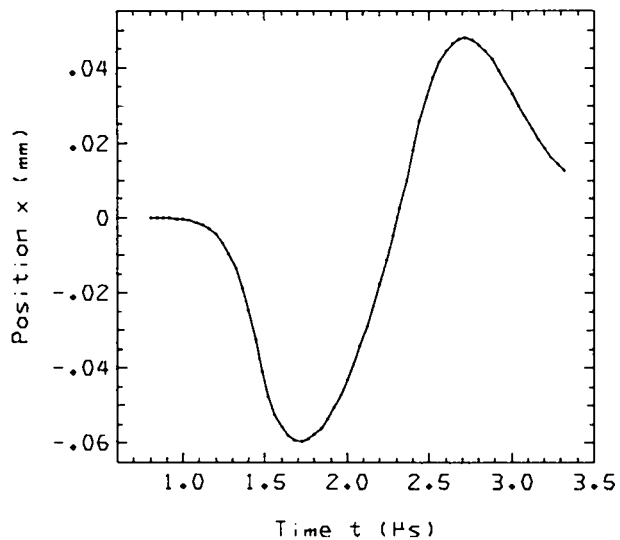


Fig. 1 (cont)

1. RARE. / DIFFERENCE / PARTICLES

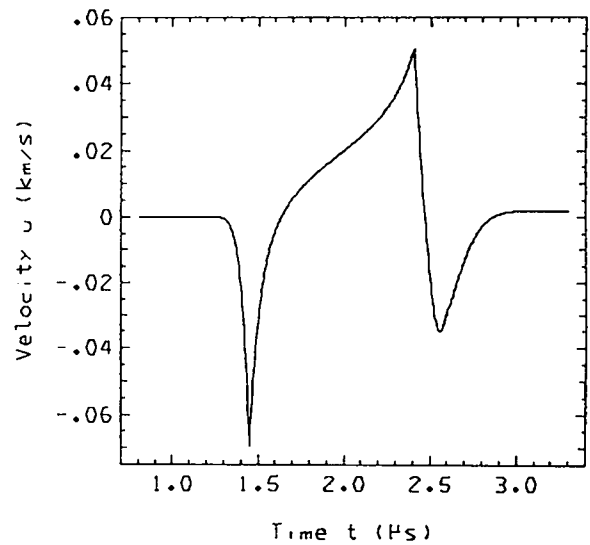
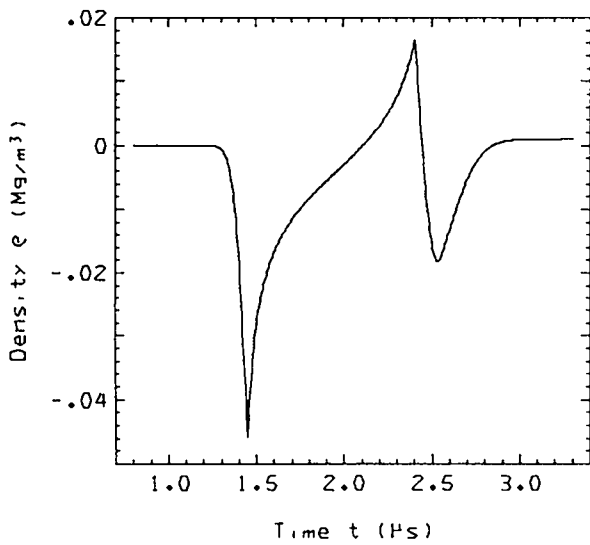
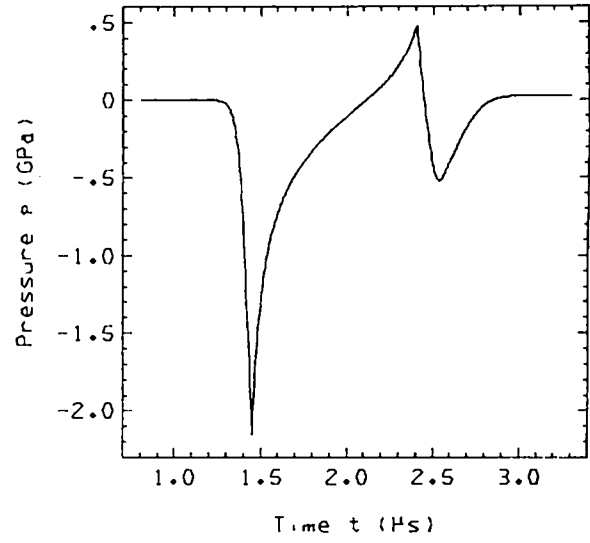
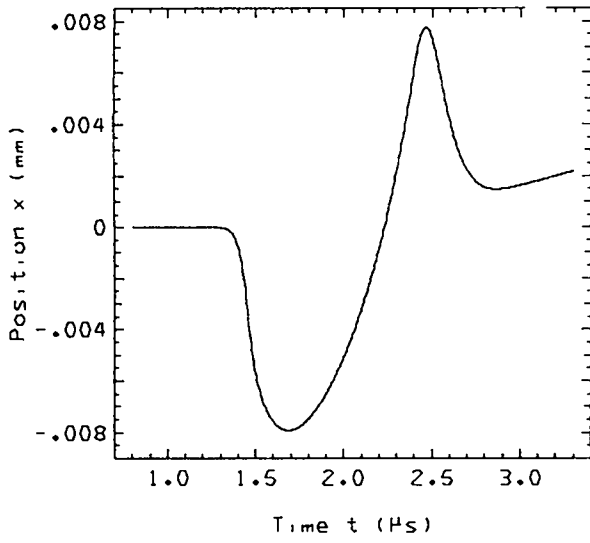


Fig. 1 (cont)

1. RARE. / DIFFERENCE / PARTICLE

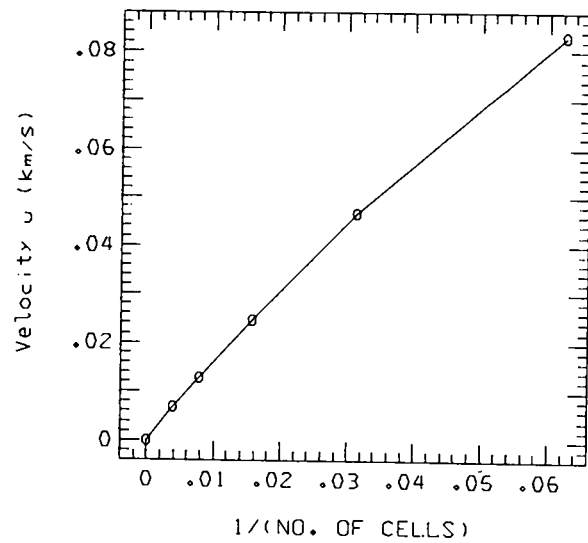
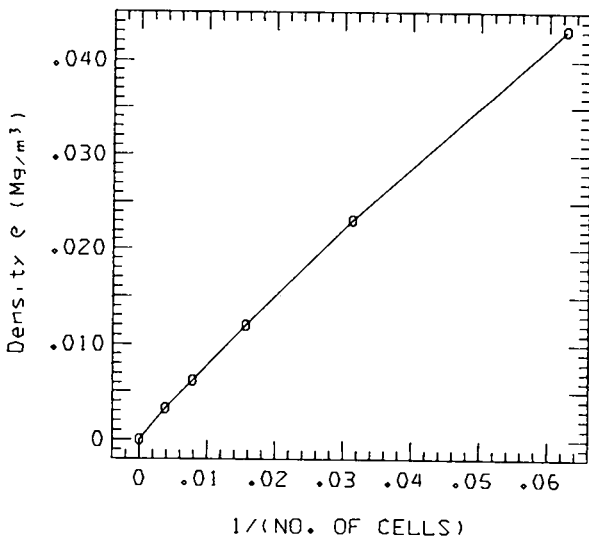
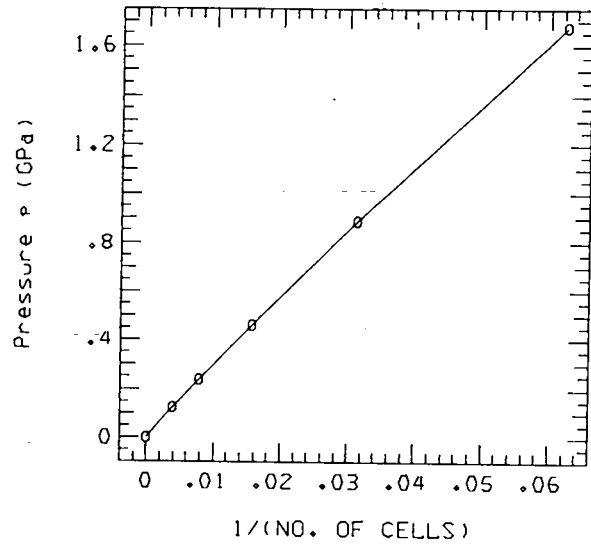
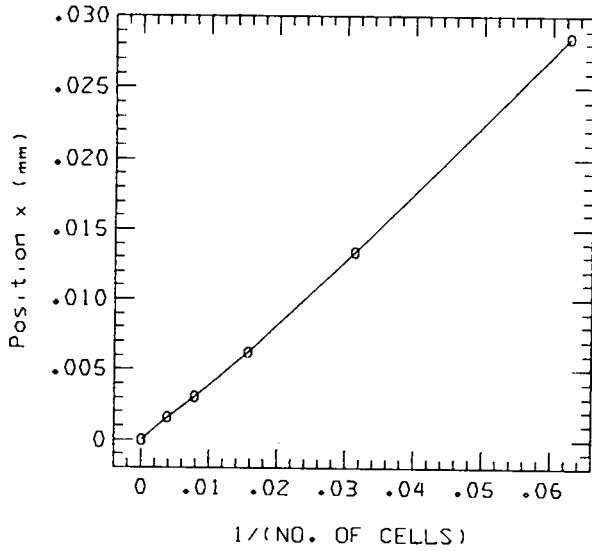


Fig. 1 (cont)

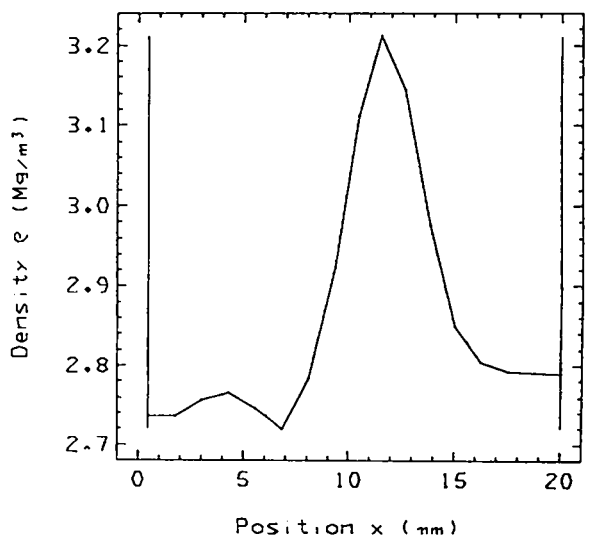
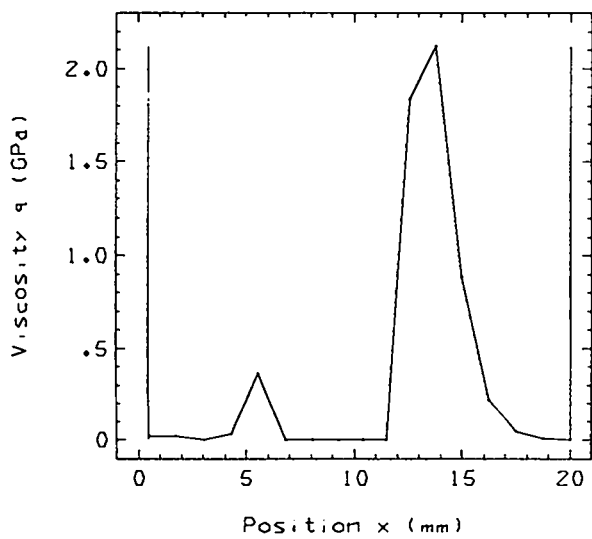
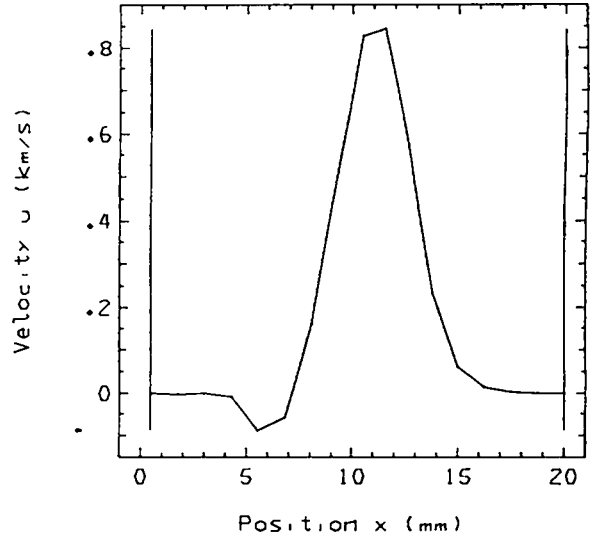
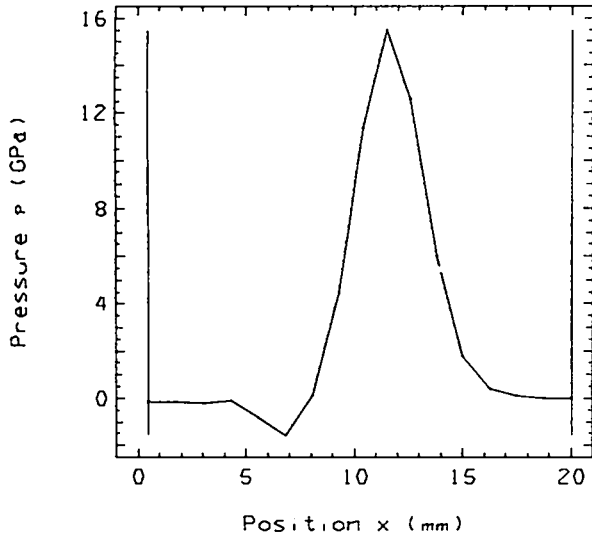


Fig. 2.
Problem 2. Shock deceleration. Standard calculation.

2. SHOCK DECEL / TIME= 1.4000E+00

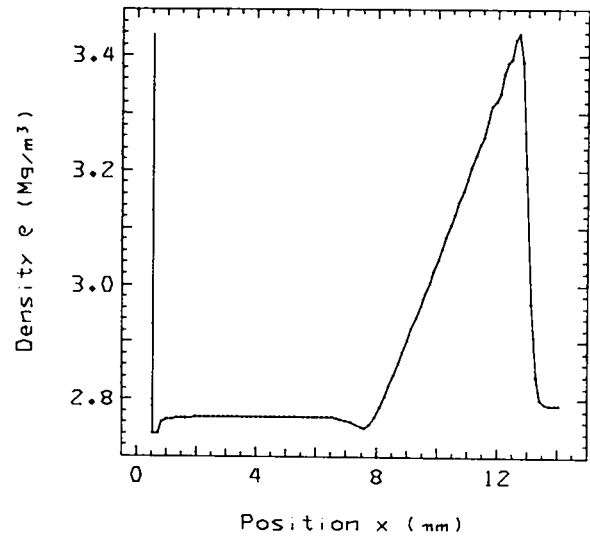
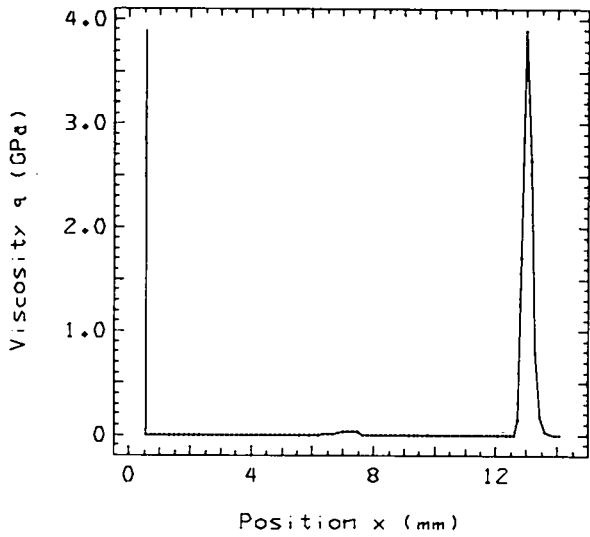
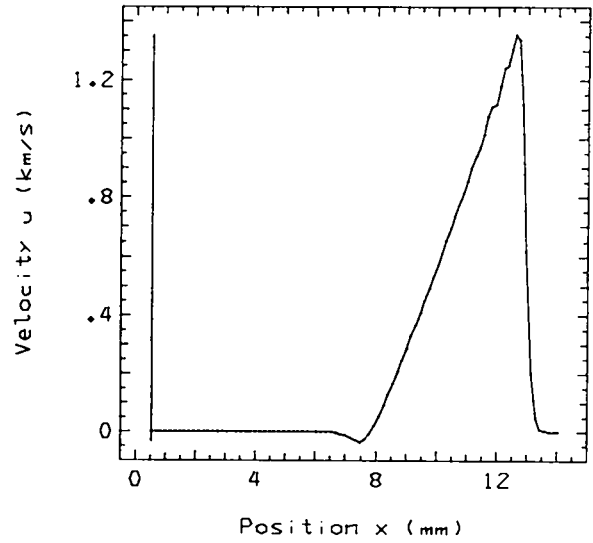
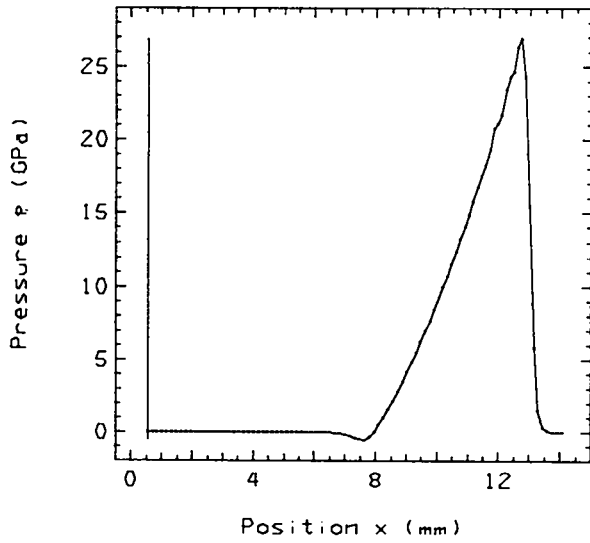


Fig. 2 (cont)

2. SHOCK DECEL / PARTICLES

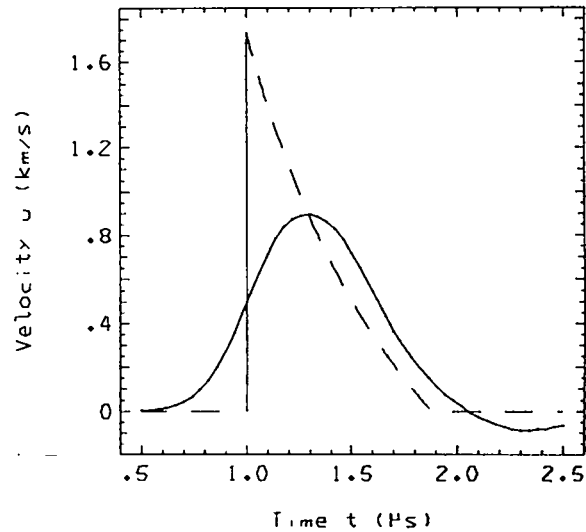
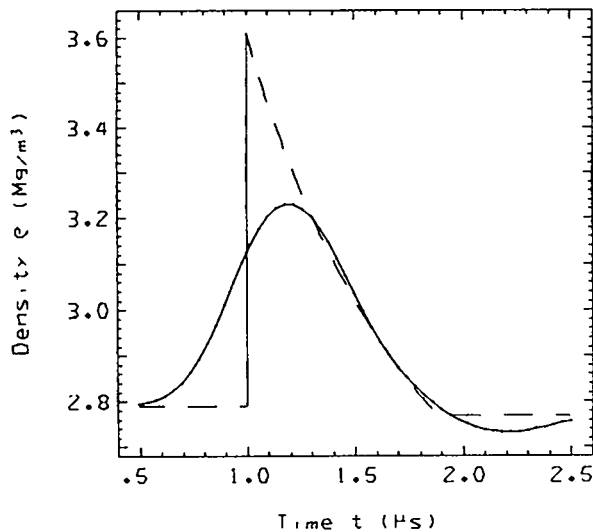
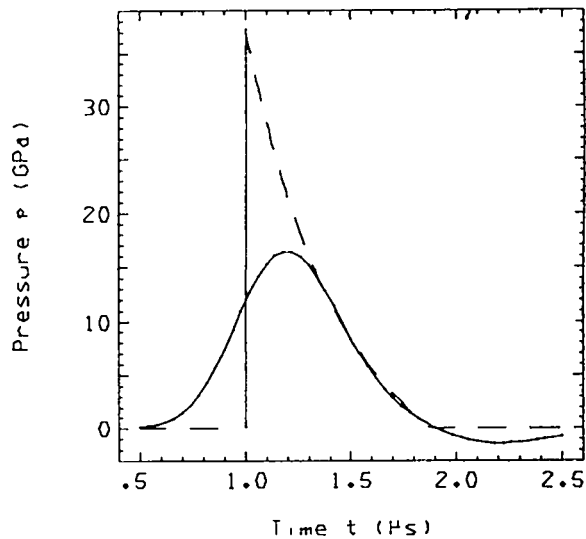
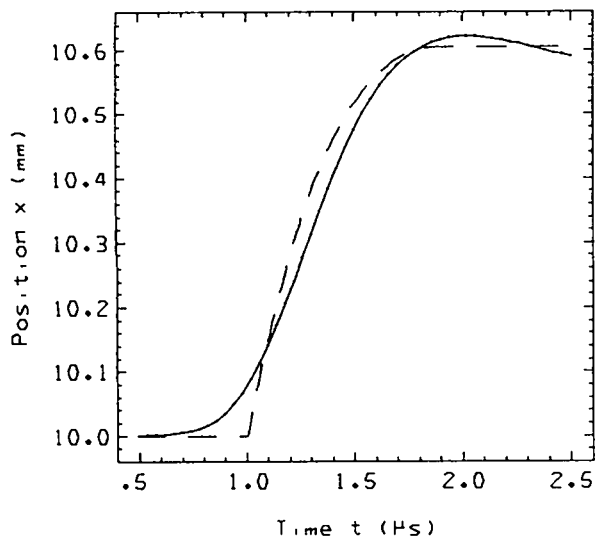


Fig. 2 (cont)

2. SHOCK DECEL / PARTICLES

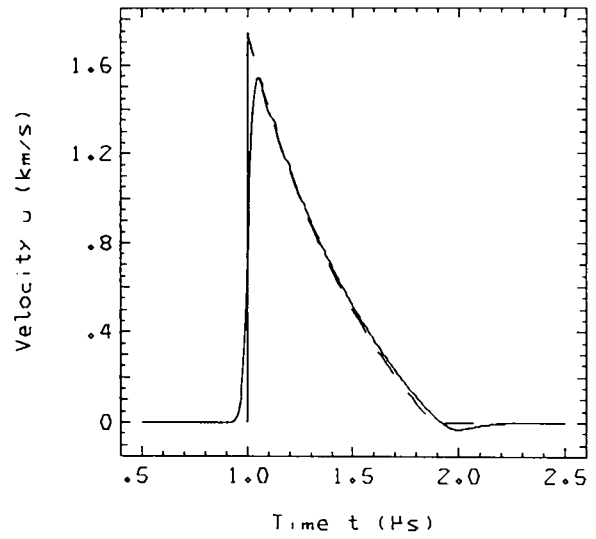
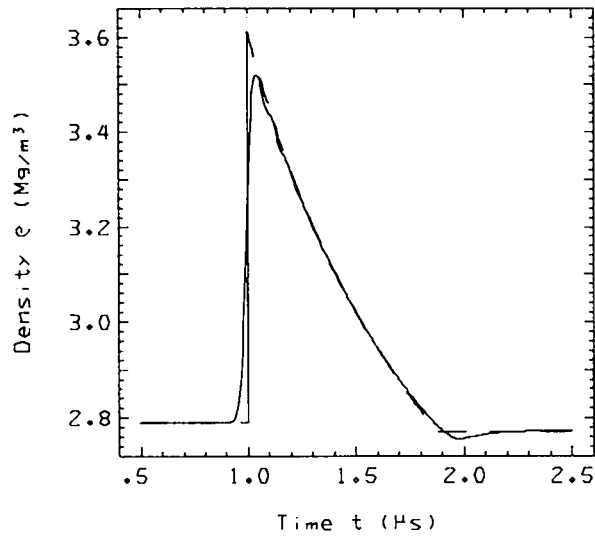
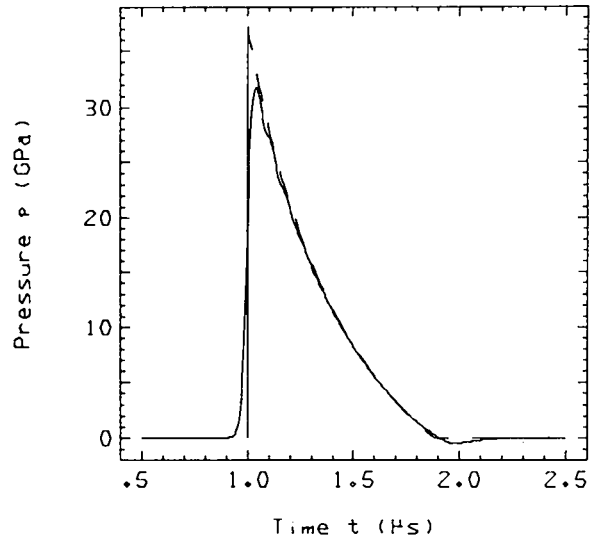
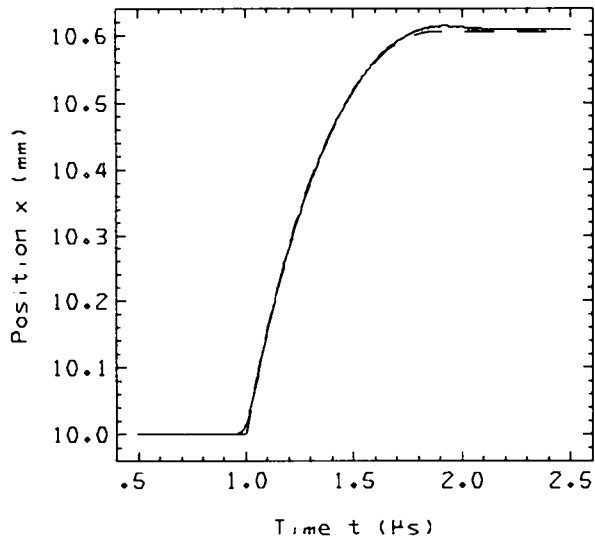
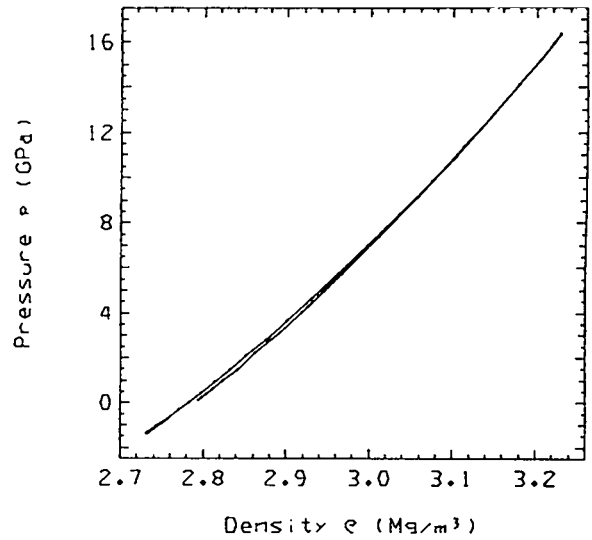
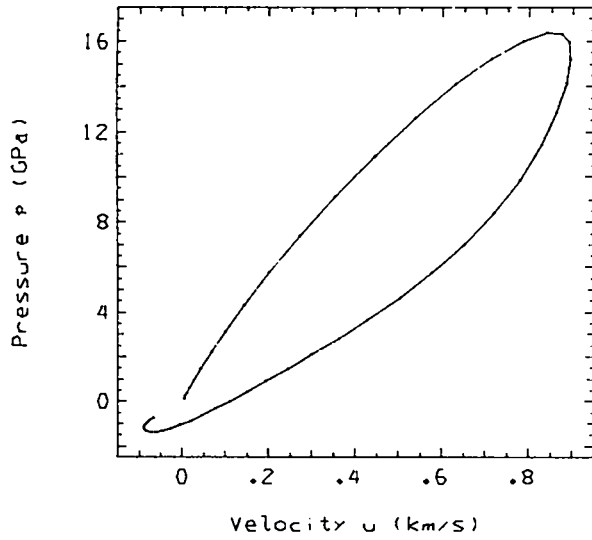


Fig. 2 (cont)

PAD3.3F6 - 75JUL14 RUN 5 LAC2A *2. SHOCK DECEL*
TFICKET1GY. .954 SEC ON RUN. 31.138 SEC ON JOB

ERUN 1. 16 CELLS 07/21/75

2. SHOCK DECEL / PARTICLES



PAD3.3F6 - 75JUL14 RUN 5 LAC2A *2. SHOCK DECEL*
TFICKET1GY. 9.822 SEC ON RUN. 40.006 SEC ON JOB

ERUN 4. 128 CELLS 07/21/75

2. SHOCK DECEL / PARTICLES

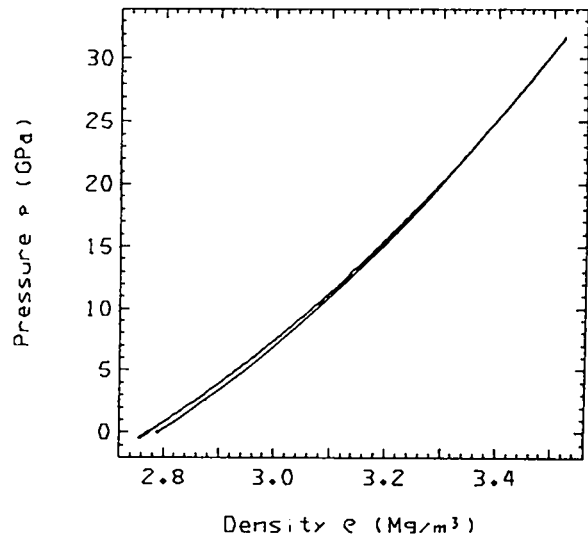
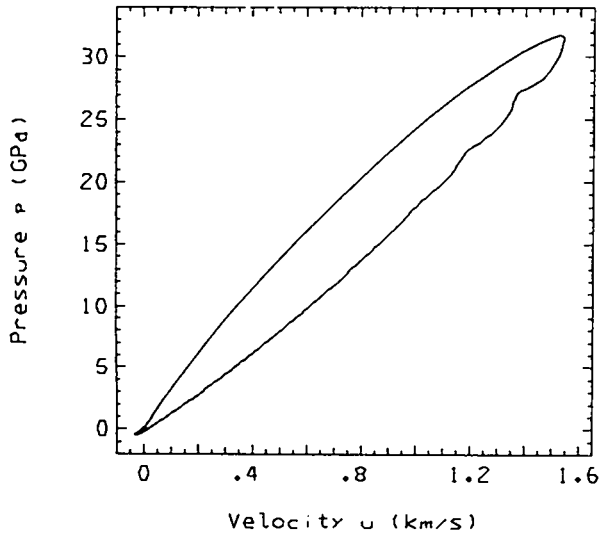


Fig. 2 (cont)

2. SHOCK DECEL / DIFFERENCE / PARTICLES

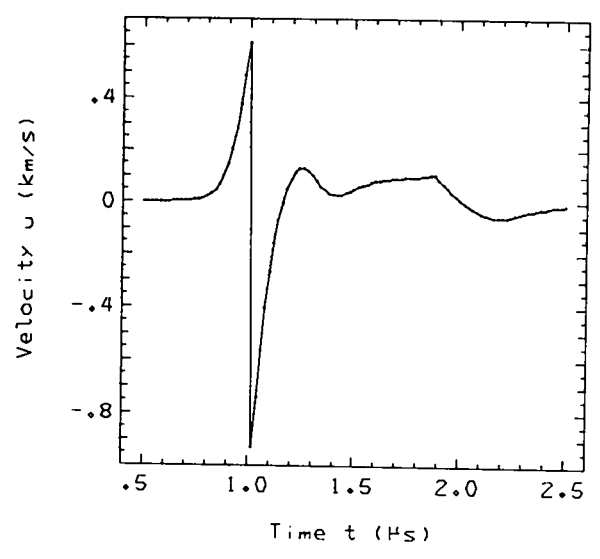
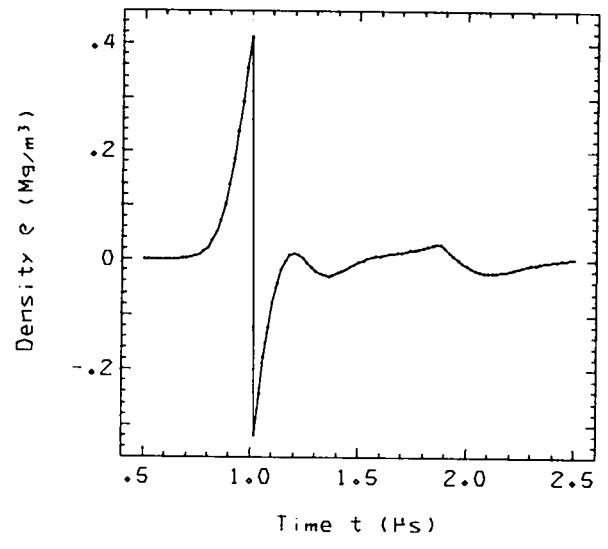
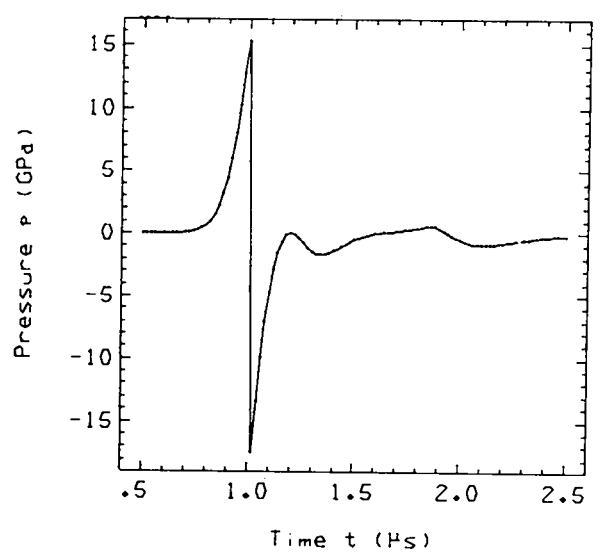
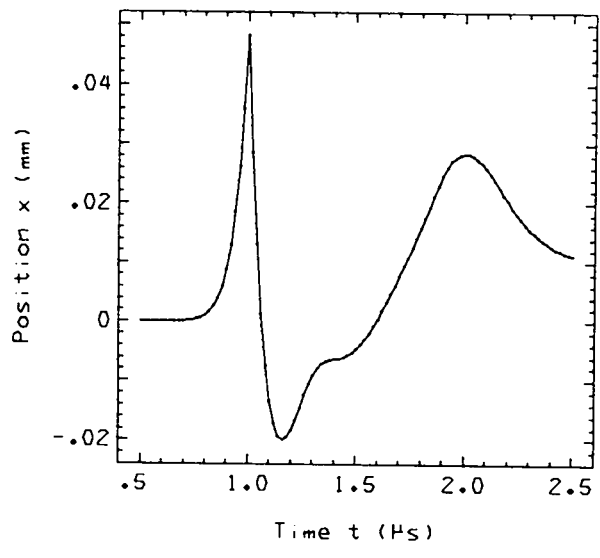


Fig. 2 (cont)

2. SHOCK DECEL / DIFFERENCE / PARTICLES

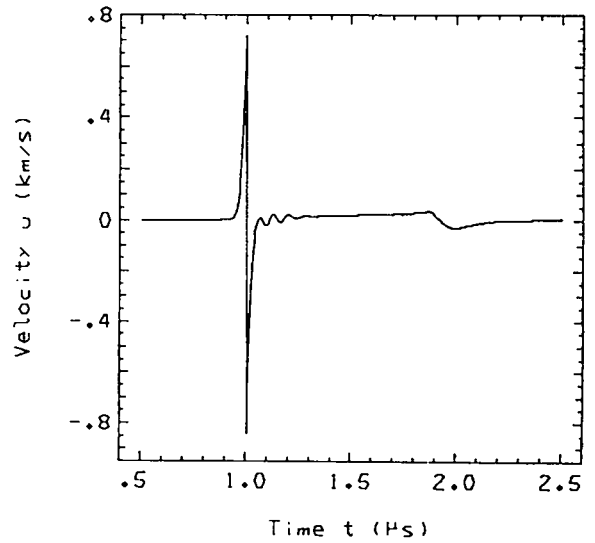
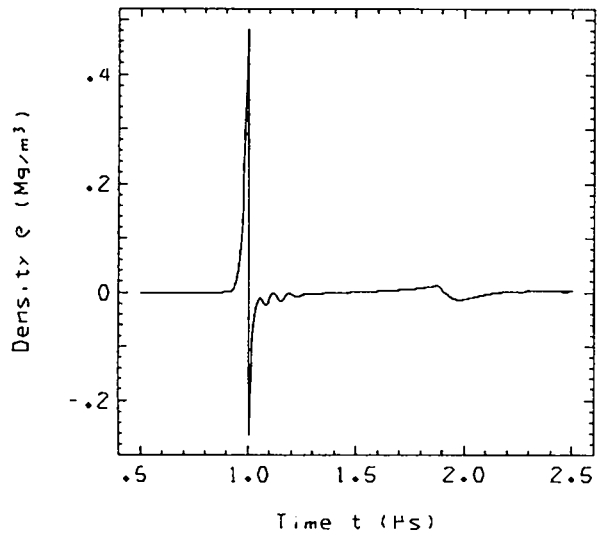
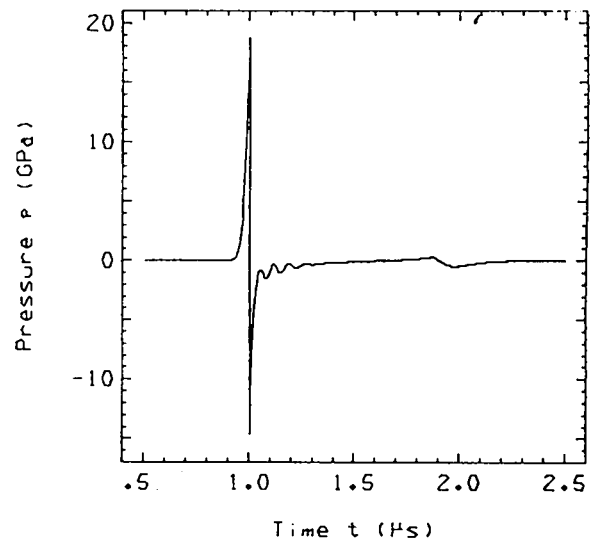
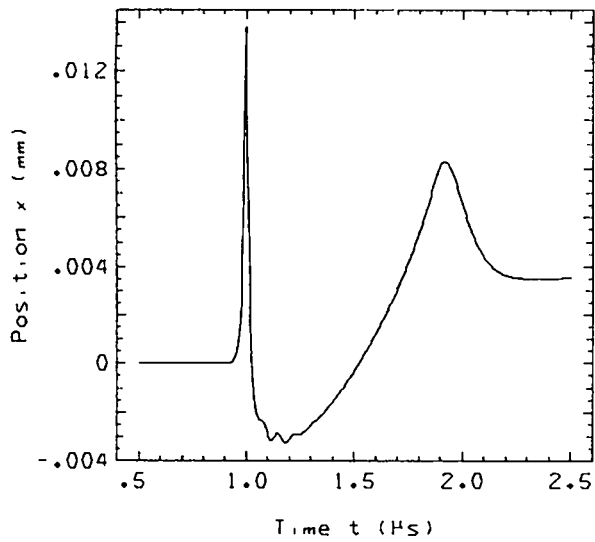


Fig. 2 (cont)

2. SHOCK DECEL / DIFFERENCE, TRUNCATED TIME / PARTICLES

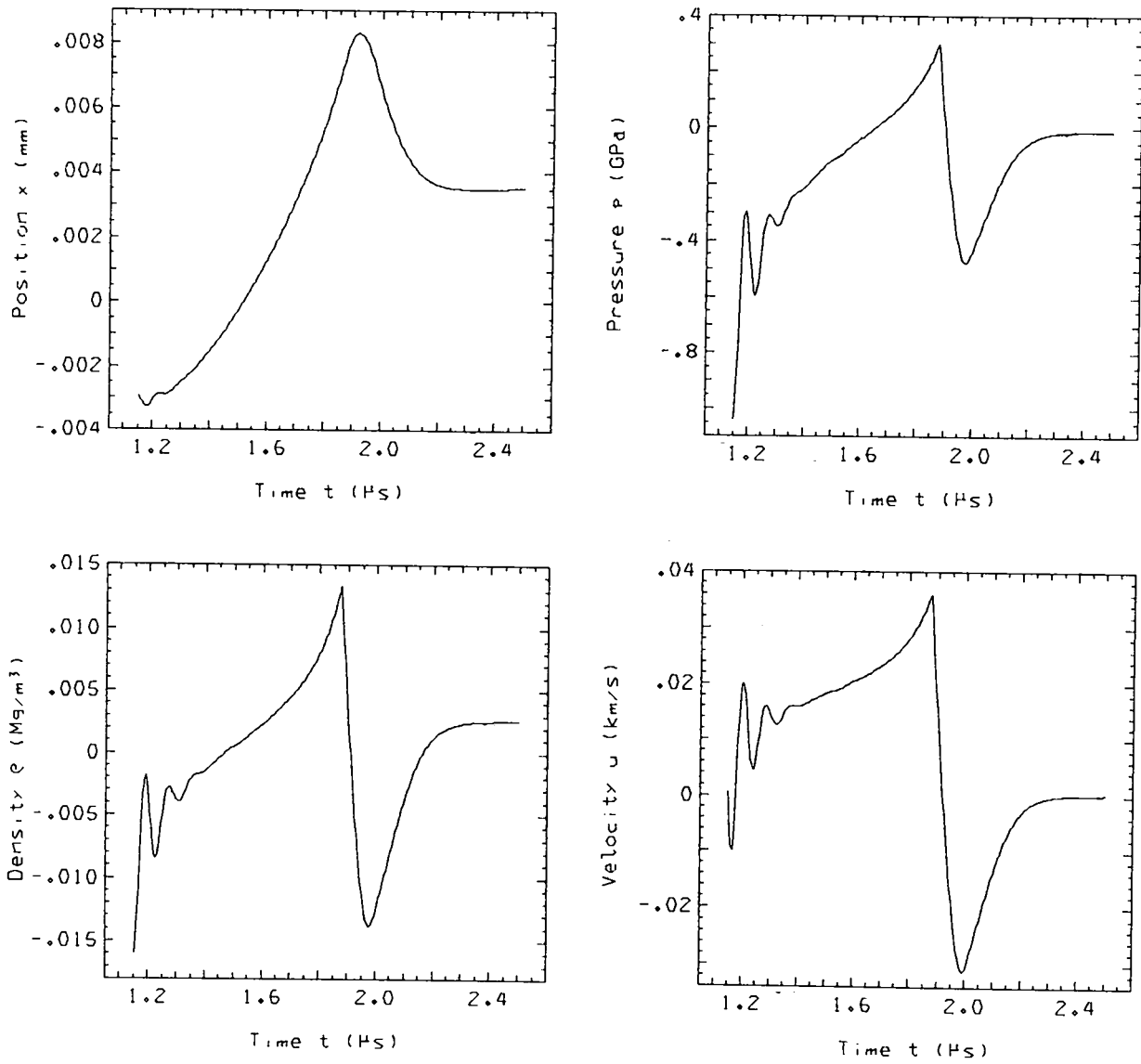


Fig. 2 (cont)

2. SHOCK DECEL / DIFFERENCE, TRUNCATED TIME / PARTICLES

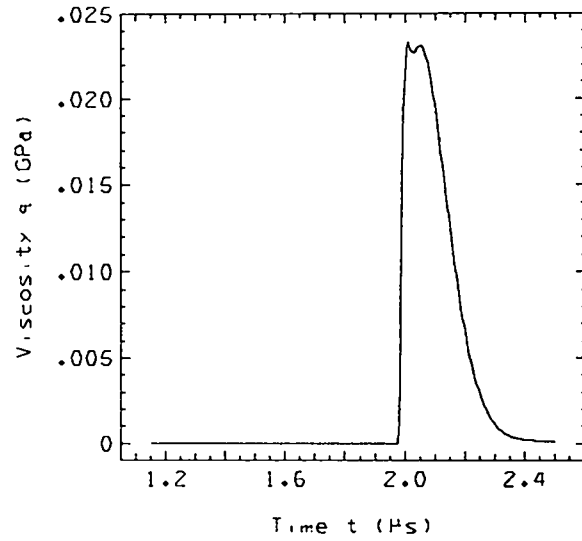
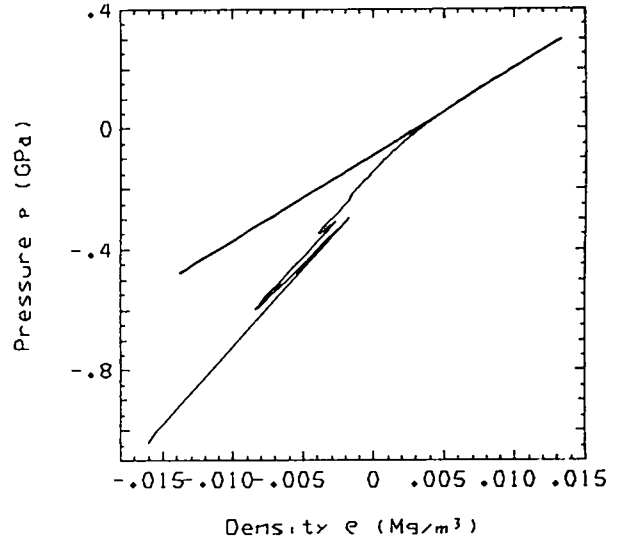
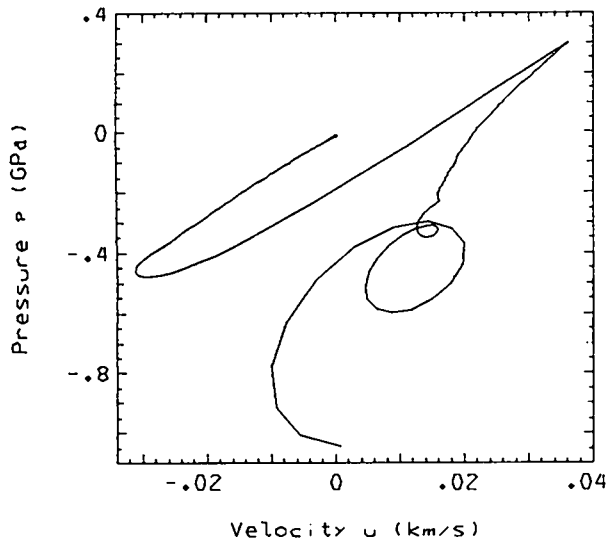


Fig. 2 (cont)

2. SHOCK DECEL / LEAD SHOCK

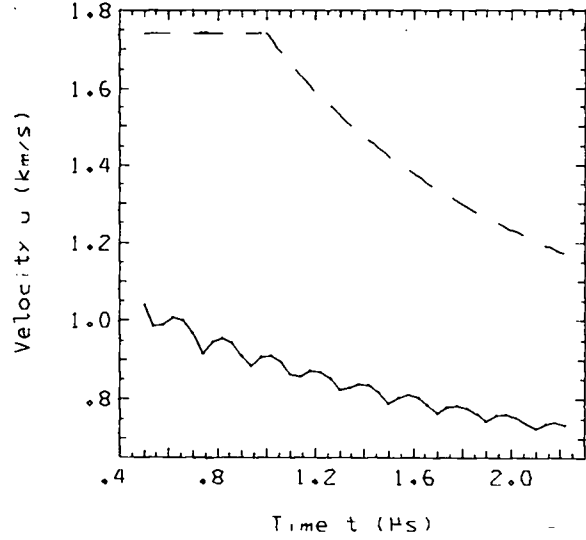
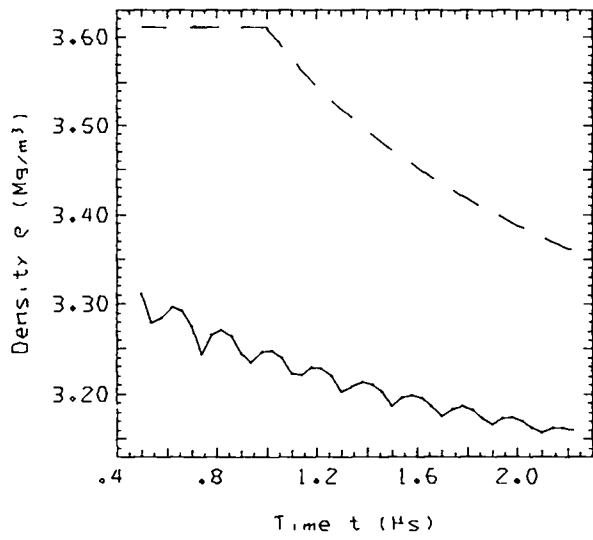
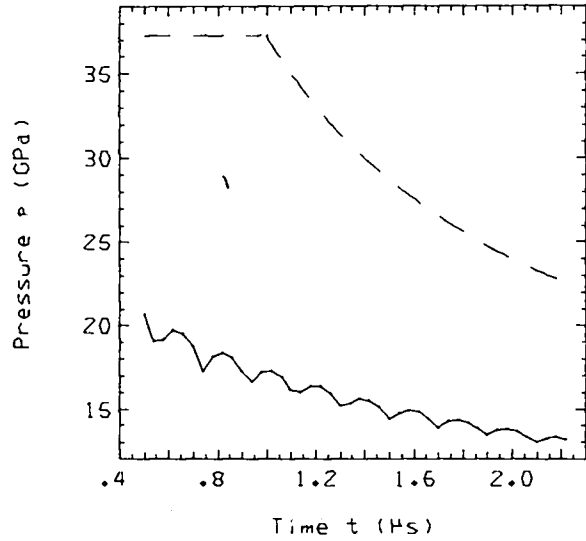
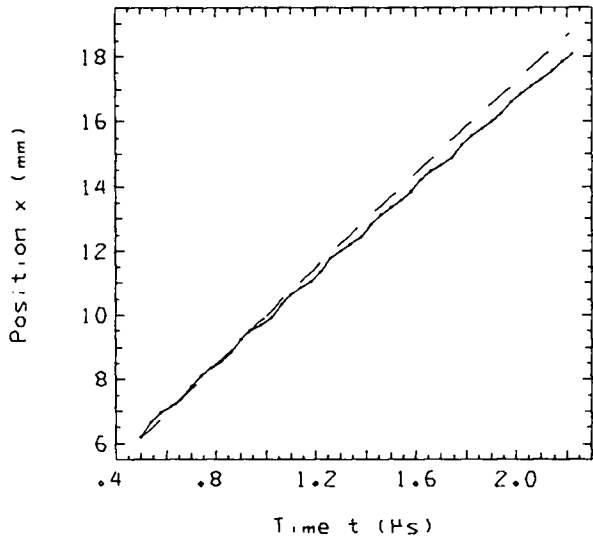


Fig. 2 (cont)

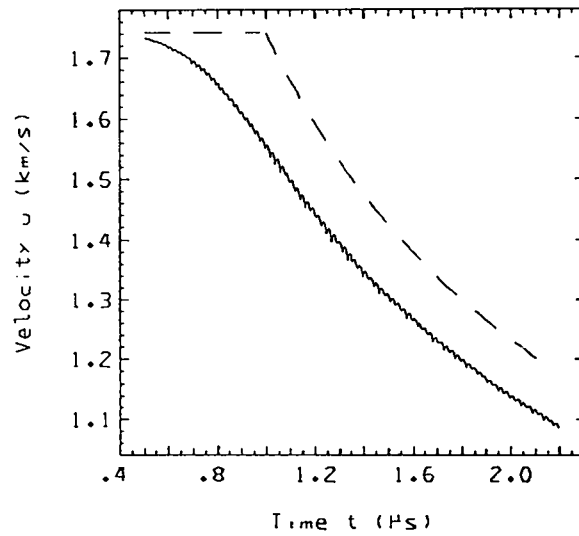
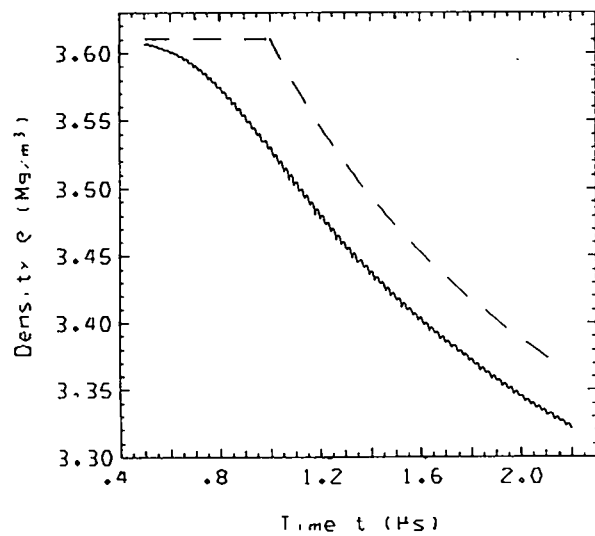
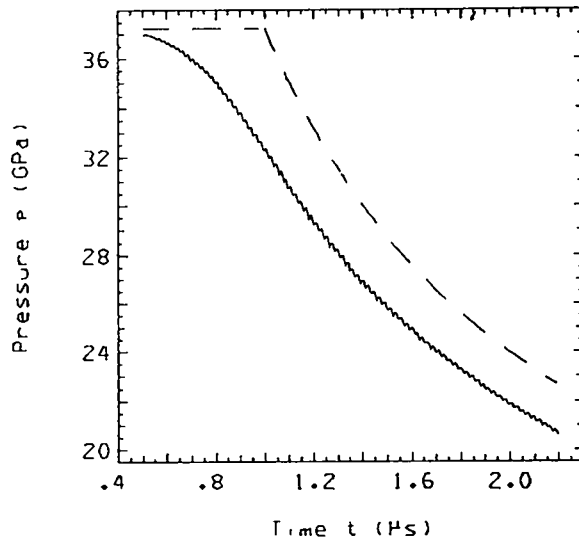
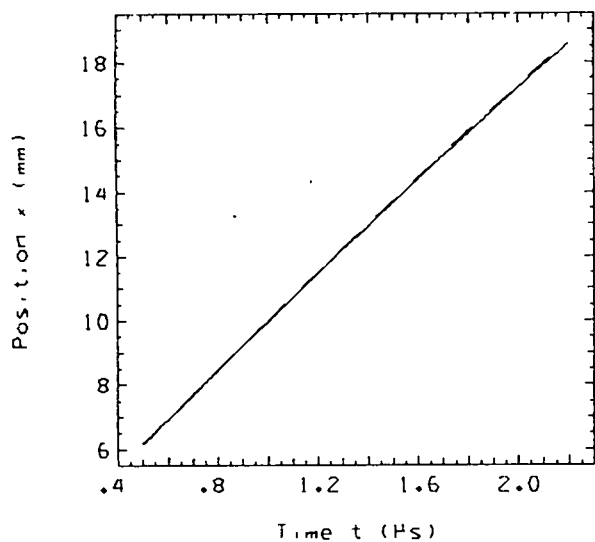


Fig. 2 (cont)

2. SHOCK DECEL / DIFFERENCE. TRUNCATED TIME / PARTICLE

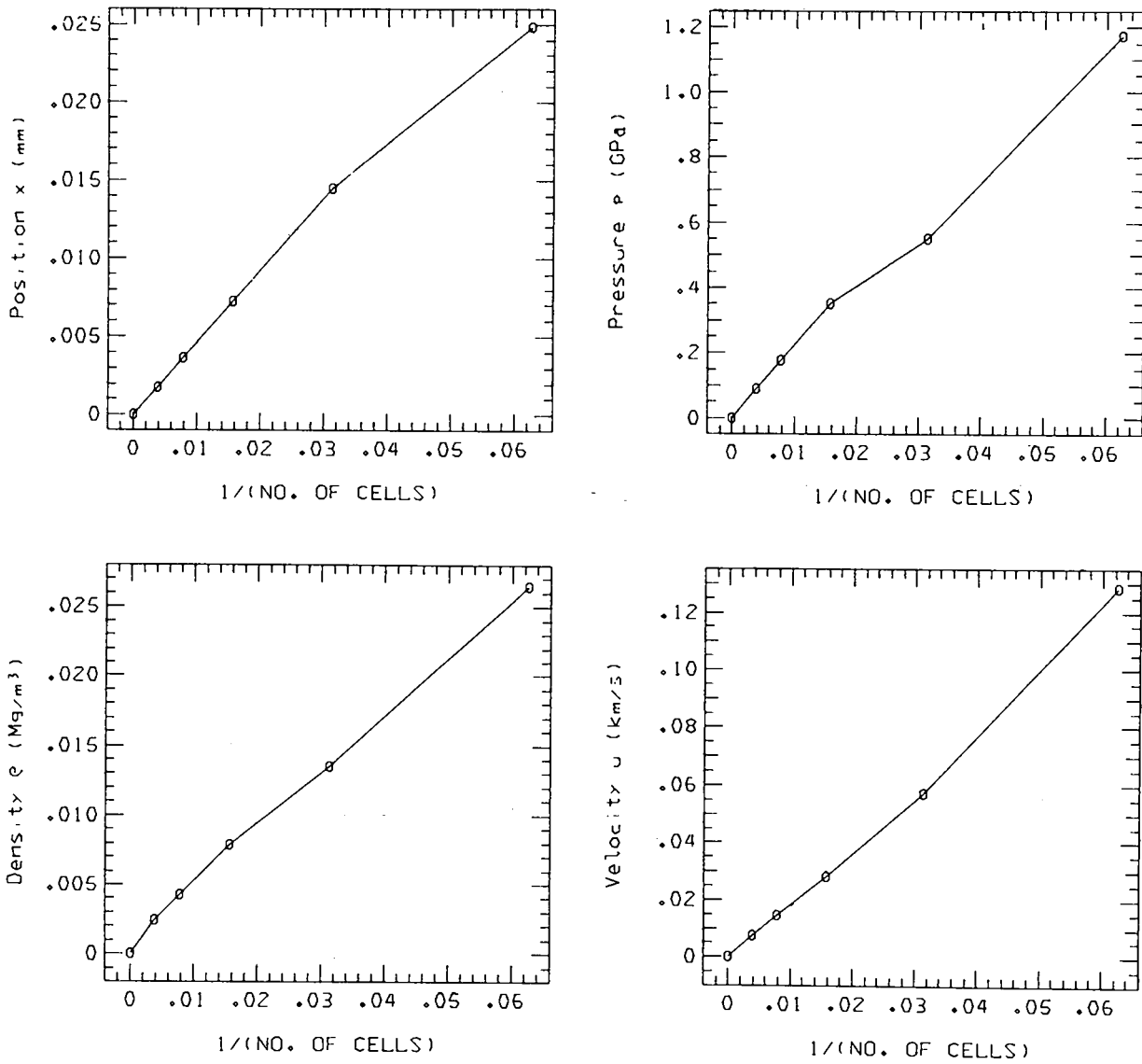


Fig. 2 (cont)

2. SHOCK DECEL / DIFFERENCE / SHOCK

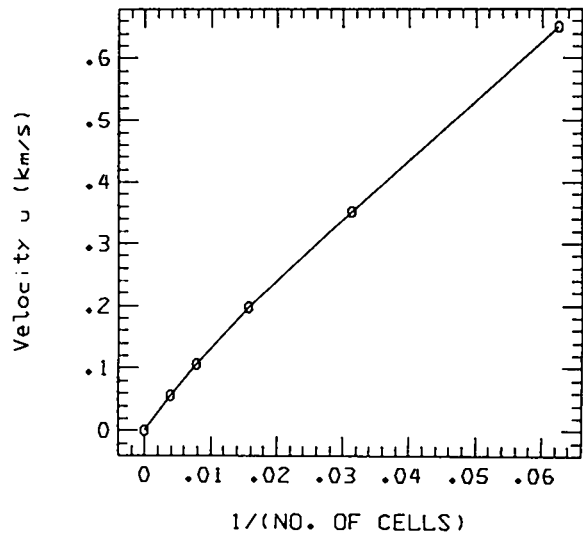
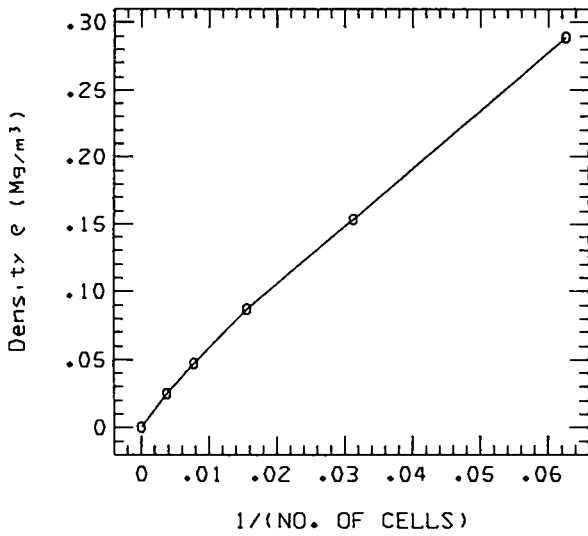
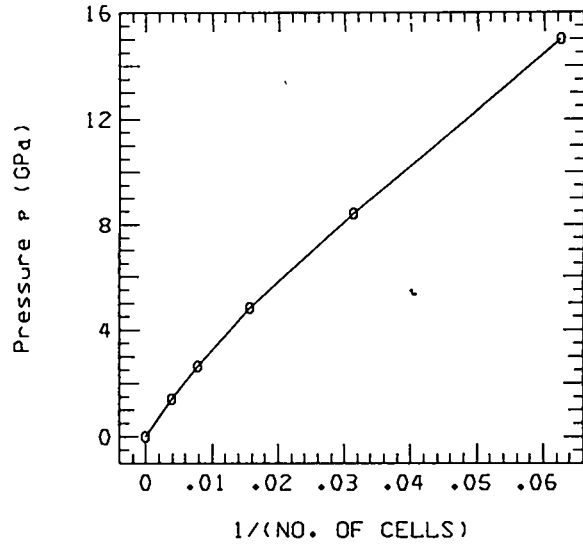
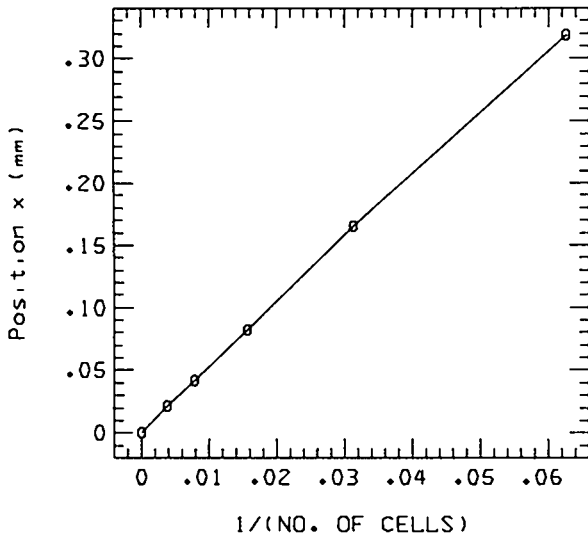


Fig. 2 (cont)

3. FREE-SURFACE DECEL. / TIME= 1.8000E+00

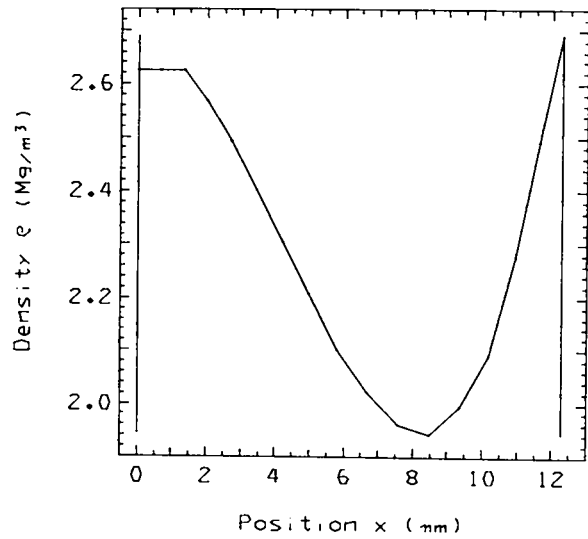
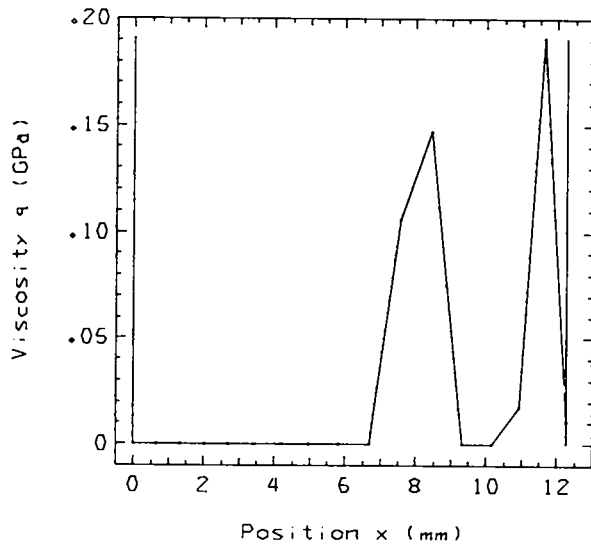
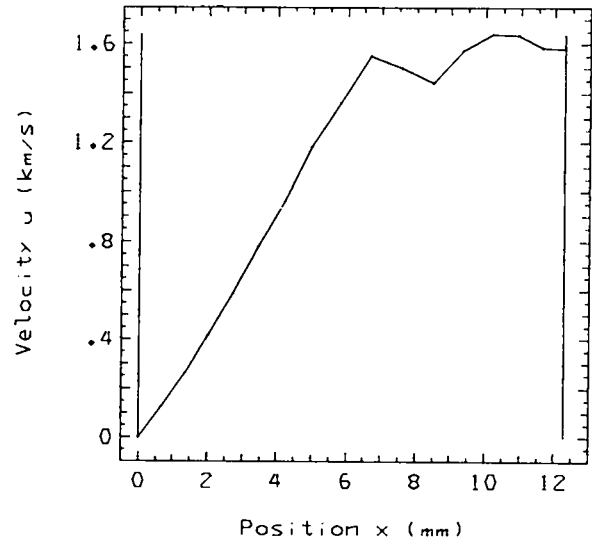
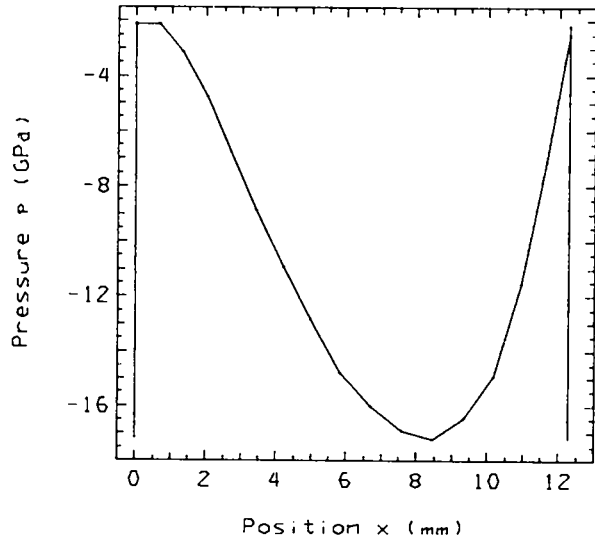


Fig. 3.
Problem 3. Free-surface deceleration. Standard calculation.

3. FREE-SURFACE DECEL. / TIME = 1.8000E+00

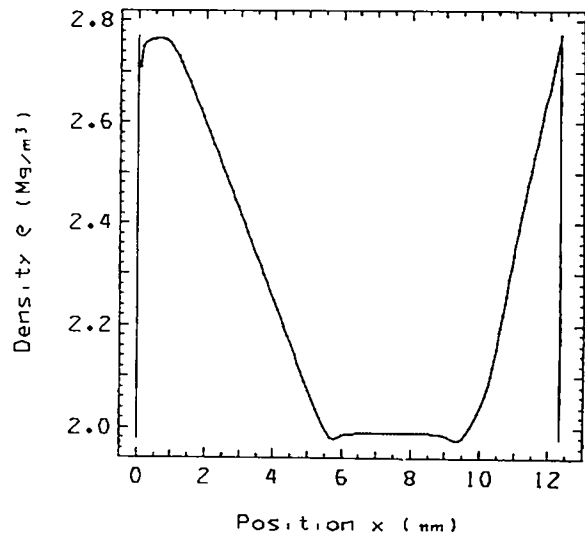
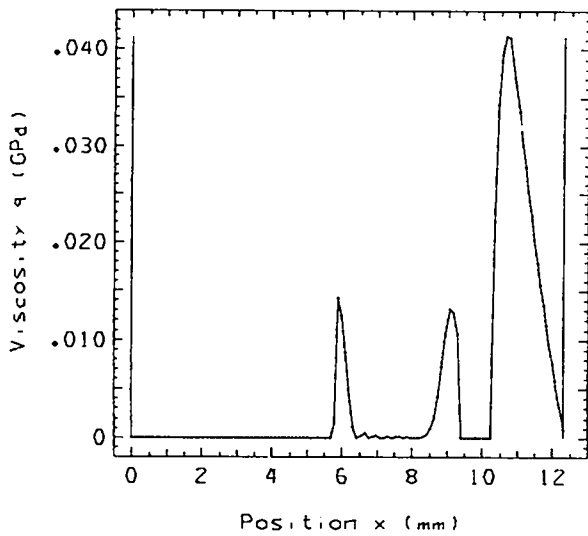
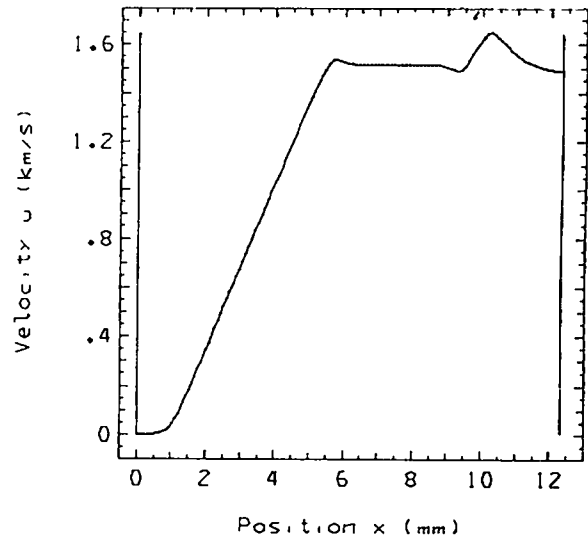
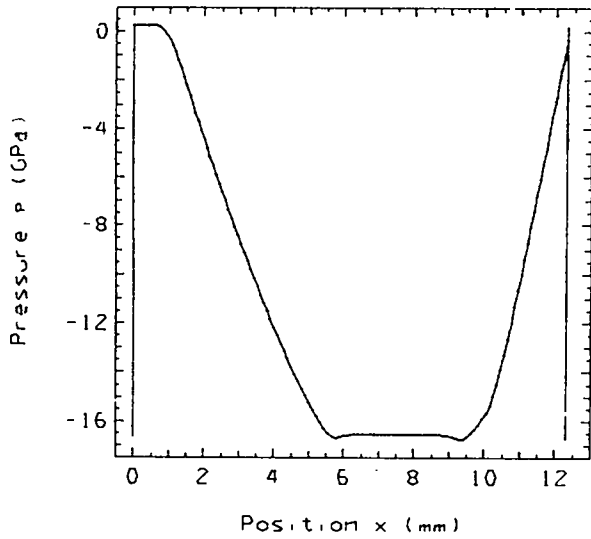


Fig. 3 (cont)

3. FREE-SURFACE DECEL. / PARTICLES

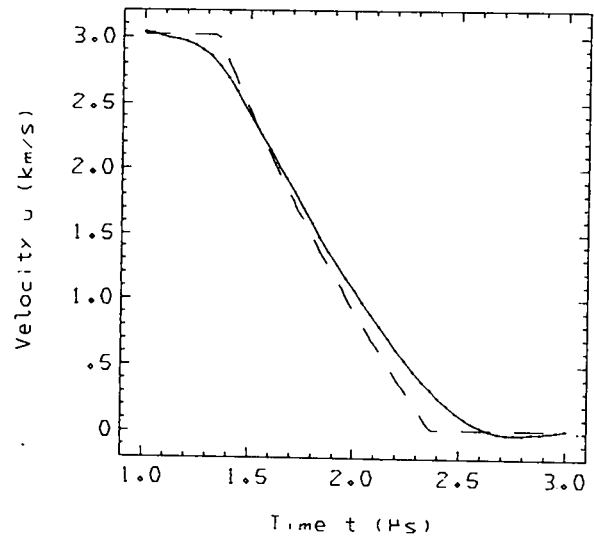
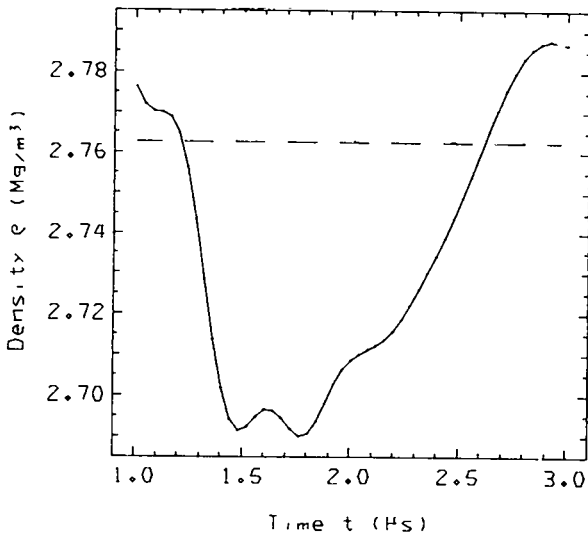
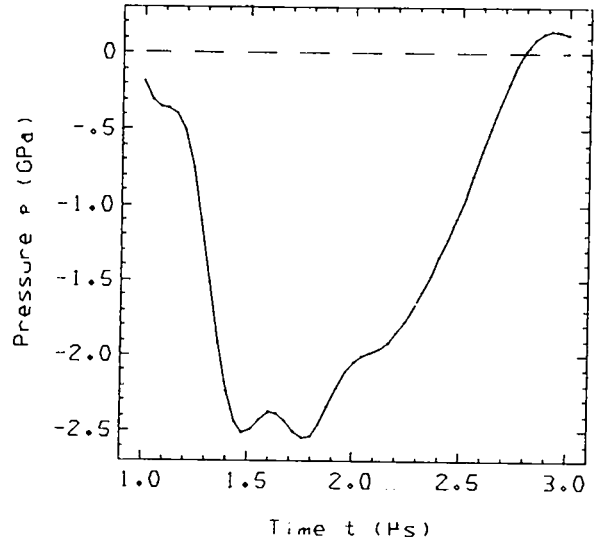
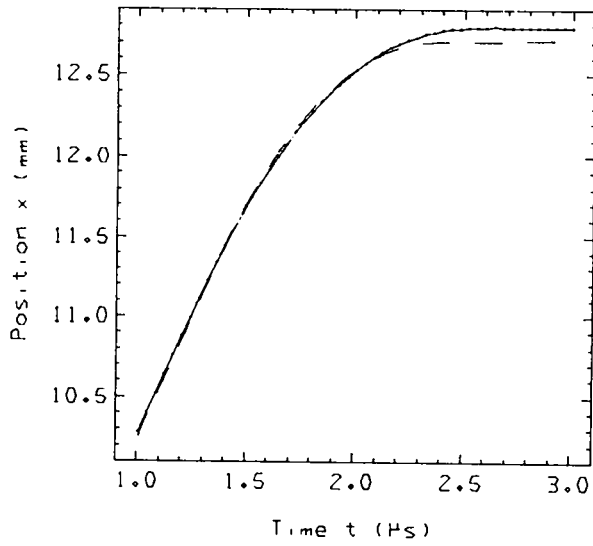


Fig. 3 (cont)

3. FREE-SURFACE DECEL. / PARTICLES

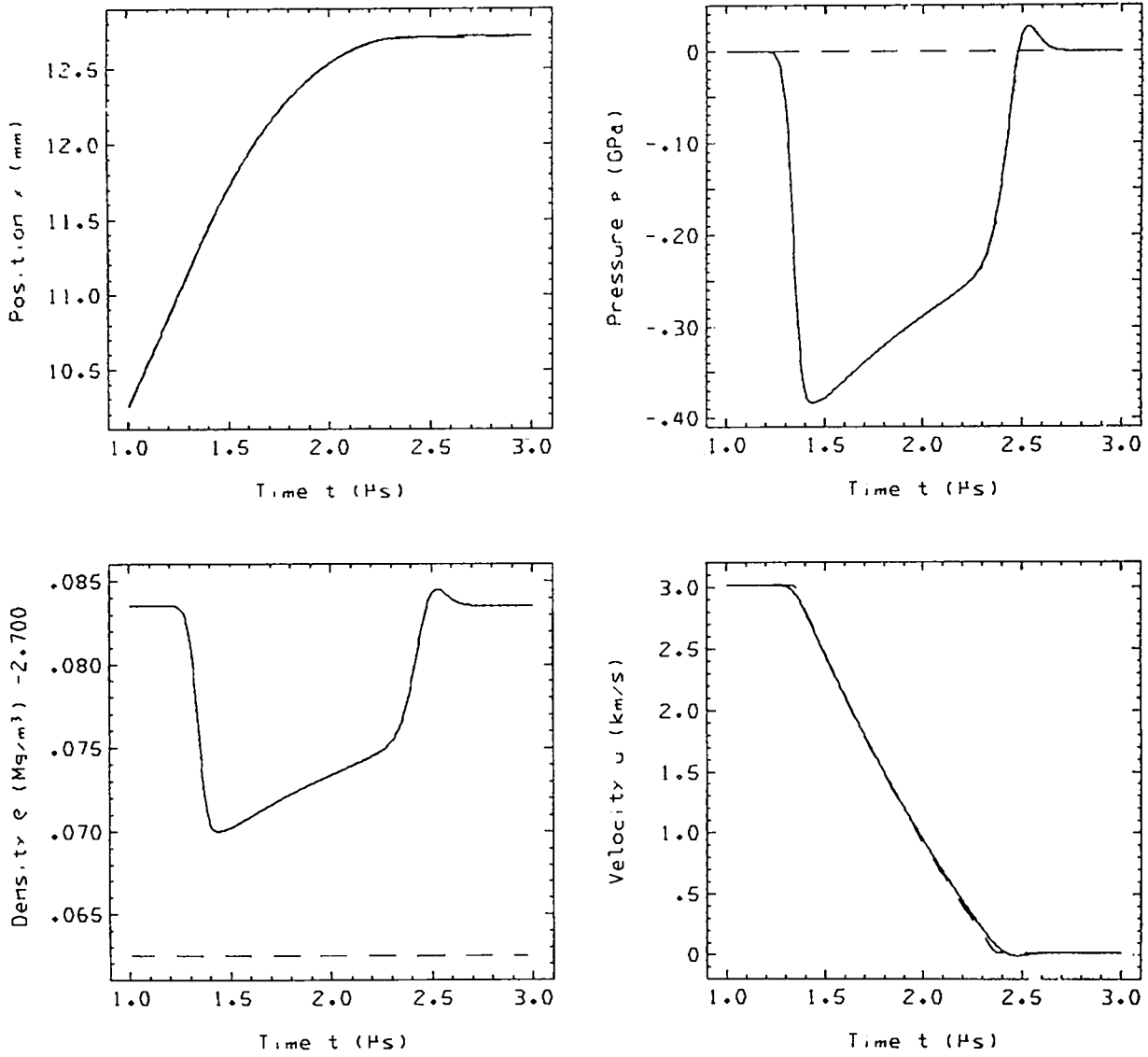


Fig. 3 (cont)

3. FREE-SURFACE DECEL. / PARTICLES

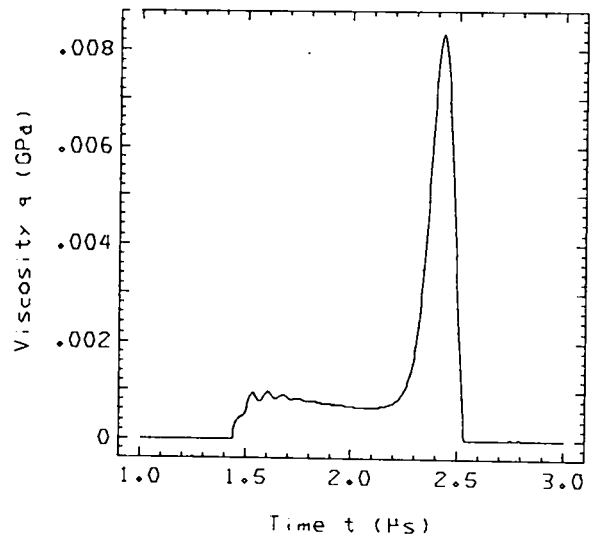
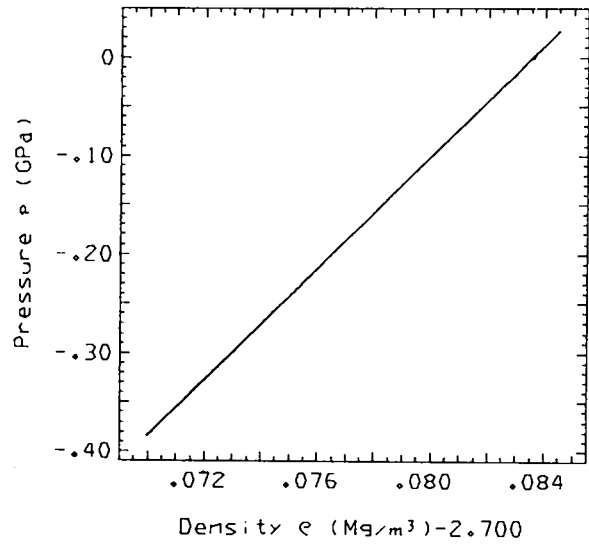
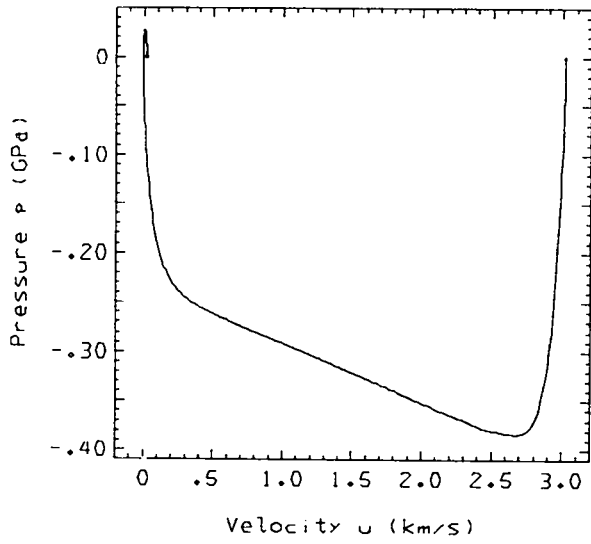


Fig. 3 (cont)

3. FREE-SURFACE DECEL. / DIFFERENCE / PARTICLES

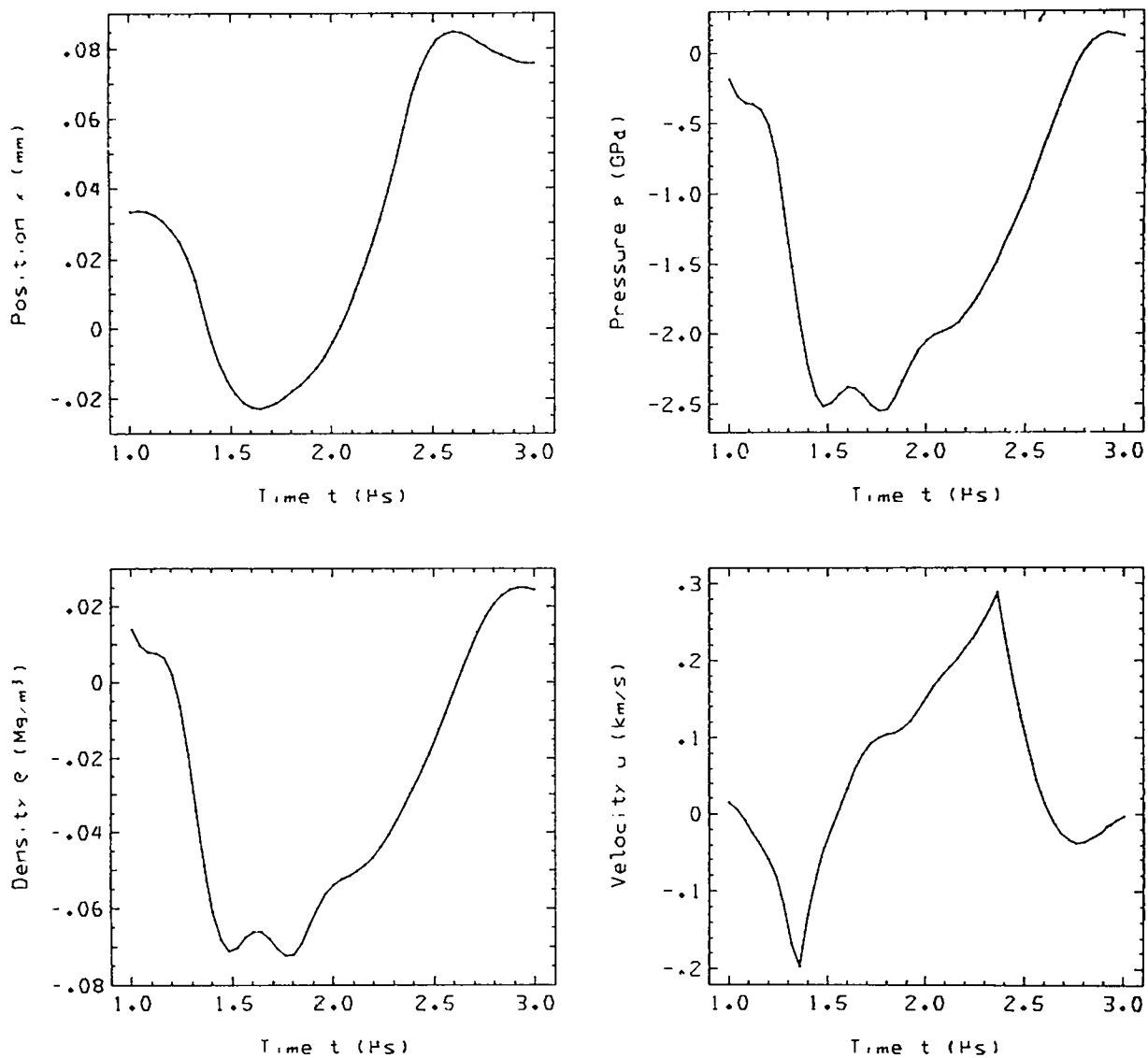


Fig. 3 (cont)

3. FREE-SURFACE DECEL. / DIFFERENCE / PARTICLES

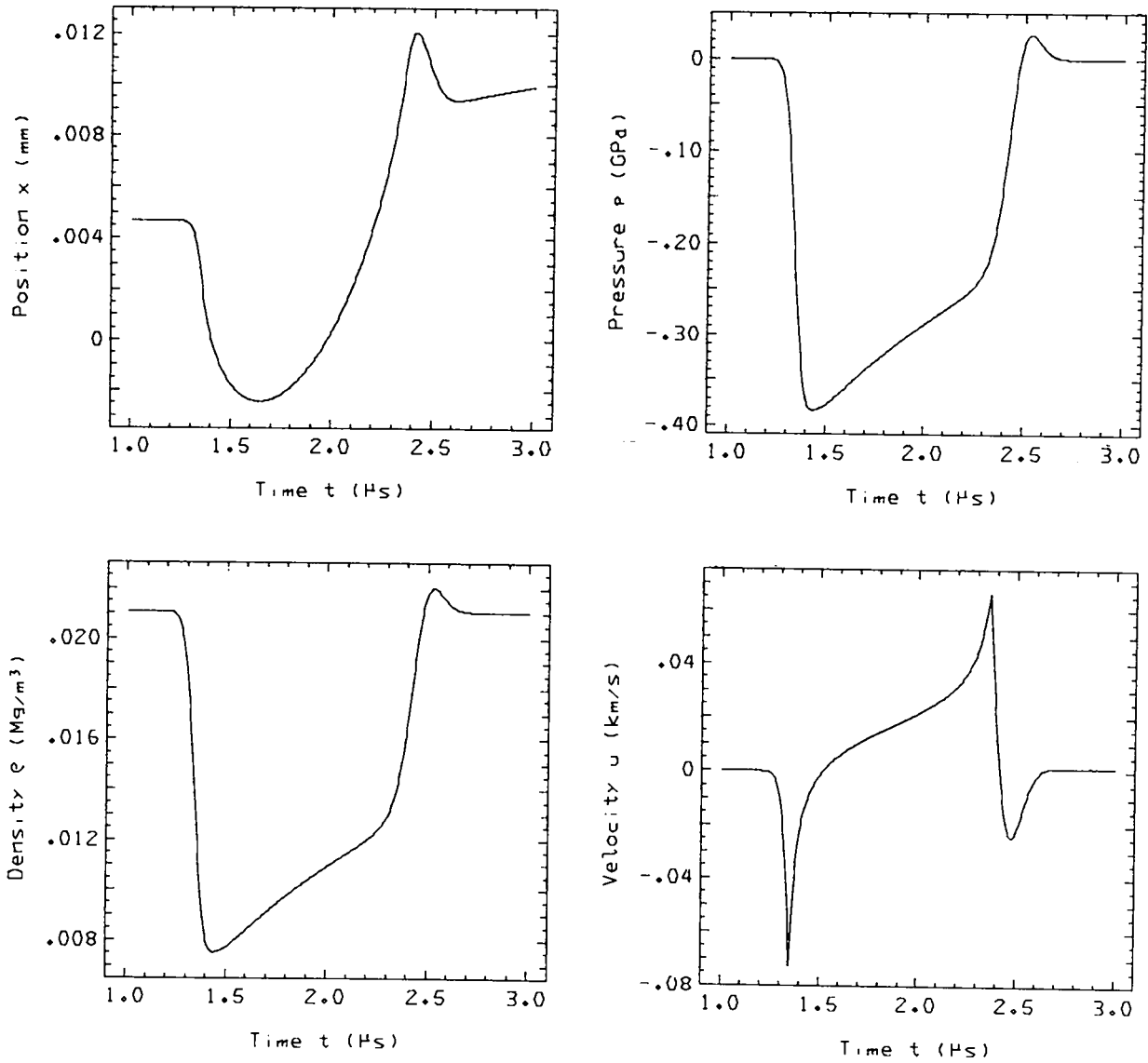


Fig. 3 (cont)

3. FREE-SURFACE DECEL. / DIFFERENCE / PARTICLE

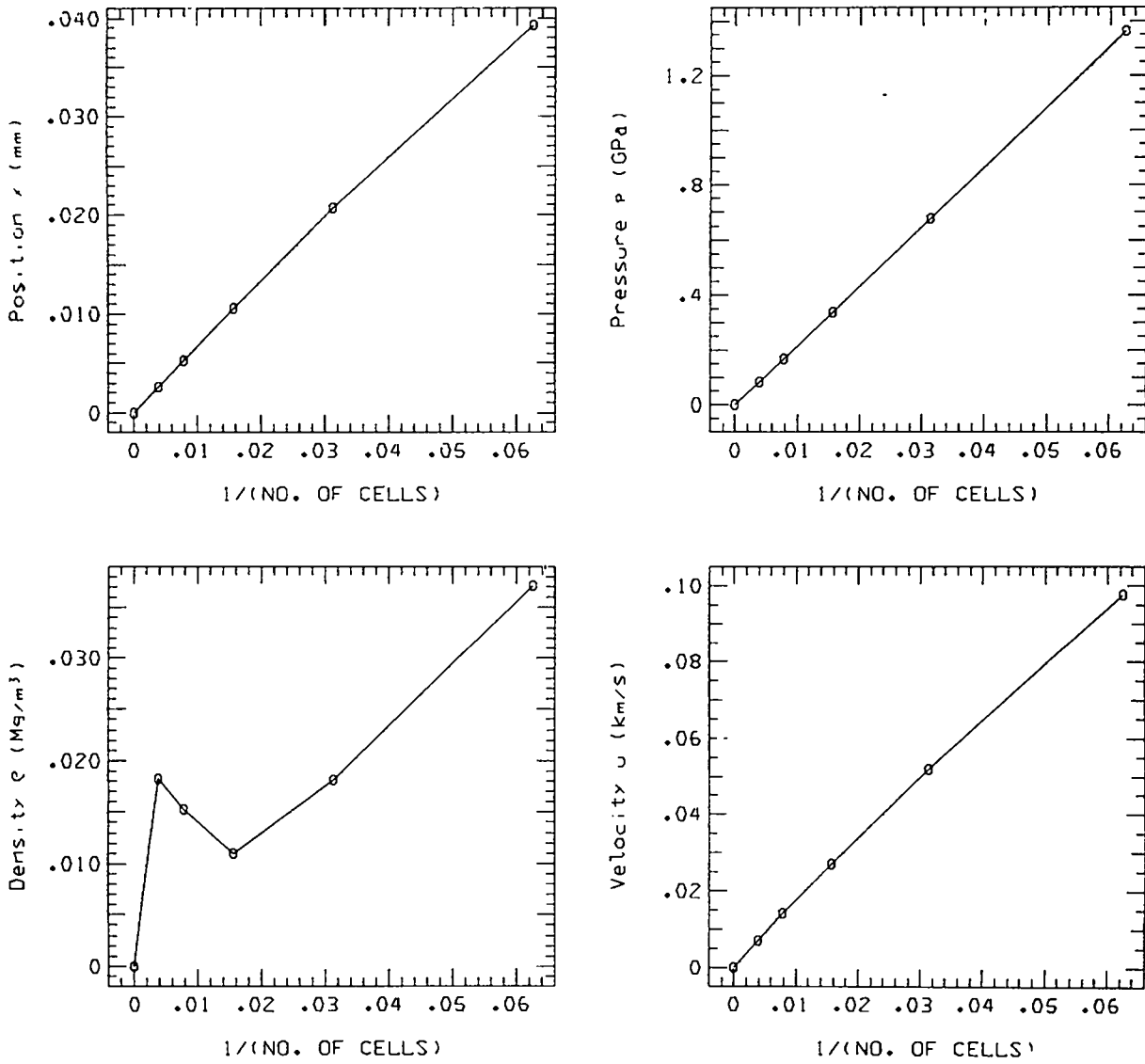


Fig. 3 (cont)

7. DECEL. SHOCK FROM HE / TIME = 2.0000E+00

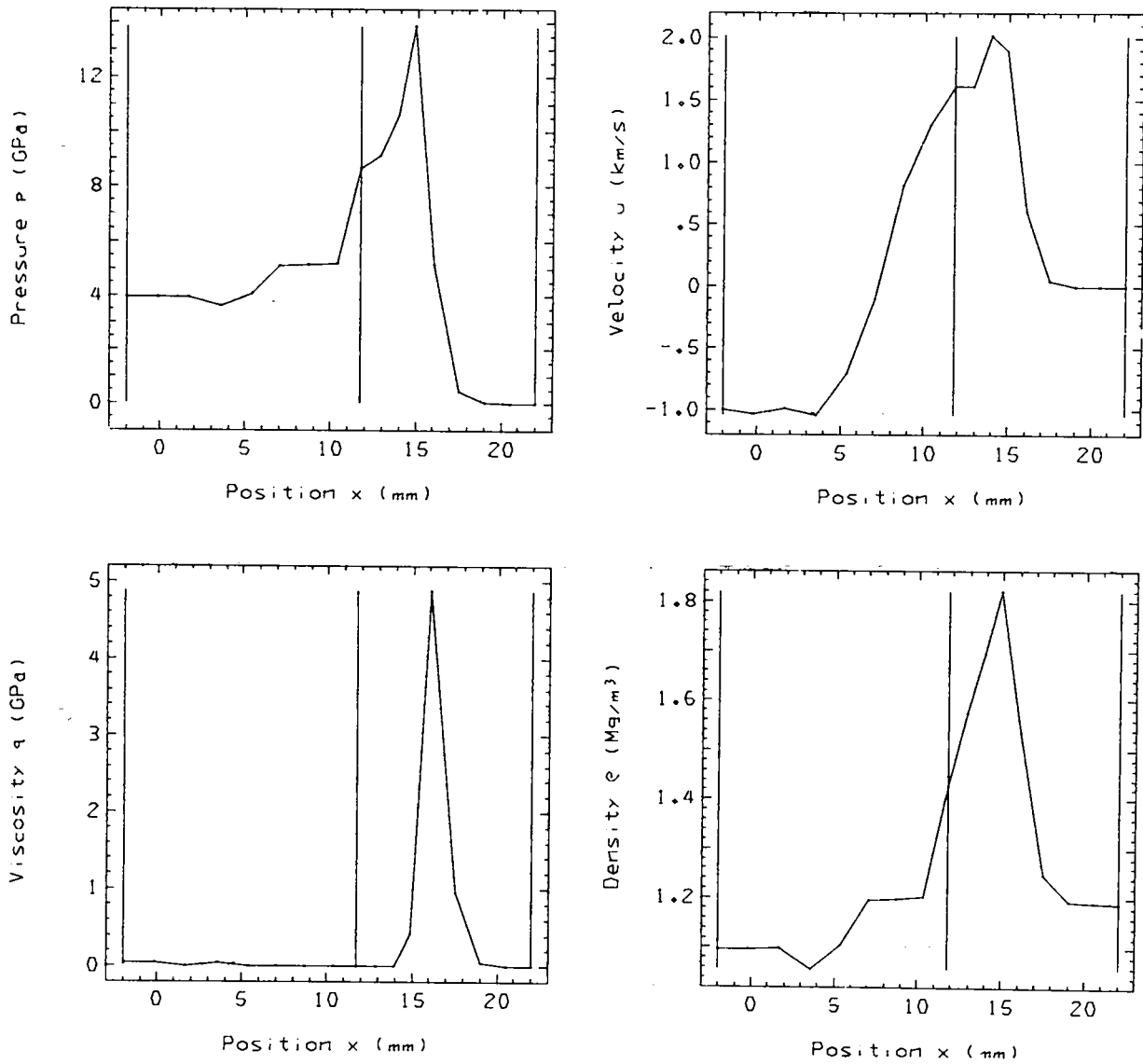


Fig. 4.
Problem 7. Decelerating shock from HE. Standard calculation.

7. DECEL. SHOCK FROM HE / TIME= 2.0000E+00

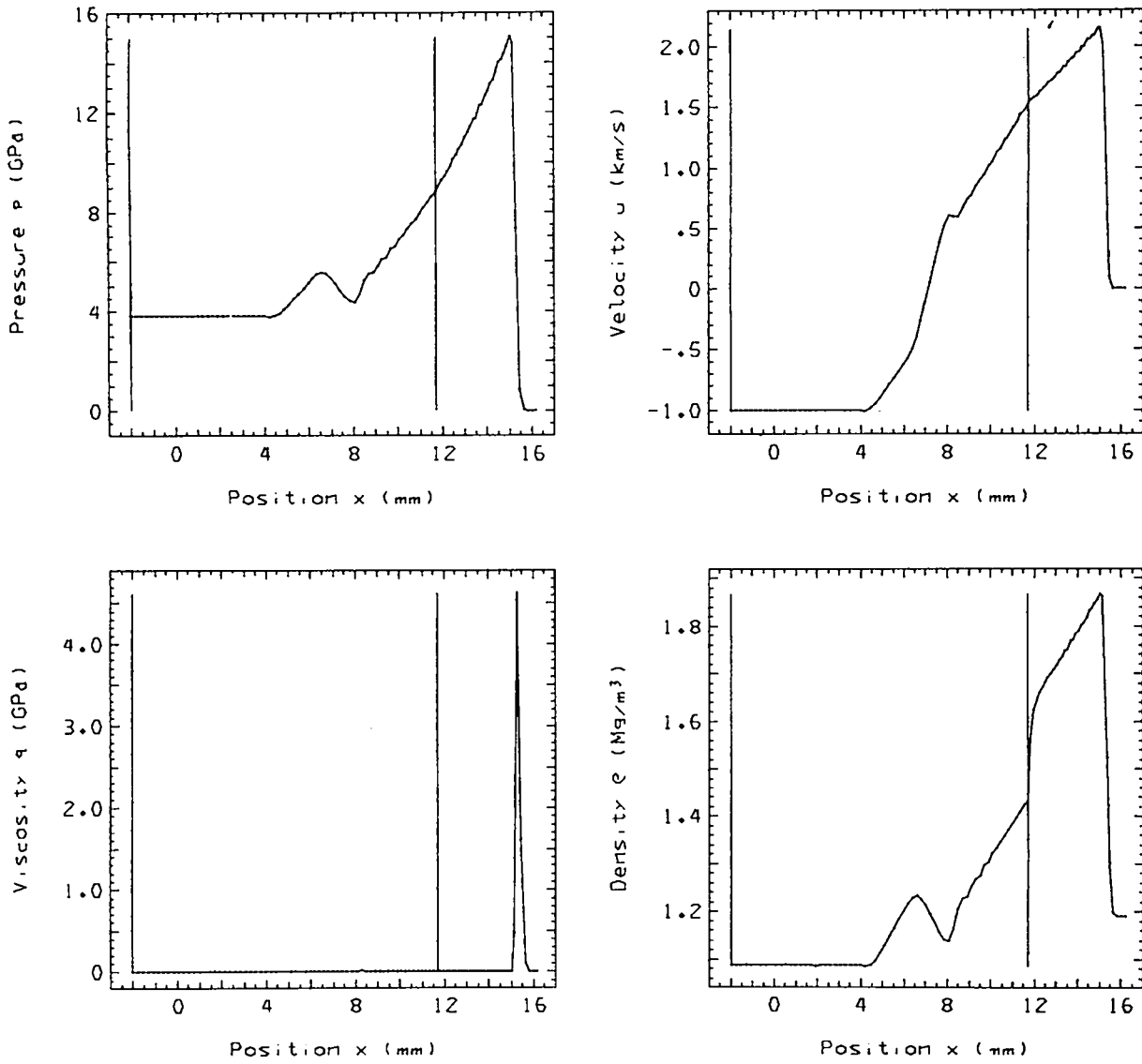


Fig. 4 (cont)

7. DECEL. SHOCK FROM HE / PARTICLES

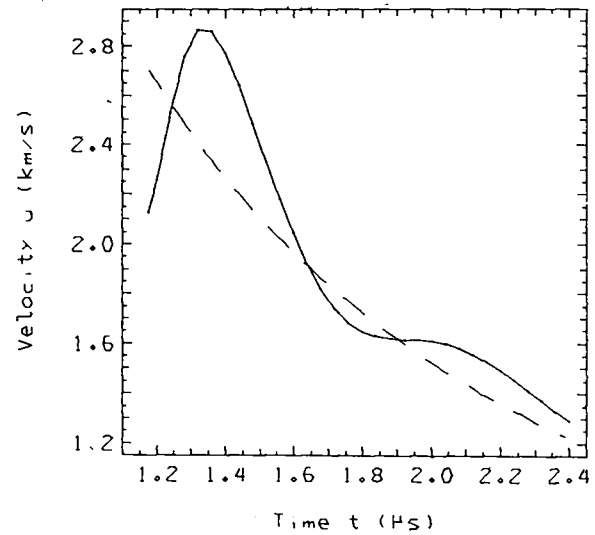
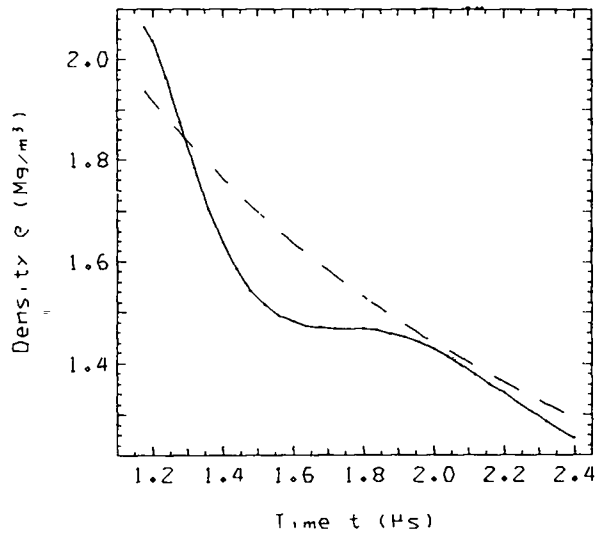
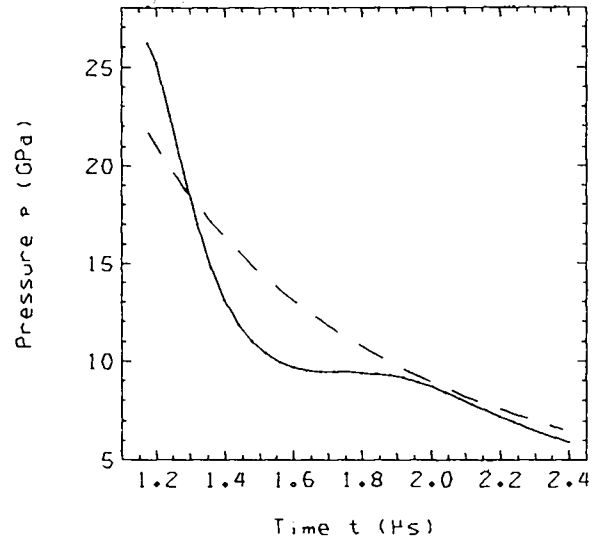
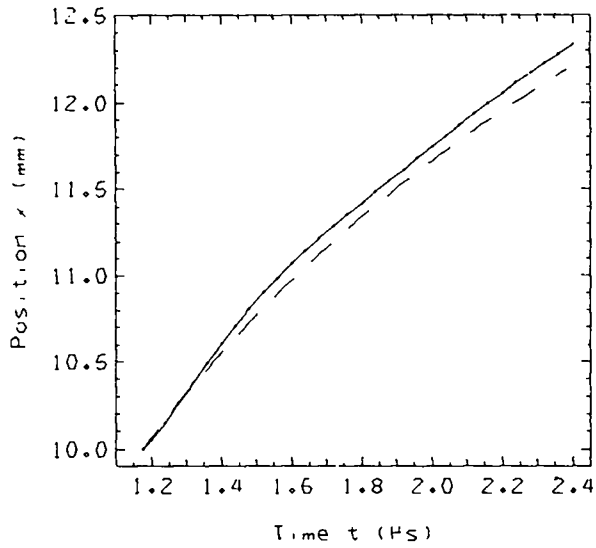


Fig. 4 (cont)

7. DECEL. SHOCK FROM HE / PARTICLES

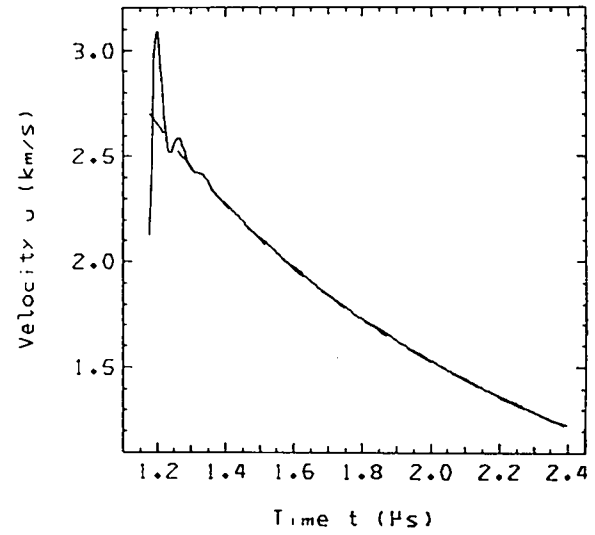
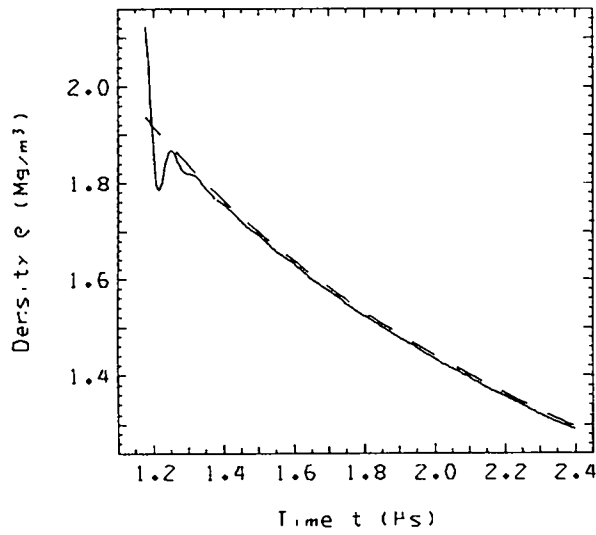
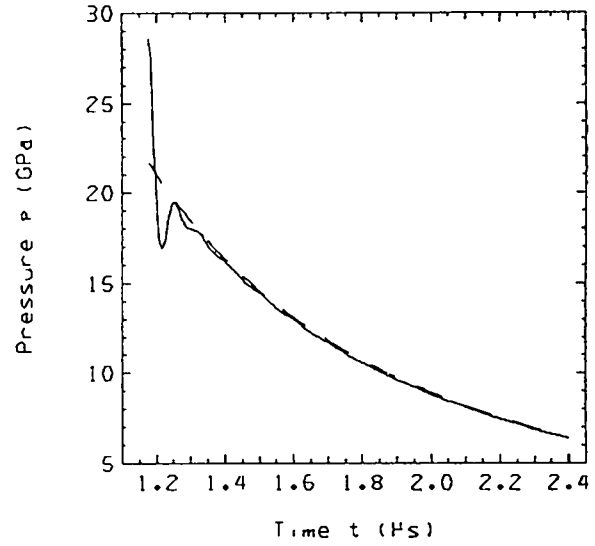
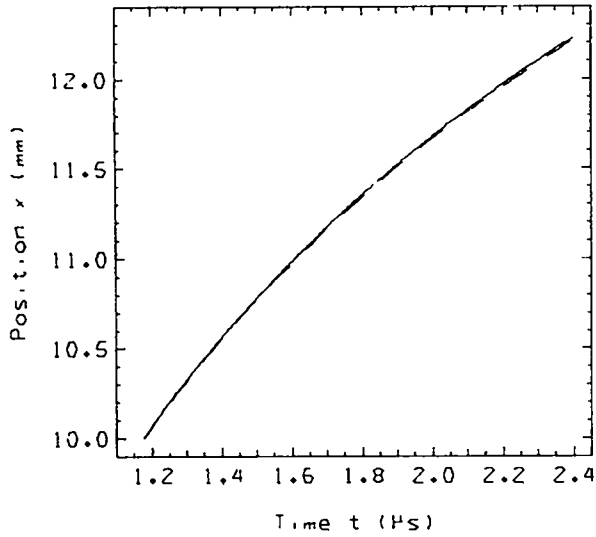


Fig. 4 (cont)

7. DECEL. SHOCK FROM HE / DIFFERENCE, TRUNCATED TIME / PARTICLES

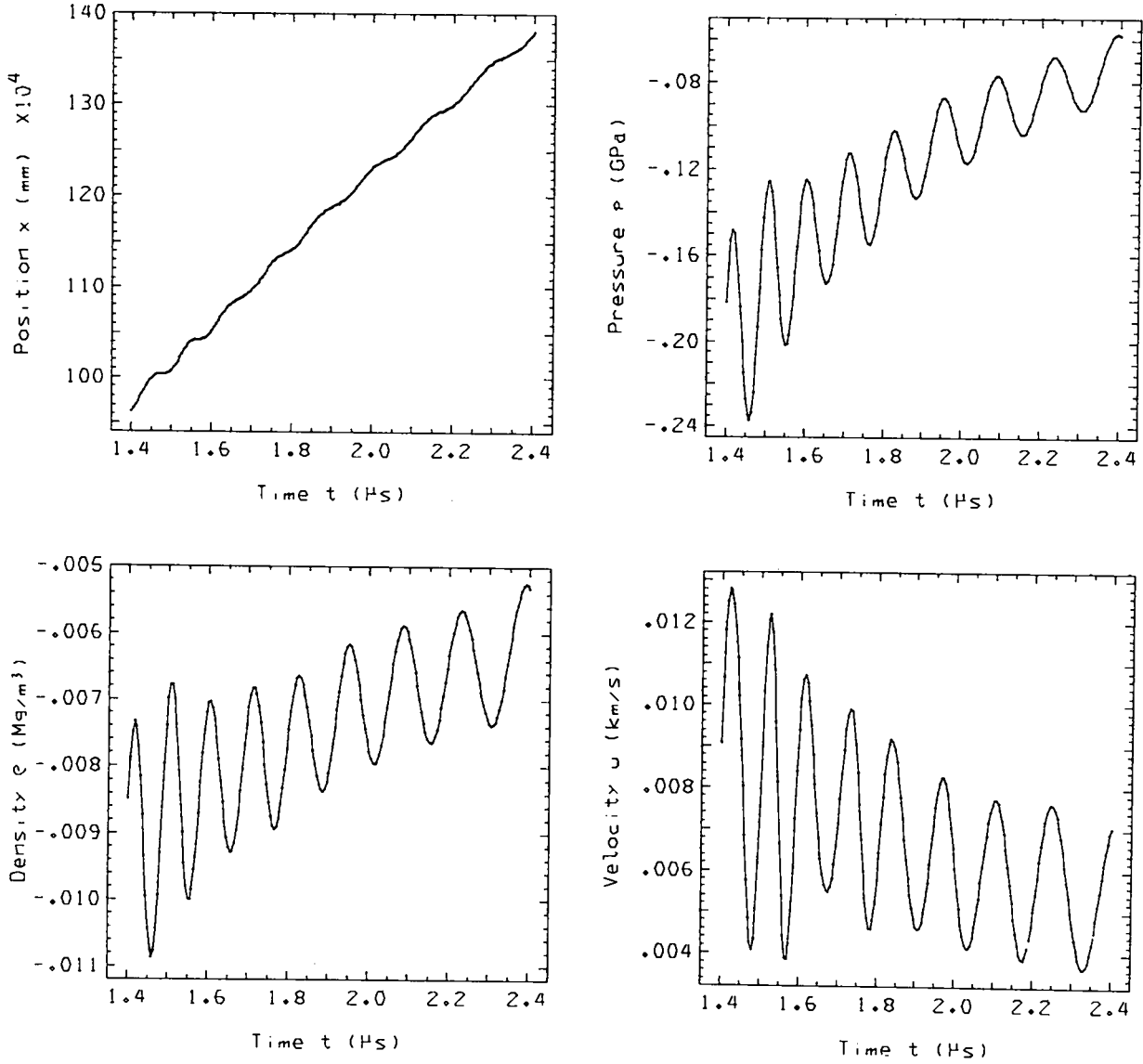
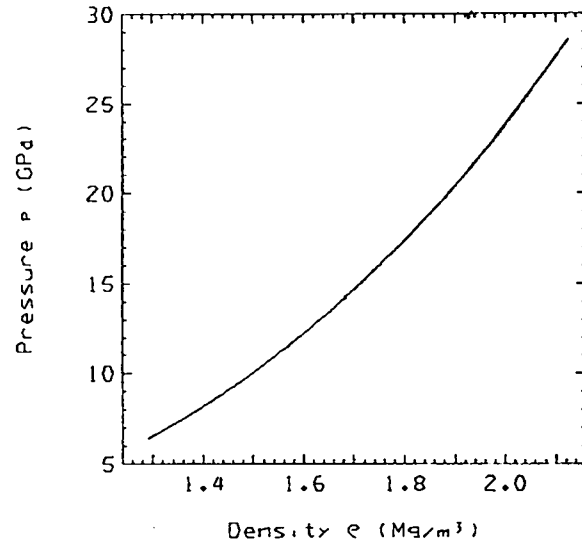
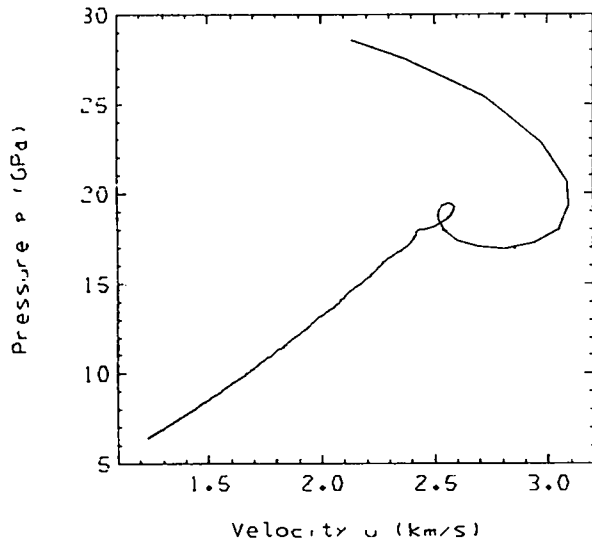


Fig. 4 (cont)

PAD3.3F6 - 75JUL14 RUN12 LAC2 *7. DECEL. SHOCK FROM HE*
IFICKETIGY. 11.538 SEC ON RUN, 155.907 SEC ON JOB

ERUN 4, 128 CELLS 07/21/75

7. DECEL. SHOCK FROM HE / PARTICLES



PAD3.3F6 - 75JUL14 RUN13 LAC2 *7. DECEL. SHOCK FROM HE*
IFICKETIGY. 3.836 SEC ON RUN, 168.065 SEC ON JOB

ERUN 4, 128 CELLS 07/21/75

7. DECEL. SHOCK FROM HE / DIFFERENCE, TRUNCATED TIME / PARTICLES

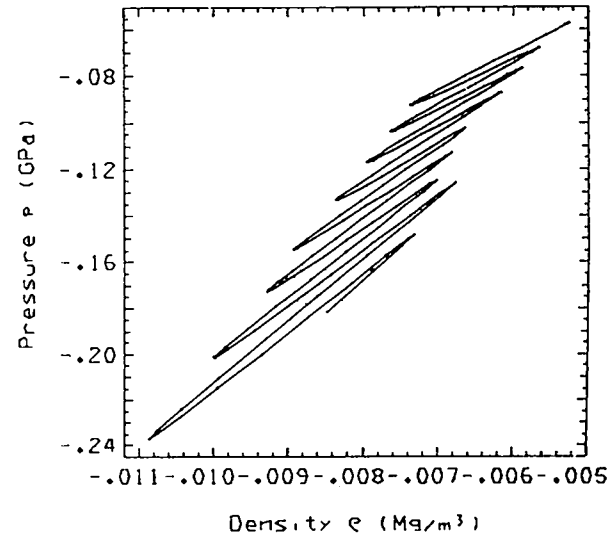
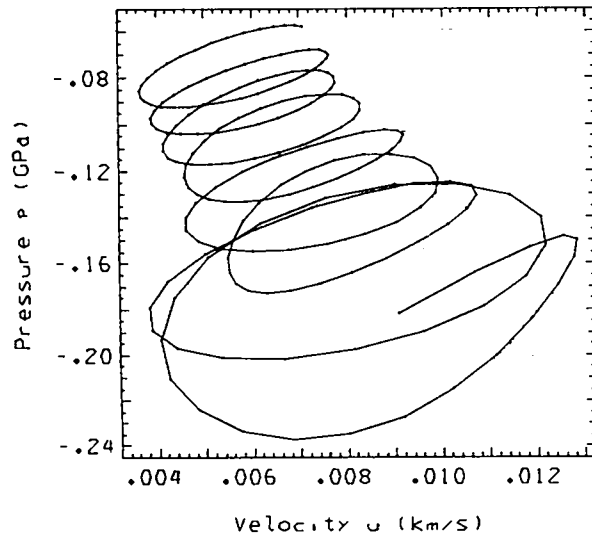


Fig. 4 (cont)

7. DECEL. SHOCK FROM HE / LEAD SHOCK

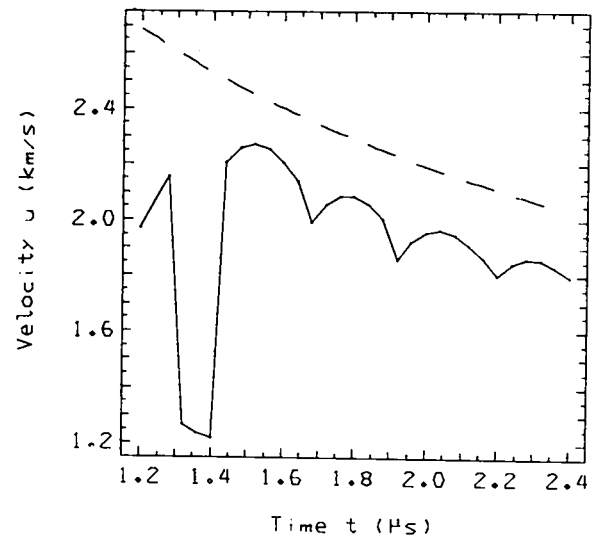
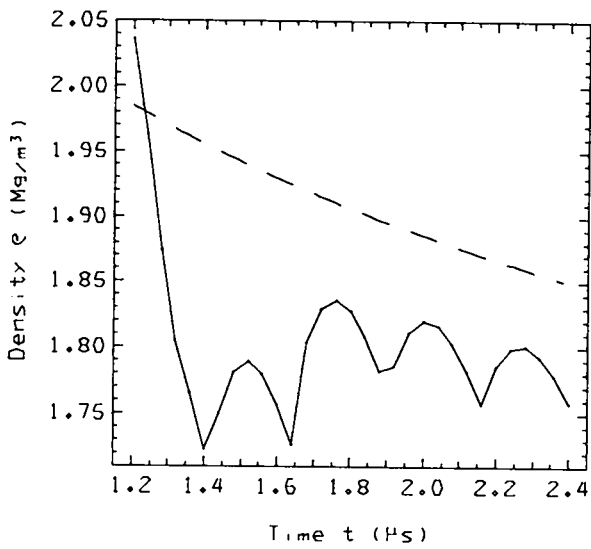
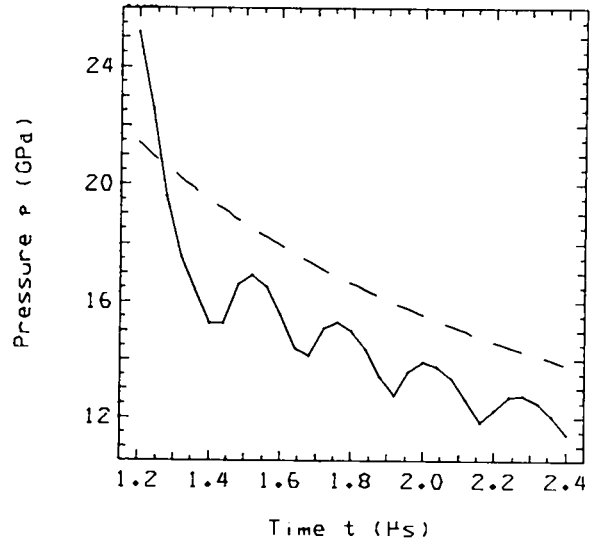
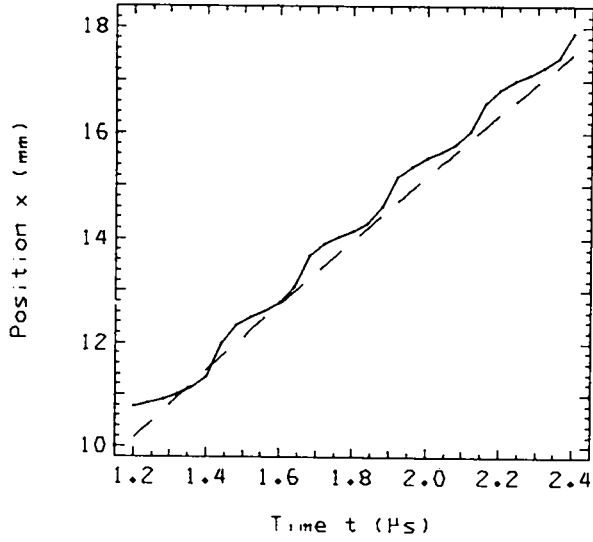


Fig. 4 (cont)

7. DECEL. SHOCK FROM HE / LEAD SHOCK

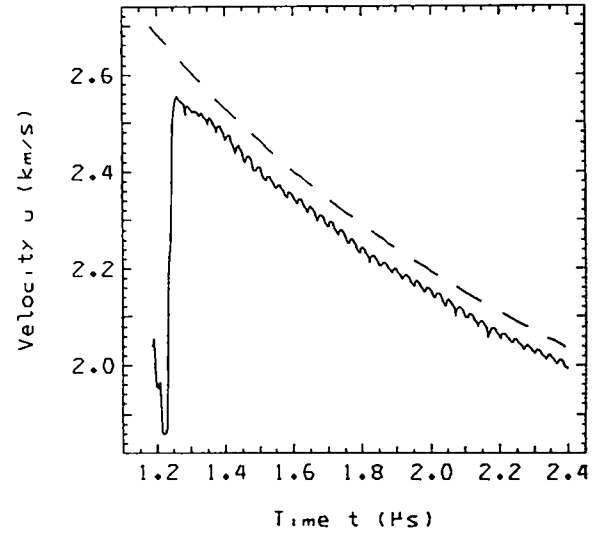
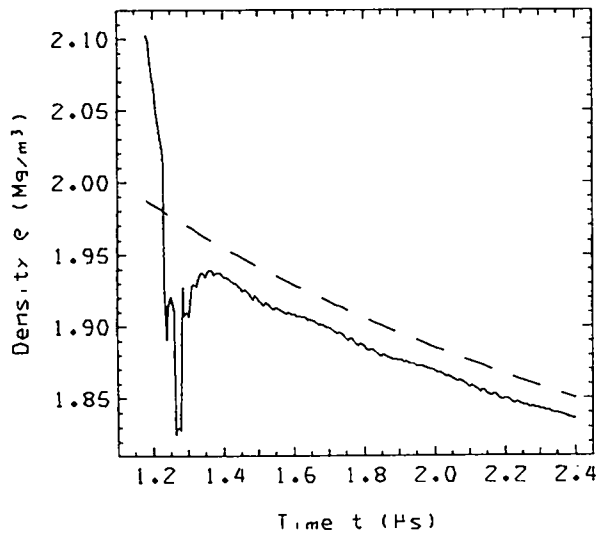
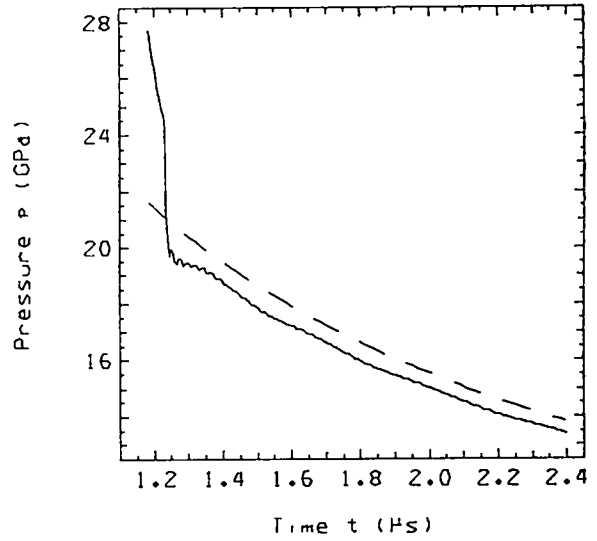
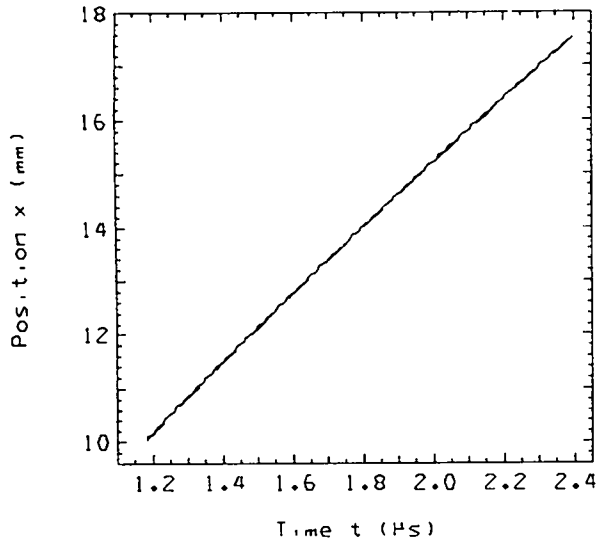


Fig. 4 (cont)

7. DECEL. SHOCK FROM HE / DIFFERENCE, TRUNCATED TIME / PARTICLE

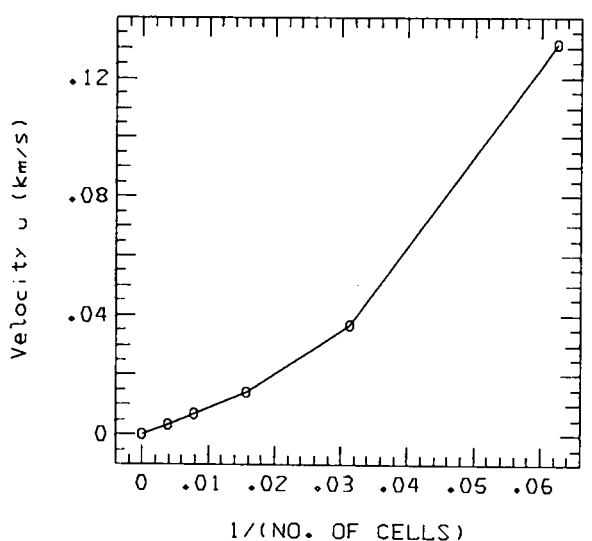
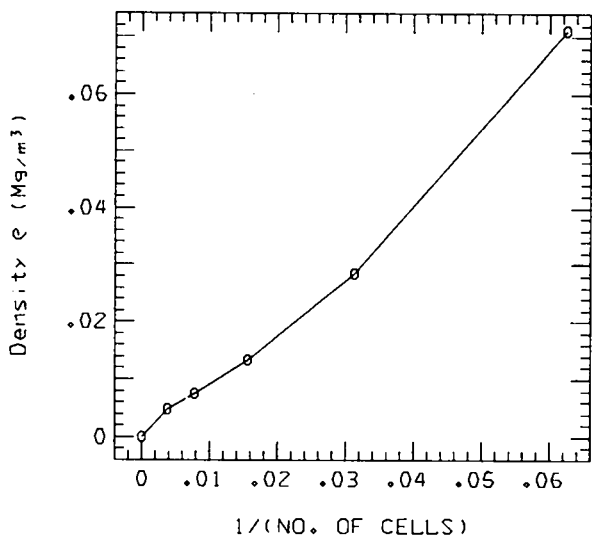
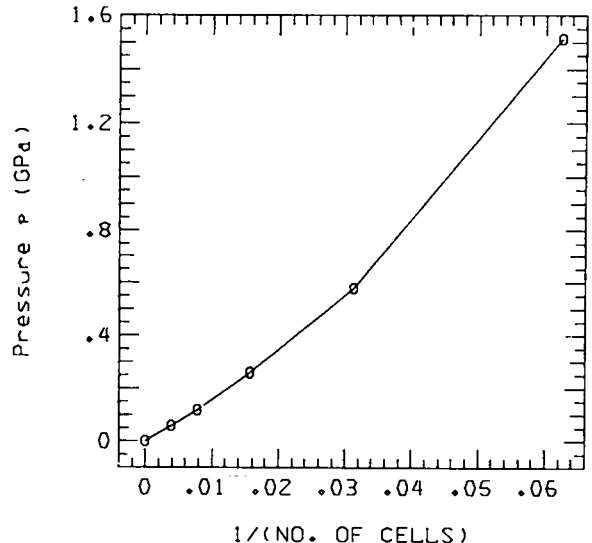
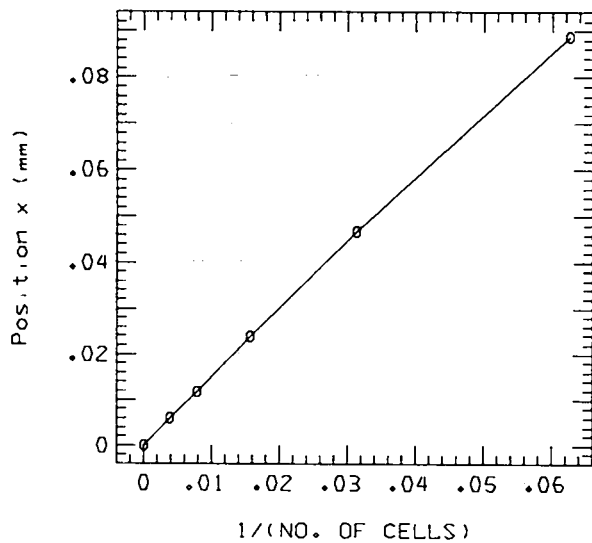


Fig. 4 (cont)

7. DECEL. SHOCK FROM HE / DIFFERENCE, TRUNCATED TIME / SHOCK

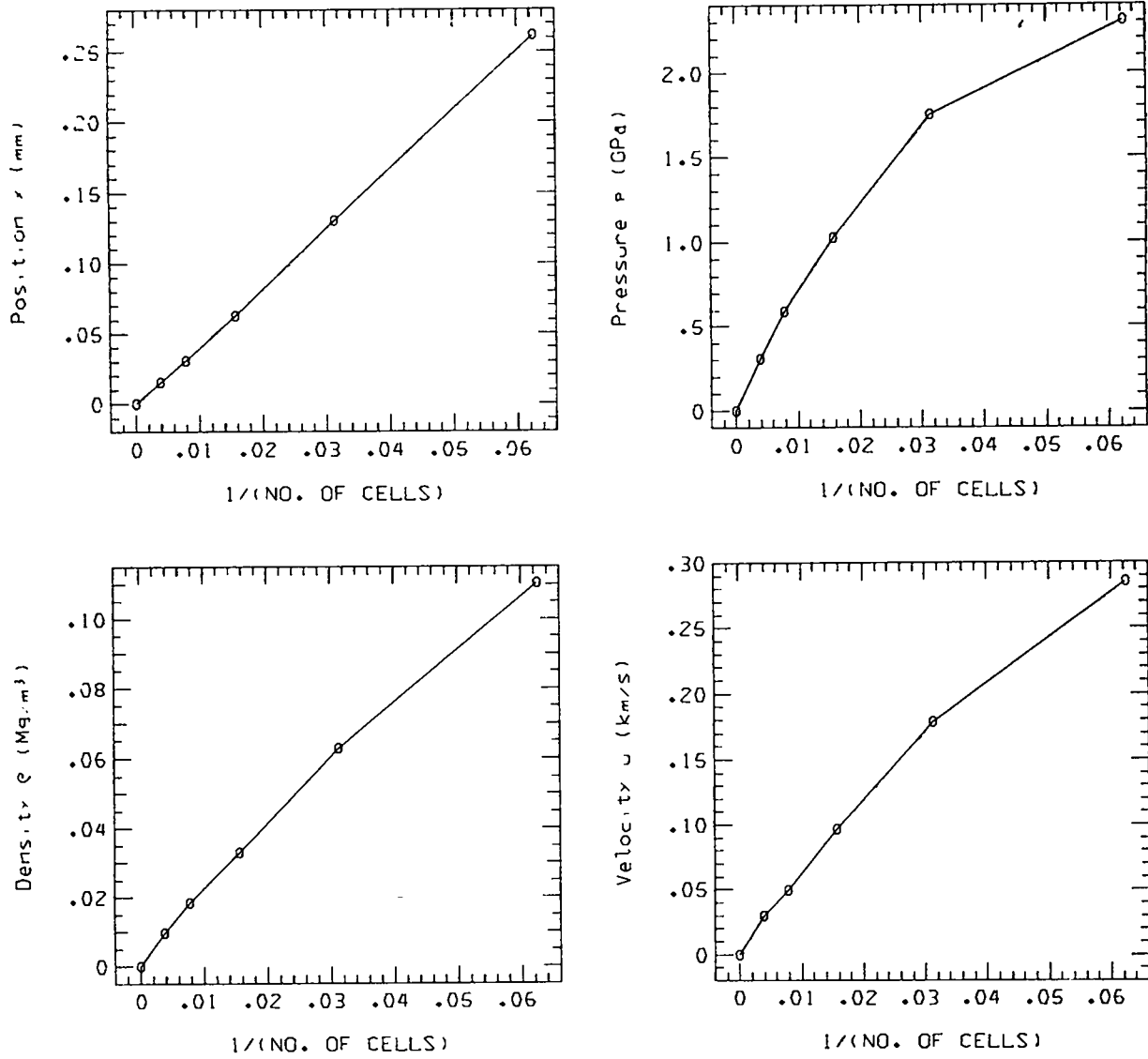


Fig. 4 (cont)

8. REVERBERATION / TIME= 8.5000E+00

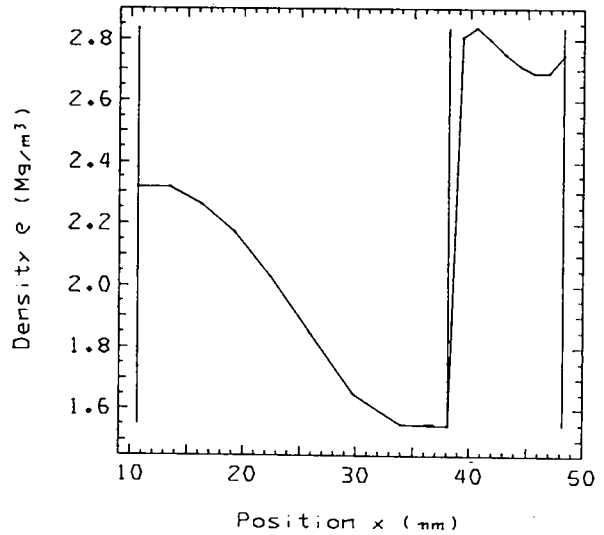
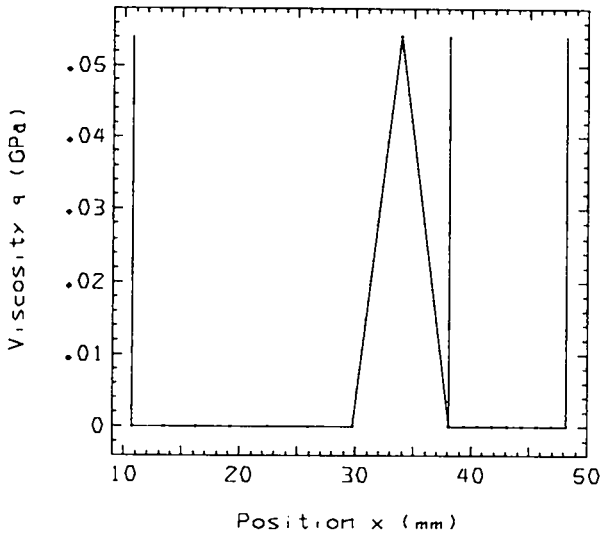
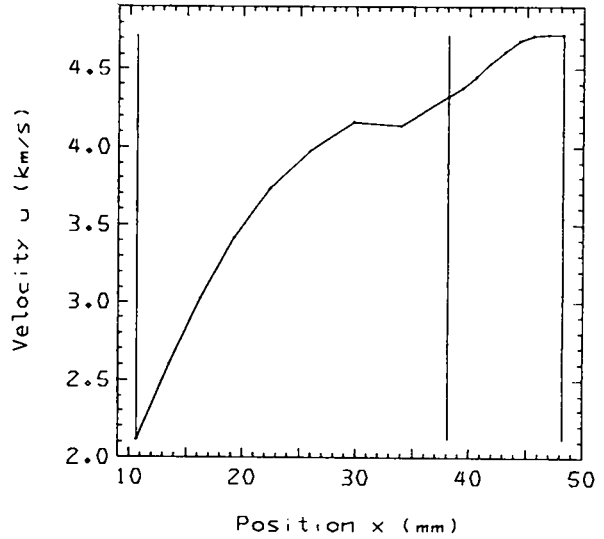
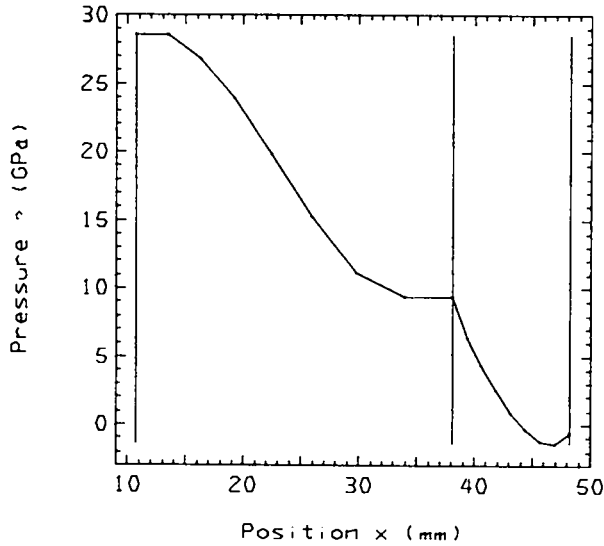


Fig. 5.
Problem 8. Reverberation. Standard calculation.

8. REVERBERATION / TIME= 8.5000E+00

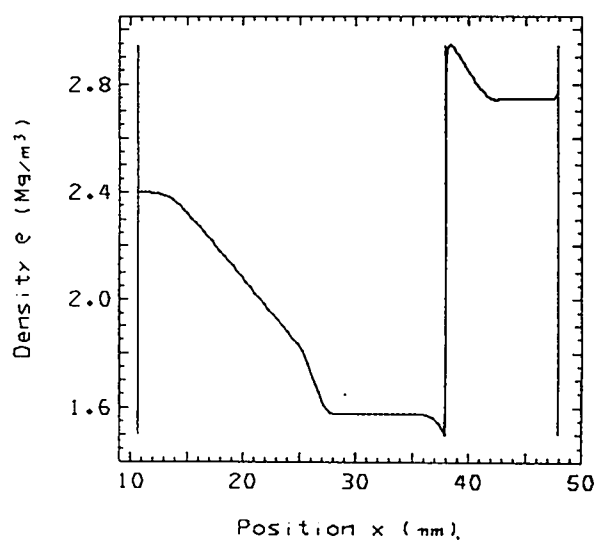
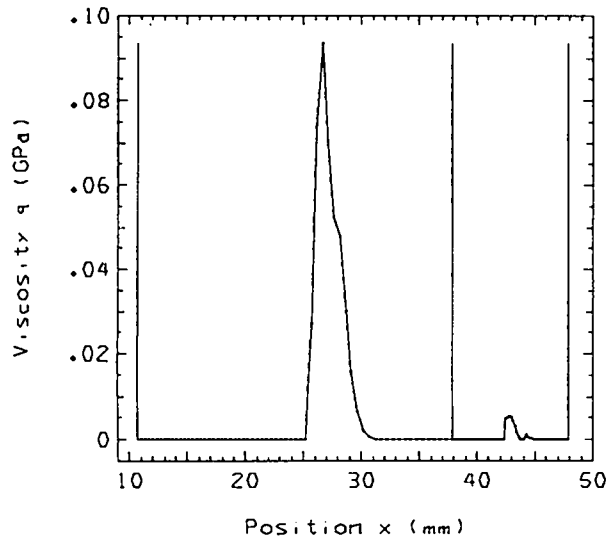
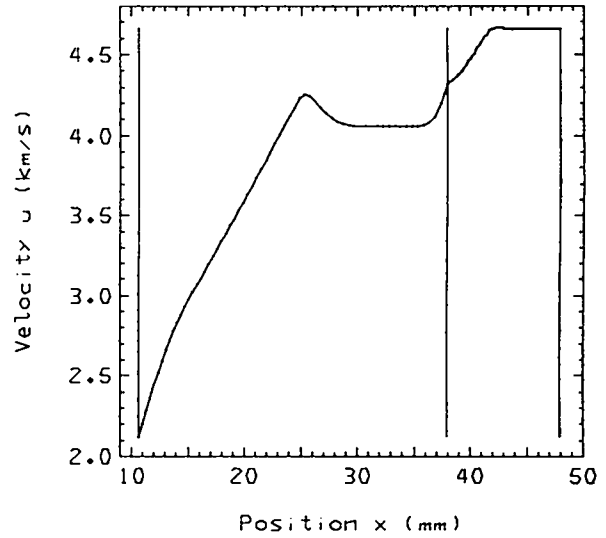
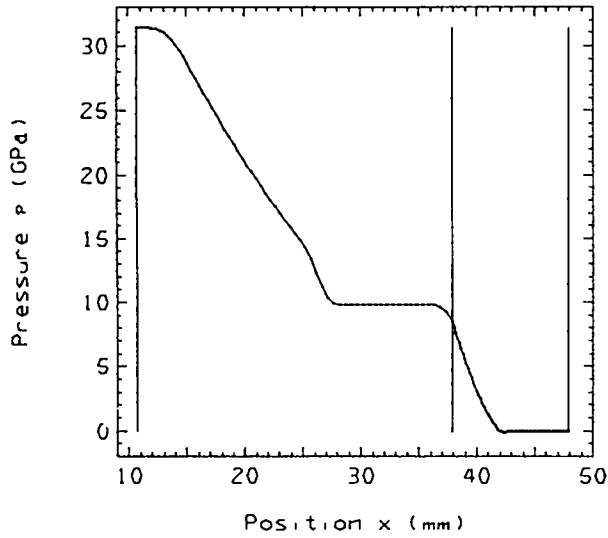


Fig. 5 (cont)

8. REVERBERATION / PARTICLES

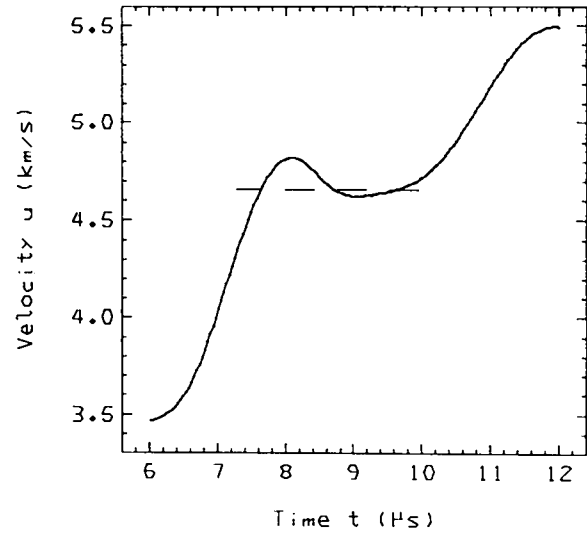
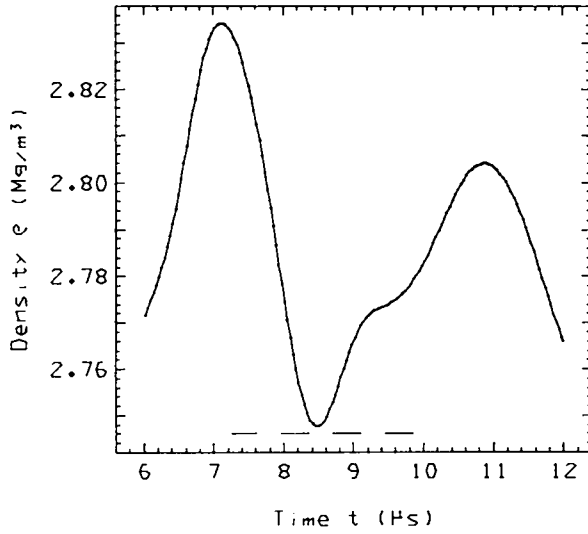
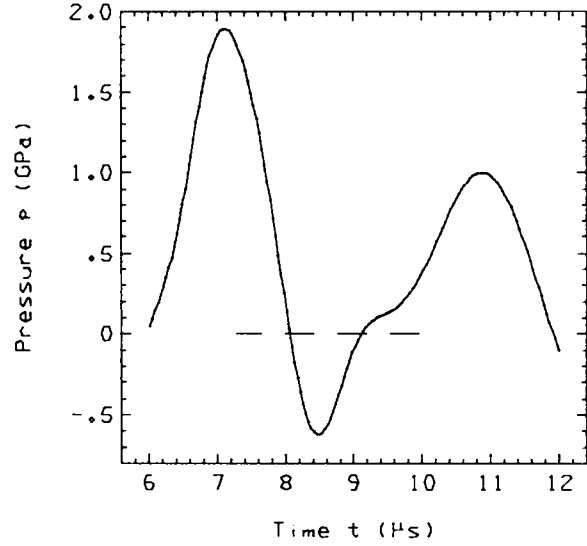
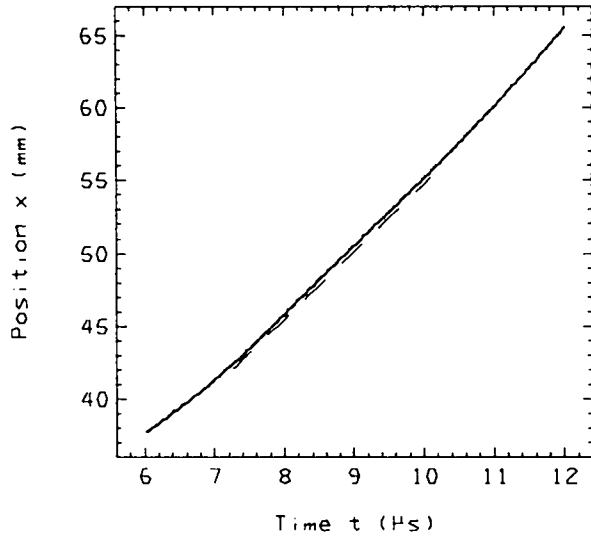


Fig. 5 (cont)

8. REVERBERATION / PARTICLES

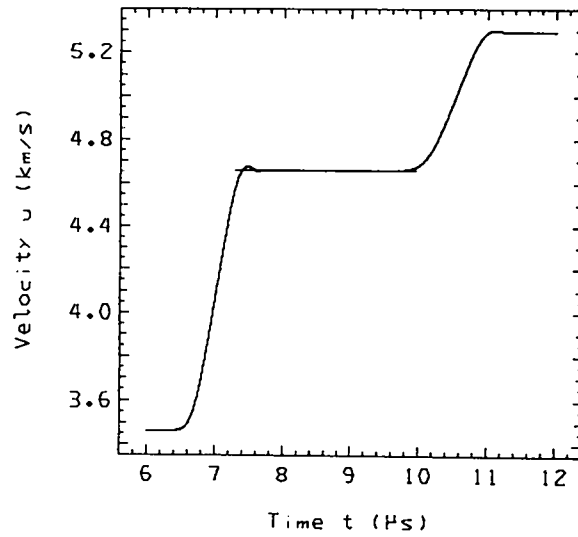
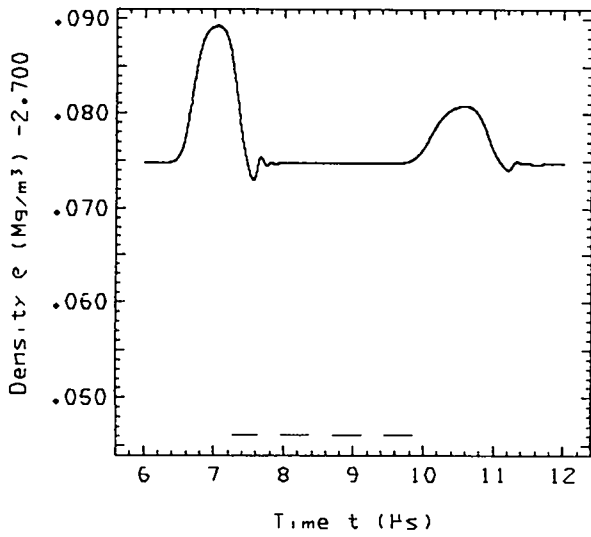
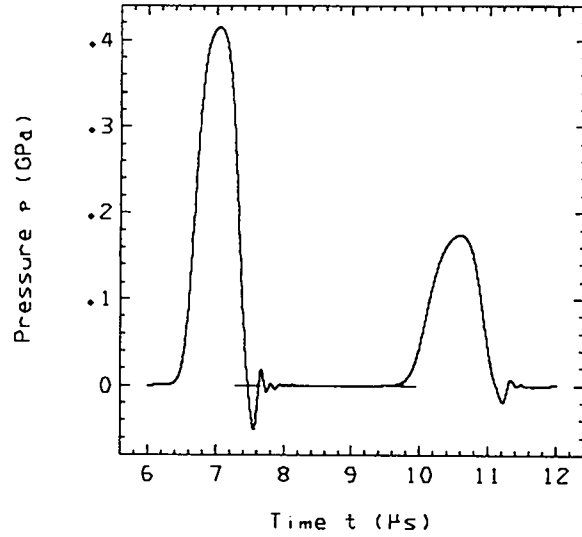
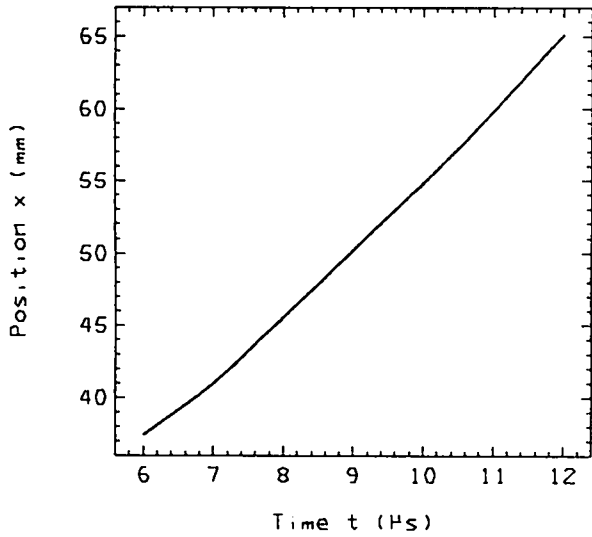


Fig. 5 (cont)

8. REVERBERATION / PARTICLES

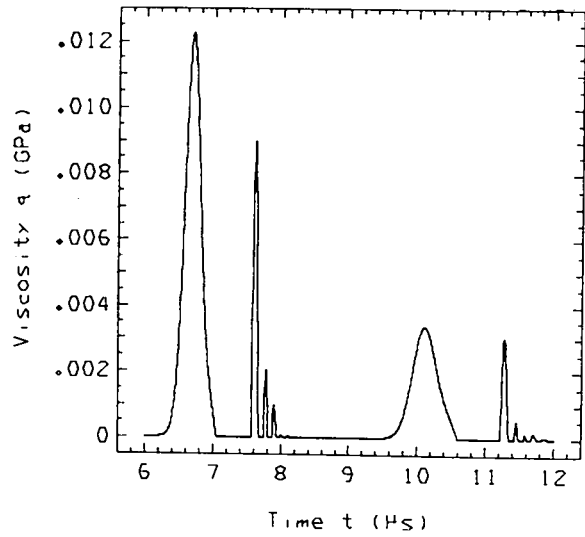
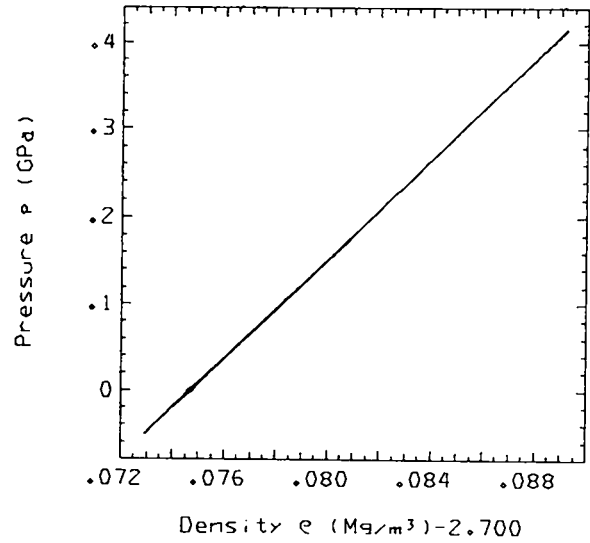
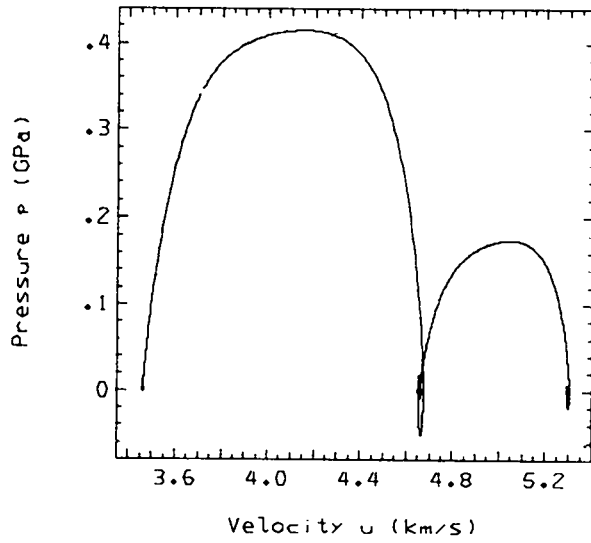


Fig. 5 (cont)

8. REVERBERATION / DIFFERENCE, TRUNCATED TIME / PARTICLES

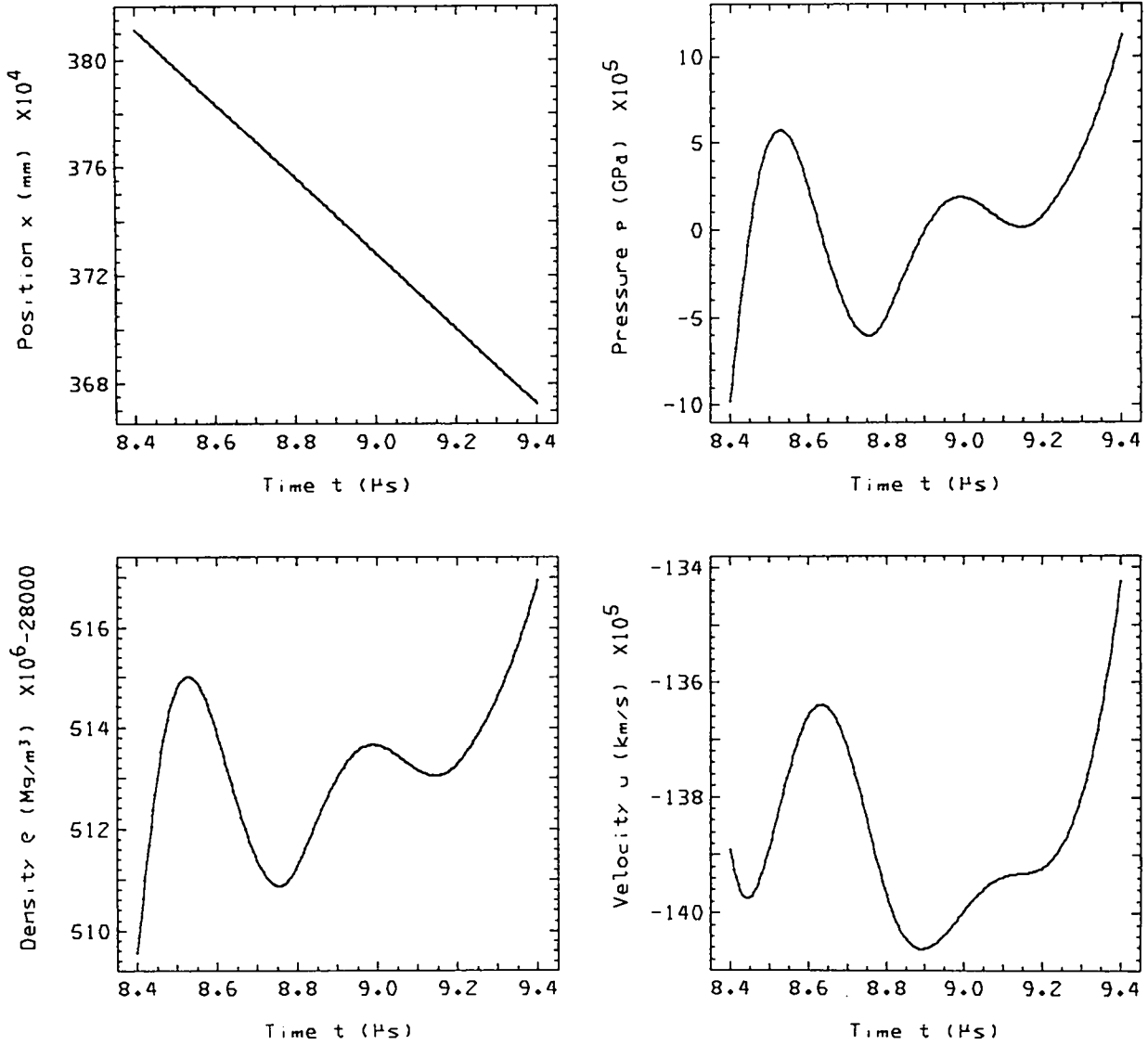


Fig. 5 (cont)

8. REVERBERATION / DIFFERENCE, TRUNCATED TIME / PARTICLES

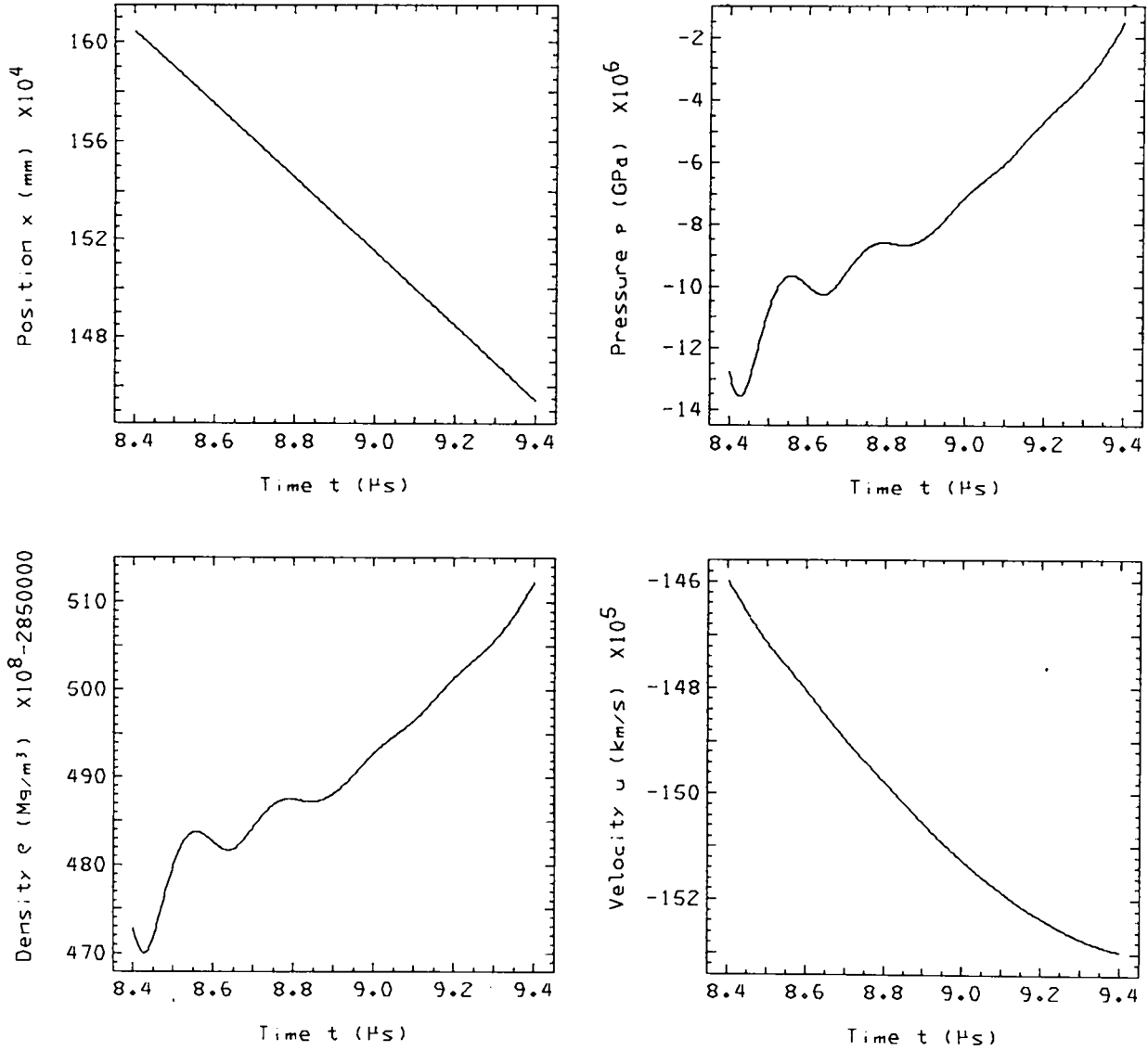


Fig. 5 (cont)

8. REVERBERATION / DIFFERENCE. TRUNCATED TIME / PARTICLES

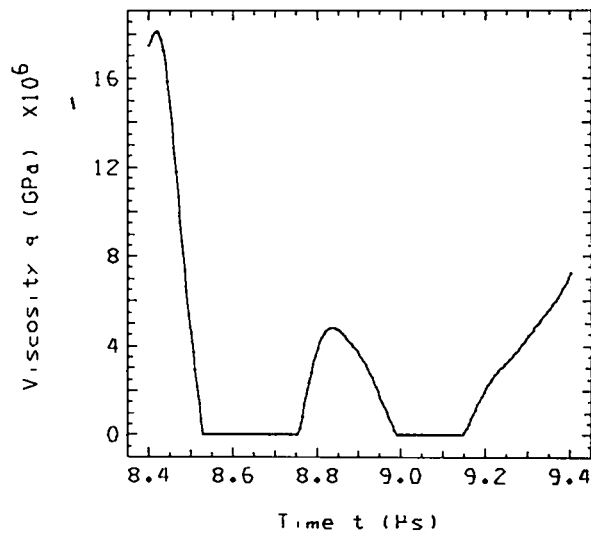
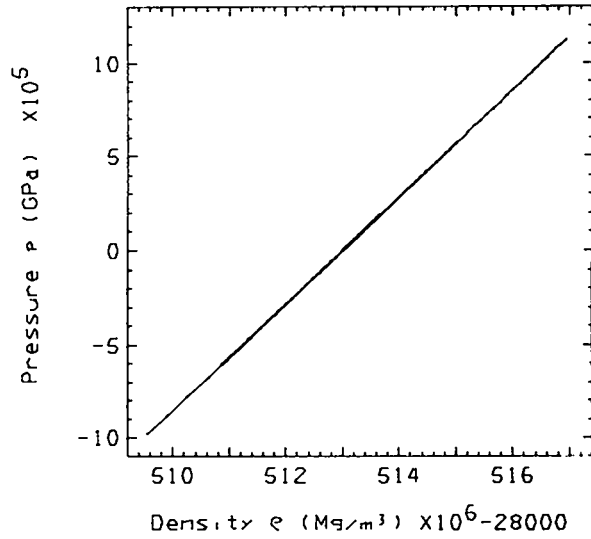
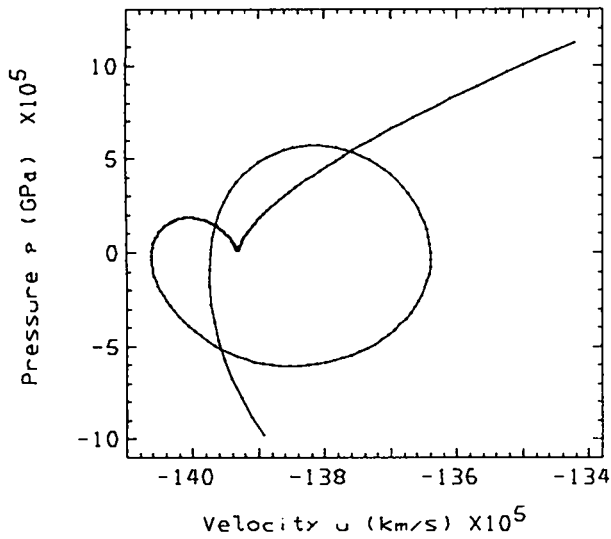


Fig. 5 (cont)

8. REVERBERATION / DIFFERENCE, TRUNCATED TIME / PARTICLE

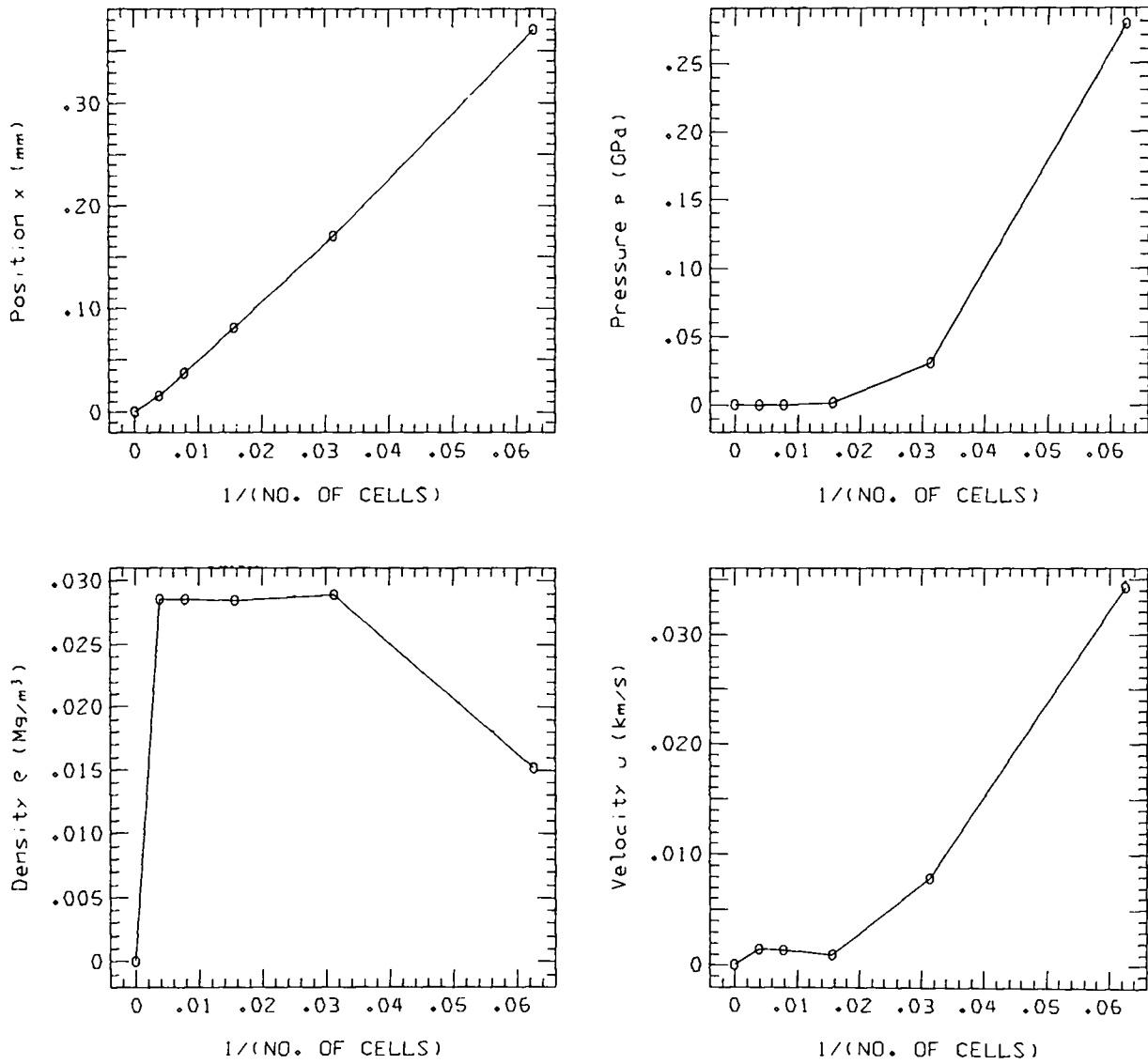


Fig. 5 (cont)

9. BLAST WAVE / TIME= 1.5000E+00

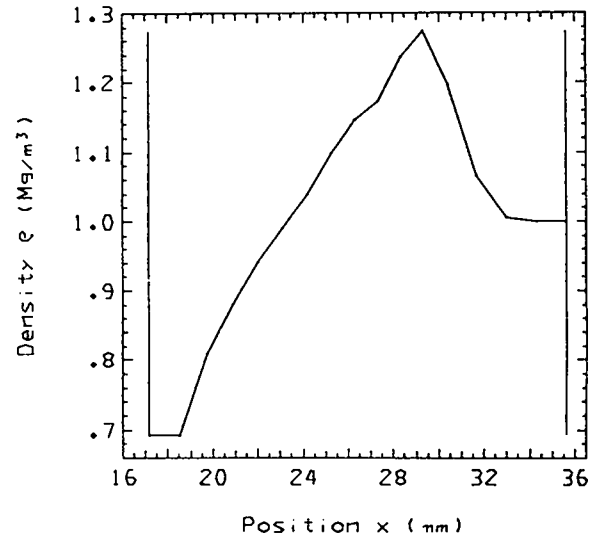
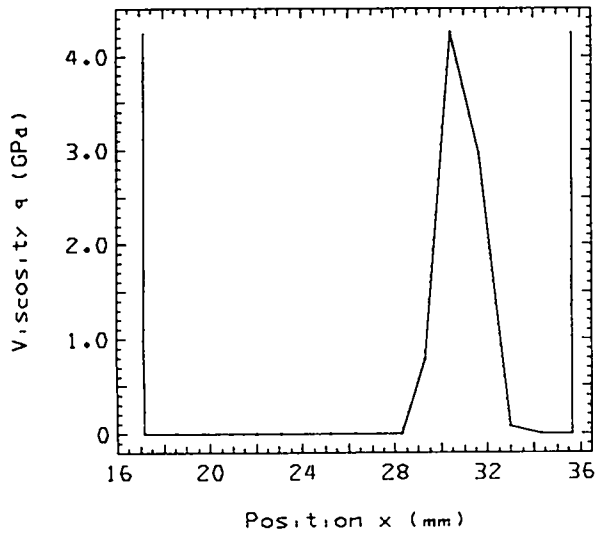
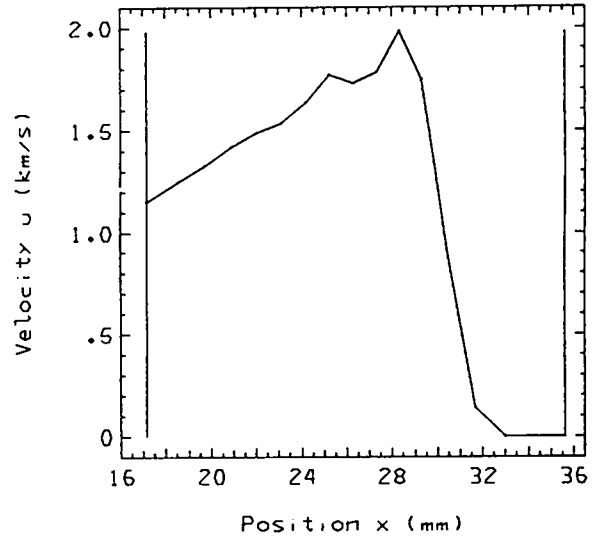
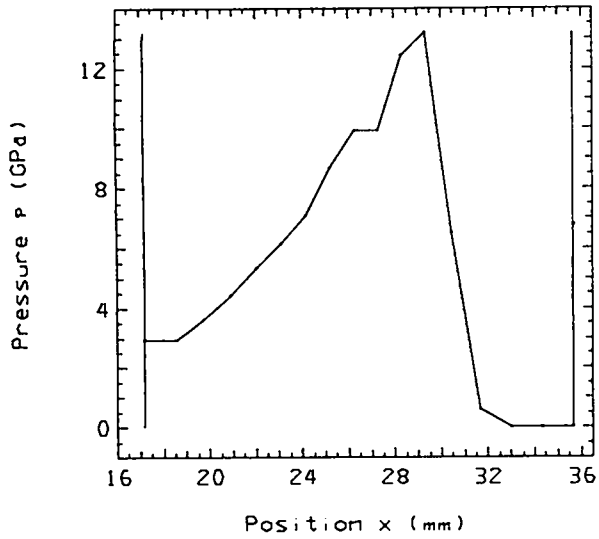


Fig. 6.
Problem 9. Blast wave. Standard calculation.

9. BLAST WAVE / TIME = 1.5000E+00

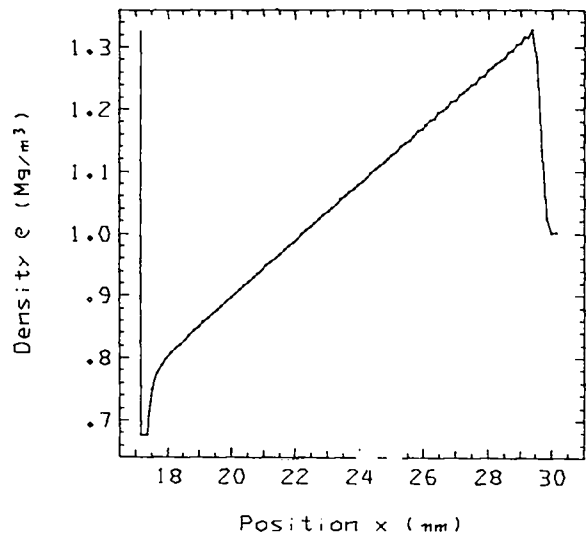
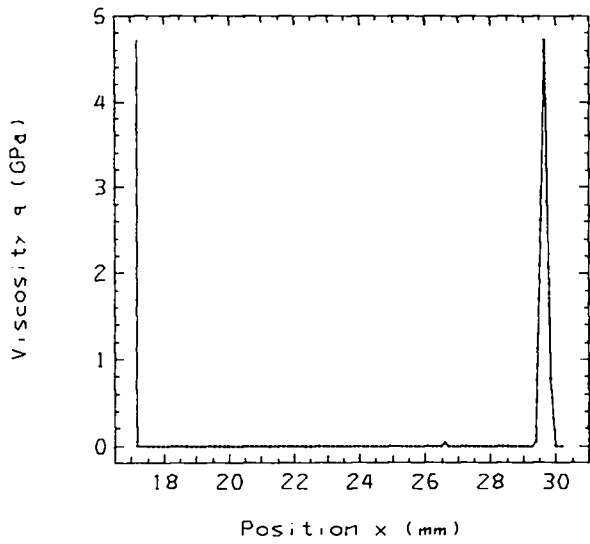
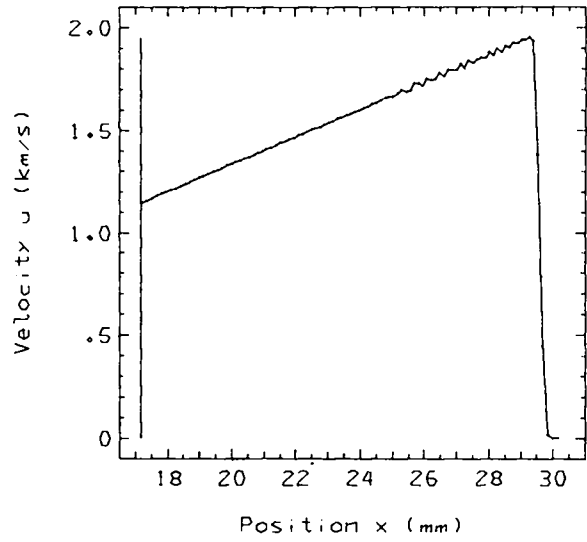
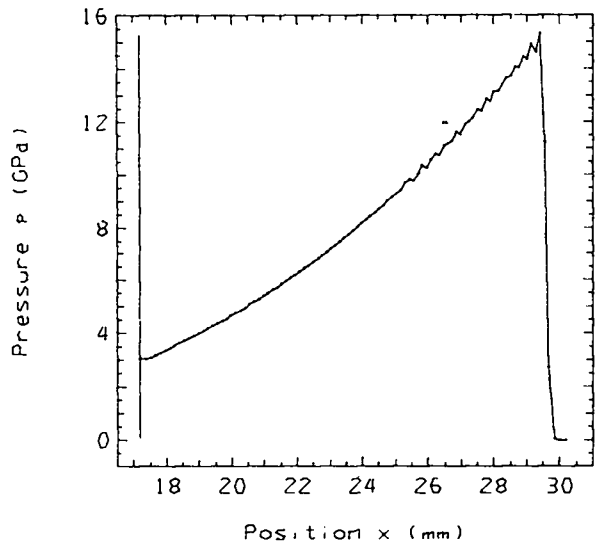


Fig. 6 (cont)

9. BLAST WAVE / PARTICLES

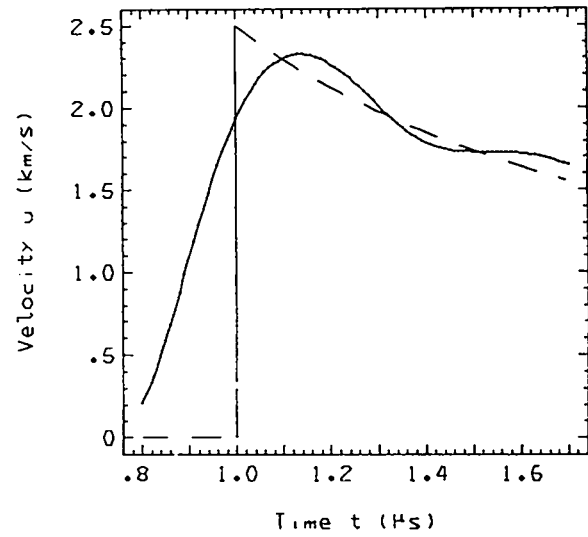
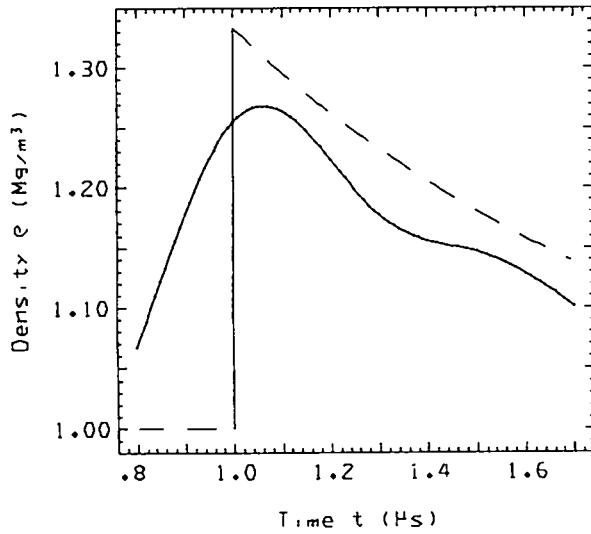
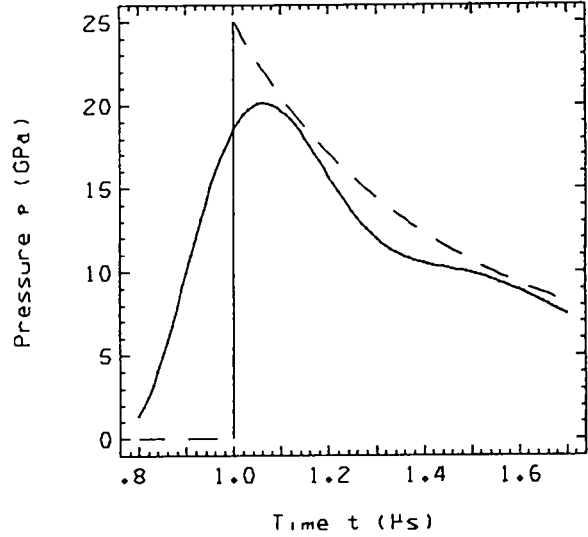
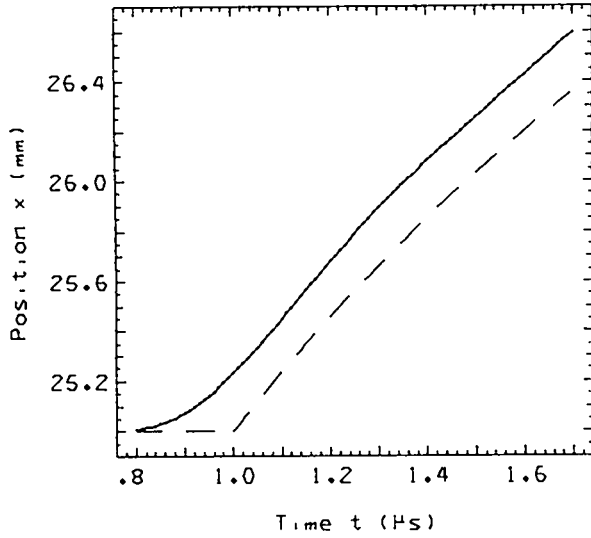


Fig. 6 (cont)

9. BLAST WAVE / PARTICLES

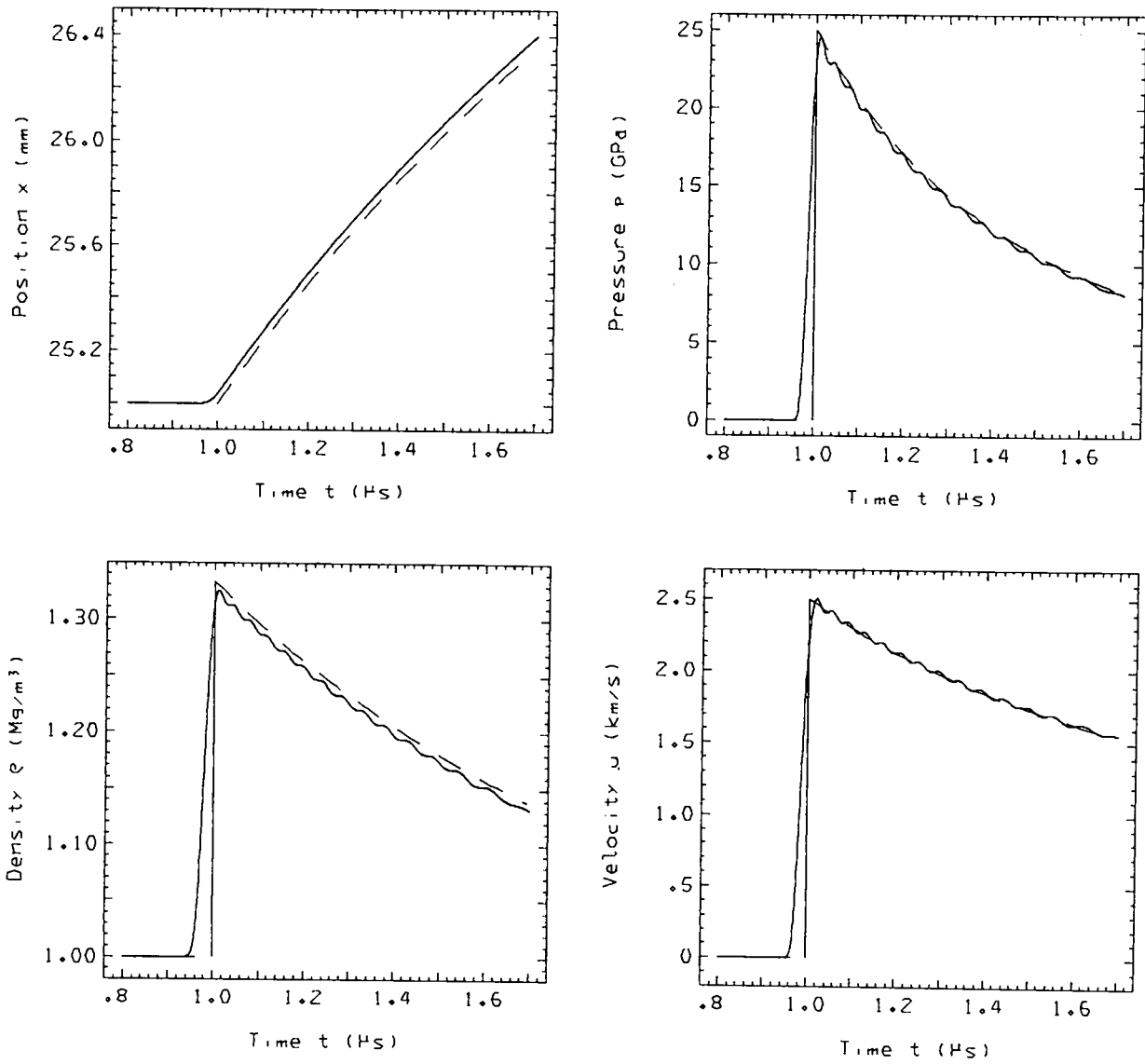


Fig. 6 (cont)

PAD3.3F6 - 75JUL14 RUN18 LAC2 *9. BLAST WAVE*
TFICKET1GY. 9.139 SEC ON RUN, 262.479 SEC ON JOB

ERUN 4, 128 CELLS 07/21/75
9. BLAST WAVE / PARTICLES

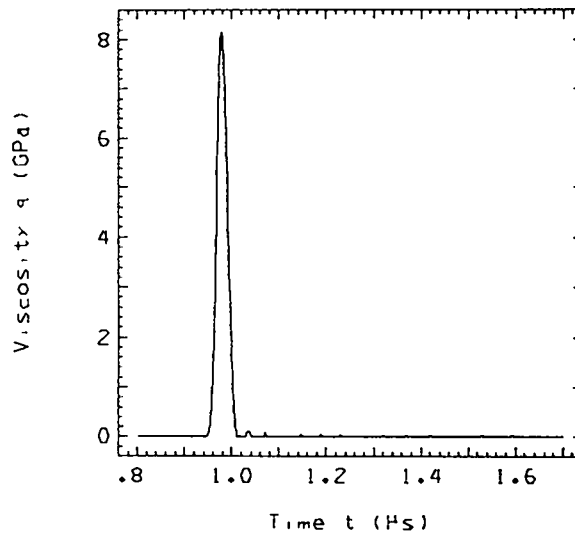
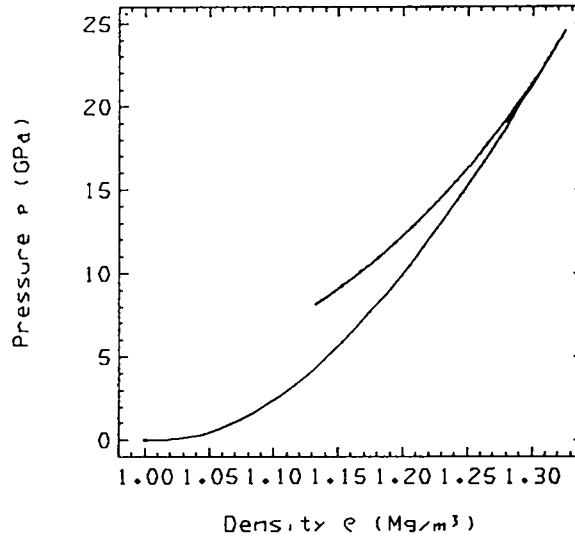
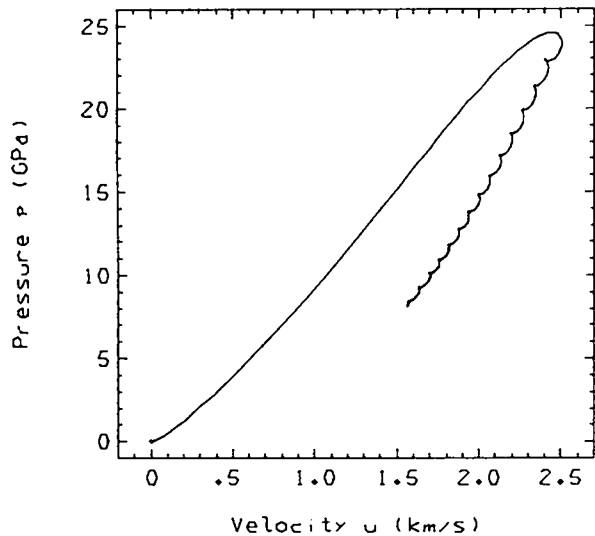


Fig. 6 (cont)

9. BLAST WAVE / DIFFERENCE, TRUNCATED TIME / PARTICLES

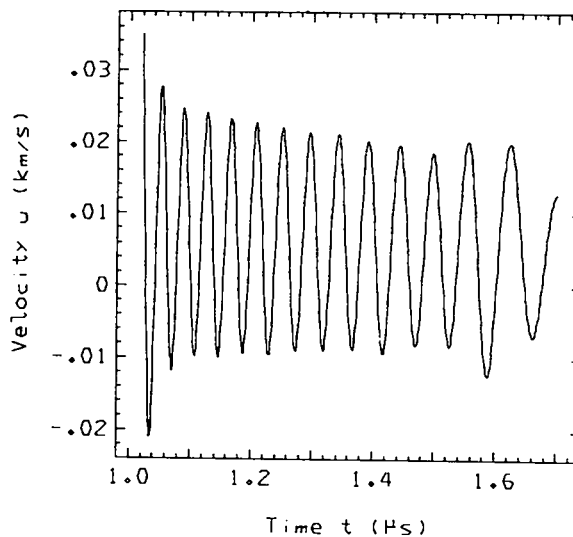
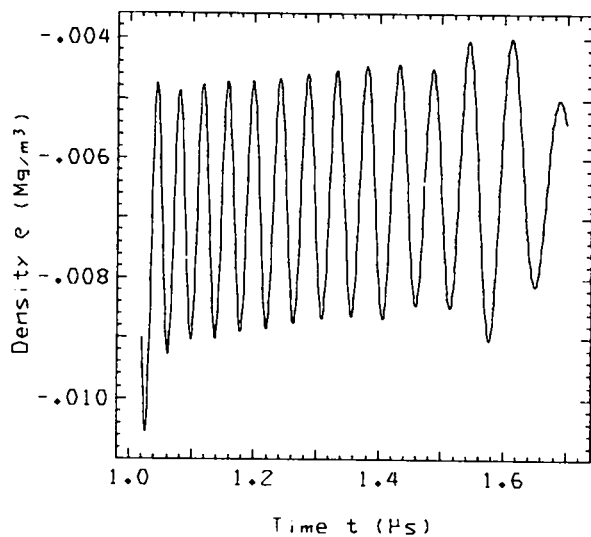
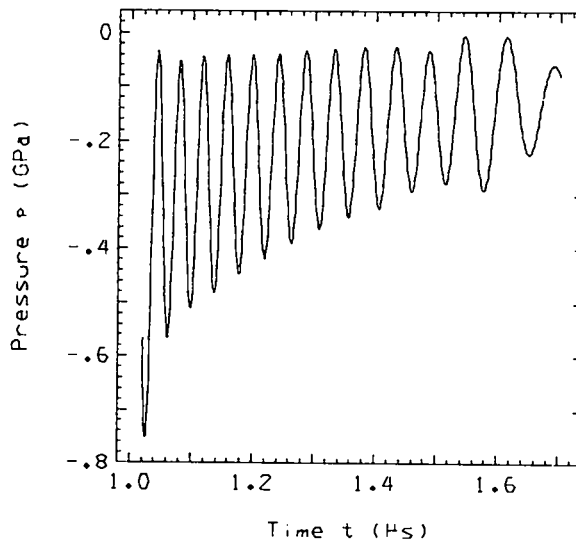
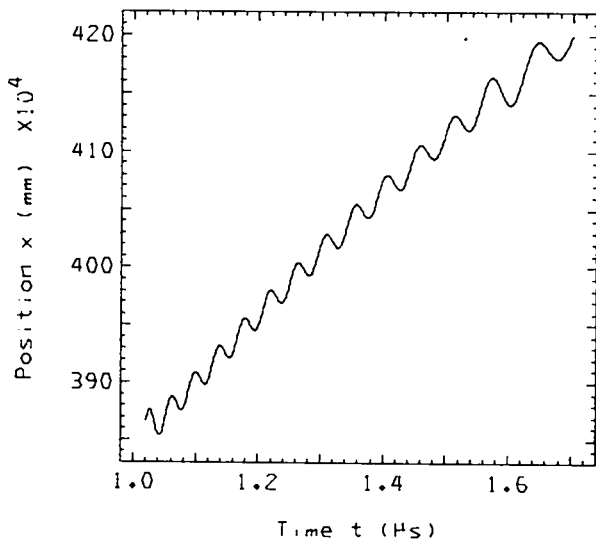


Fig. 6 (cont)

9. BLAST WAVE / DIFFERENCE, TRUNCATED TIME / PARTICLES
(to t = 2)

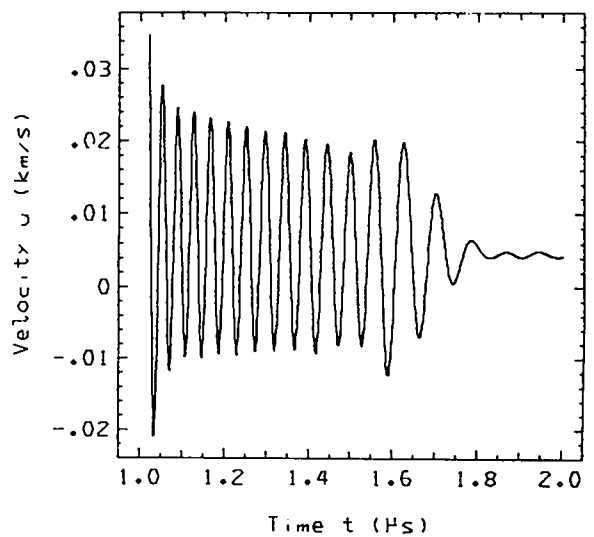
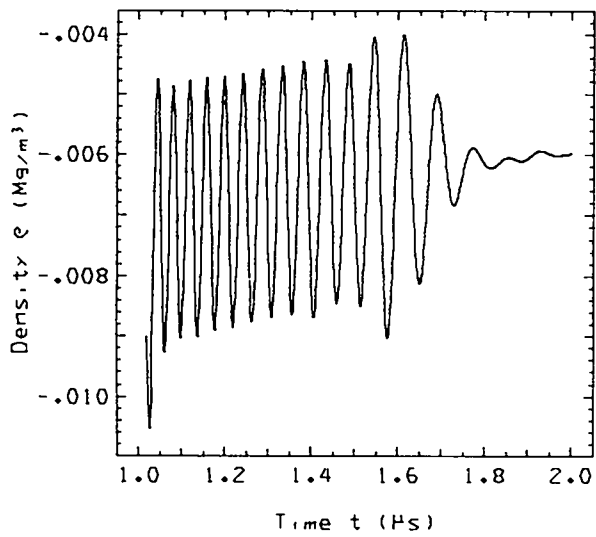
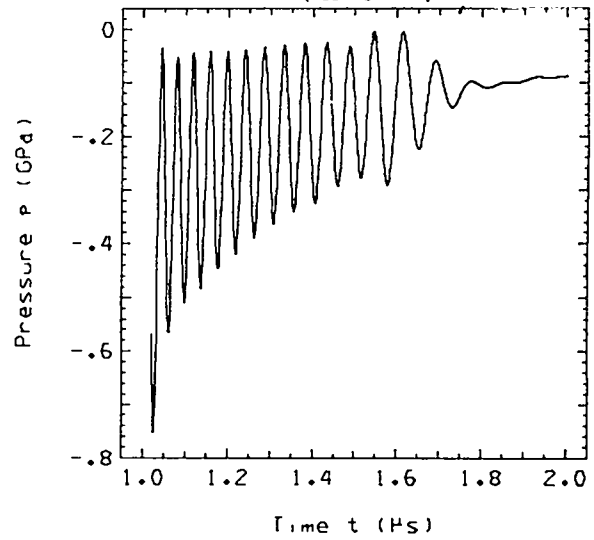
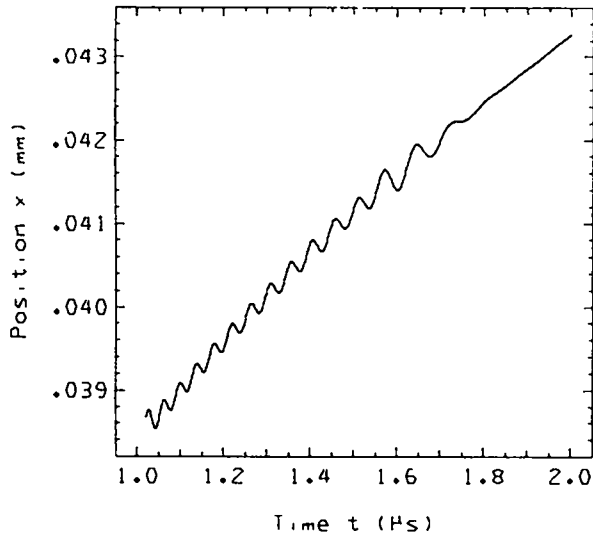


Fig. 6 (cont)

9. BLAST WAVE / DIFFERENCE, TRUNCATED TIME / PARTICLES

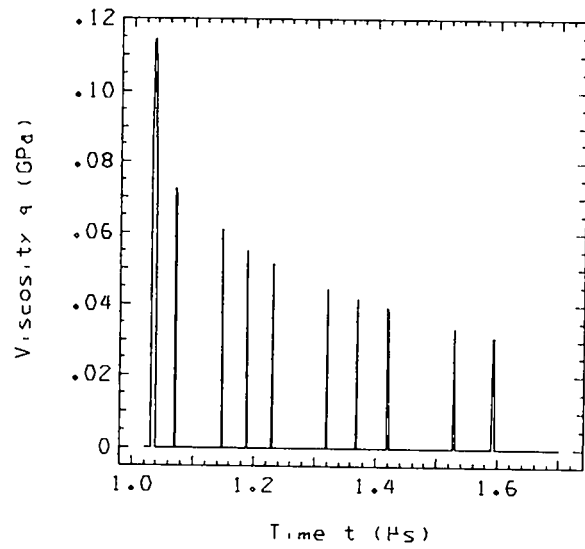
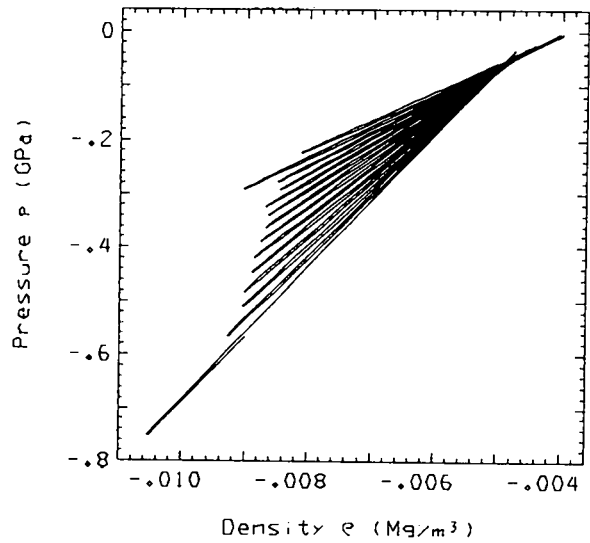
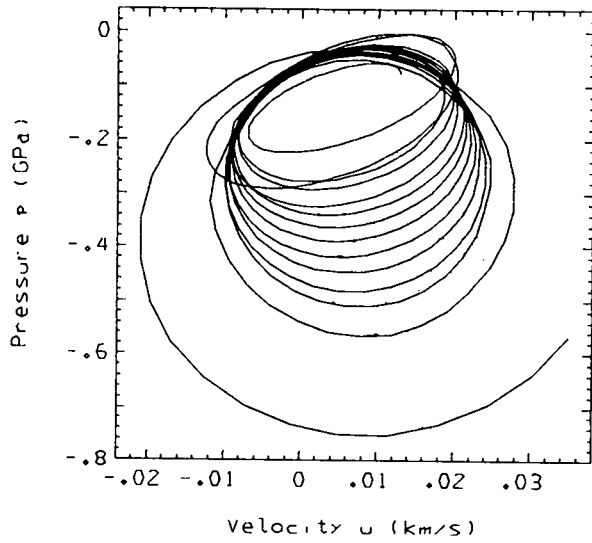


Fig. 6 (cont)

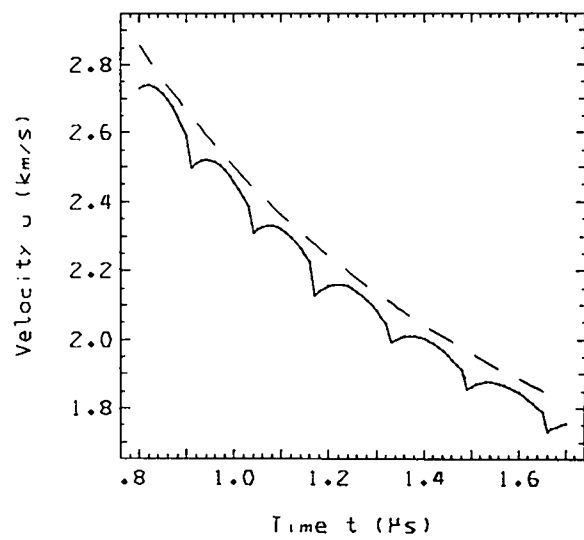
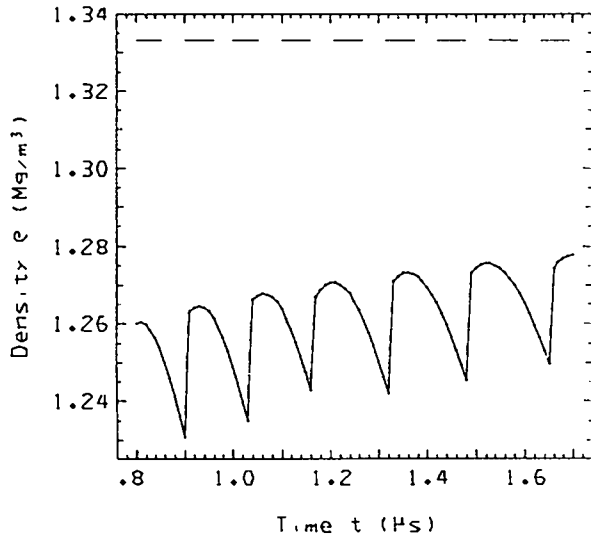
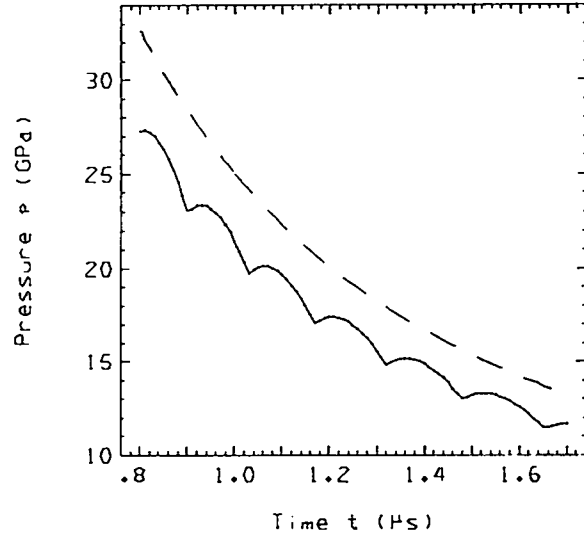
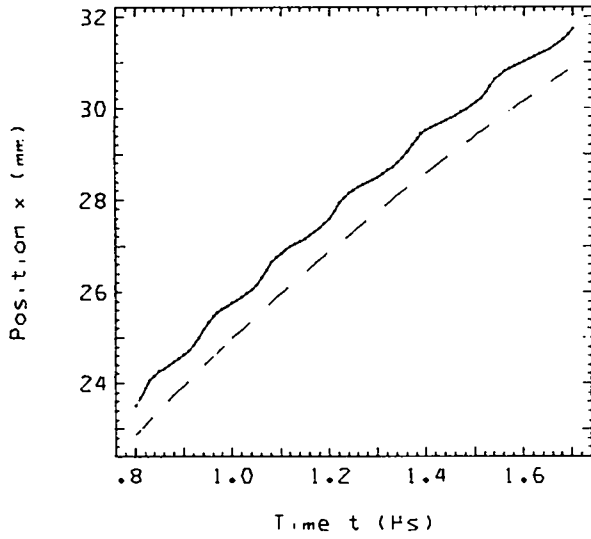


Fig. 6 (cont)

9. BLAST WAVE / LEAD SHOCK

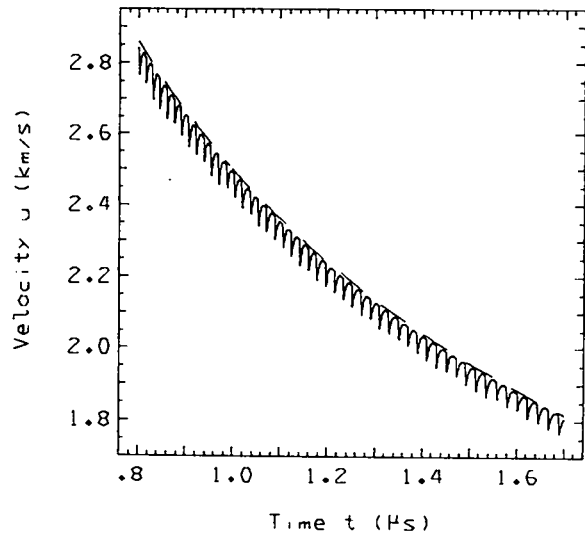
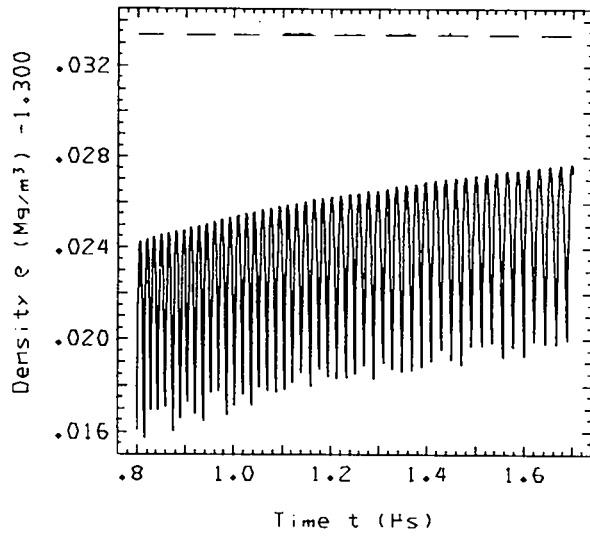
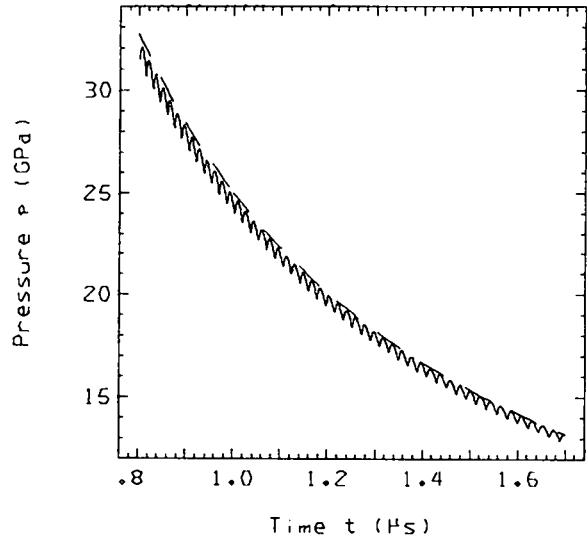
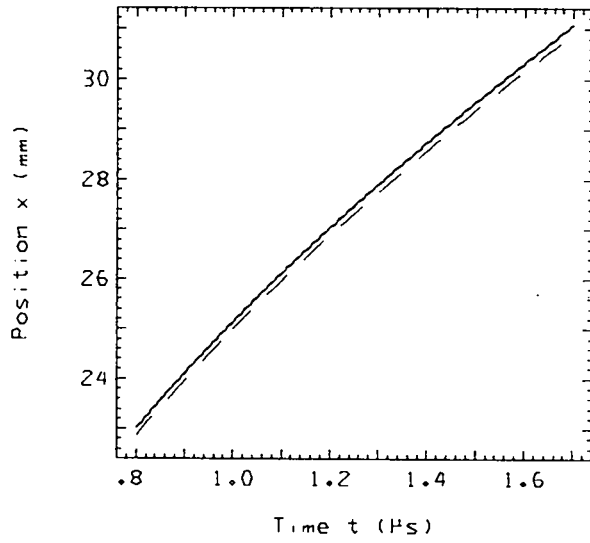


Fig. 6 (cont)

9. BLAST WAVE / DIFFERENCE / LEAD SHOCK

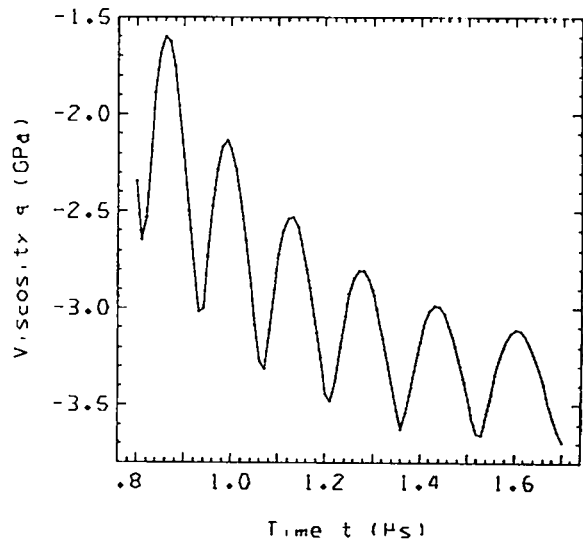
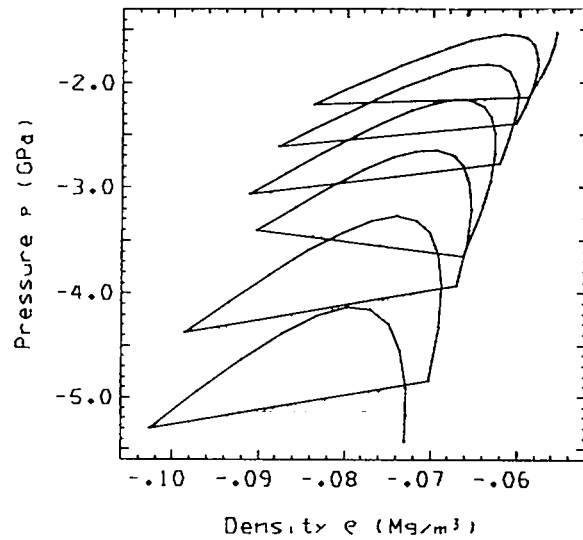
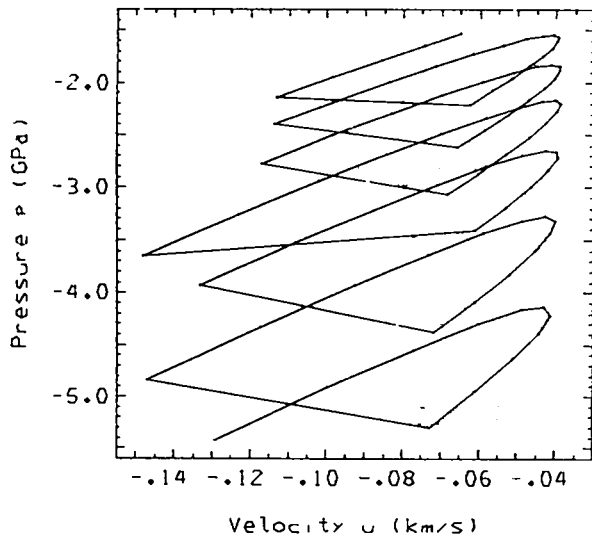


Fig. 6 (cont)

9. BLAST WAVE / DIFFERENCE, TRUNCATED TIME / PARTICLE

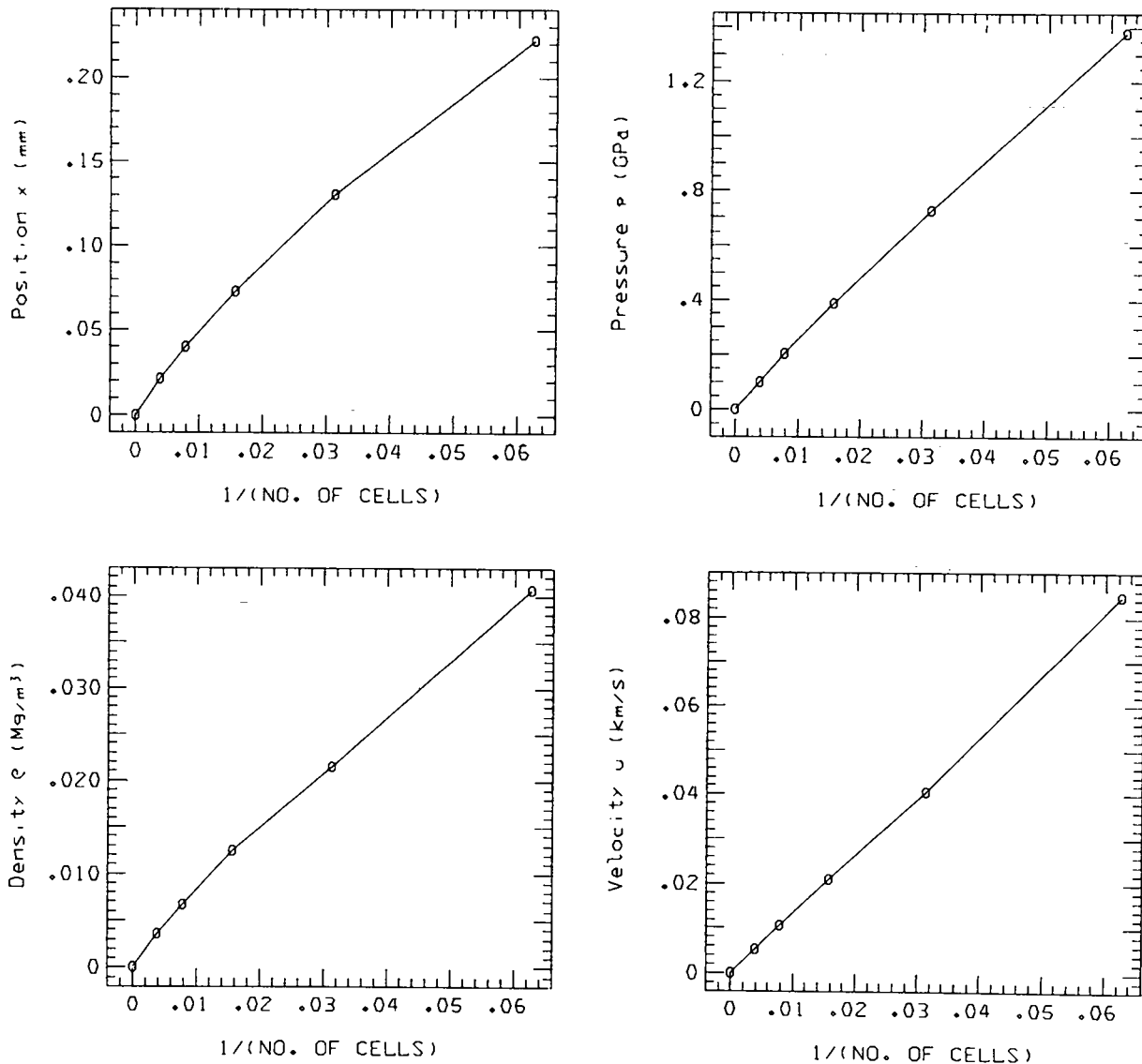


Fig. 6 (cont)

9. BLAST WAVE / DIFFERENCE / SHOCK

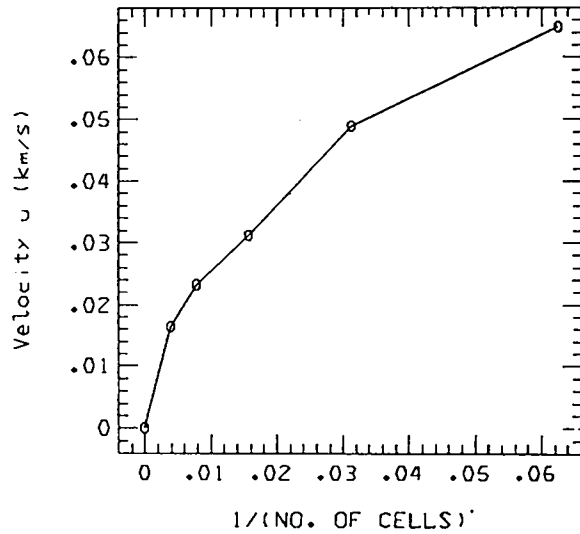
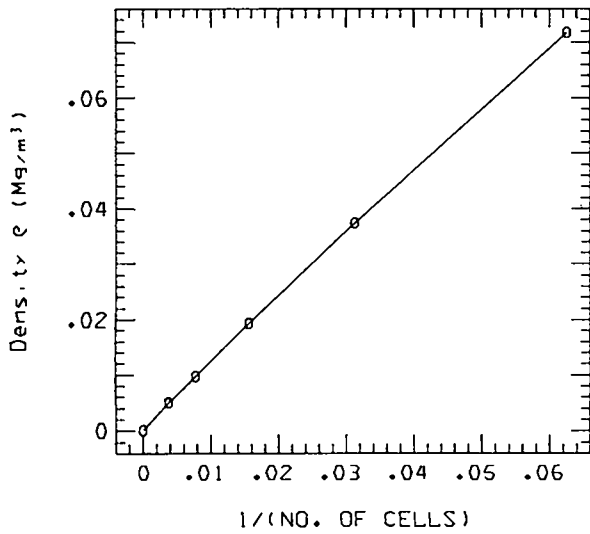
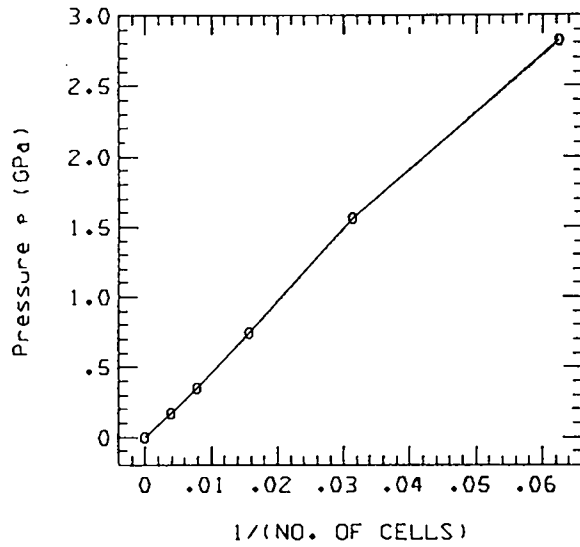
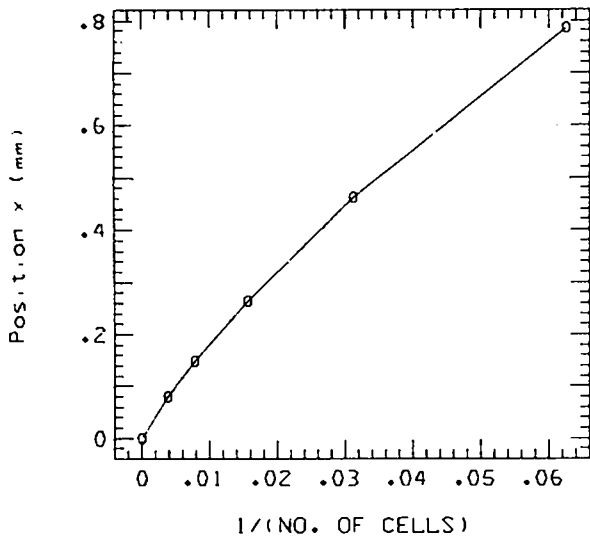


Fig. 6 (cont)

10. STEADY DETONATION / TIME= 1.7000E+00

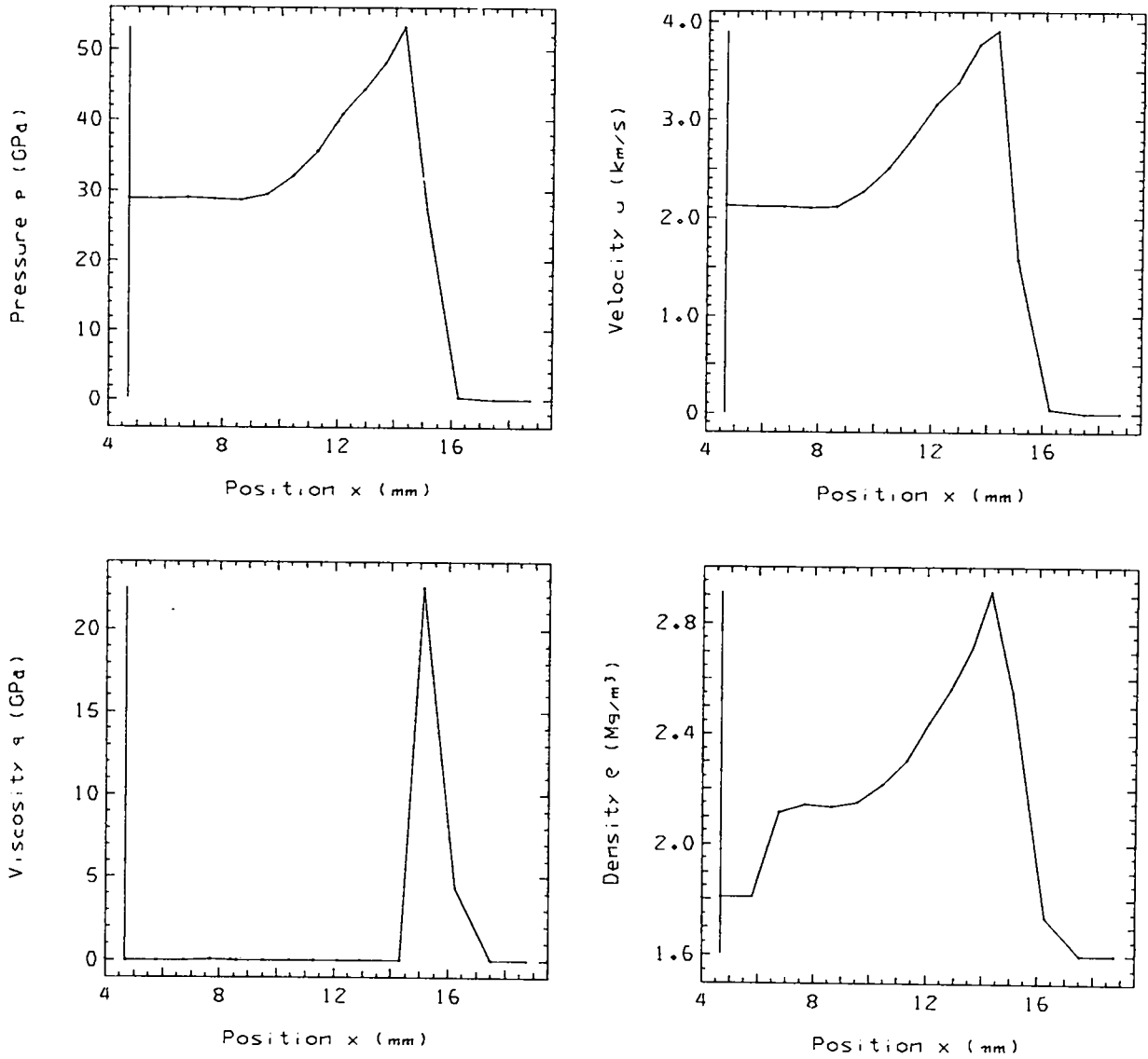


Fig. 7.
Problem 10. Steady detonation. Standard calculation.

10. STEADY DETONATION / TIME= 1.7000E+00

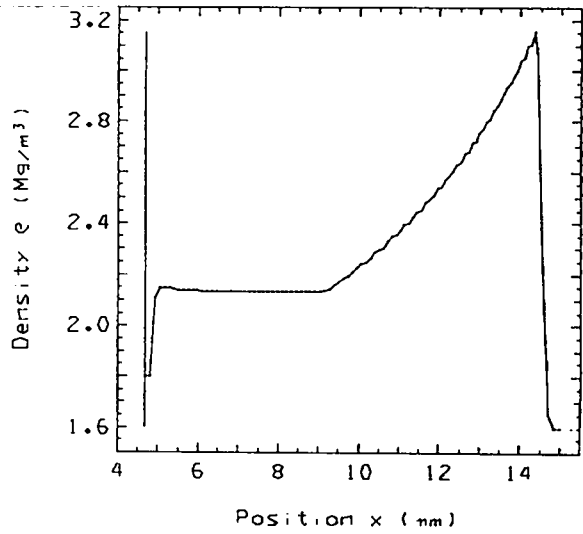
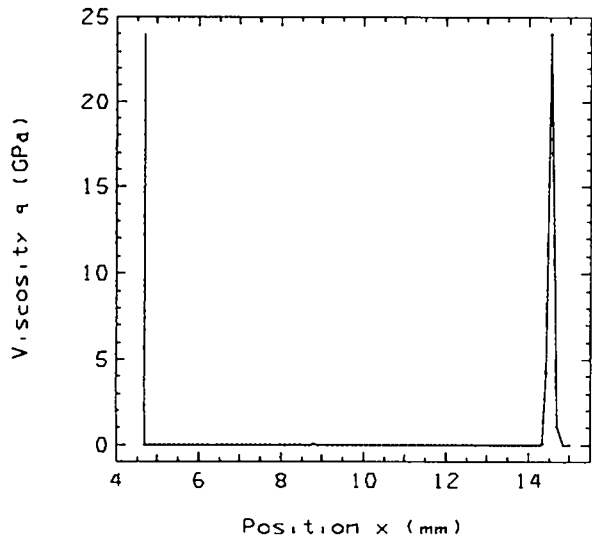
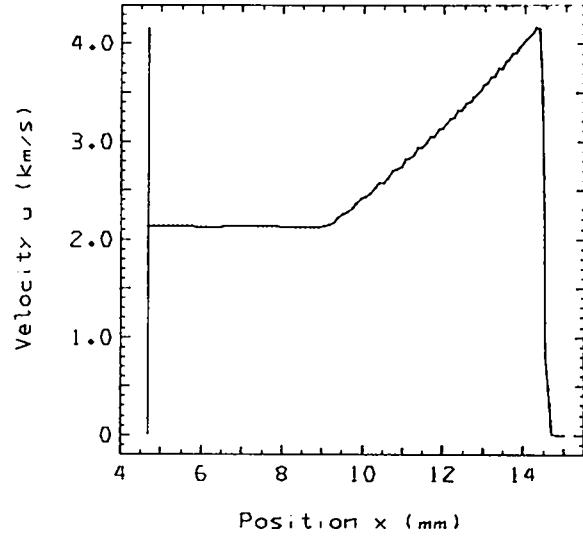
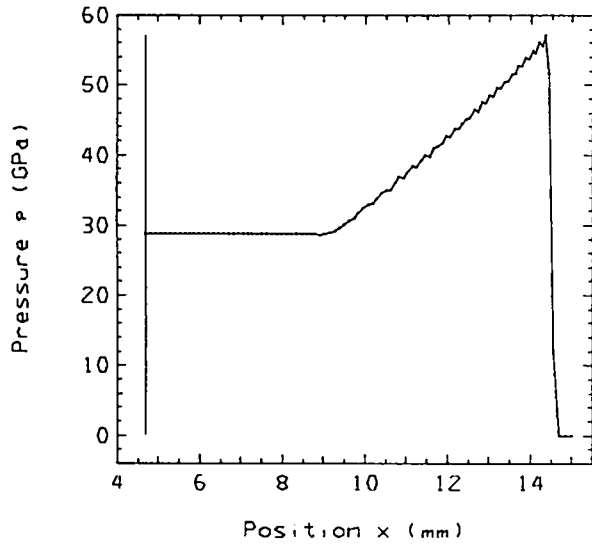
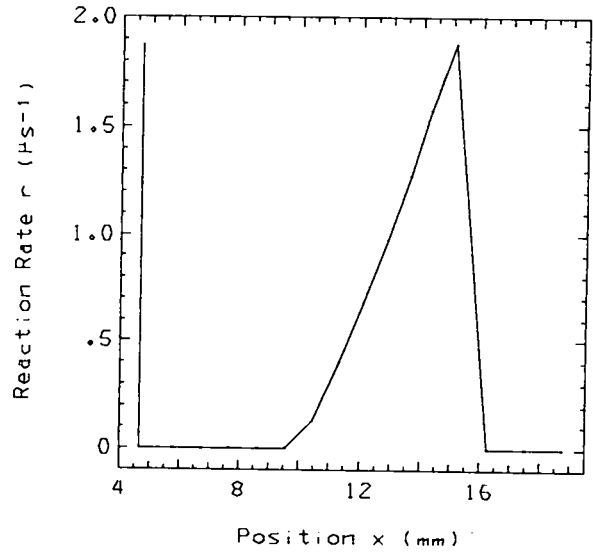
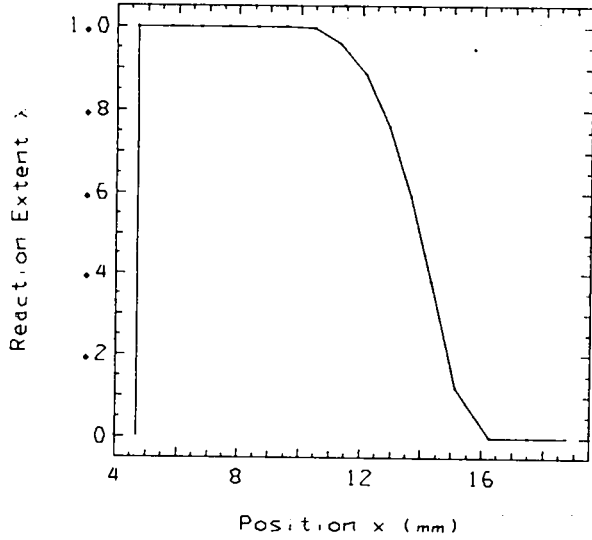


Fig. 7 (cont)

PAD3.3F6 - 75JUL14 RUN22 LAC2 *10. STEADY DETONATION*
TFICKET1GY. .339 SEC ON RUN, 314.430 SEC ON JOB

ERUN 1. 16 CELLS 07/21/75

10. STEADY DETONATION / TIME= 1.7000E+00



PAD3.3F6 - 75JUL14 RUN22 LAC2 *10. STEADY DETONATION*
TFICKET1GY. 9.825 SEC ON RUN, 323.916 SEC ON JOB

ERUN 4. 128 CELLS 07/21/75

10. STEADY DETONATION / TIME= 1.7000E+00

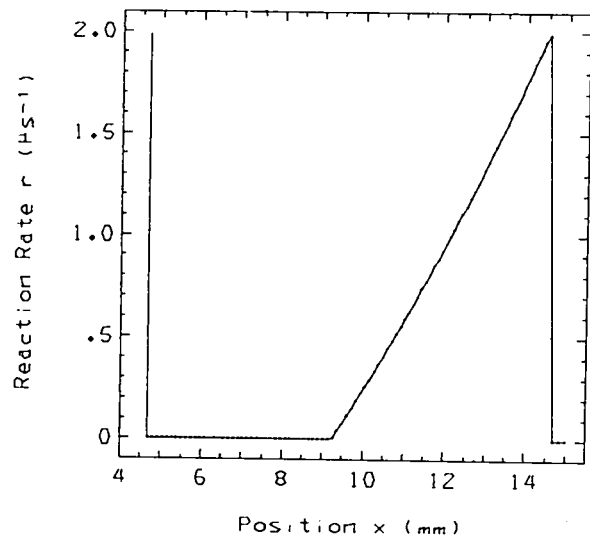
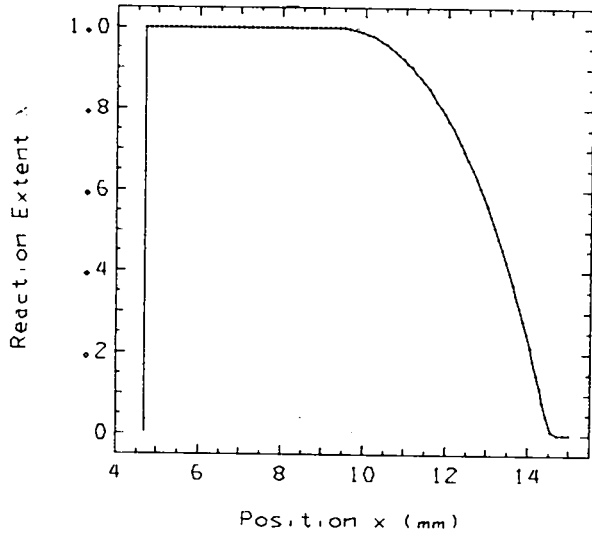


Fig. 7 (cont)

10. STEADY DETONATION / PARTICLES

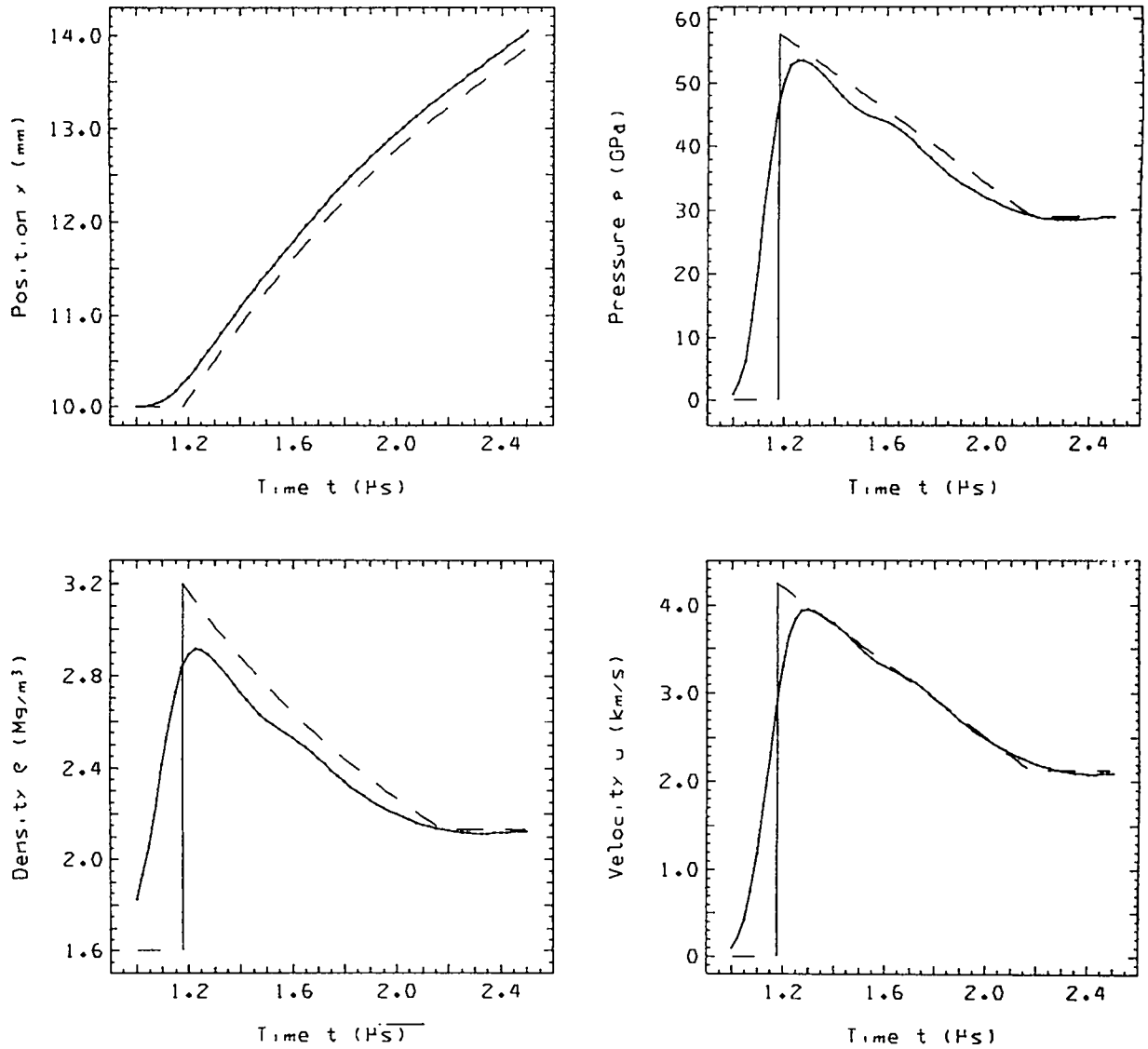


Fig. 7 (cont)

10. STEADY DETONATION / PARTICLES

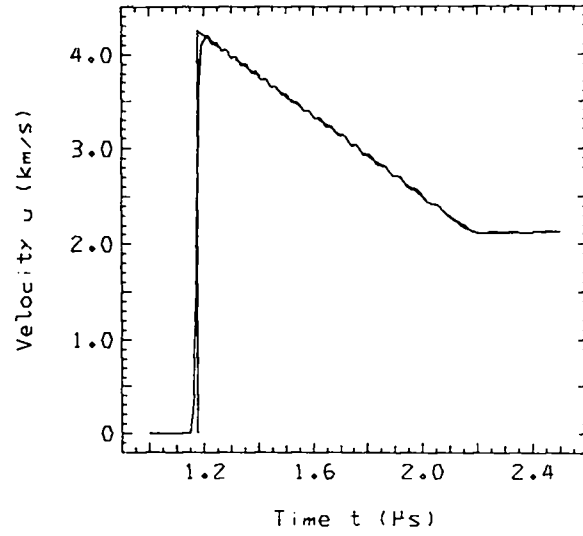
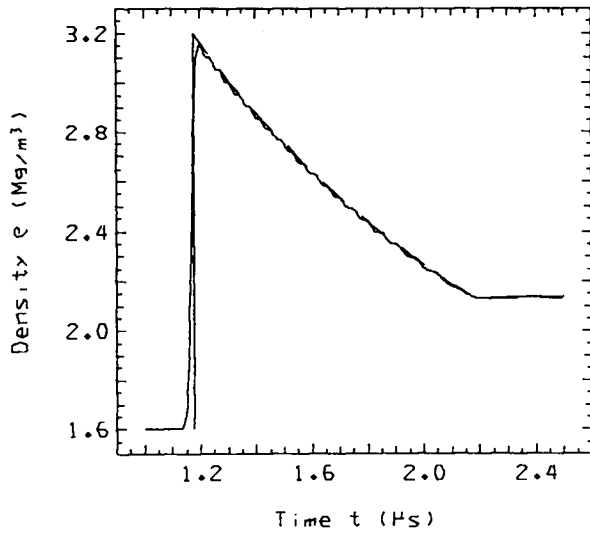
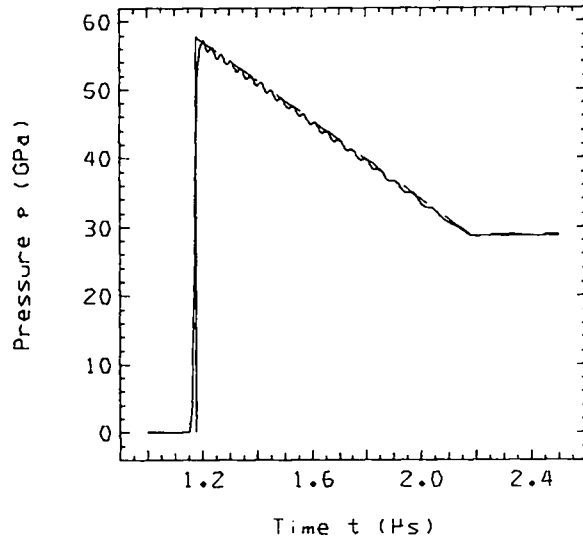
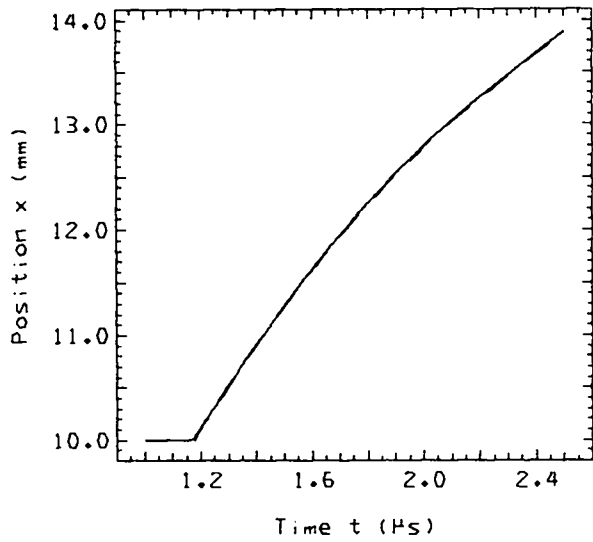
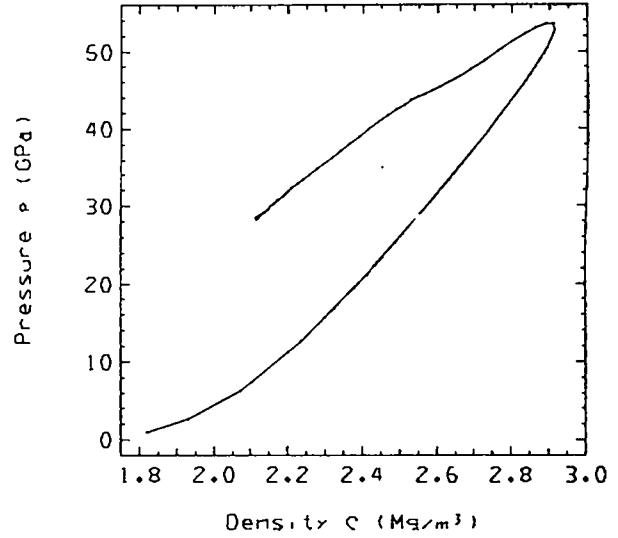
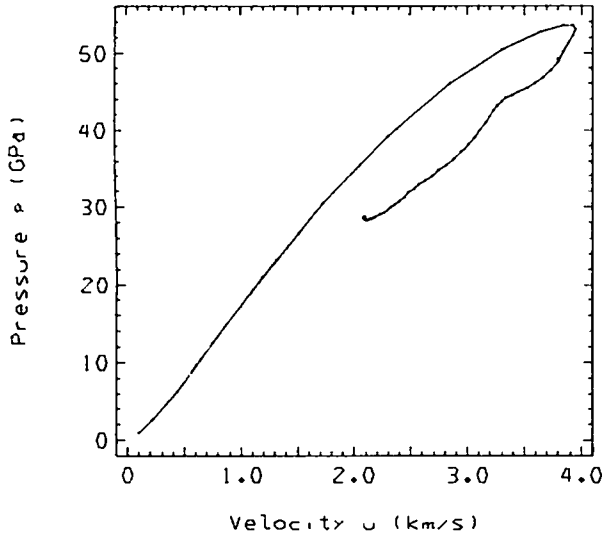


Fig. 7 (cont)

PAD3.3F6 - 75JUL14 RUN22 LAC2 *10. STEADY DETONATION*
TFICKETIGY. 1.096 SEC ON RUN. 315.187 SEC ON JOB

ERUN 1. 16 CELLS 07/21/75

10. STEADY DETONATION / PARTICLES



PAD3.3F6 - 75JUL14 RUN22 LAC2 *10. STEADY DETONATION*
TFICKETIGY. 13.530 SEC ON RUN. 327.621 SEC ON JOB

ERUN 4. 128 CELLS 07/21/75

10. STEADY DETONATION / PARTICLES

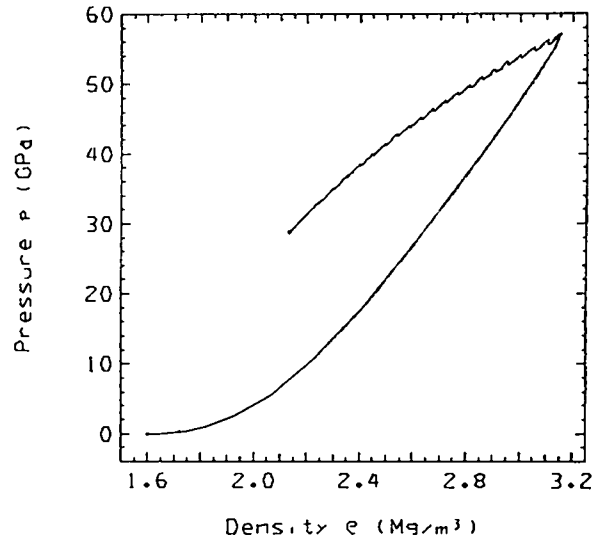
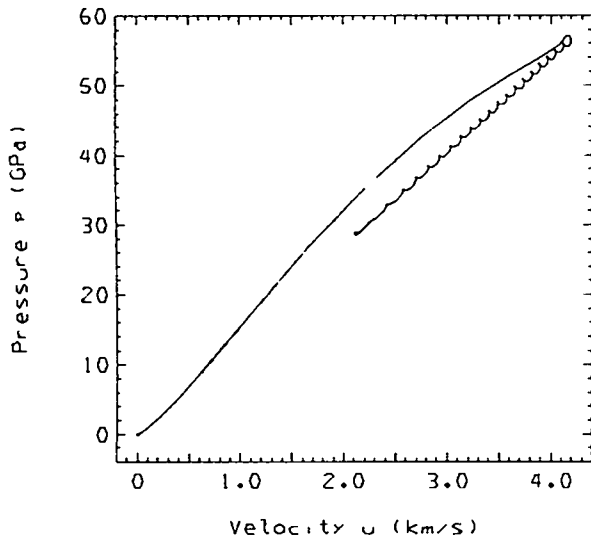


Fig. 7 (cont)

10. STEADY DETONATION / DIFFERENCE, TRUNCATED TIME / PARTICLES

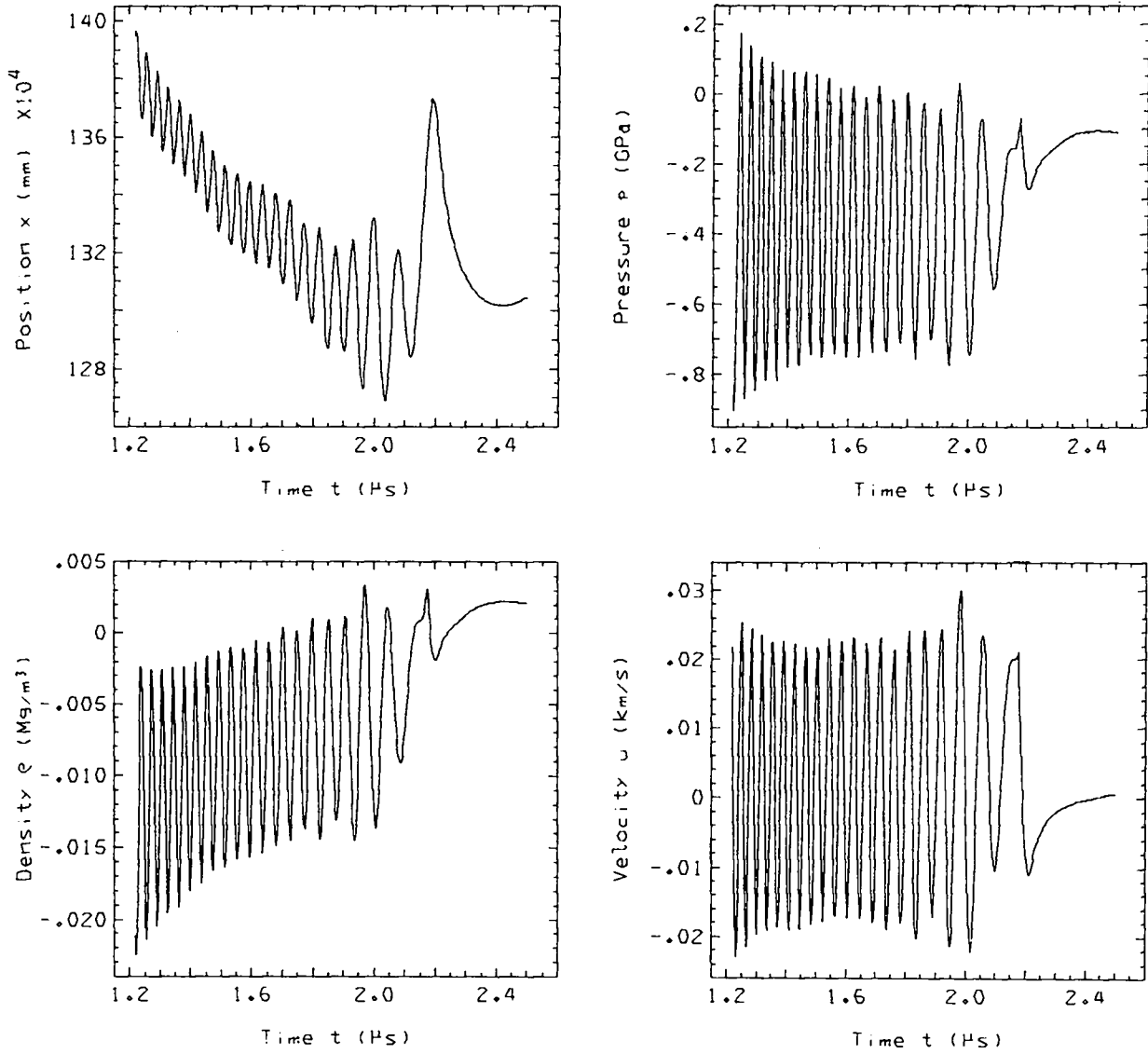


Fig. 7 (cont)

10. STEADY DETONATION / DIFFERENCE, TRUNCATED TIME / PARTICLES

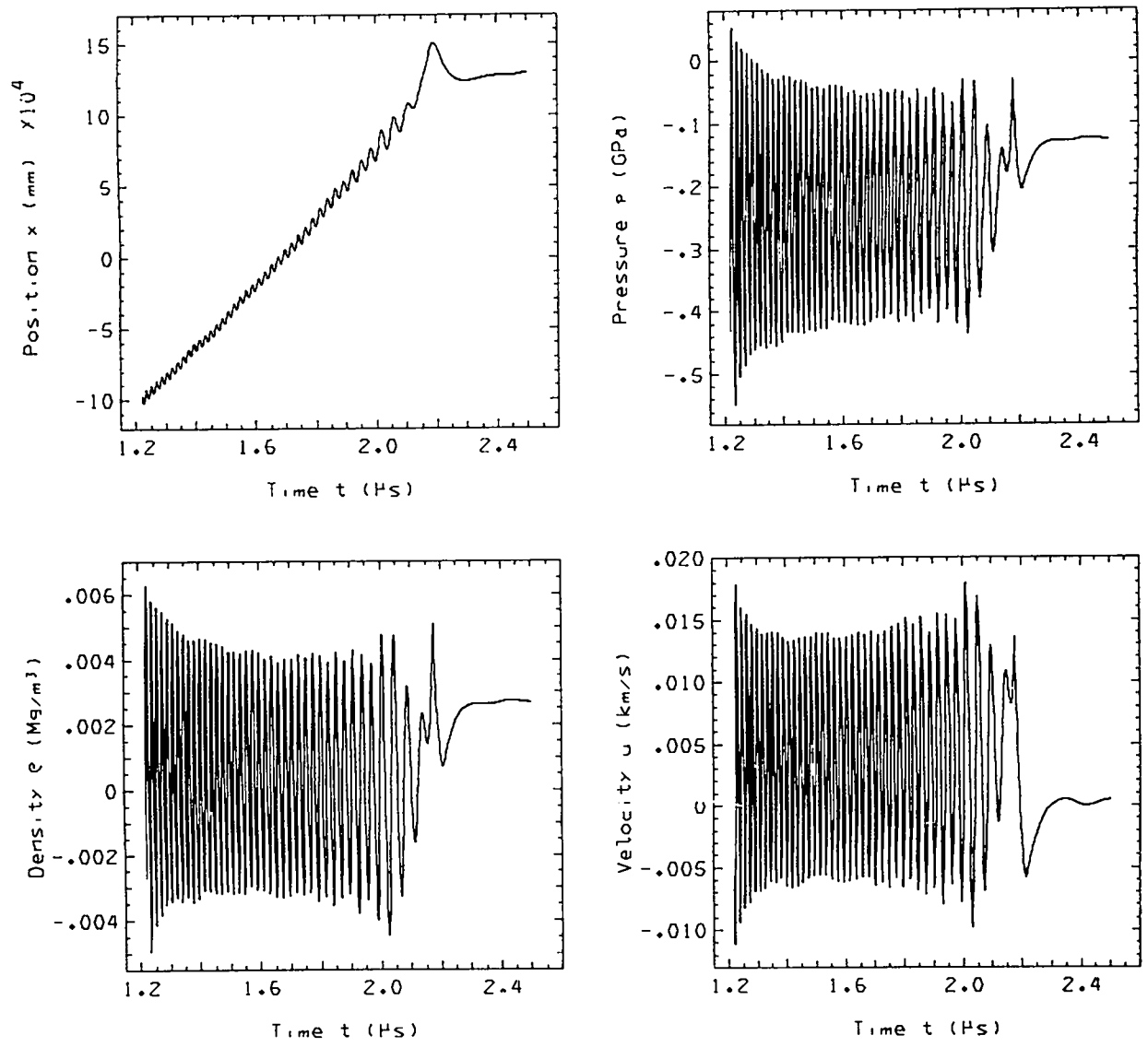


Fig. 7 (cont)

10. STEADY DETONATION / DIFFERENCE, TRUNCATED TIME / PARTICLES

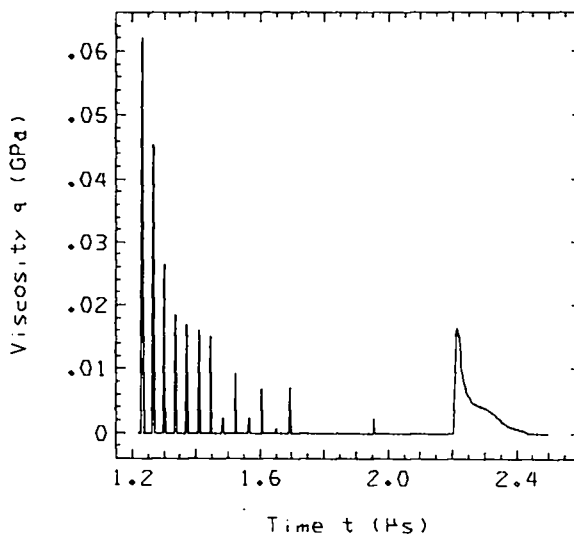
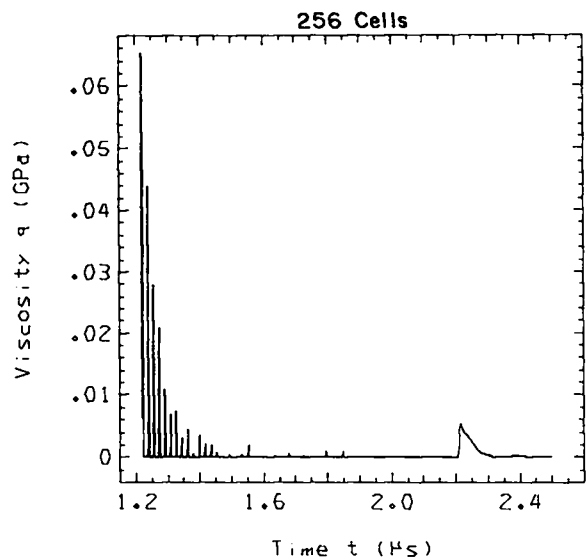
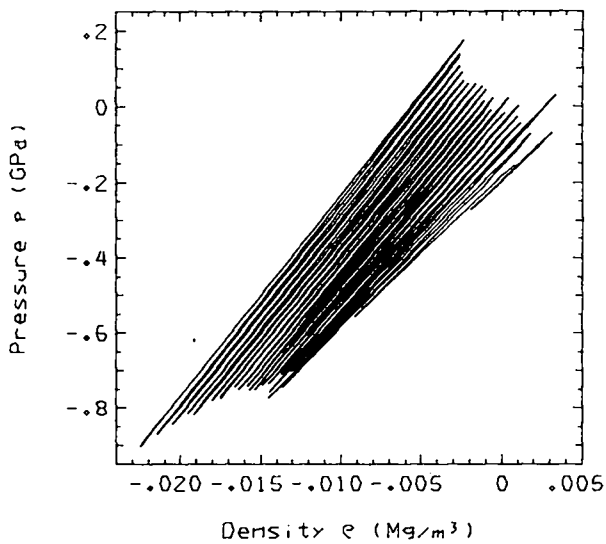
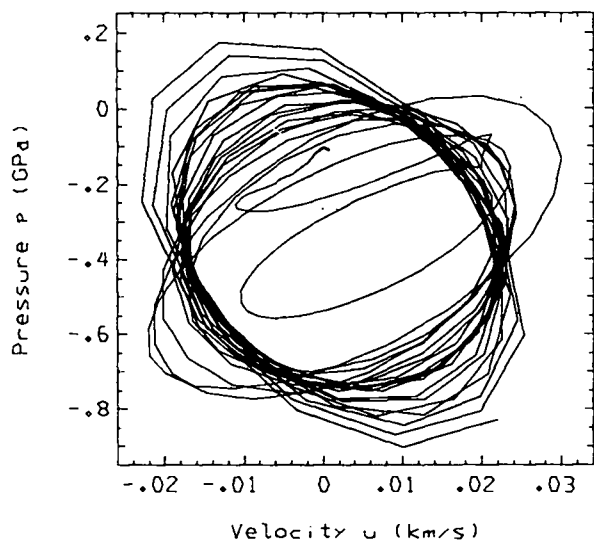


Fig. 7 (cont)

10. STEADY DETONATION / LEAD SHOCK

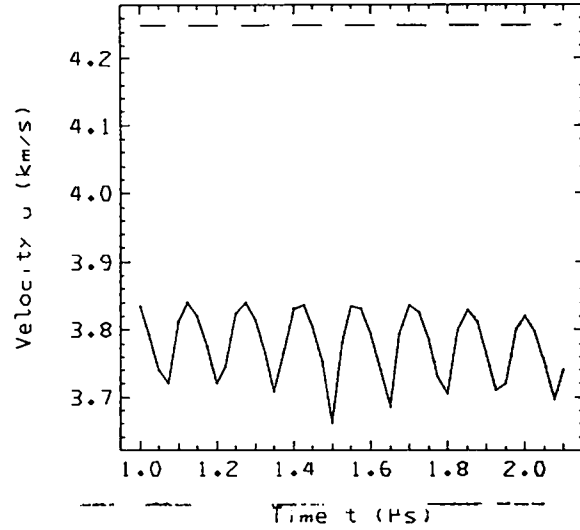
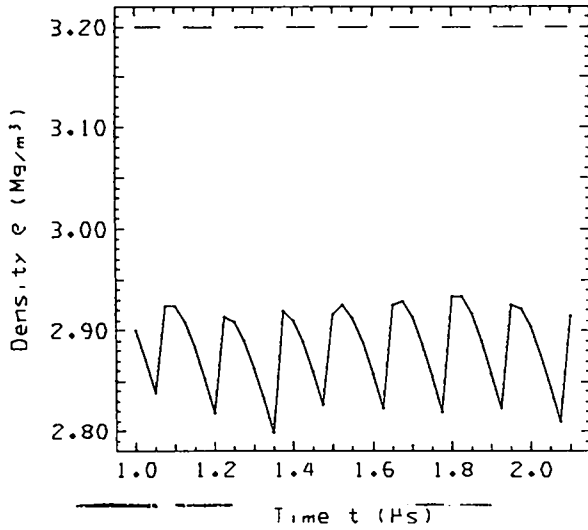
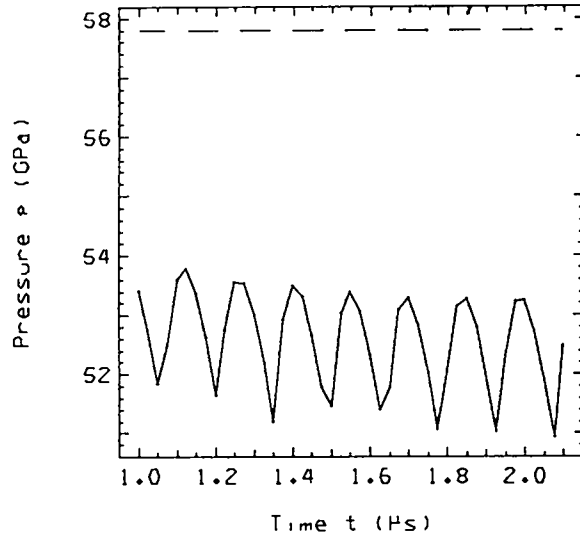
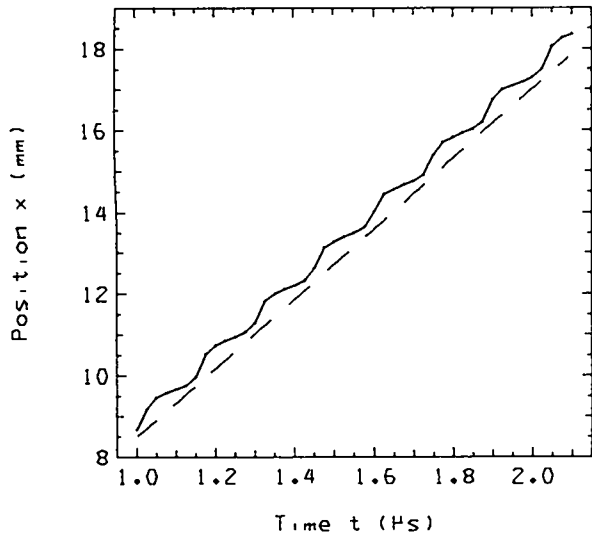


Fig. 7 (cont)

10. STEADY DETONATION / DIFFERENCE / LEAD SHOCK

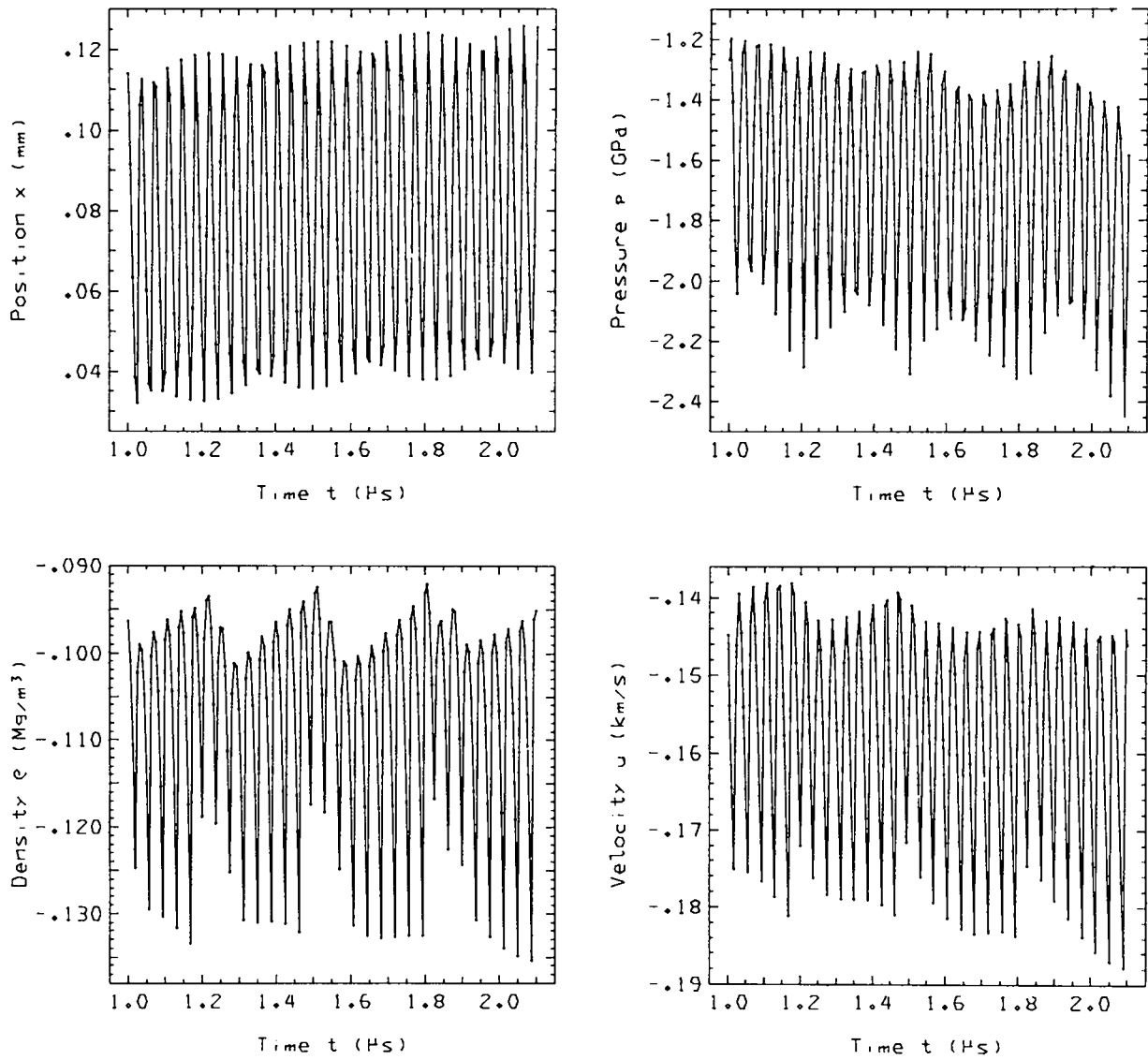


Fig. 7 (cont)

10. STEADY DETONATION / DIFFERENCE / LEAD SHOCK

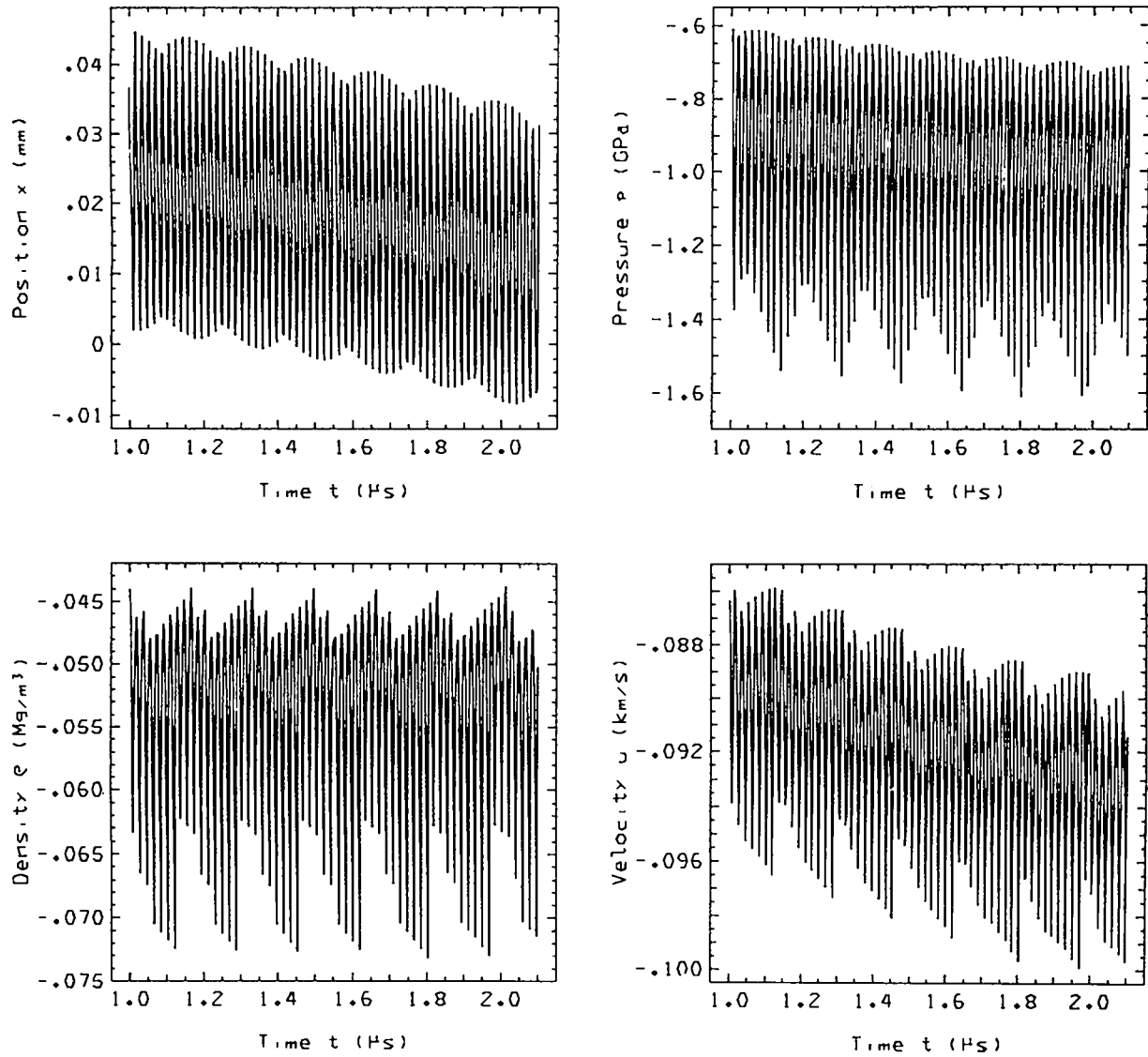


Fig. 7 (cont)

10. STEADY DETONATION / DIFFERENCE, TRUNCATED TIME / PARTICLE

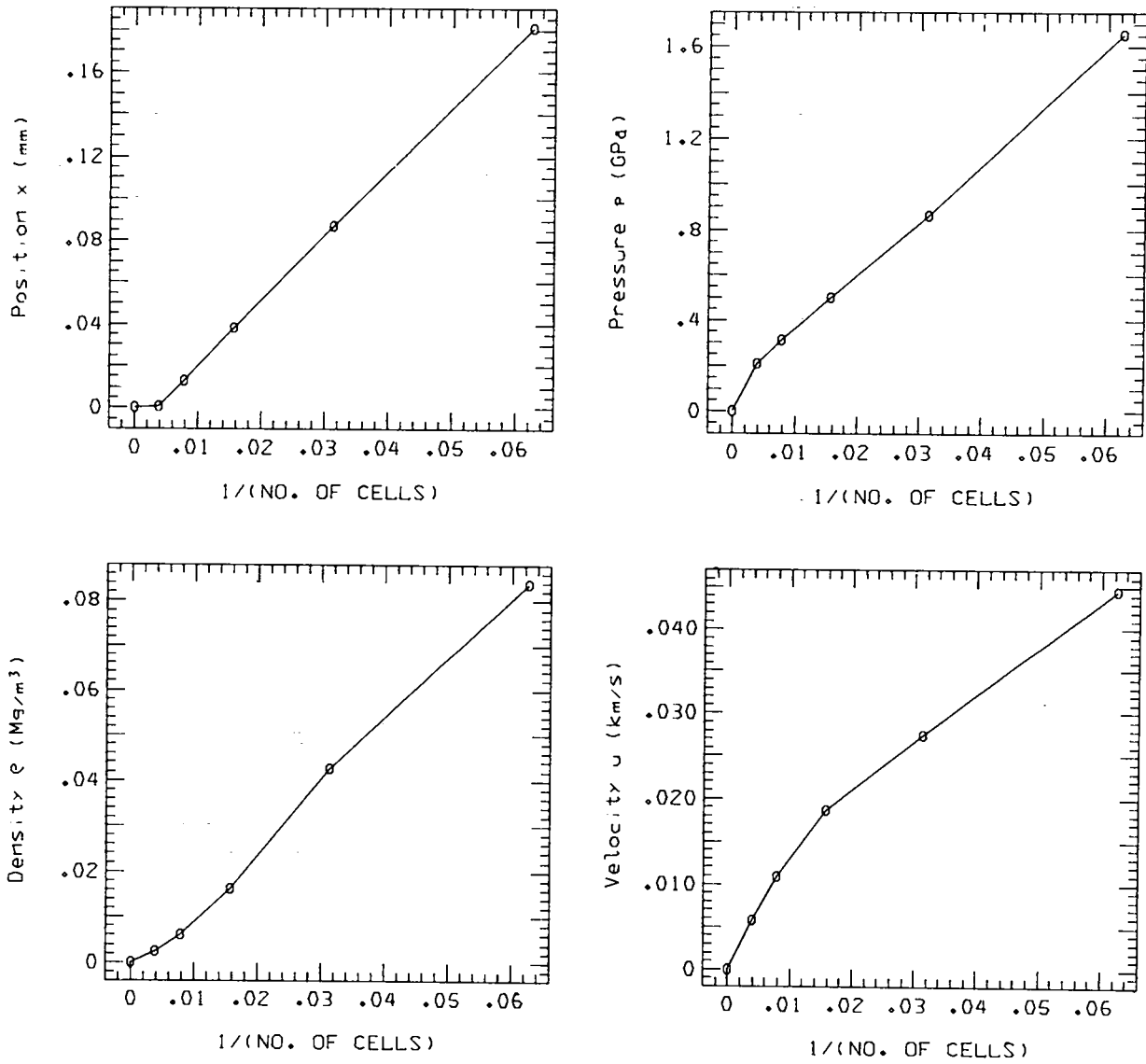


Fig. 7 (cont)

10. STEADY DETONATION / DIFFERENCE / SHOCK

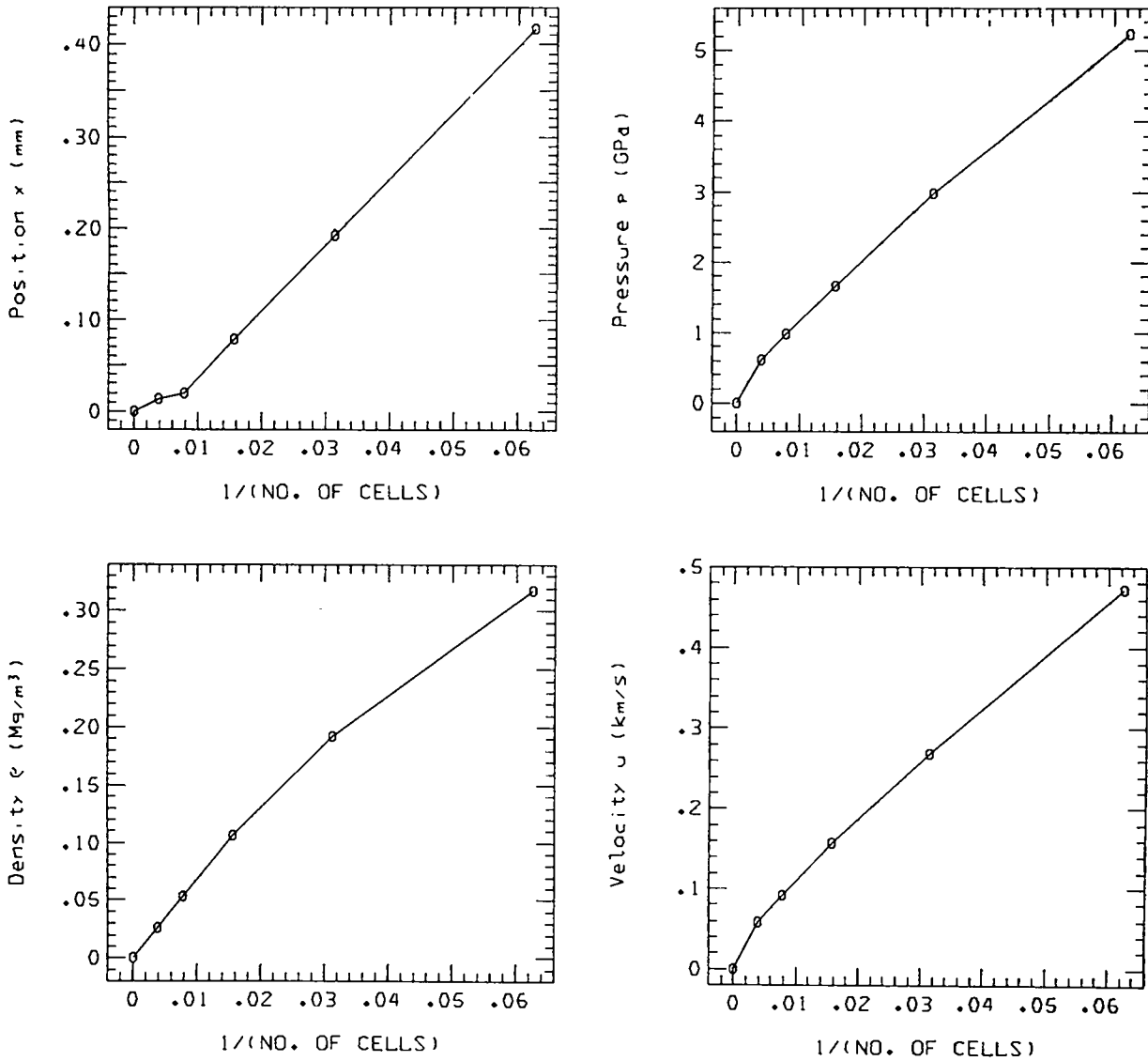


Fig. 7 (cont)

2. SHOCK DECEL., Q = 0, 1.414 / TIME = 1.4000E+00

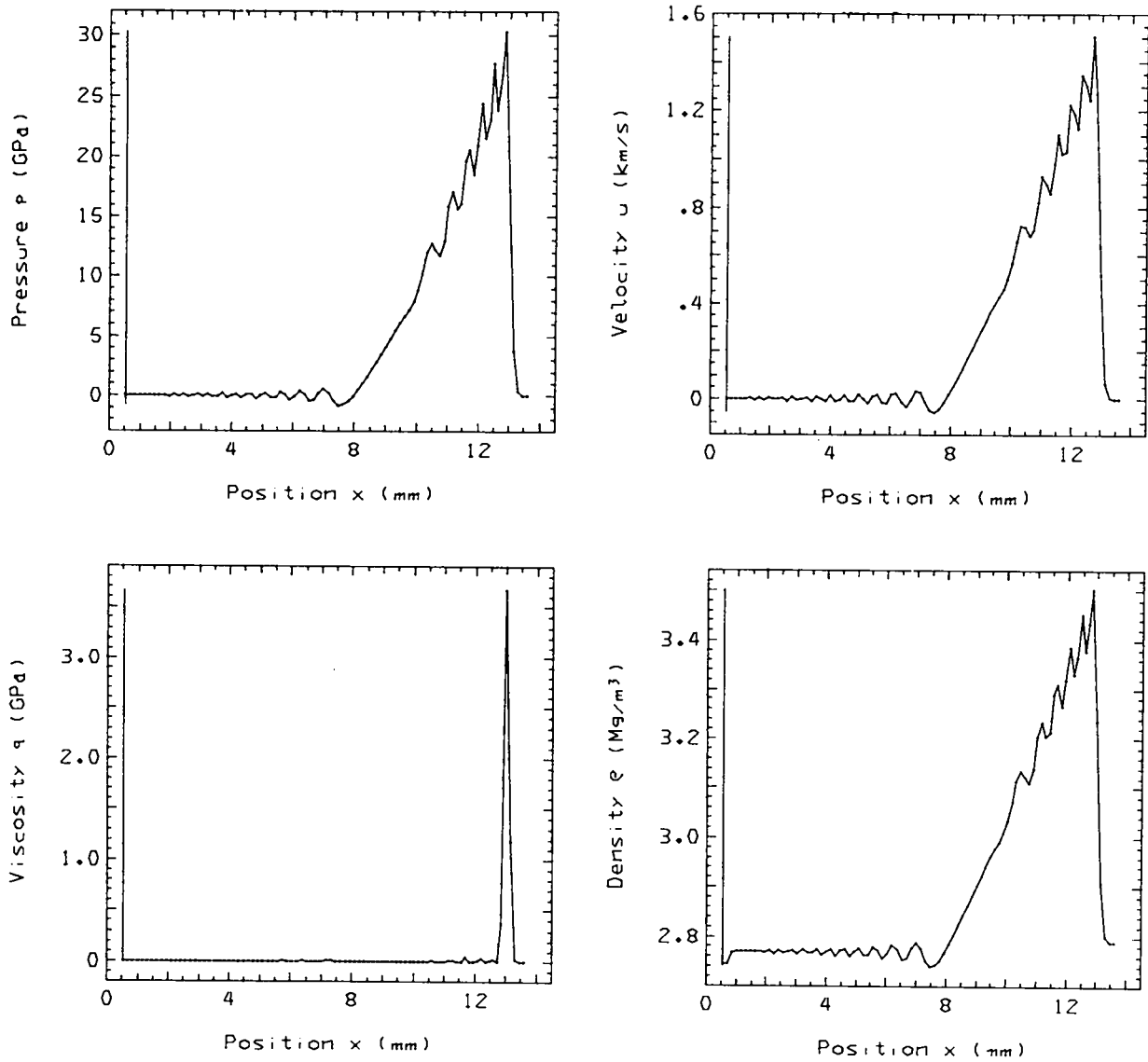


Fig. 8.
Problem 2. $q = 0, 1.414$, quadratic.

2. SHOCK DECEL., Q = 0, 1.414 / PARTICLES

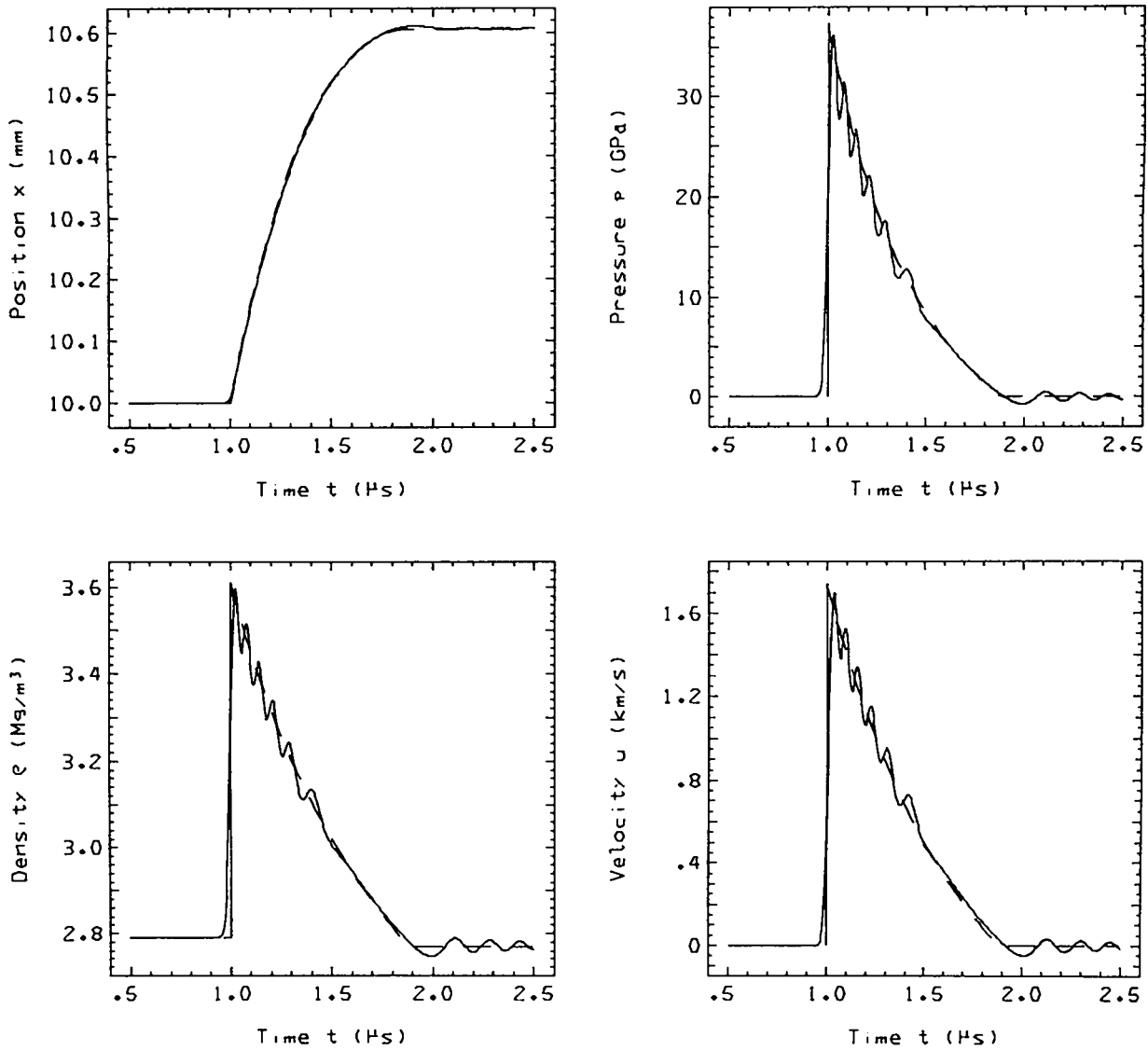


Fig. 8 (cont)

2. SHOCK DECEL., Q = 0, 1.414 / DIFFERENCE, TRUNCATED TIME / PARTICLES

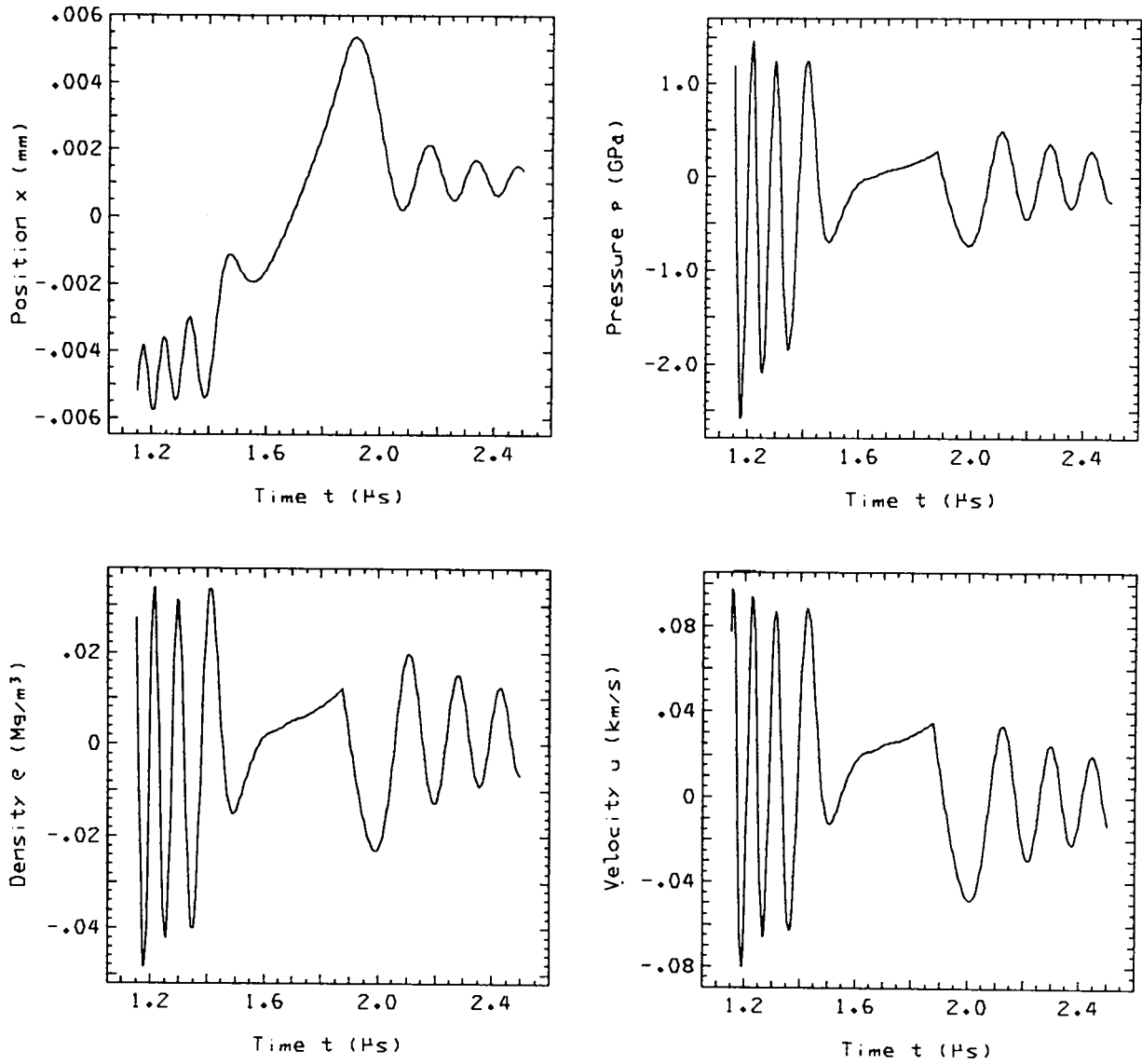


Fig. 8 (cont)

2. SHOCK DECEL.. Q = 0, 1.414 / DIFFERENCE, TRUNCATED TIME / PARTICLES

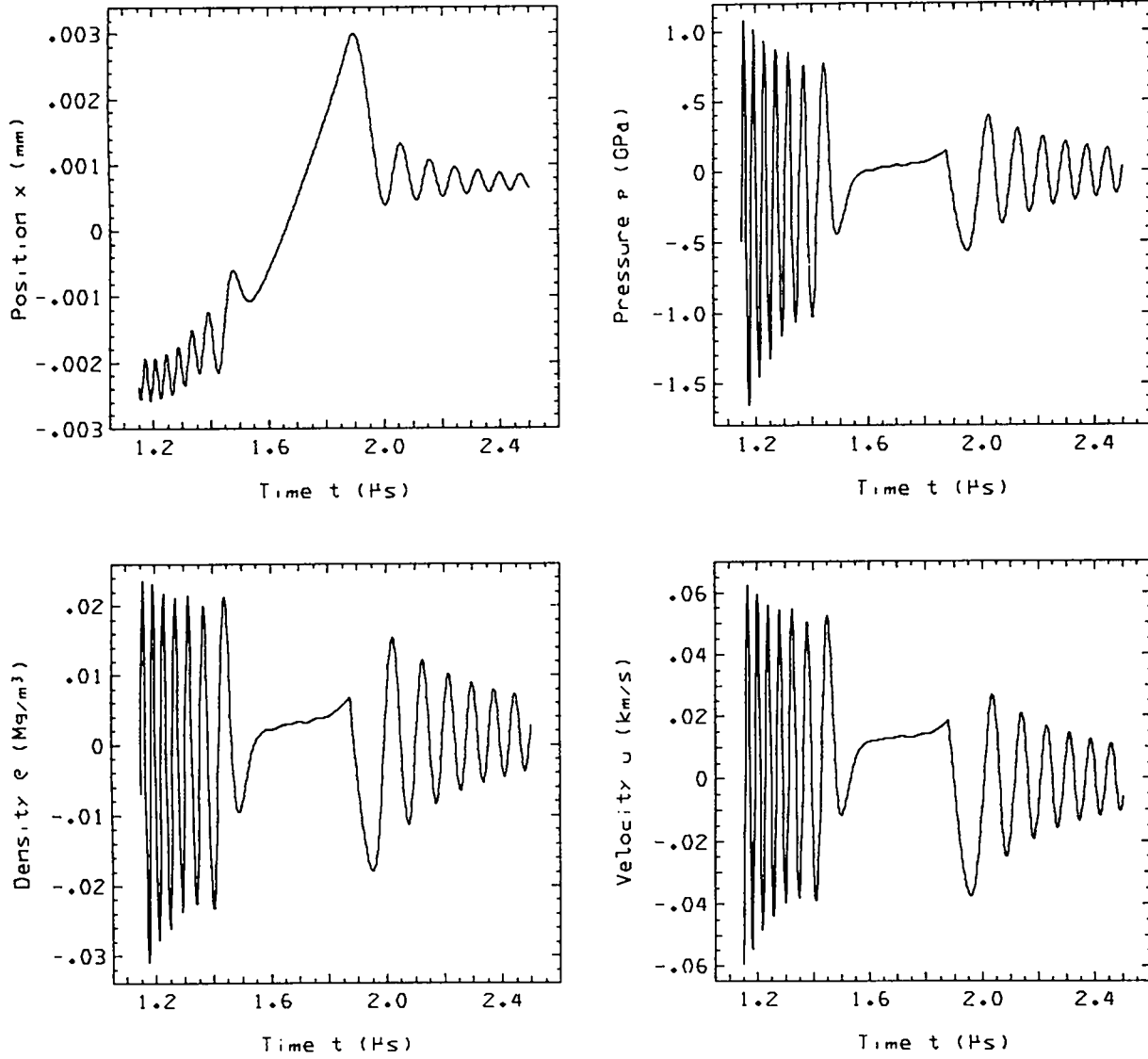


Fig. 8 (cont)

PAD3.3F6 - 75JUL14 RUN21 LAC3 *SHOCK DECEL., Q = 0, 1.414*
TFICKET1AW, 6.760 SEC ON RUN, 237.711 SEC ON JOB

ERUN 4, 128 CELLS 07/22/75

2. SHOCK DECEL., Q = 0, 1.414 / DIFFERENCE, TRUNCATED TIME / PARTICLES

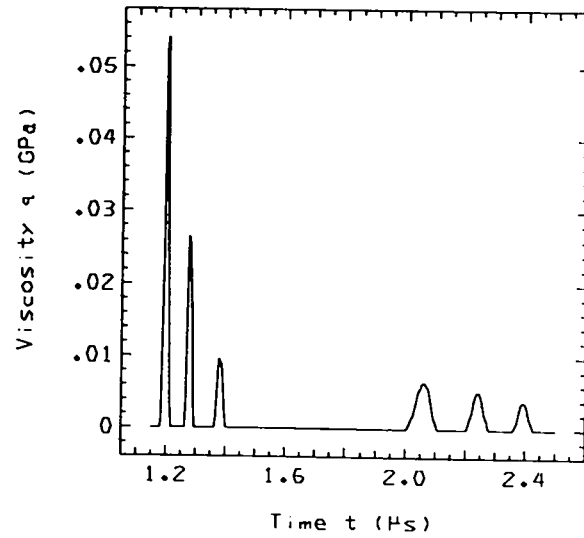
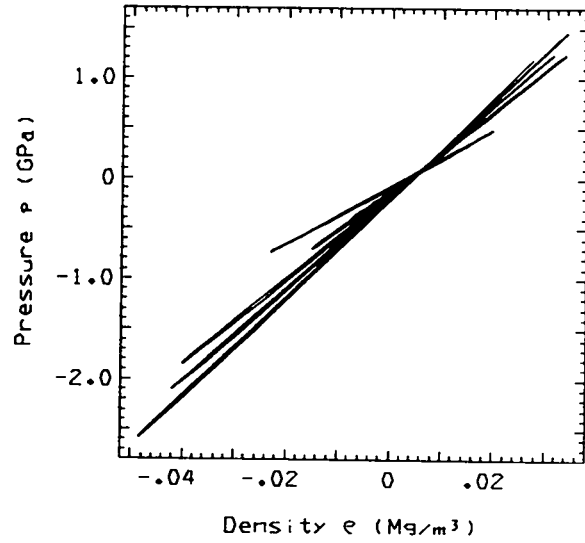
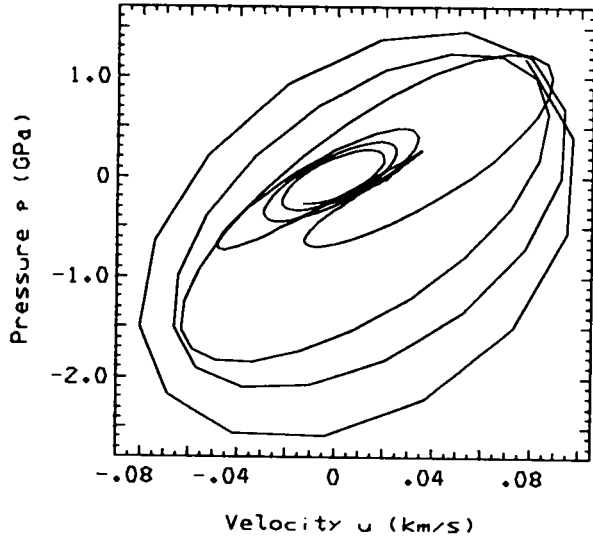


Fig. 8 (cont)

2. SHOCK DECEL., Q = 0, 1.414 / LEAD SHOCK

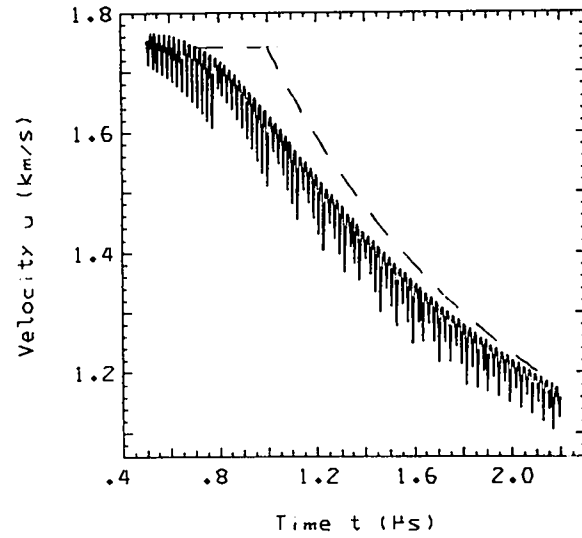
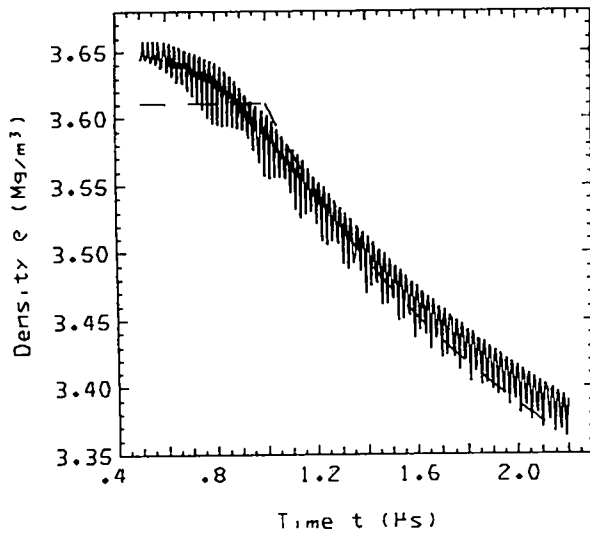
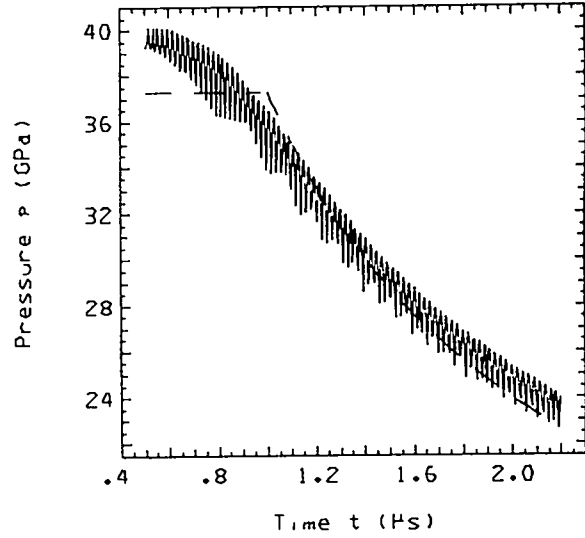
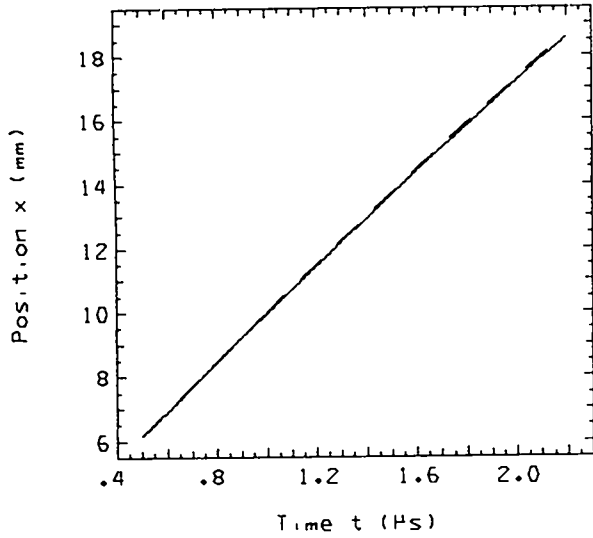


Fig. 8 (cont)

7. DECEL. SHOCK FROM HE. Q = 0.3, 0 / TIME = 2.0000E+00

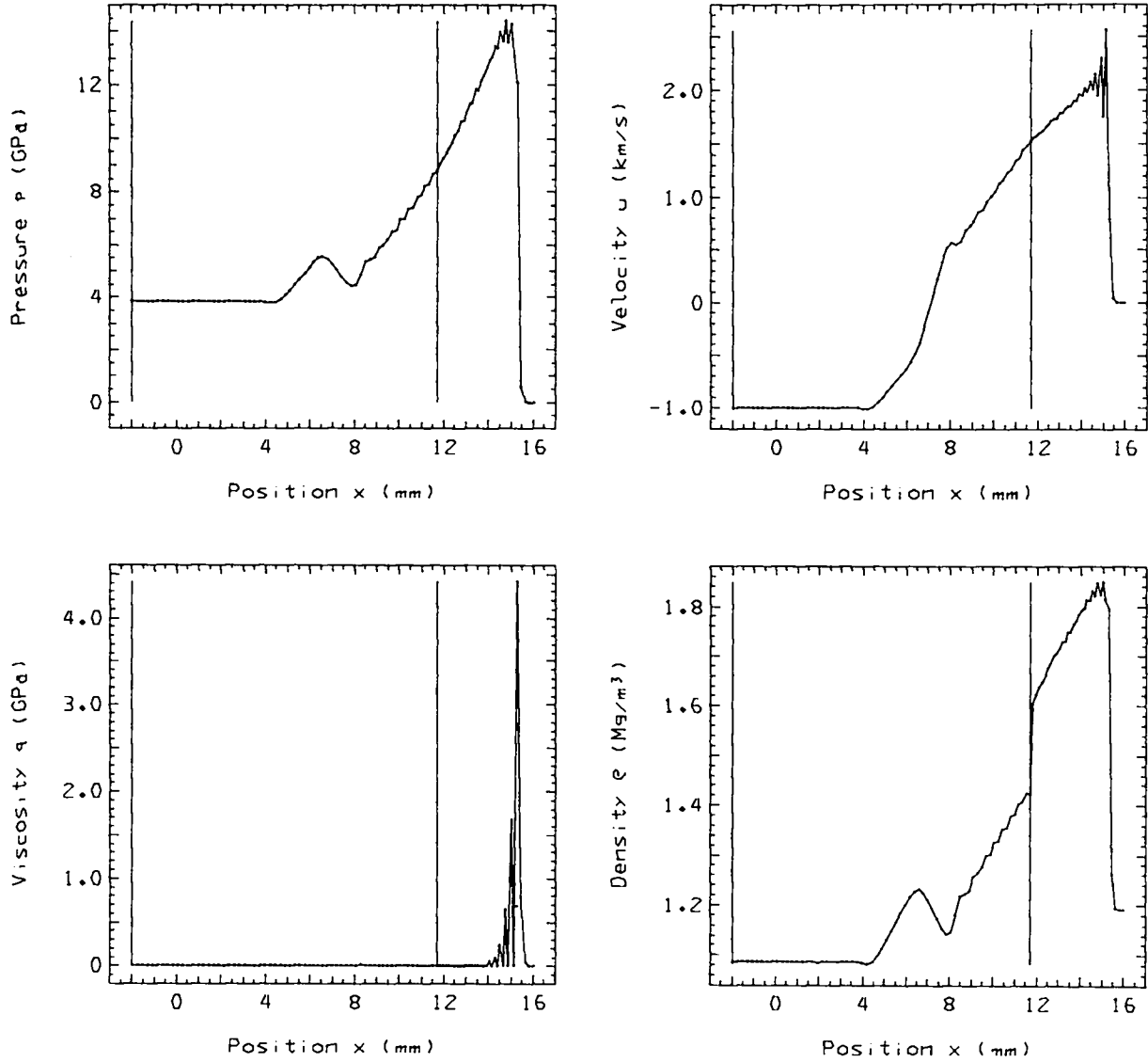


Fig. 9.
Problem 7. $q = 0.3, 0$, linear underdamped.

7. DECEL. SHOCK FROM HE, Q = 0.3, 0 / PARTICLES

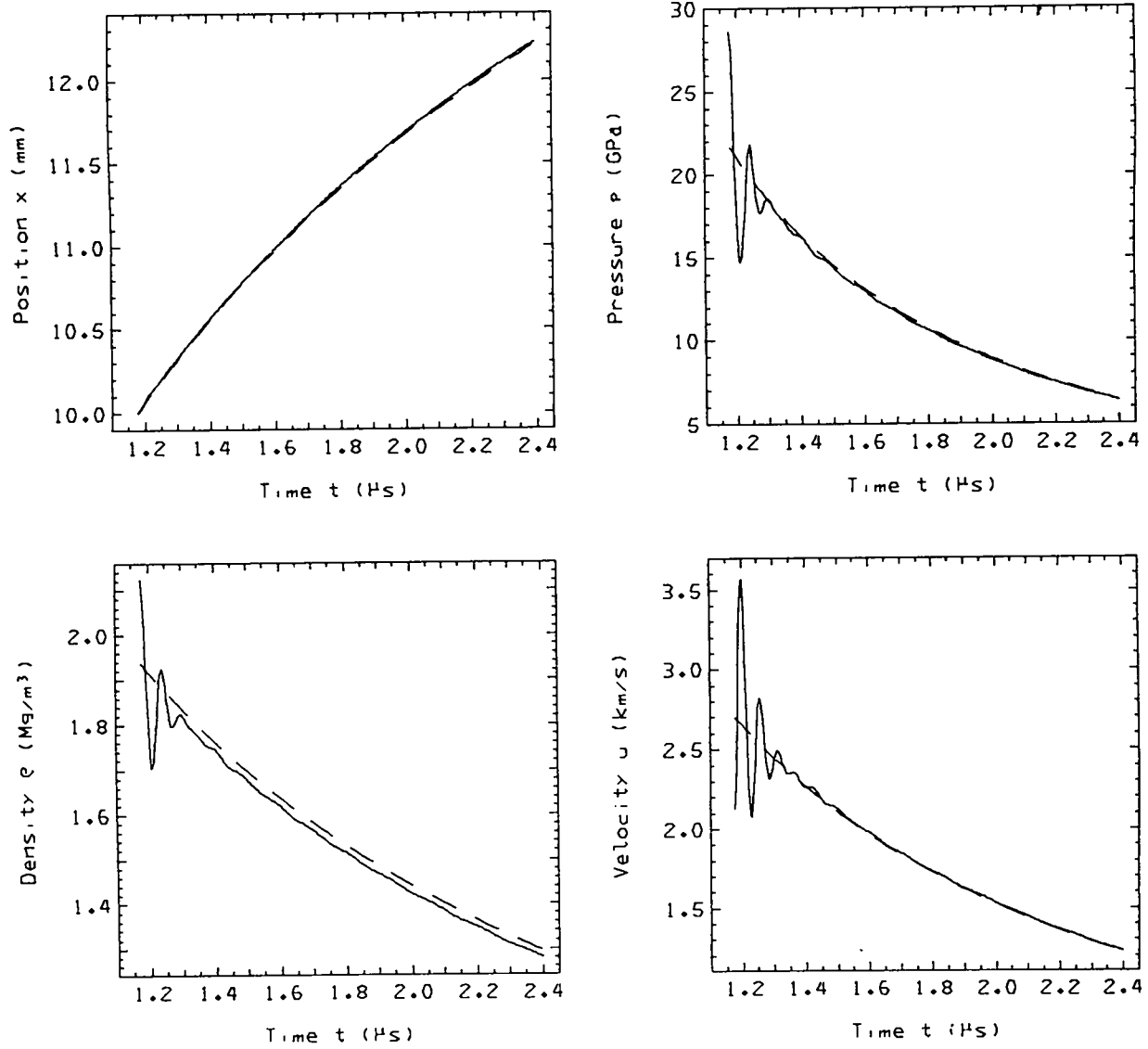


Fig. 9 (cont)

7. DECEL. SHOCK FROM HE, Q = 0.3, 0 / DIFFERENCE, TRUNCATED TIME / PARTICLES

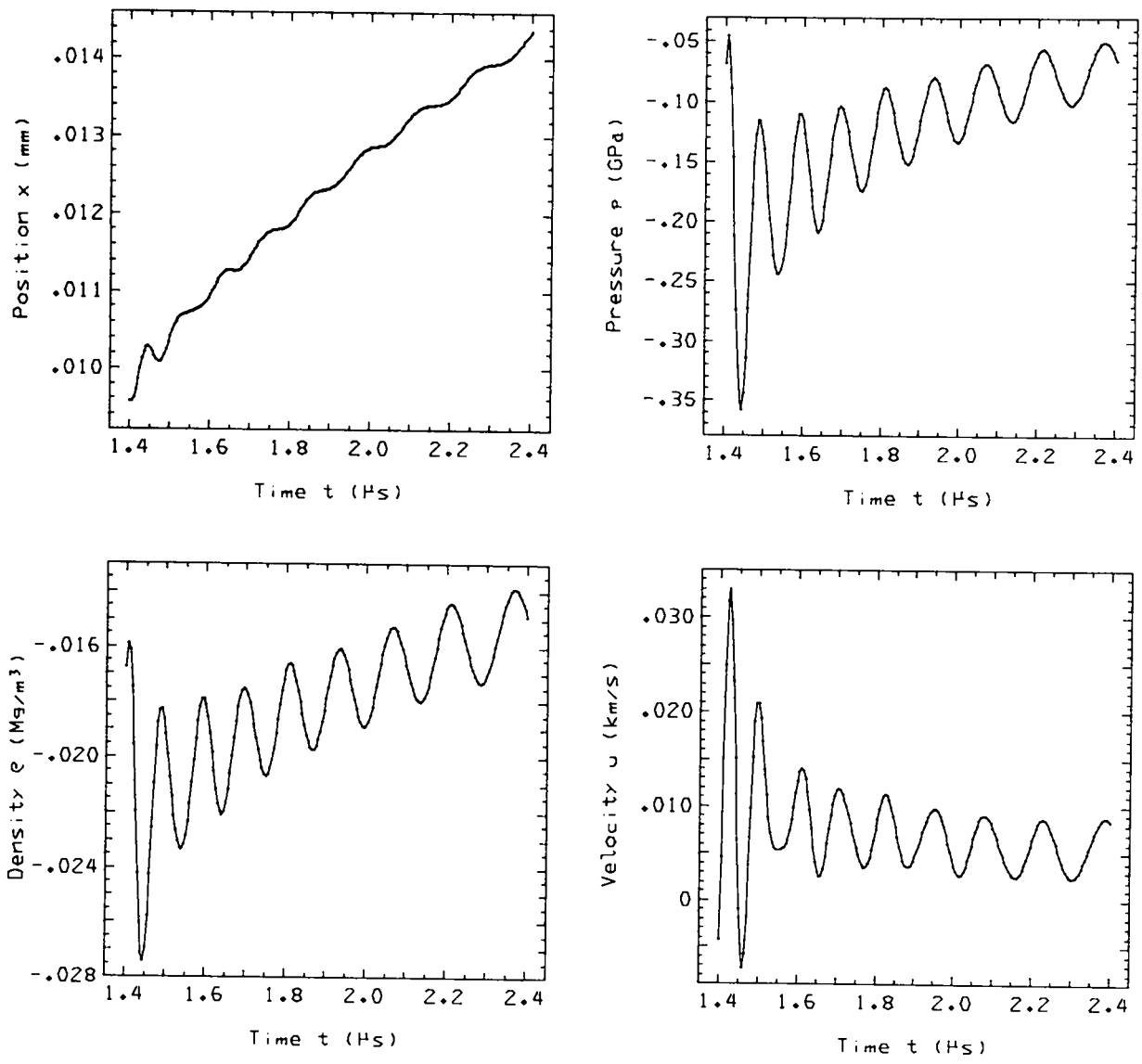


Fig. 9 (cont)

7. DECEL. SHOCK FROM HE, Q = 0.3, 0 / LEAD SHOCK

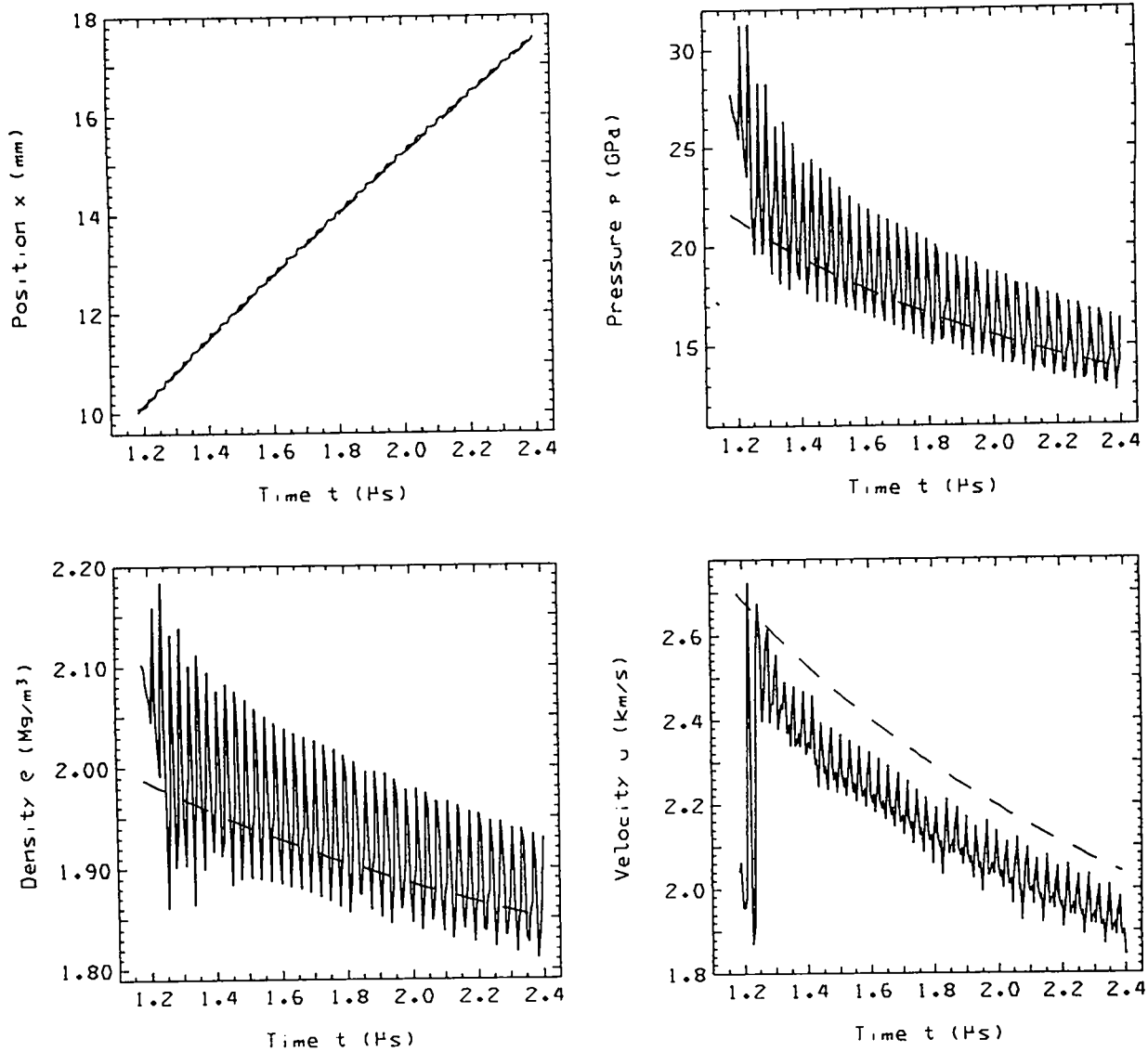


Fig. 9 (cont)

7. DECEL. SHOCK FROM HE. Q = 0.5, 0 / TIME= 2.0000E+00

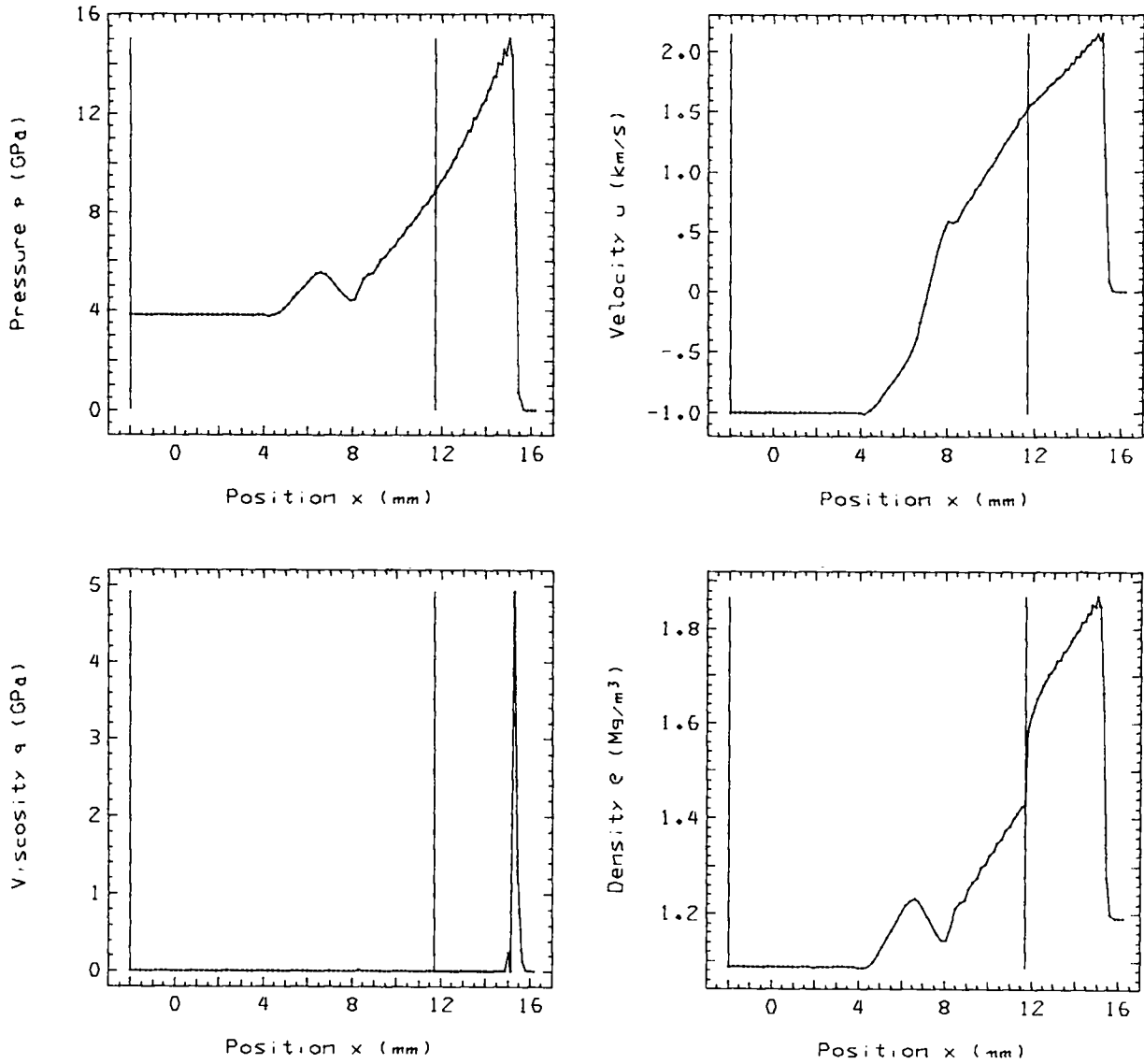


Fig. 10.
Problem 7. $q = 0.5, 0$, linear critically damped.

7. DECEL. SHOCK FROM HE. $\theta = 0.5, 0$ / PARTICLES

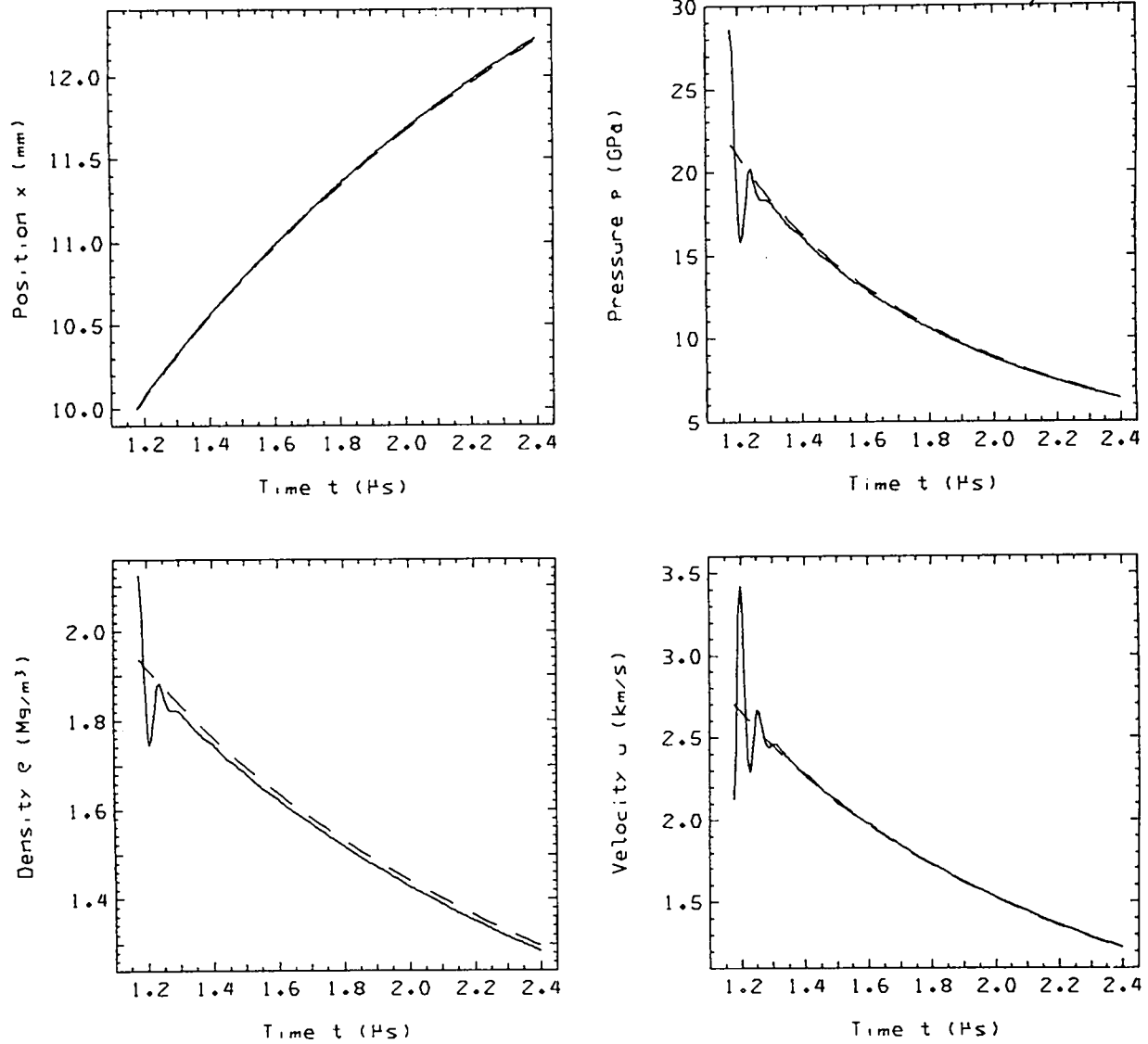


Fig. 10 (cont)

7. DECEL. SHOCK FROM HE, Q = 0.5, 0 / DIFFERENCE, TRUNCATED TIME / PARTICLES

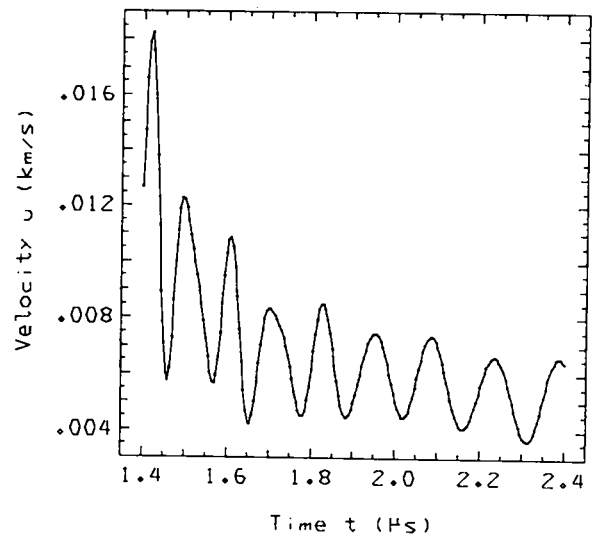
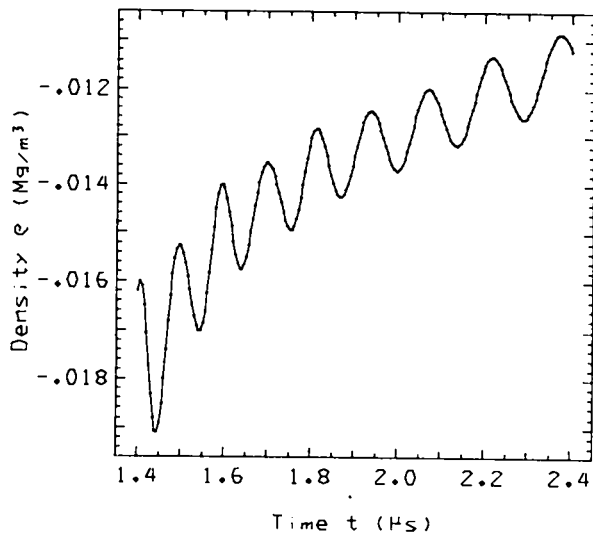
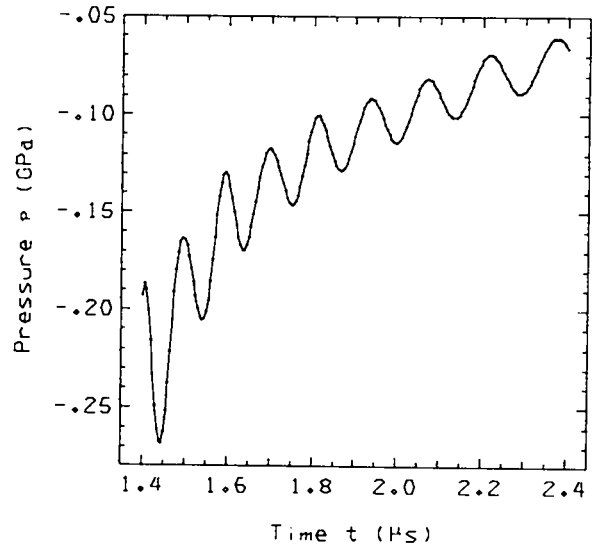
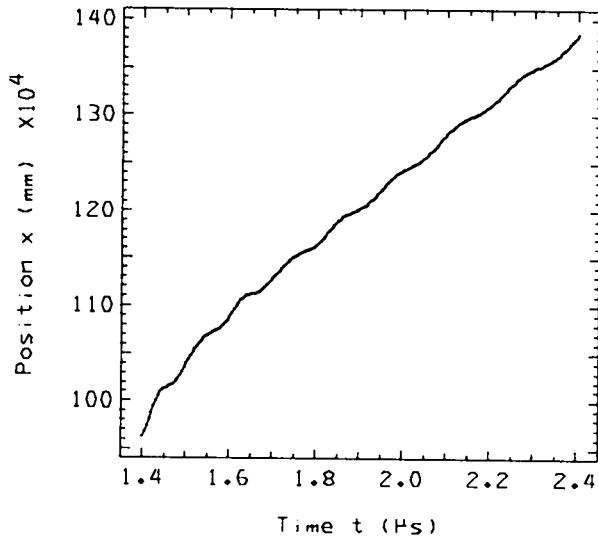


Fig. 10 (cont)

7. DECEL. SHOCK FROM HE, Q = 0.5, 0 / LEAD SHOCK

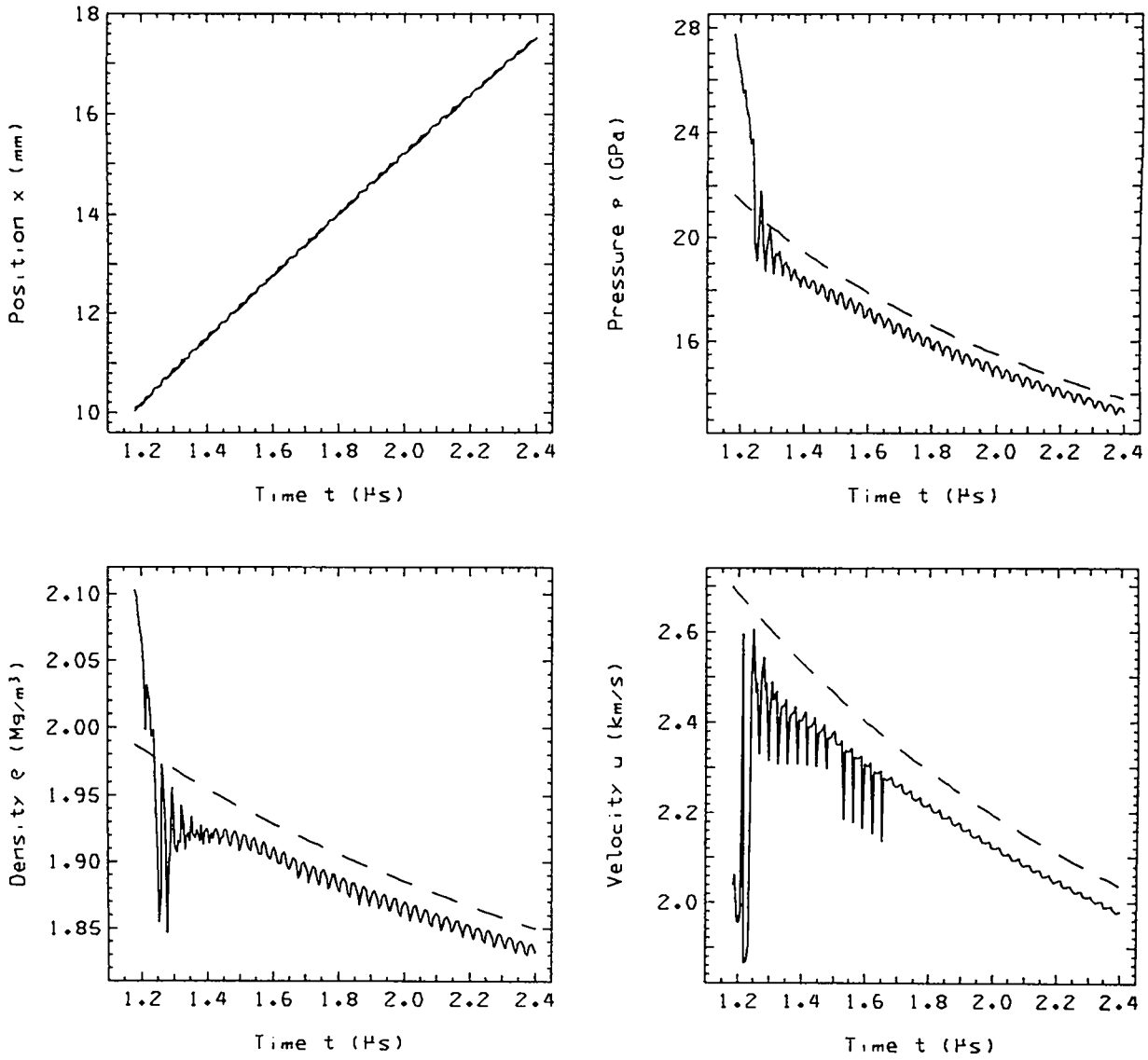


Fig. 10 (cont)

7. DECEL. SHOCK FROM HE, Q = 0.7, 0 / TIME= 2.0000E+00

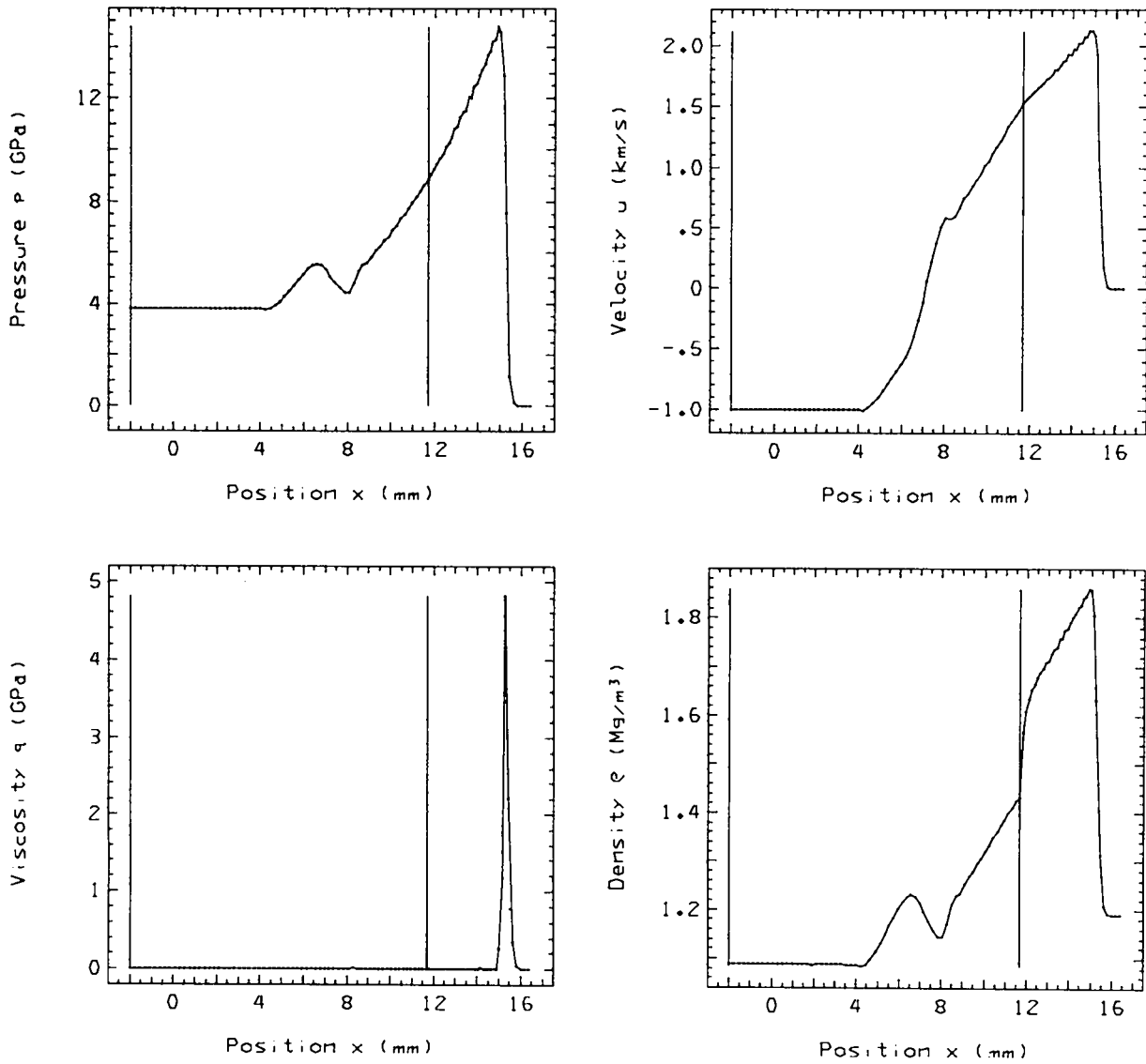


Fig. 11.
Problem 7. $q = 0.7, 0$, linear overdamped.

7. DECEL. SHOCK FROM HE, $\theta = 0.7, 0^\circ$ / PARTICLES

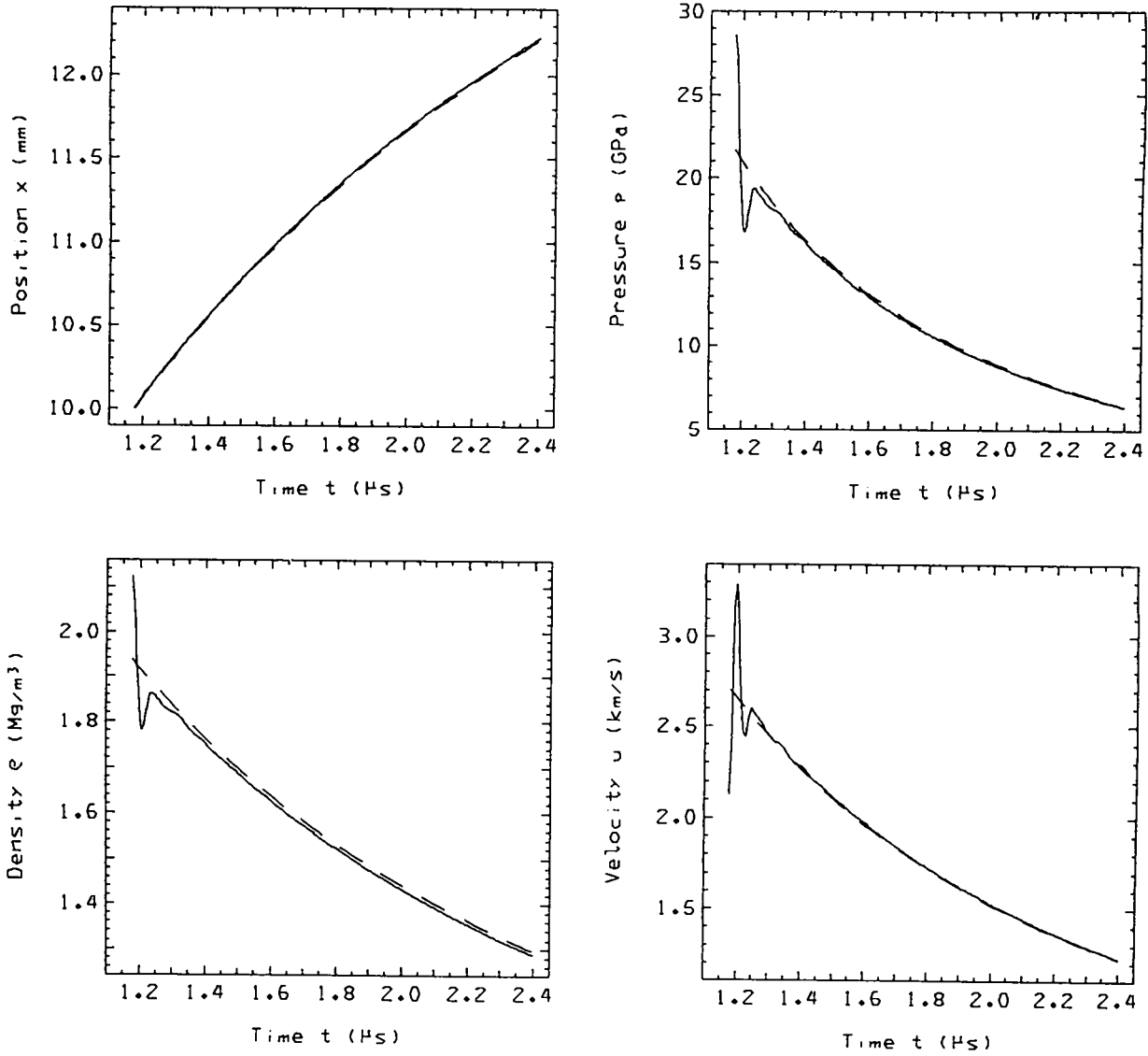


Fig. 11 (cont)

7. DECEL. SHOCK FROM HE, Q = 0.7, 0 / DIFFERENCE. TRUNCATED TIME / PARTICLES

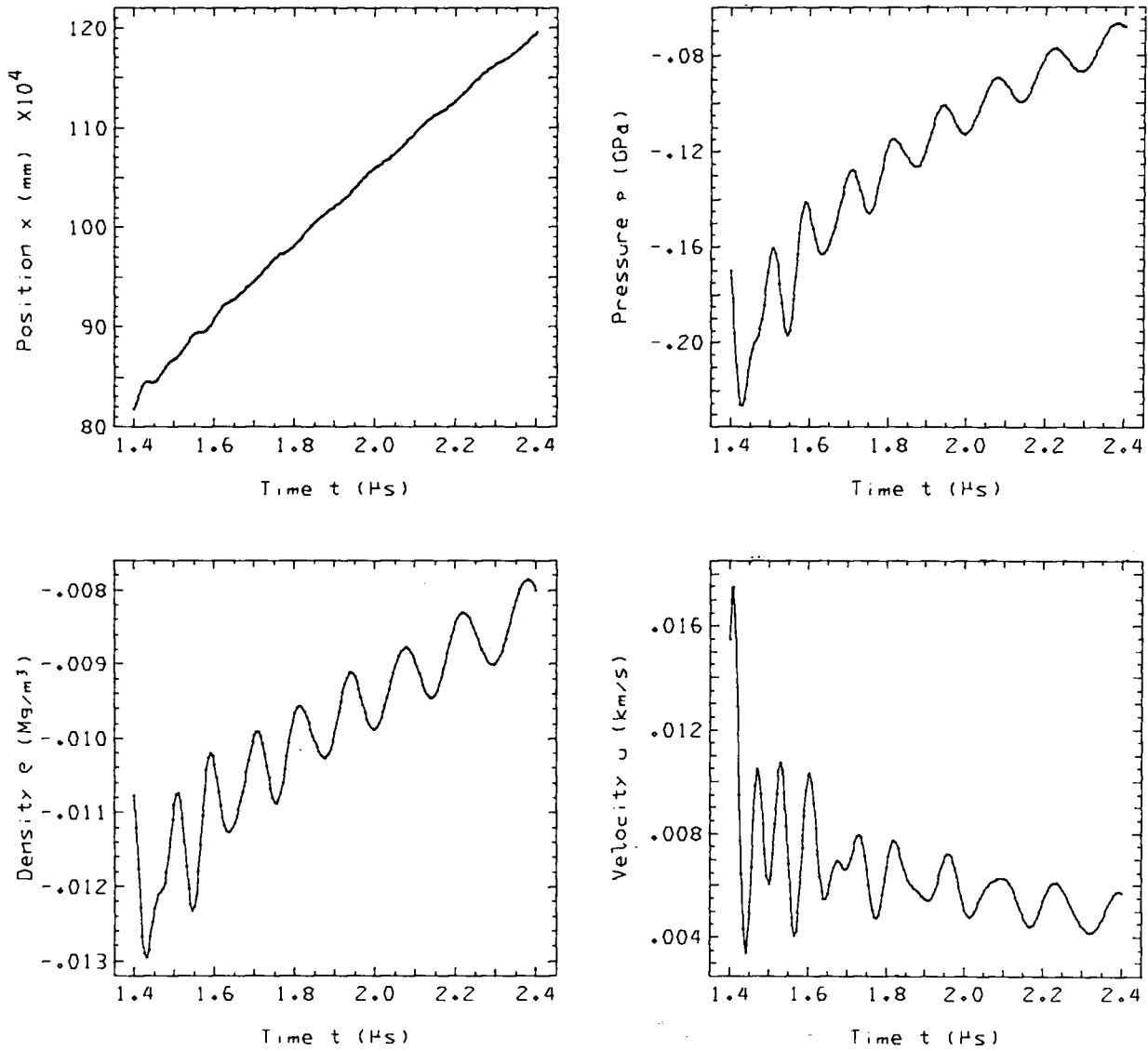


Fig. 11 (cont)

7. DECEL. SHOCK FROM HE, $\theta = 0.7, 0^\circ$ / LEAD SHOCK

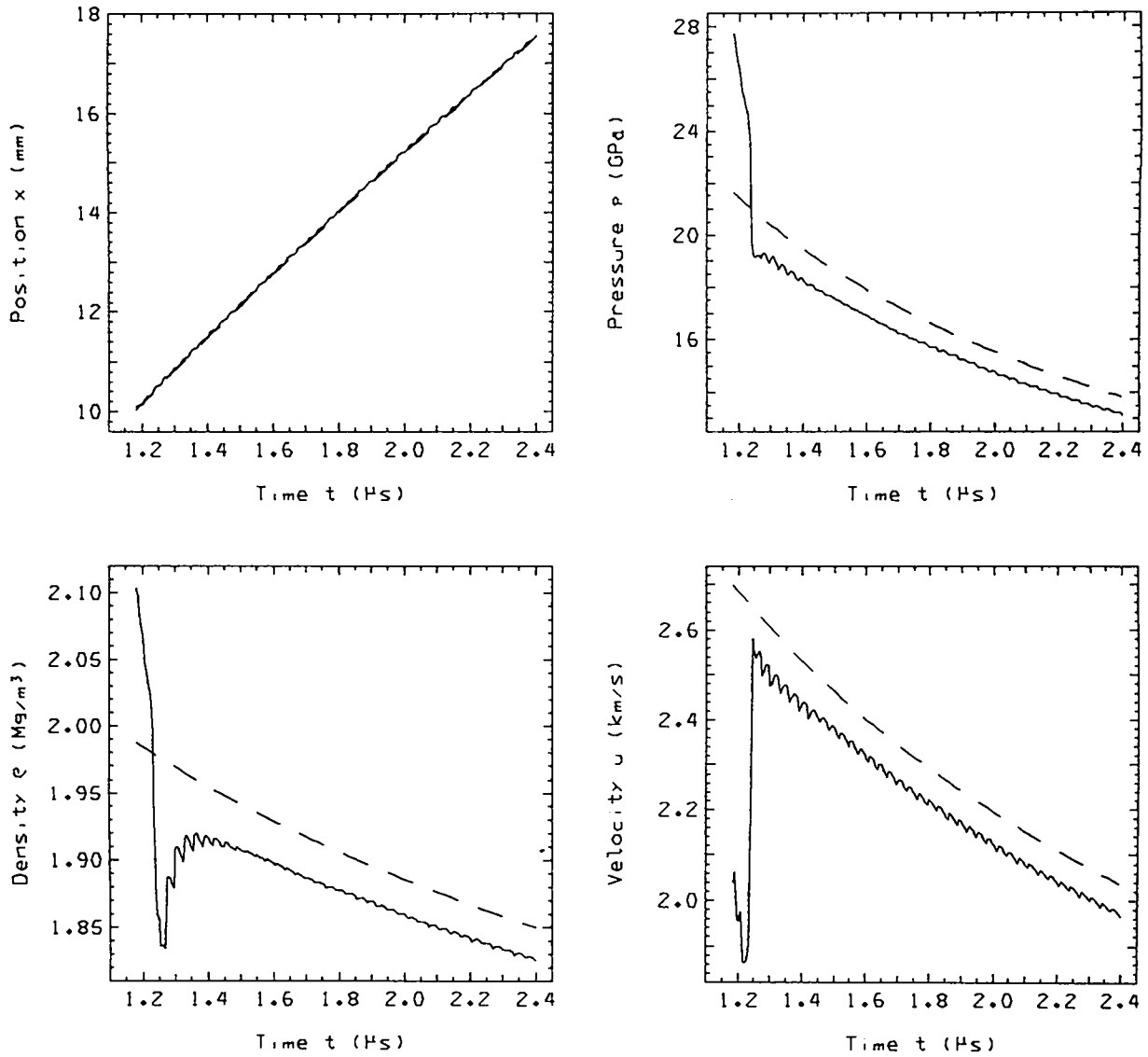


Fig. 11 (cont)

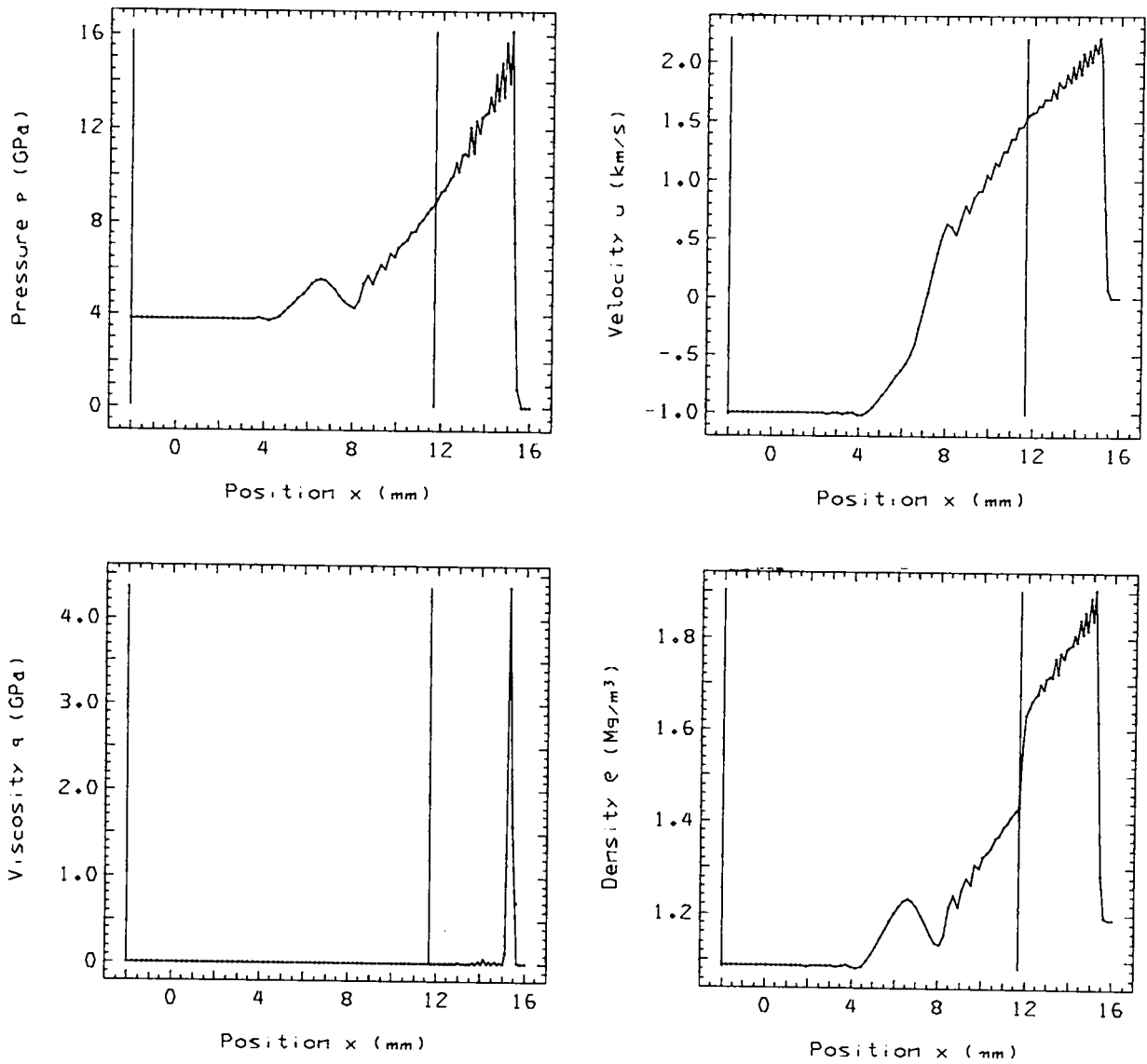


Fig. 12.
Problem 7. $q = 0, 1.414$, quadratic.

7. DECEL. SHOCK FROM HE, Q = 0, 1.414 / PARTICLES

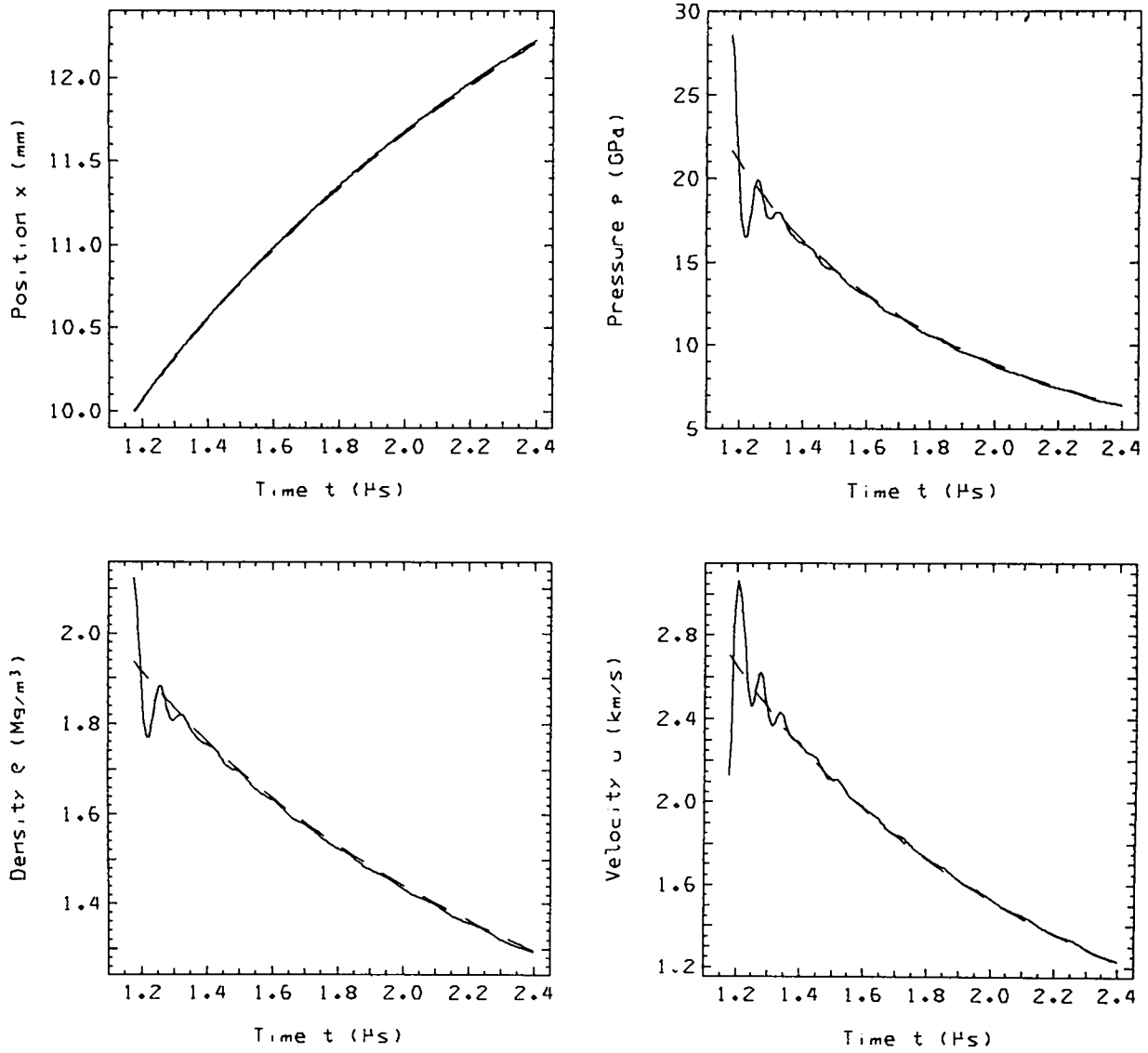


Fig. 12 (cont)

PAD3.3F6 - 75JUL14 RUN 9 LAG2 *7. DECEL. SHOCK FROM HE, Q = 0, 1.414* ERUN 4, 128 CELLS 07/22/75
 TFICKETIAW, 5.722 SEC ON RUN, 78.655 SEC ON JOB
 7. DECEL. SHOCK FROM HE, Q = 0, 1.414 / DIFFERENCE, TRUNCATED TIME / PARTICLES

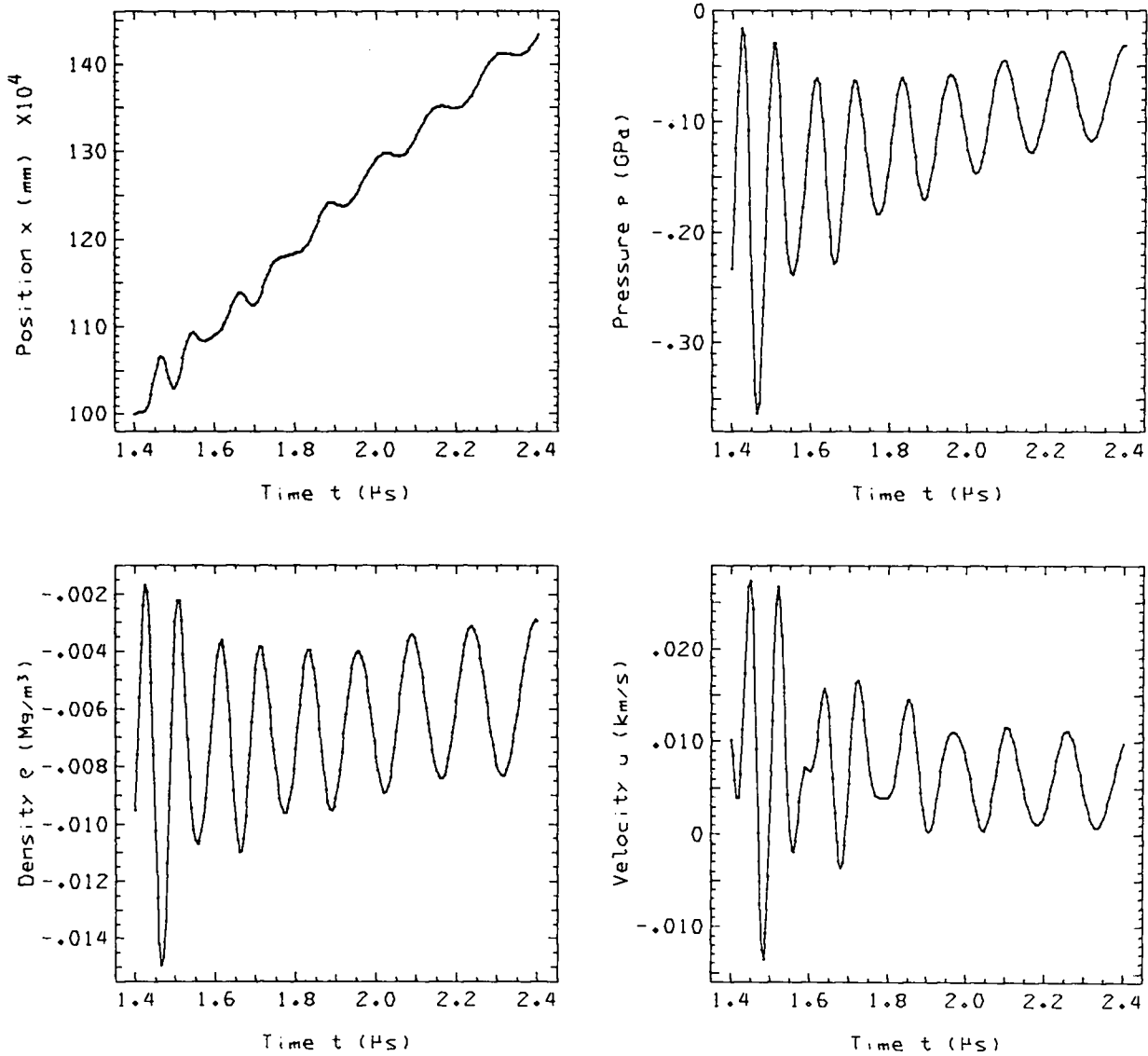


Fig. 12 (cont)

7. DECEL. SHOCK FROM HE, $Q = 0.1414$ / LEAD SHOCK

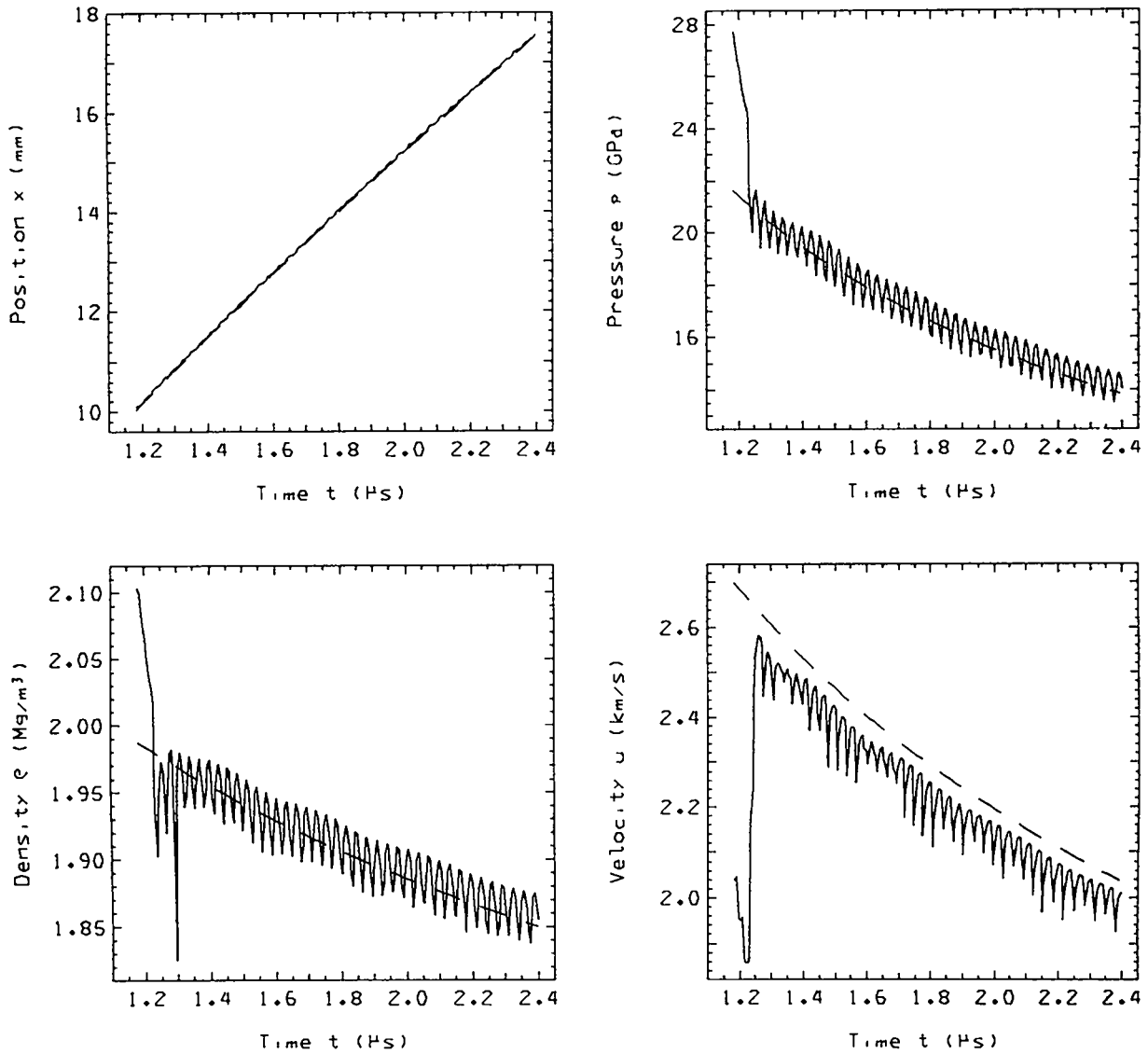


Fig. 12 (cont)

7. DECEL. SHOCK FROM HE. Q = 0. 0. 2 / TIME = 2.0000E+00

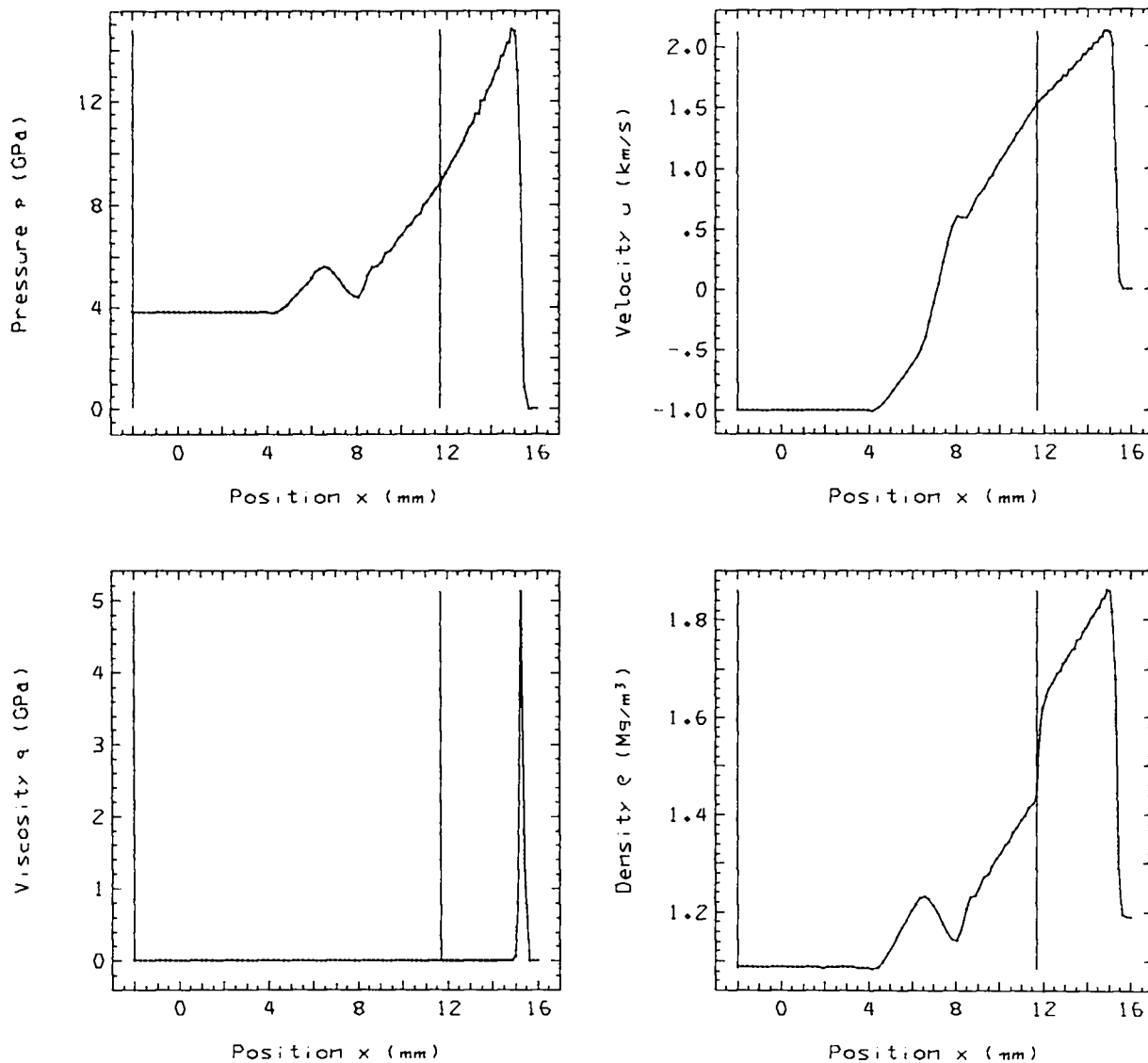


Fig. 13.
Problem 7. $q = 0, 0, 2$, PIC.

7. DECEL. SHOCK FROM HE, Q = 0. 0. 2 / PARTICLES

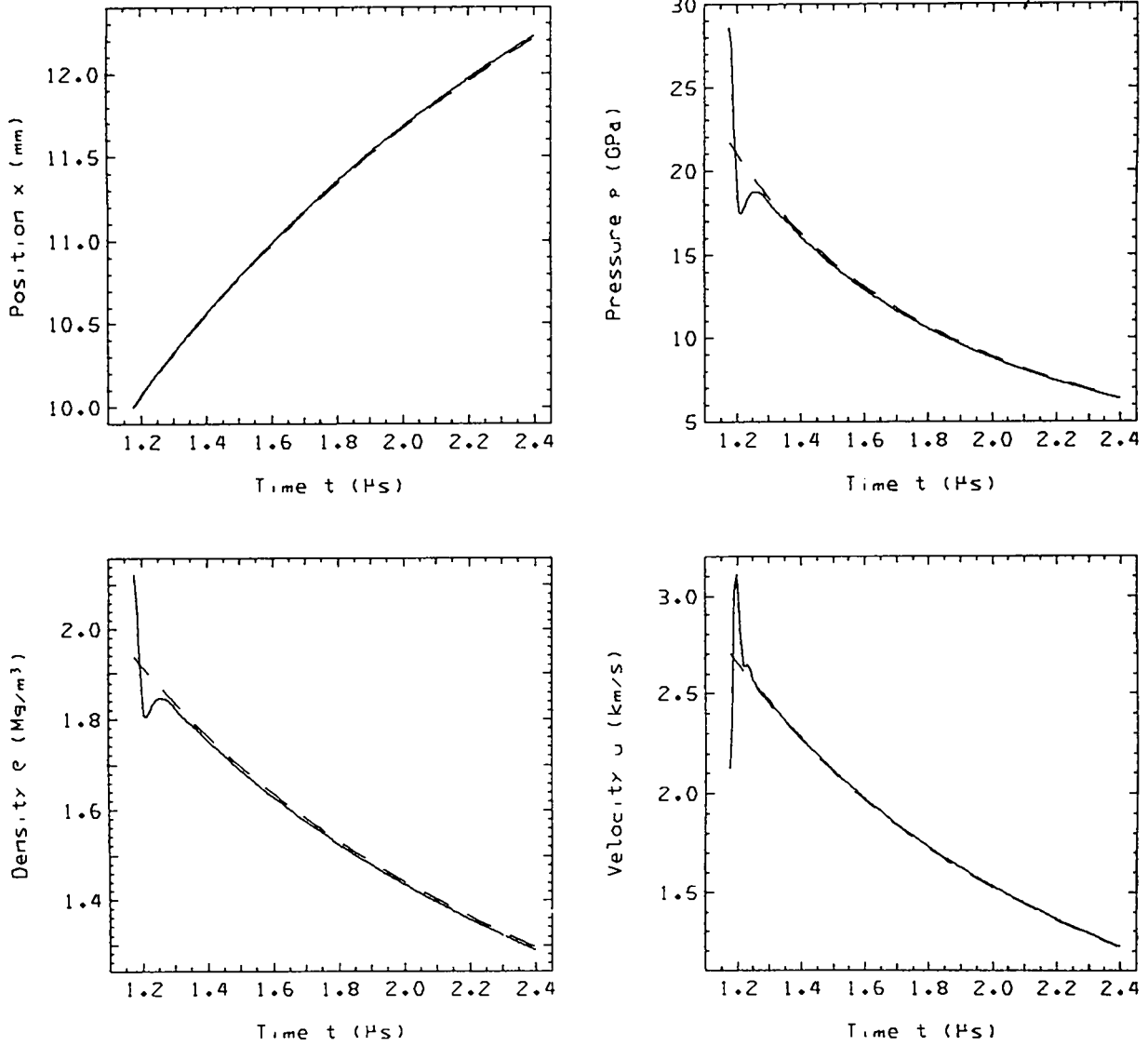


Fig. 13 (cont)

PAD3.3F6 - 75JUL14 RUN11 LAC2 *7. DECEL. SHOCK FROM HE, Q = 0, 0, 2* ERUN 4, 128 CELLS 07/22/75
TFICKETIAW, 5.747 SEC ON RUN, 97.882 SEC ON JOB
7. DECEL. SHOCK FROM HE, Q = 0, 0, 2 / DIFFERENCE, TRUNCATED TIME / PARTICLES

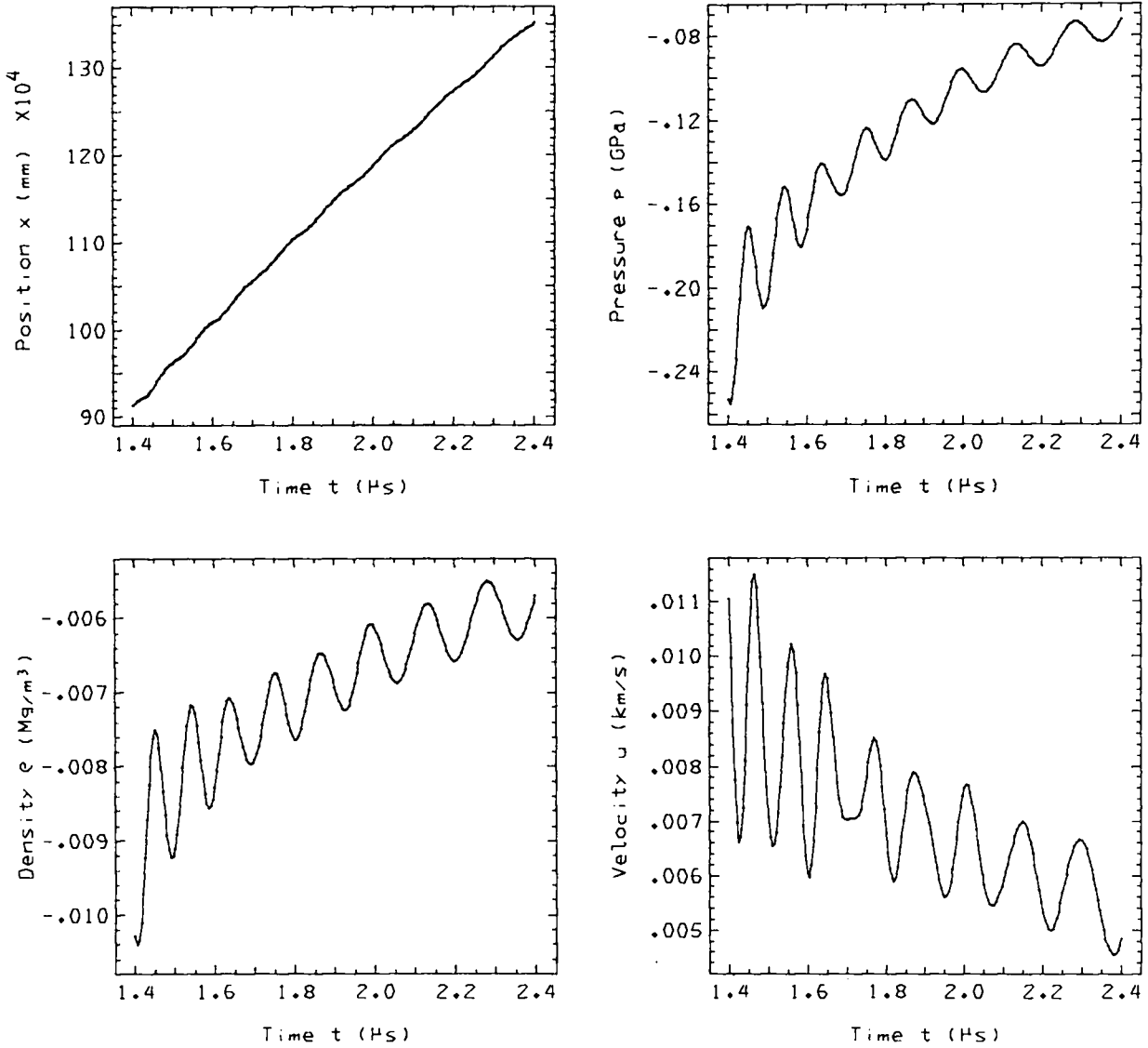


Fig. 13 (cont)

7. DECEL. SHOCK FROM HE, Q = 0, 0, 2 / LEAD SHOCK

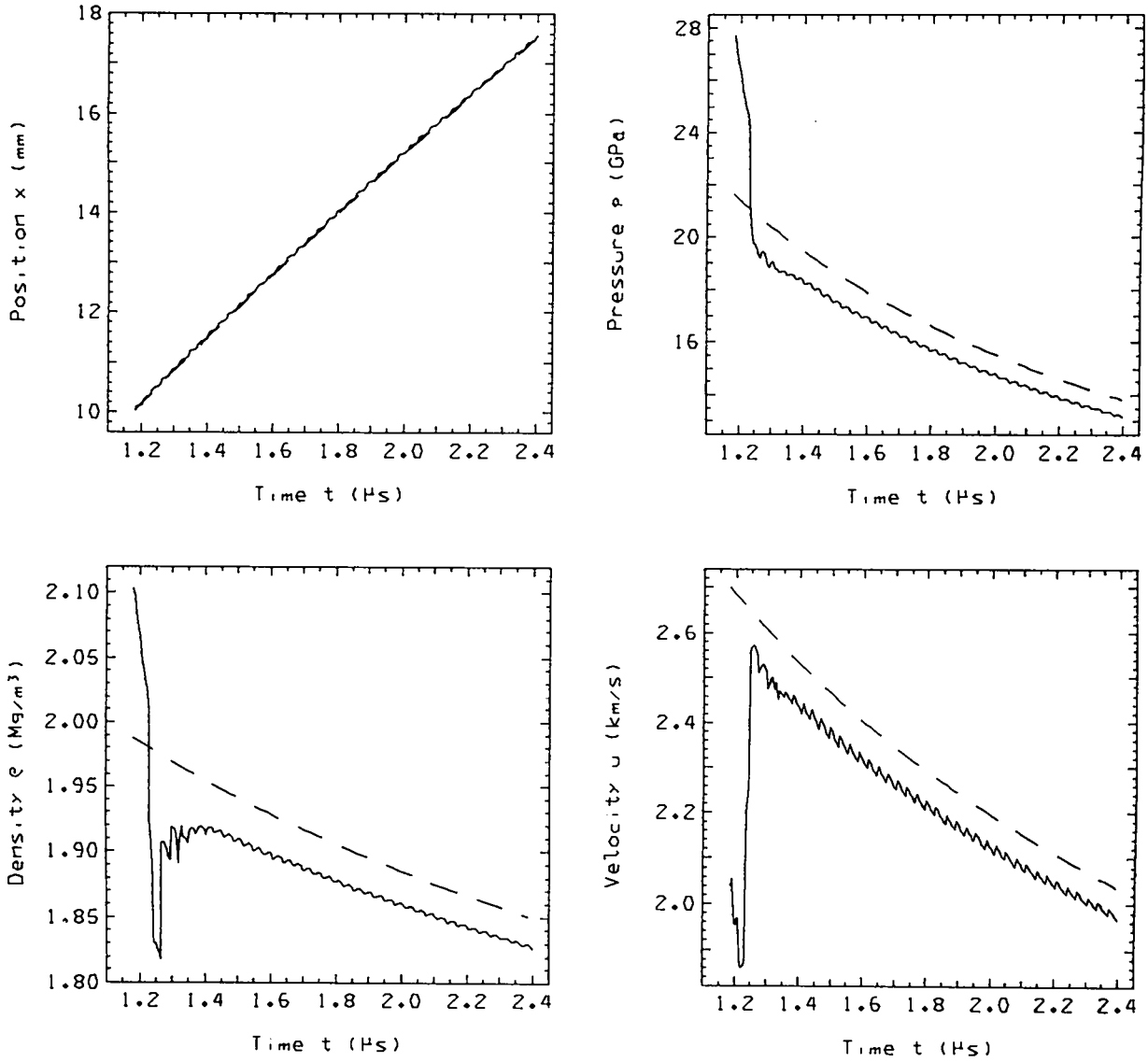


Fig. 13 (cont)

7. DECEL. SHOCK FROM HE. HALF DEL T / TIME= 2.0000E+00

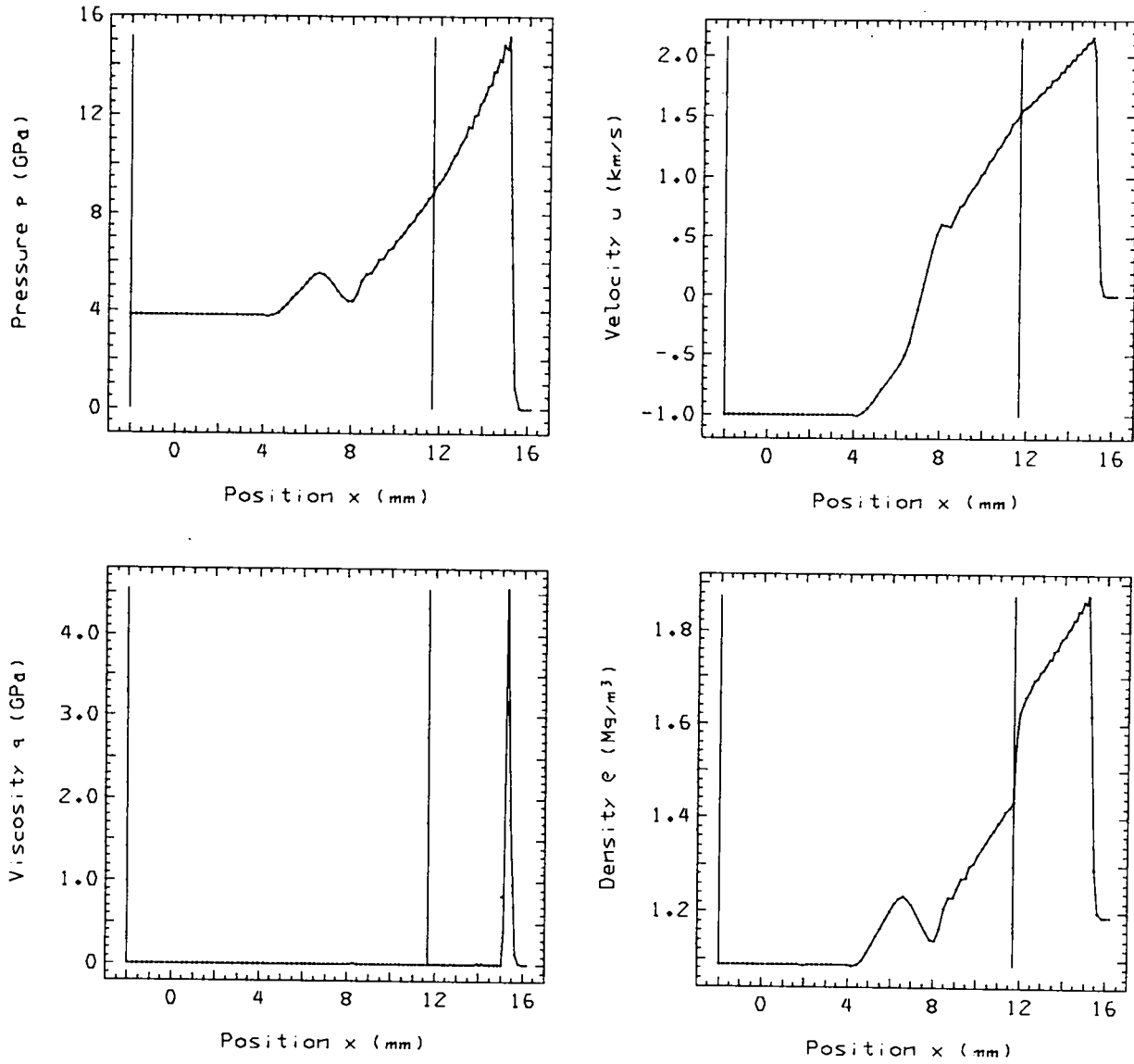


Fig. 14.
Problem 7. Δt halved.

7. DECEL. SHOCK FROM HE, HALF DEL T / PARTICLES

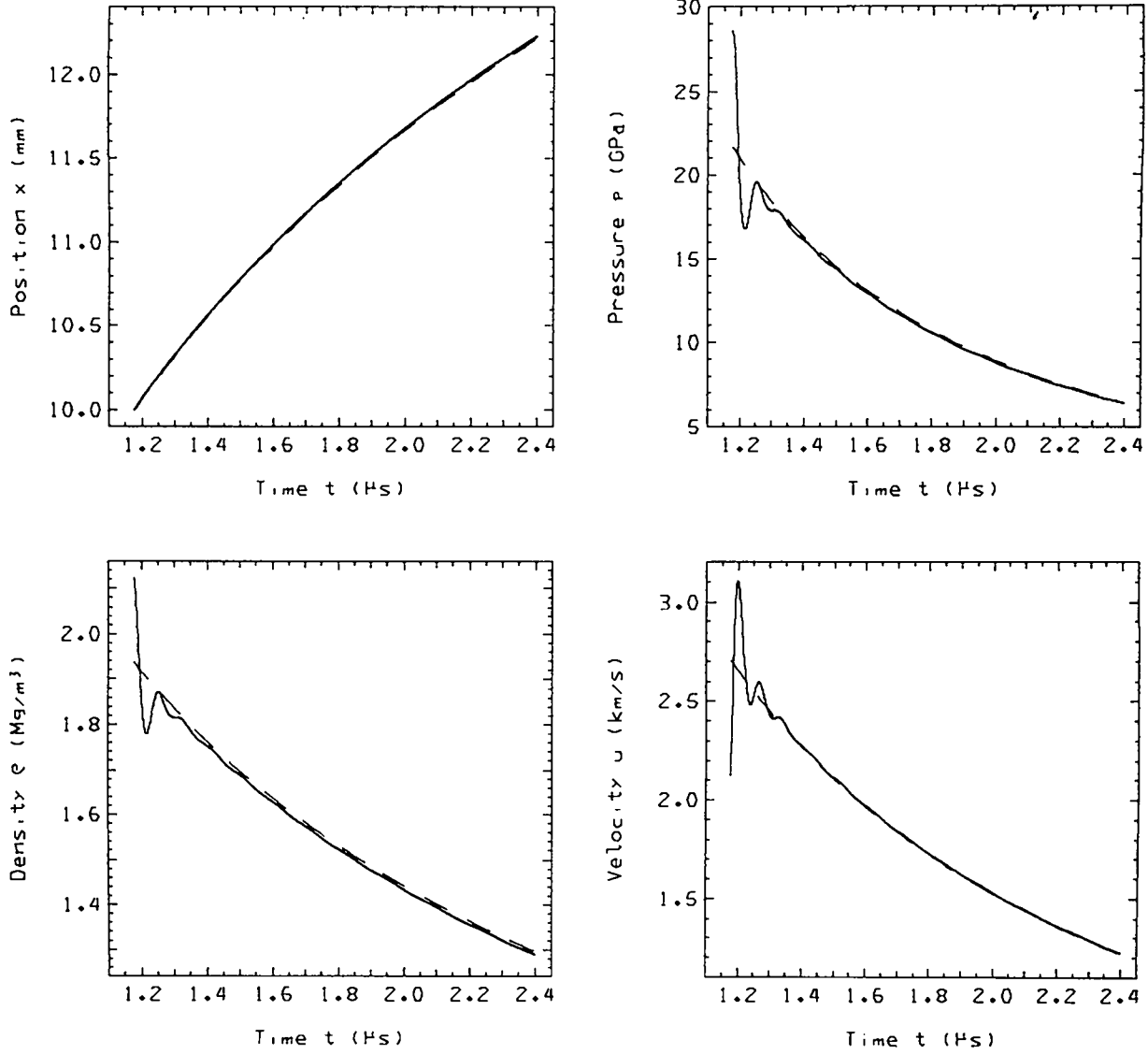


Fig. 14 (cont)

7. DECEL. SHOCK FROM HE, HALF DEL T / DIFFERENCE, TRUNCATED TIME / PARTICLES

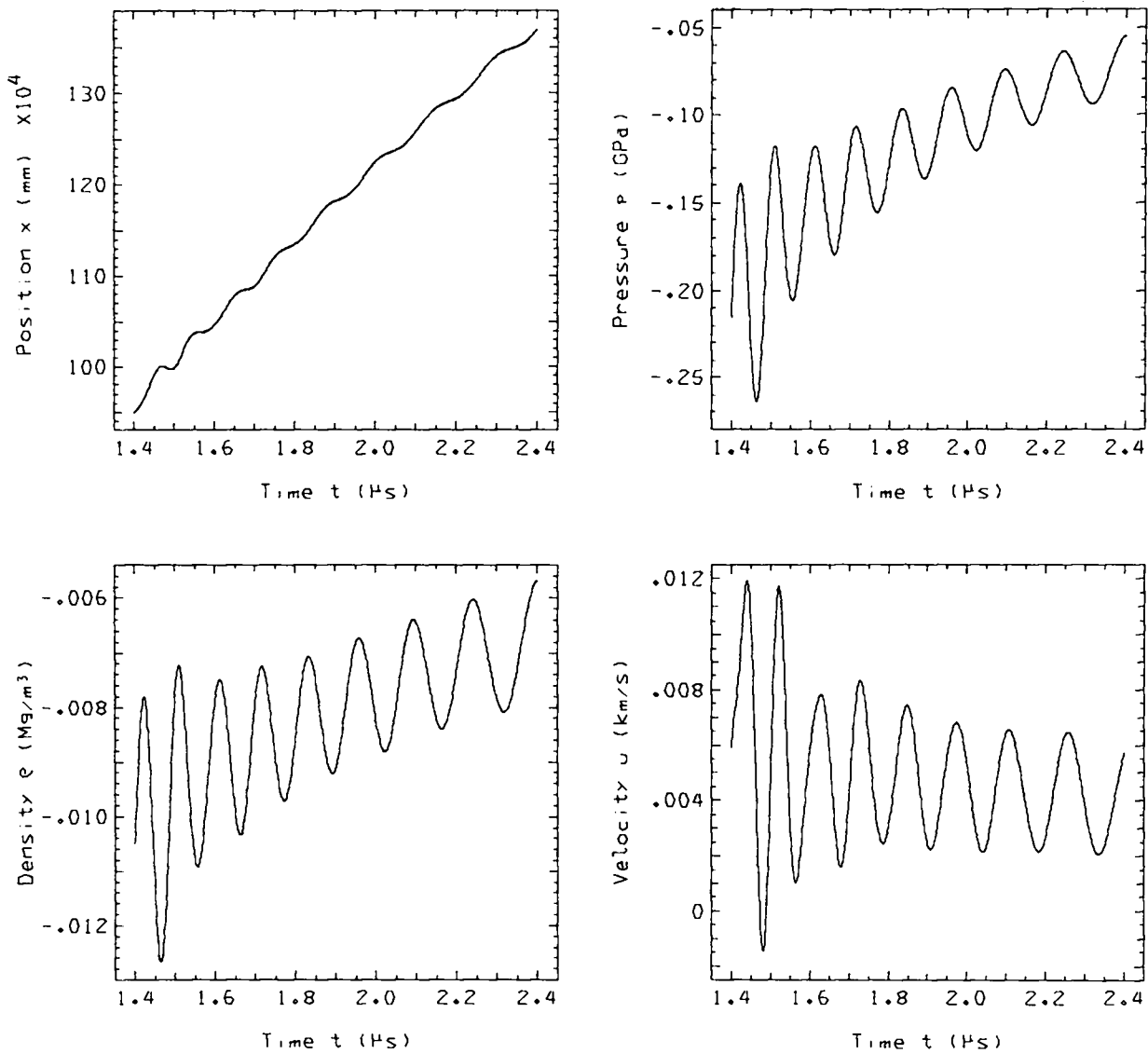


Fig. 14 (cont)

7. DECEL. SHOCK FROM HE, HALF DEL T / LEAD SHOCK

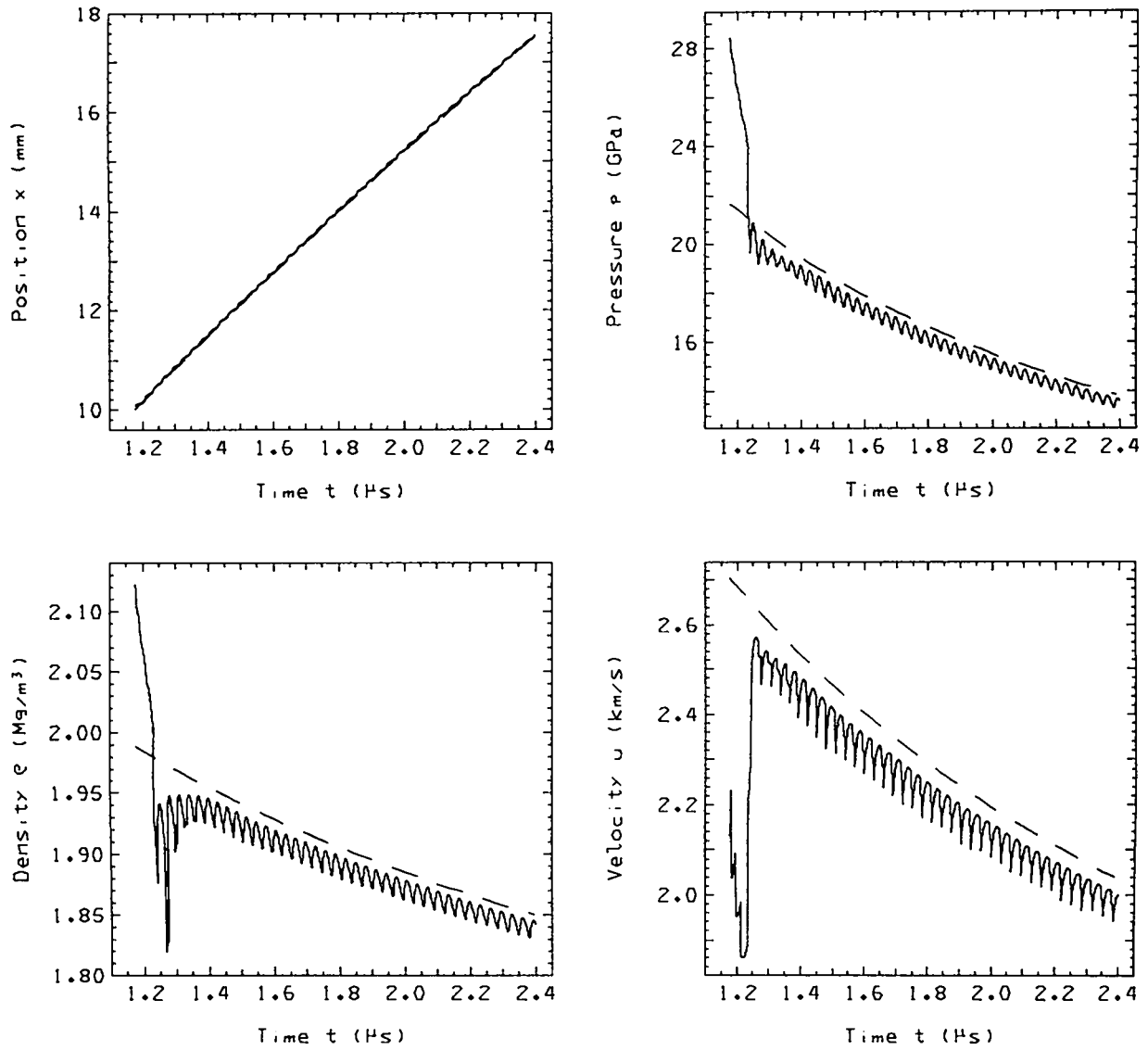


Fig. 14 (cont)

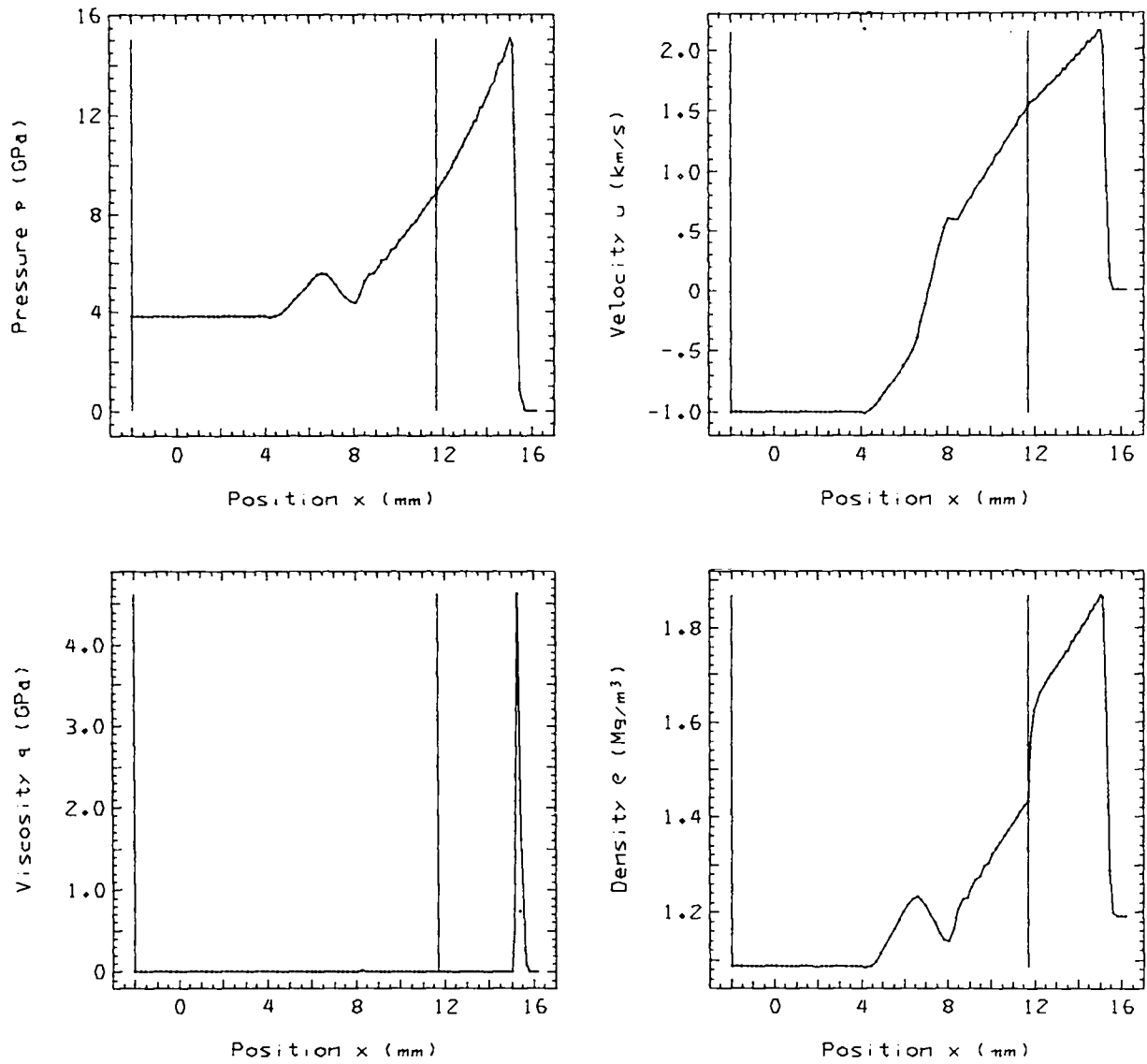


Fig. 15.
 Problem 7. Δt doubled.

7. DECEL. SHOCK FROM HE, TWICE DEL T / PARTICLES

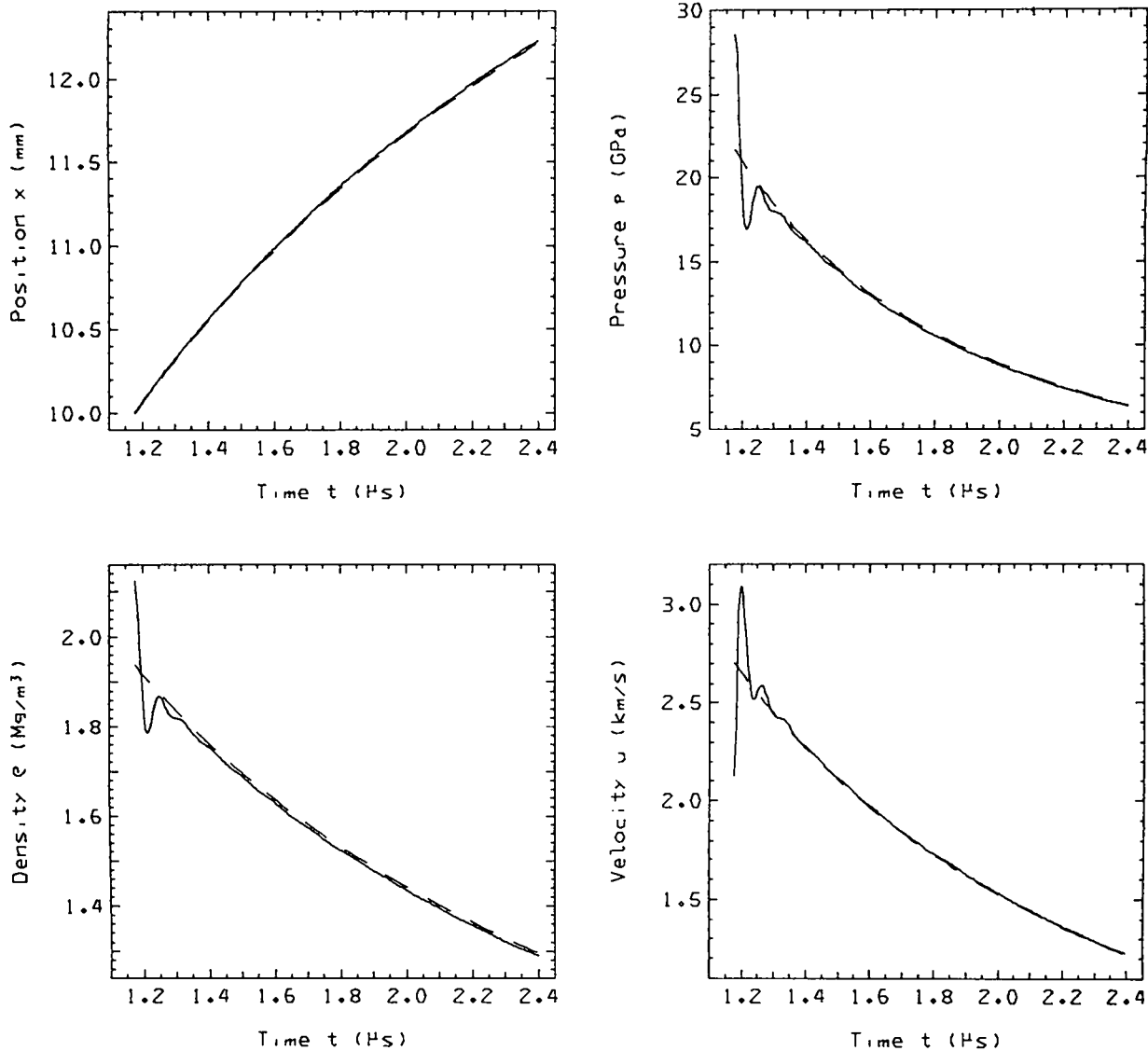


Fig. 15 (cont)

7. DECEL. SHOCK FROM HE. TWICE DEL T / DIFFERENCE, TRUNCATED TIME / PARTICLES

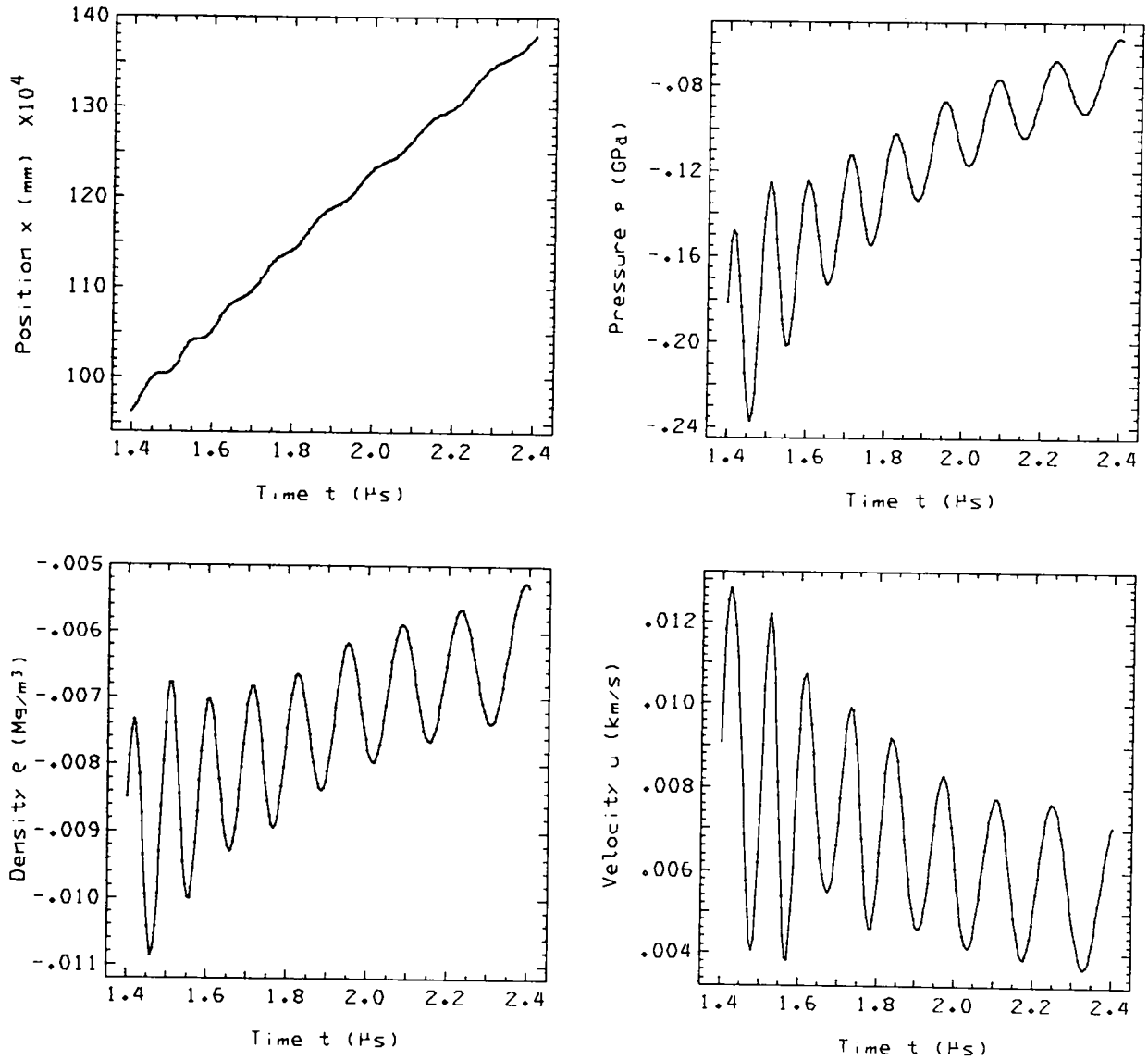


Fig. 15 (cont)

7. DECEL. SHOCK FROM HE, TWICE DEL T / LEAD SHOCK

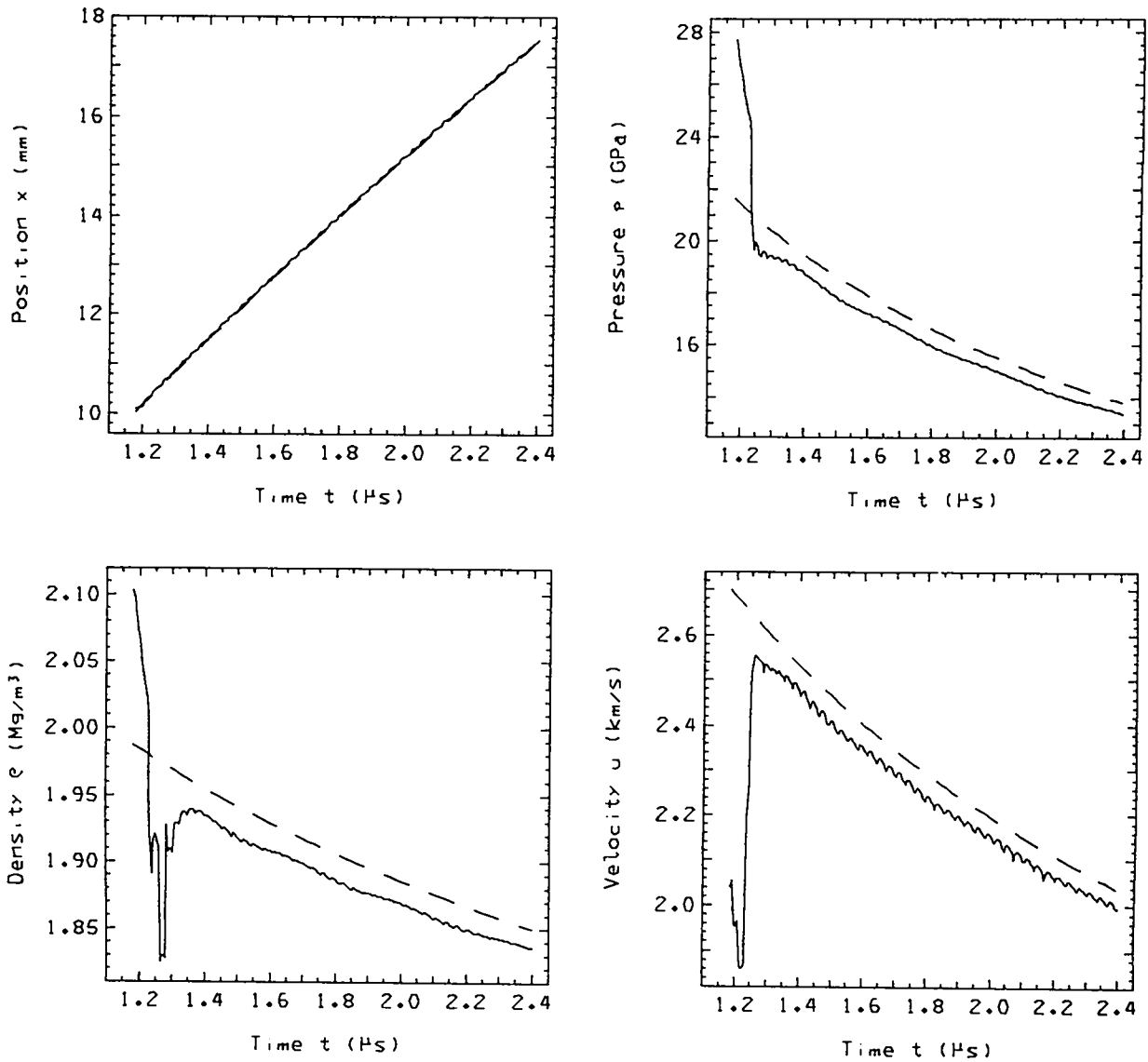


Fig. 15 (cont)

7. DECEL. SHOCK FROM HE, 6/10 CELLS / TIME= 2.0000E+00

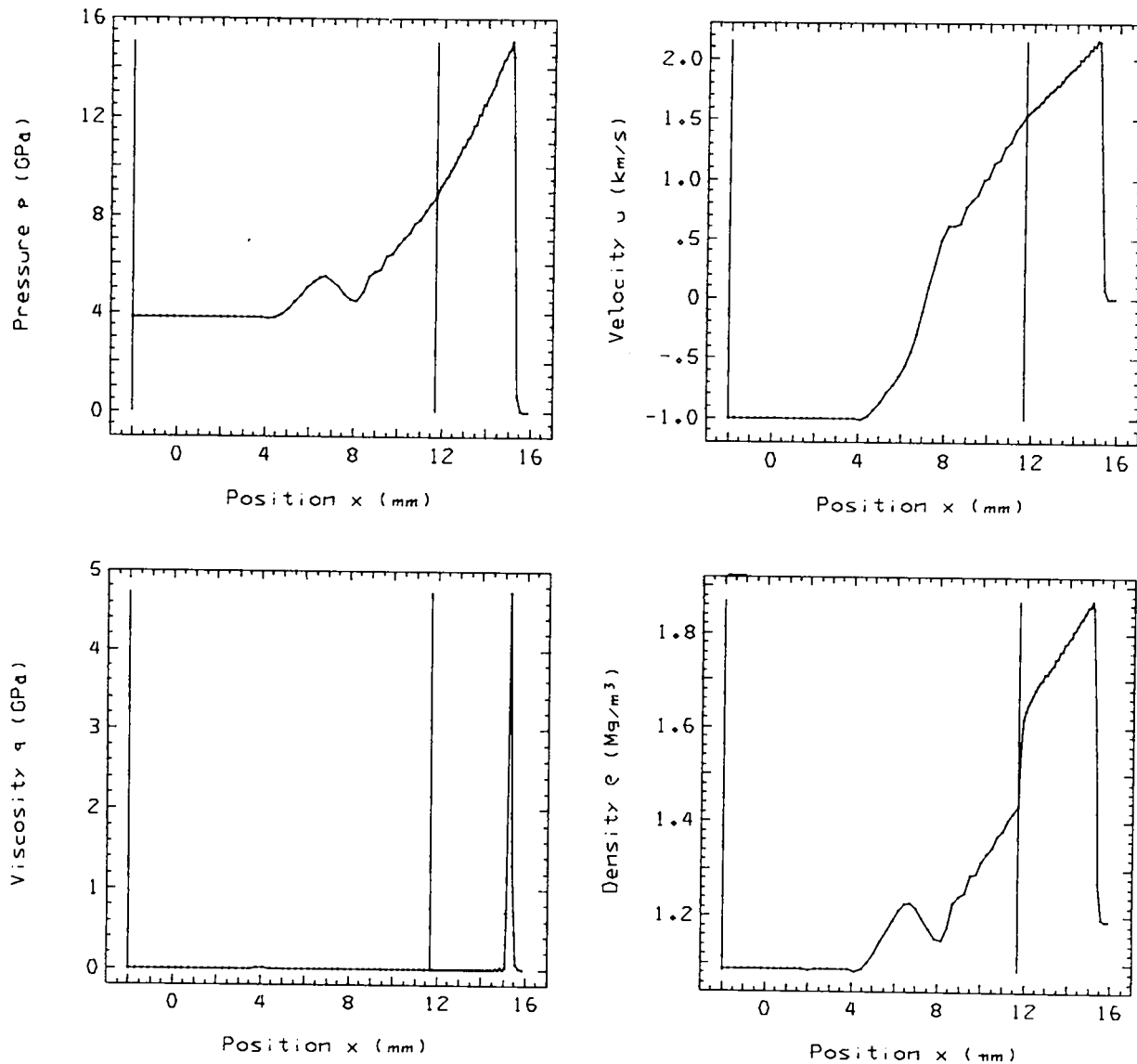


Fig. 16.
Problem 7. 6/10 cells in HE/inert.

7. DECEL. SHOCK FROM HE, 6/10 CELLS / PARTICLES

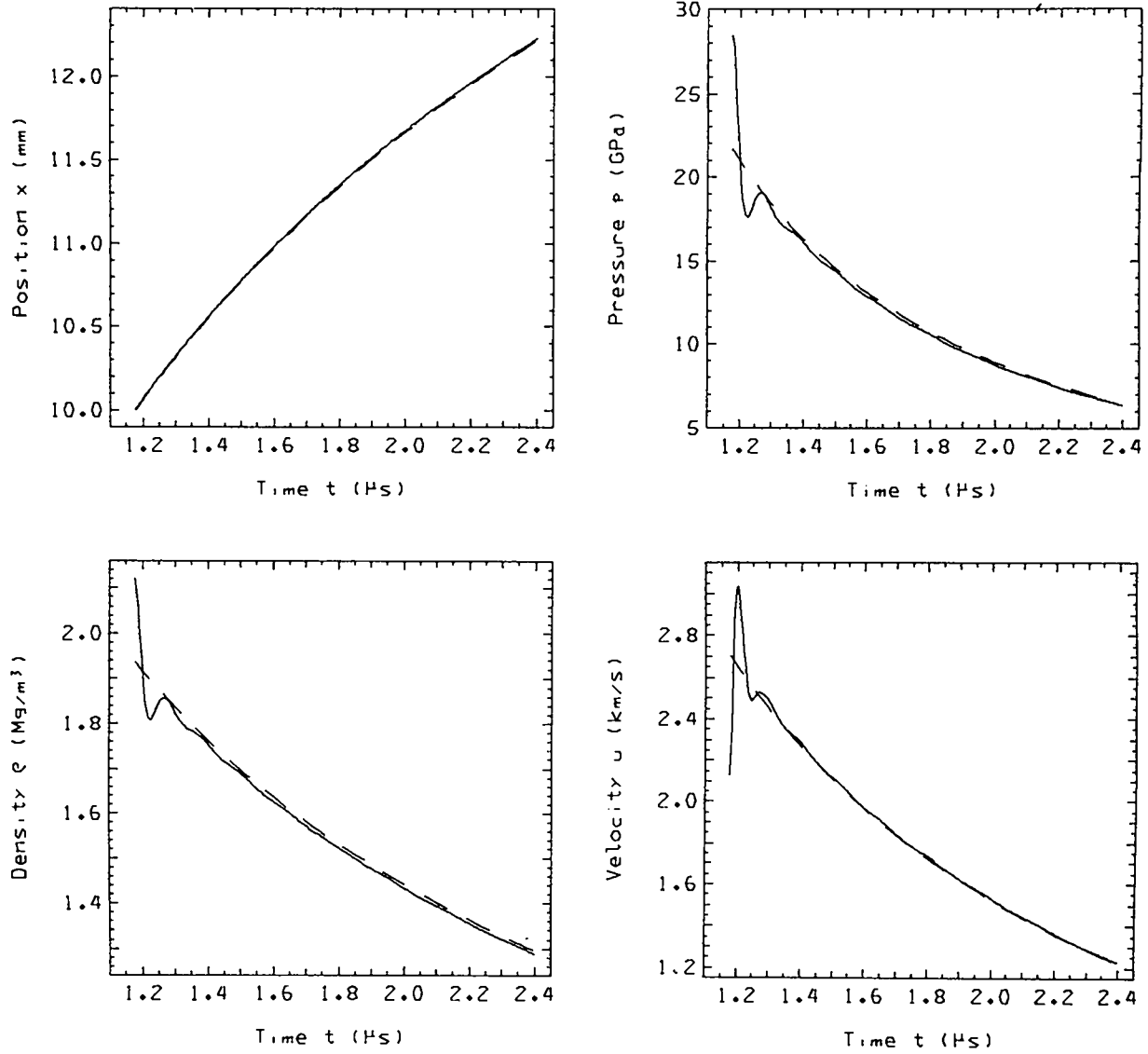


Fig. 16 (cont)

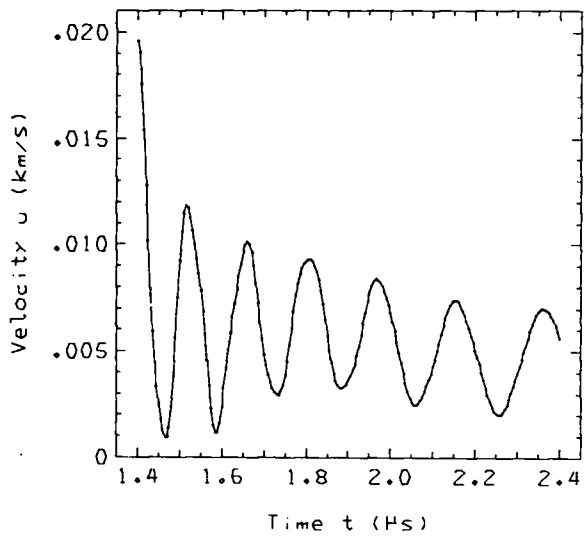
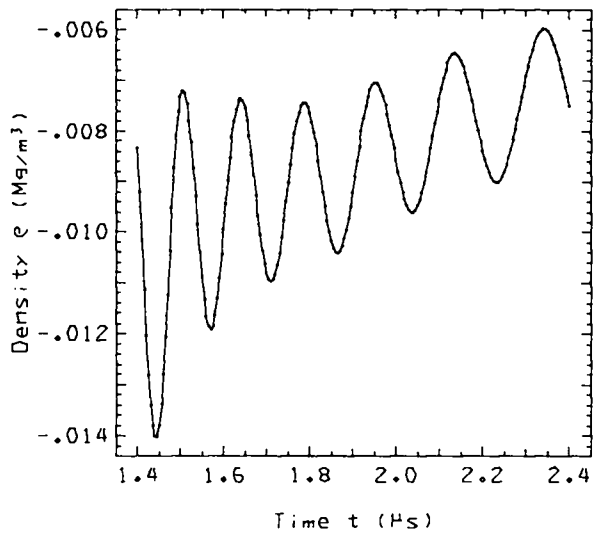
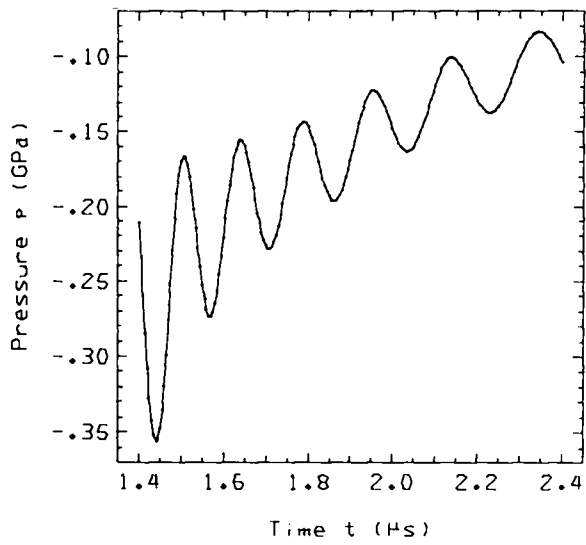
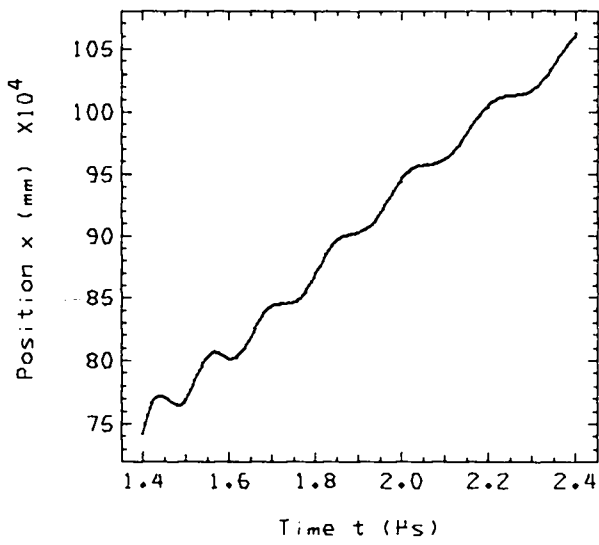


Fig. 16 (cont)

7. DECEL. SHOCK FROM HE, 6/10 CELLS / LEAD SHOCK

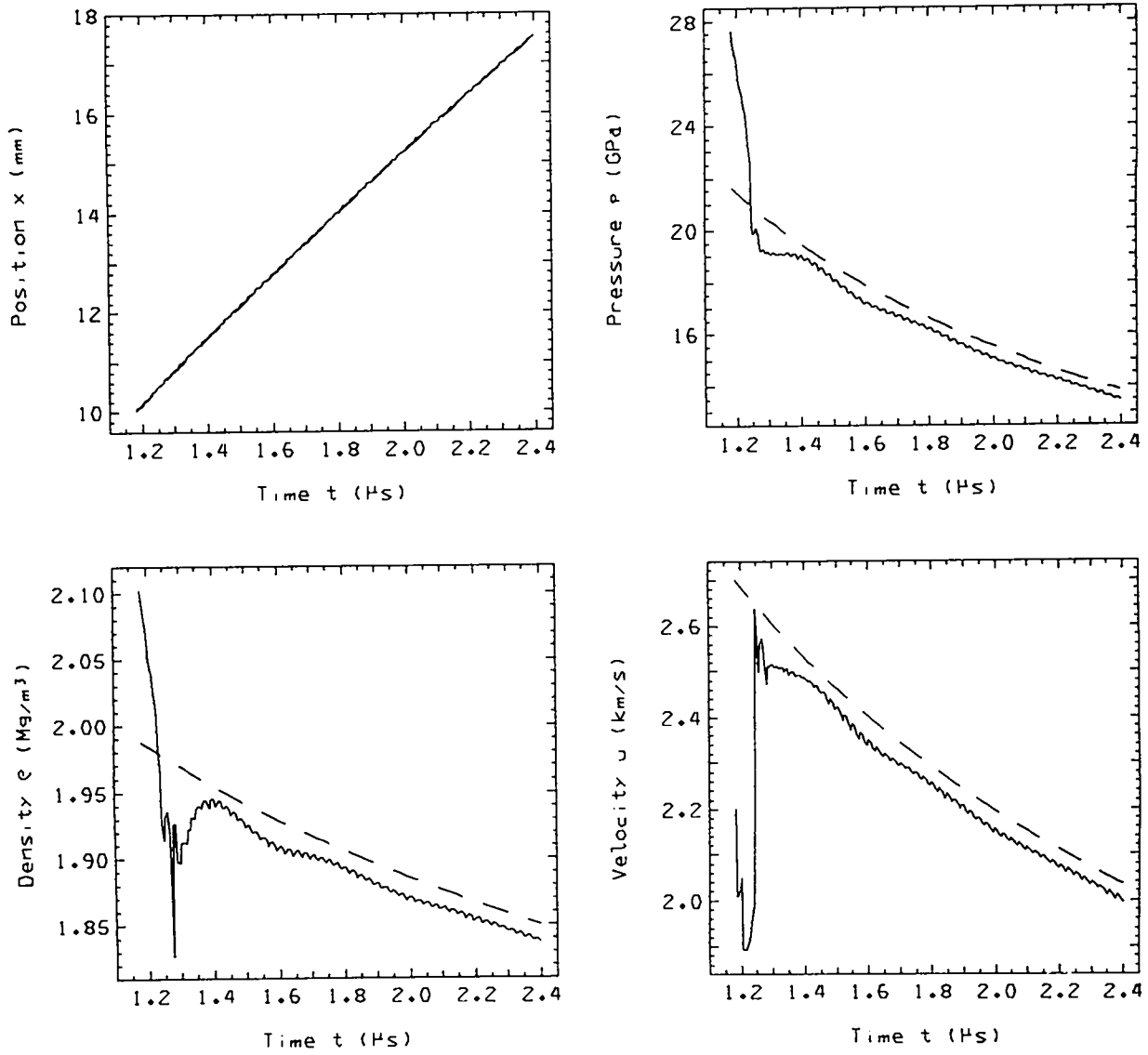


Fig. 16 (cont)

8. REVERBERATION, Q = 0, 1.414 / TIME= 8.5000E+00

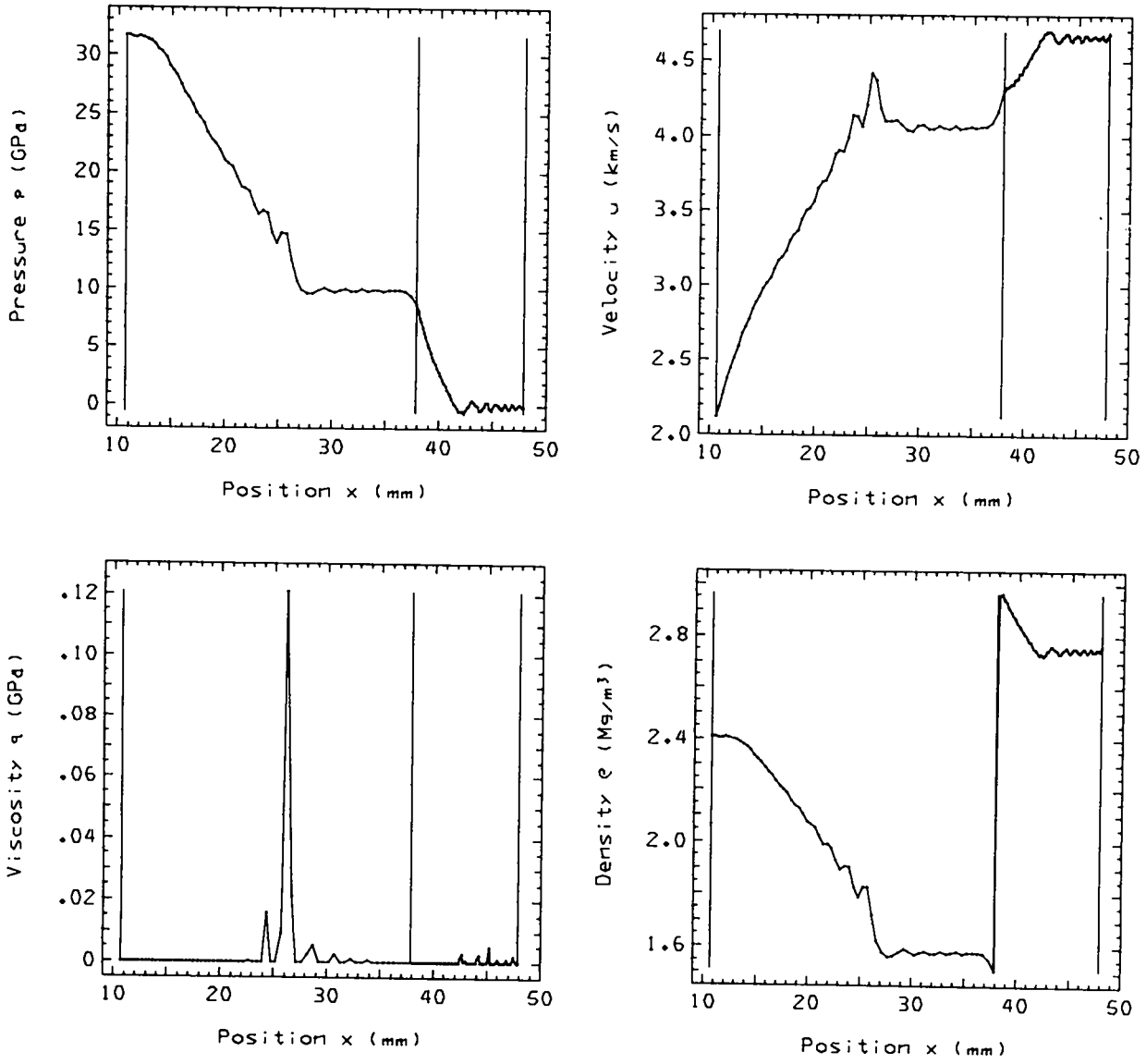


Fig. 17.
Problem 8. $q = 0, 1.414$, quadratic.

8. REVERBERATION, Q = 0.1414 / PARTICLES

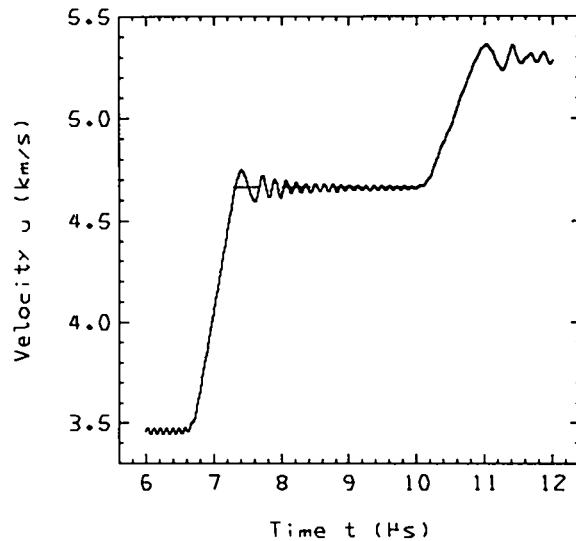
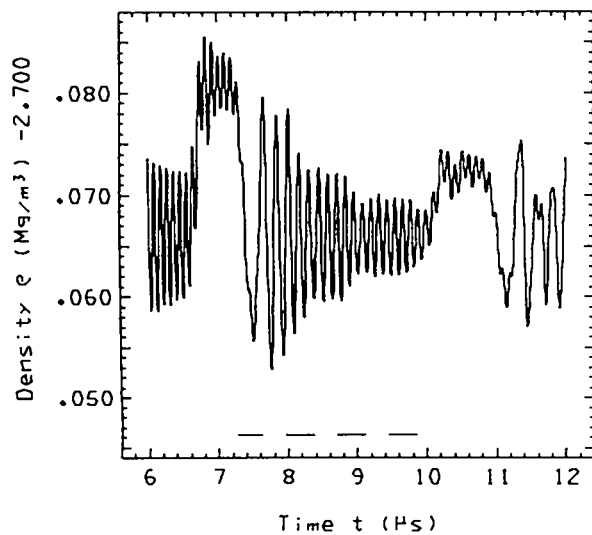
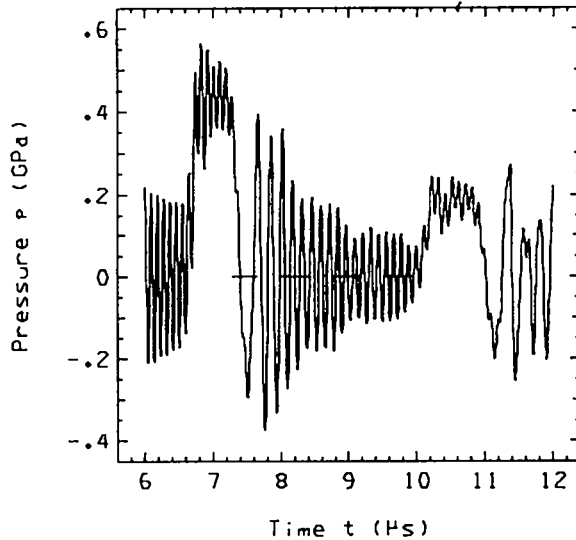
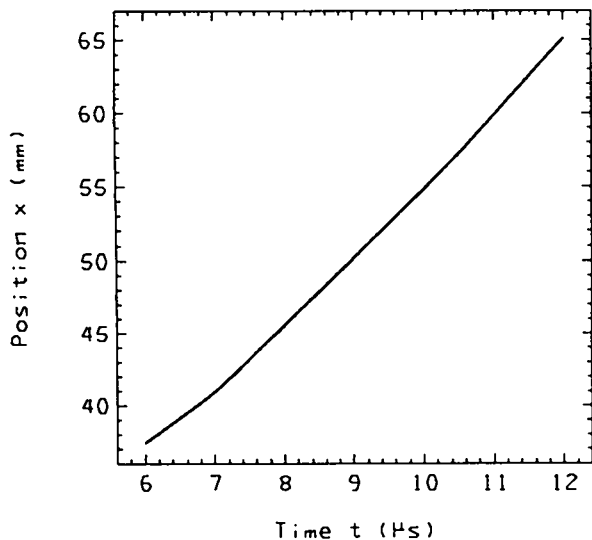


Fig. 17 (cont)

8. REVERBERATION, Q = 0. 1.414 / DIFFERENCE, TRUNCATED TIME / PARTICLES

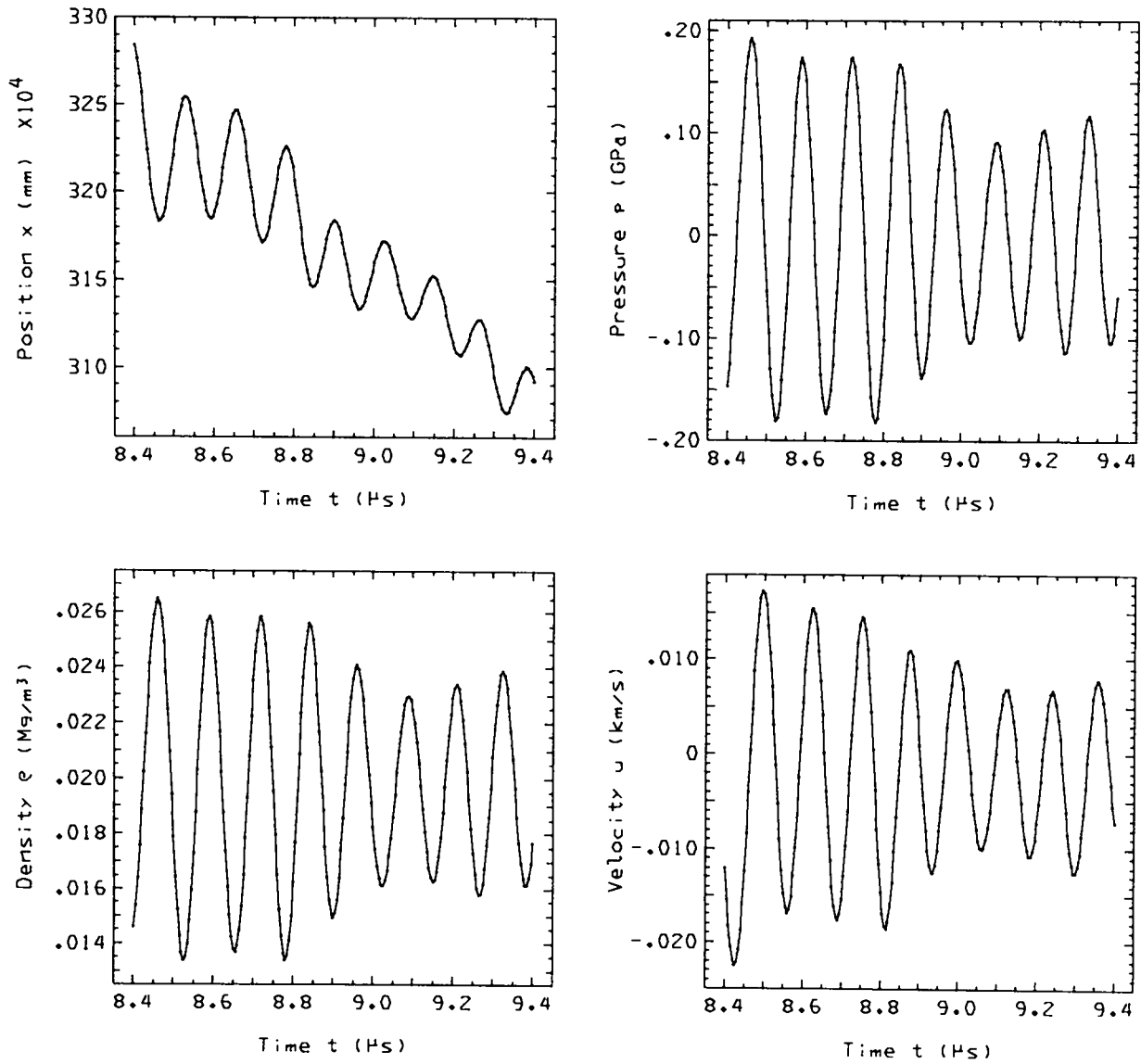


Fig. 17 (cont)

8. REVERBERATION, Q = 0. 1.414 / DIFFERENCE, TRUNCATED TIME / PARTICLES

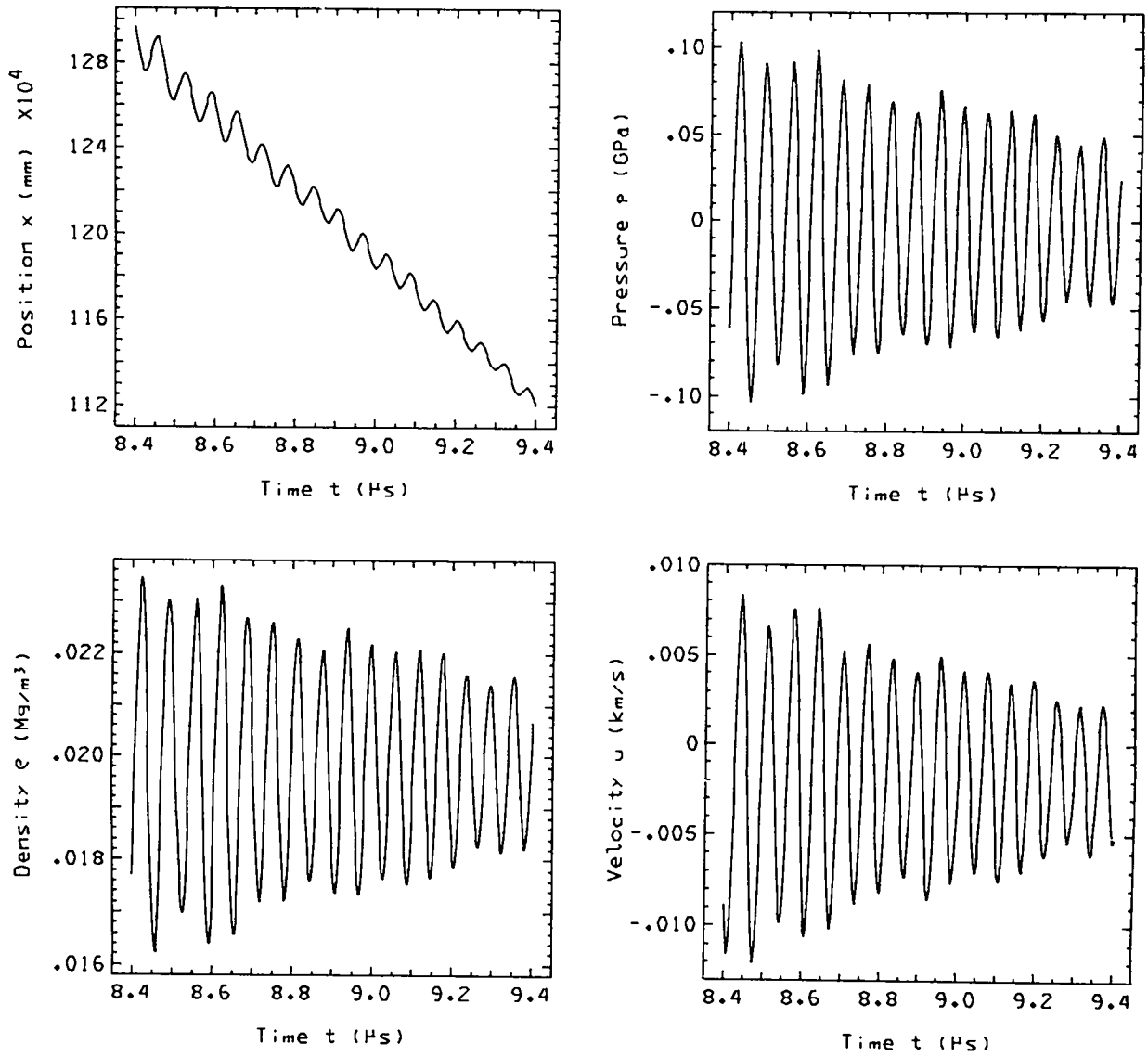


Fig. 17 (cont)

8. REVERBERATION, Q = 0, 1.414 / PARTICLES

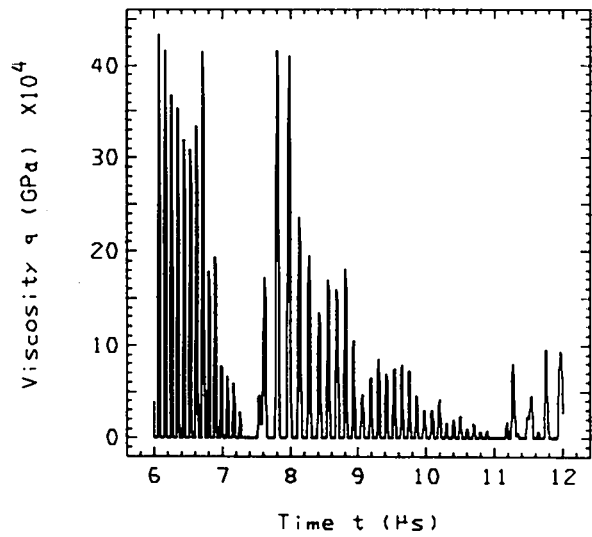
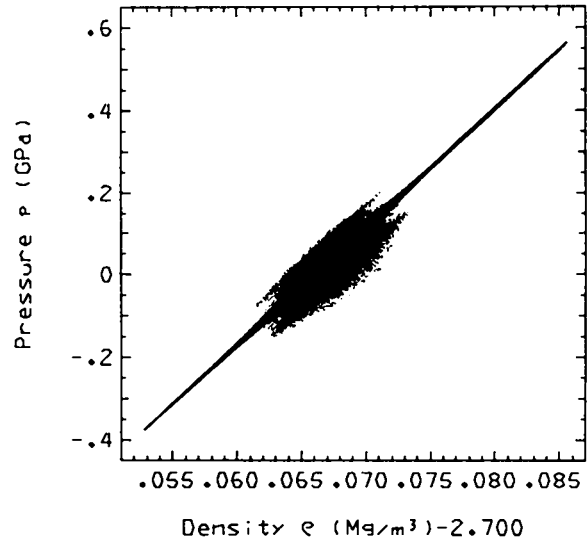
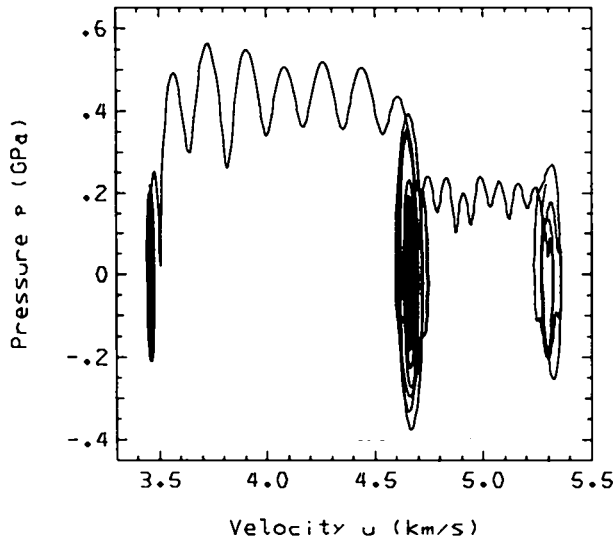


Fig. 17 (cont)

8. REVERBERATION, Q = 0. 1.414 / DIFFERENCE, TRUNCATED TIME / PARTICLE

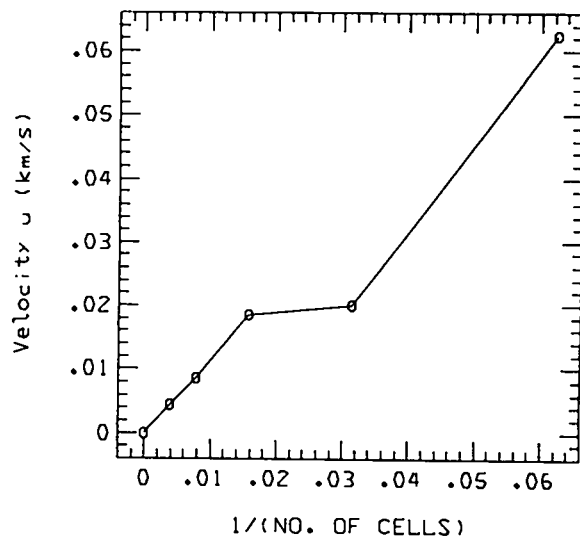
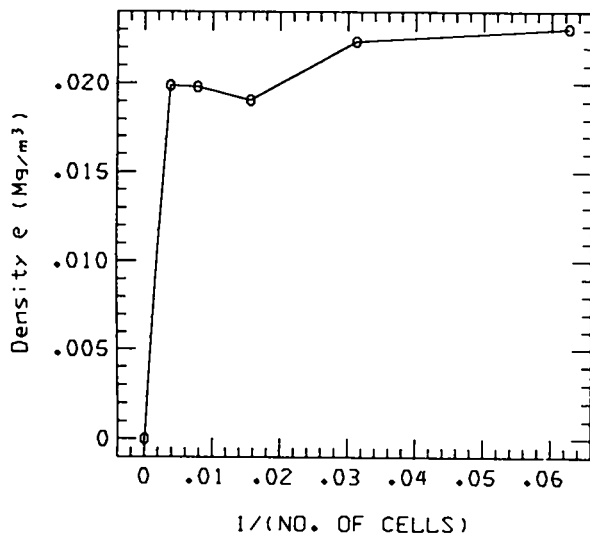
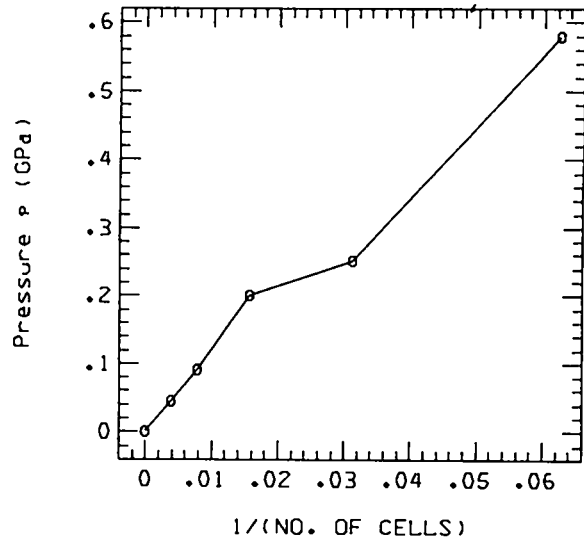
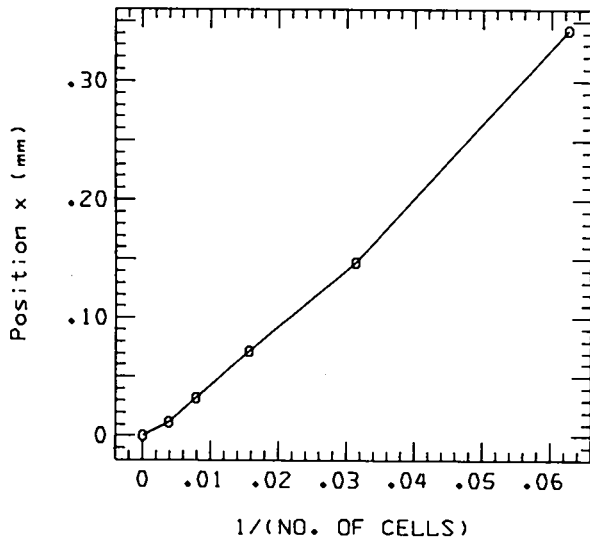


Fig. 17 (cont)

10. STEADY DETONATION, Q = 0, 1.414 / TIME = 1.7000E+00

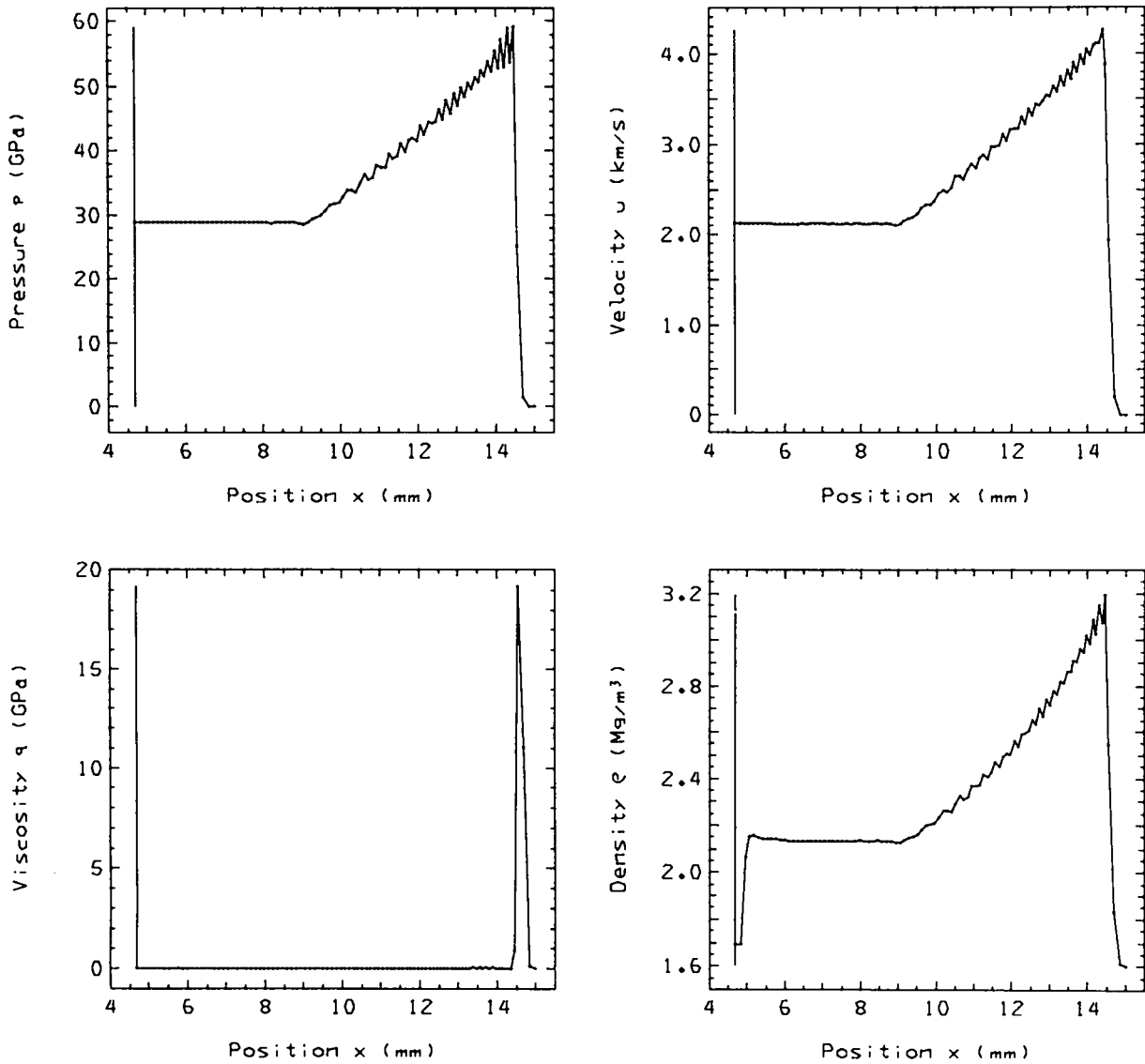


Fig. 18.
Problem 10. $q = 0, 1.414$, quadratic.

10. STEADY DETONATION, Q = 0. 1.414 / TIME= 1.7000E+00

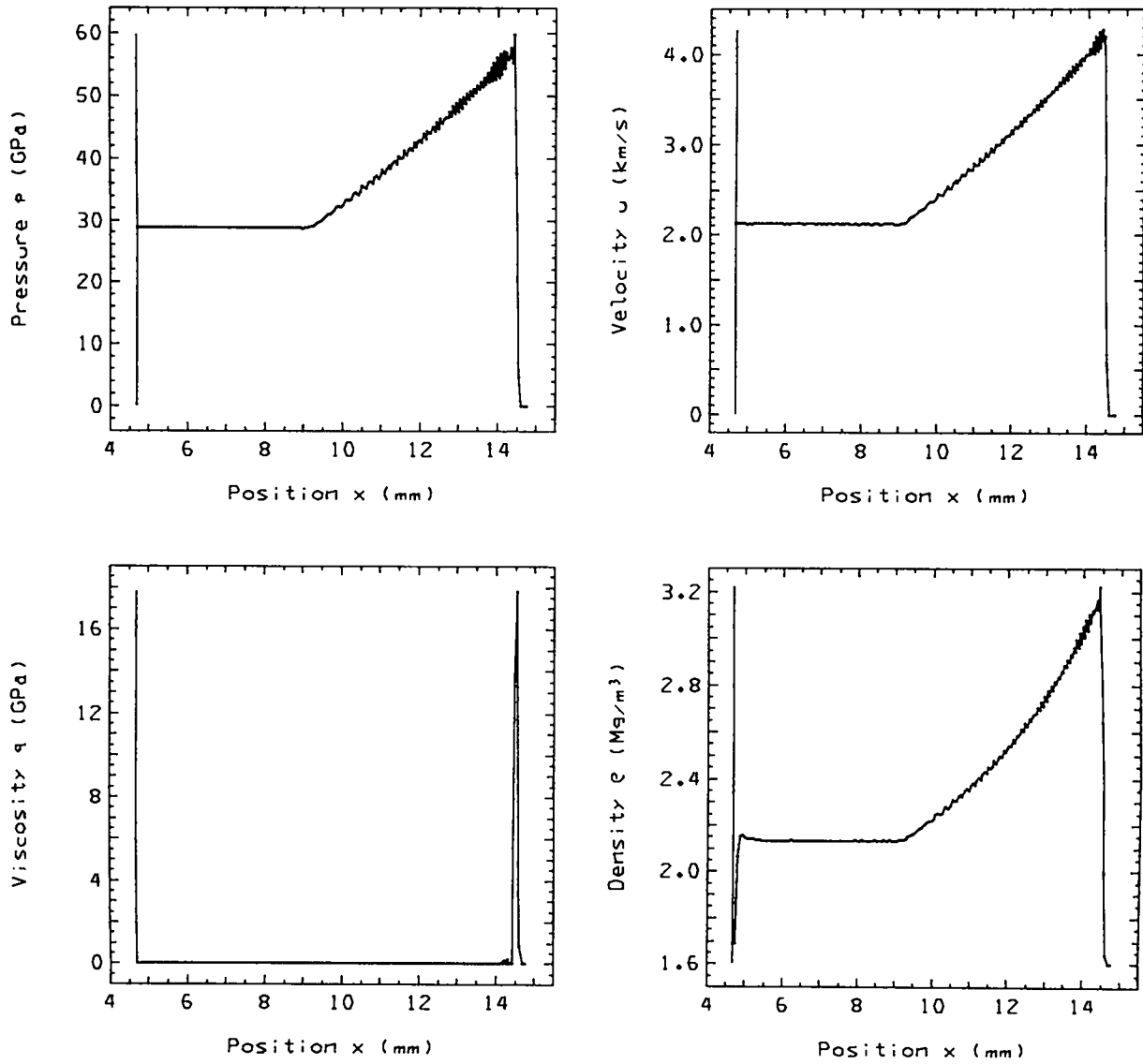


Fig. 18 (cont)

10. STEADY DETONATION, Q = 0. 1.414 / PARTICLES

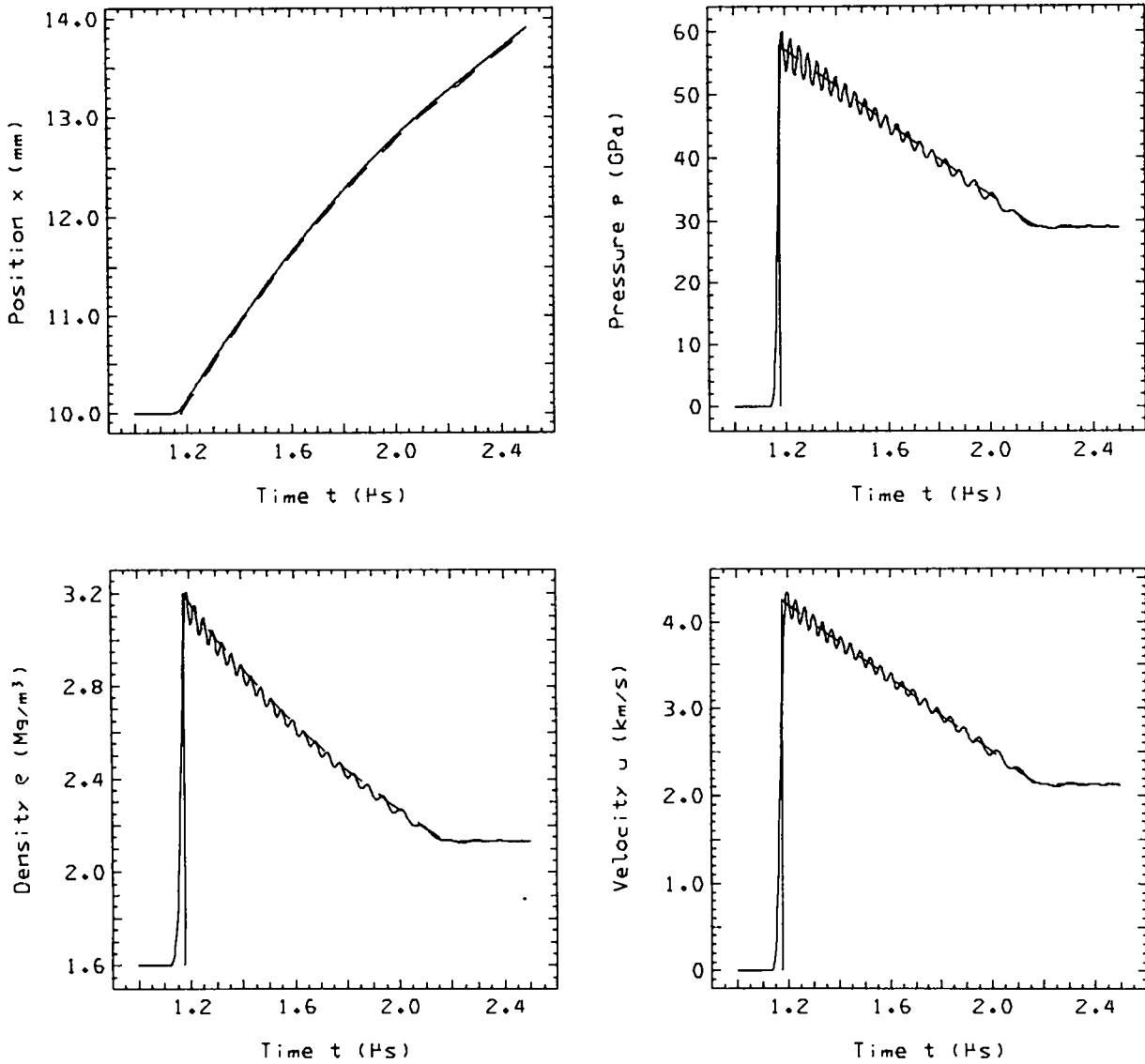


Fig. 18 (cont)

10. STEADY DETONATION, Q = 0, 1.414 / DIFFERENCE, TRUNCATED TIME / PARTICLES

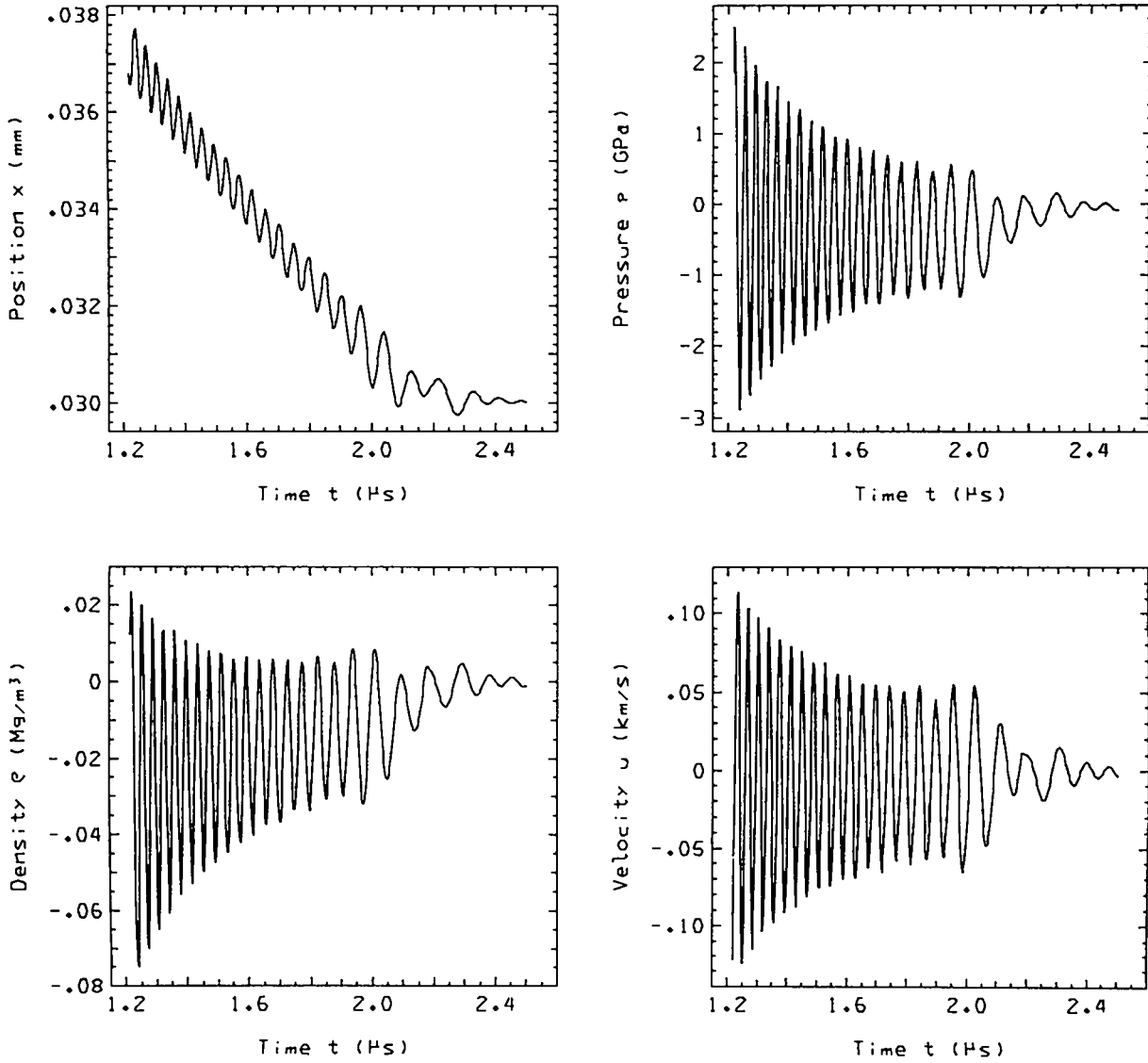


Fig. 18 (cont)

10. STEADY DETONATION, Q = 0, 1.414 / DIFFERENCE, TRUNCATED TIME / PARTICLES

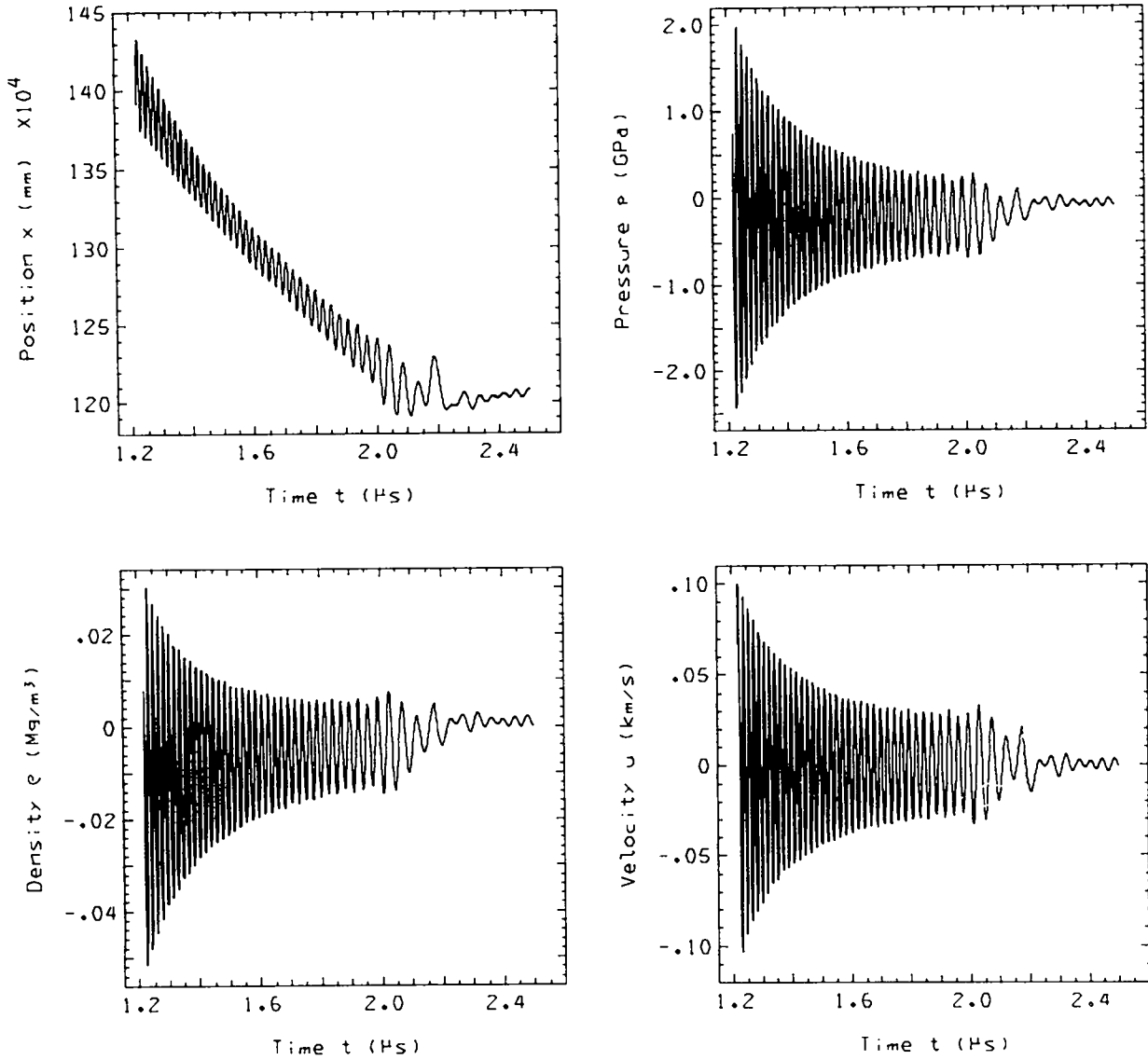


Fig. 18 (cont)

PAD3.3F6 - 75JUL14 RUN 7 LAC2 *10. STEADY DETONATION. Q = 0. 1.414*
TFICKET114K. 10.781 SEC ON RUN, 165.793 SEC ON JOB

ERUN 4, 128 CELLS 07/24/75

10. STEADY DETONATION, Q = 0. 1.414 / DIFFERENCE, TRUNCATED TIME / PARTICLES

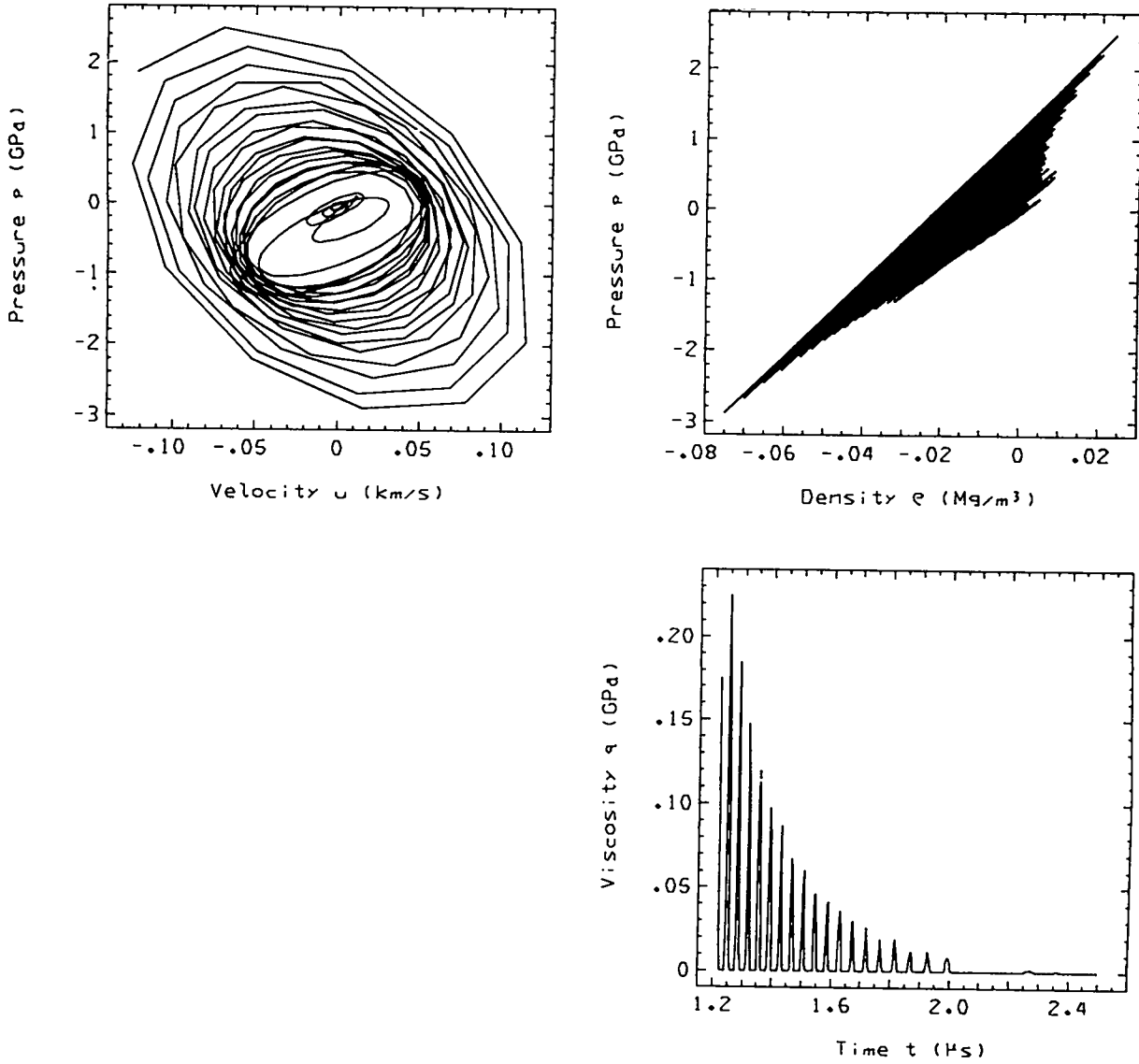


Fig. 18 (cont)

10. STEADY DETONATION, Q = 0, 1.414 / DIFFERENCE / LEAD SHOCK

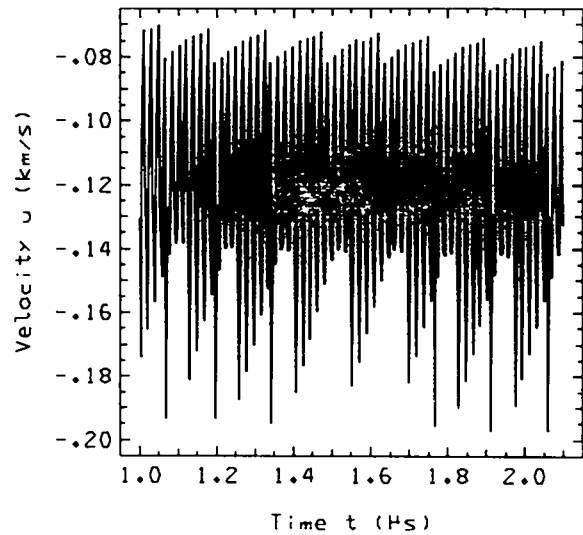
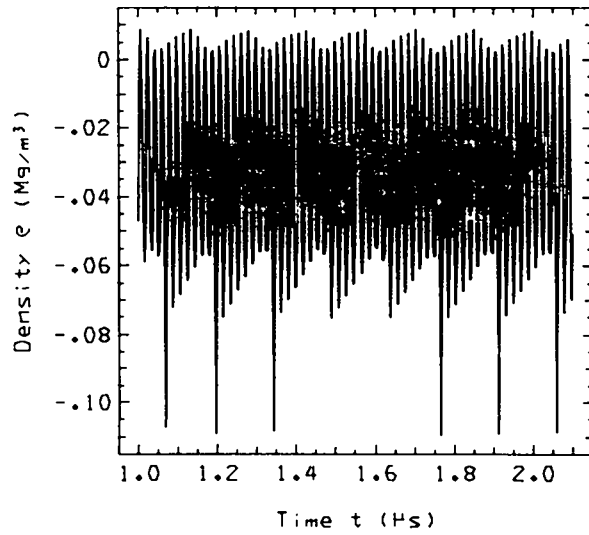
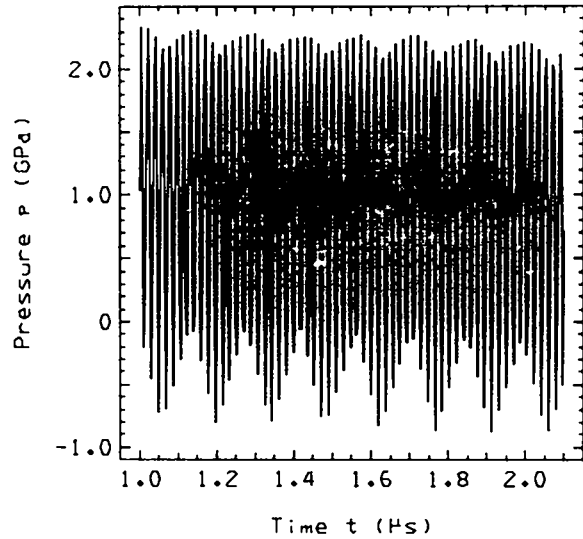
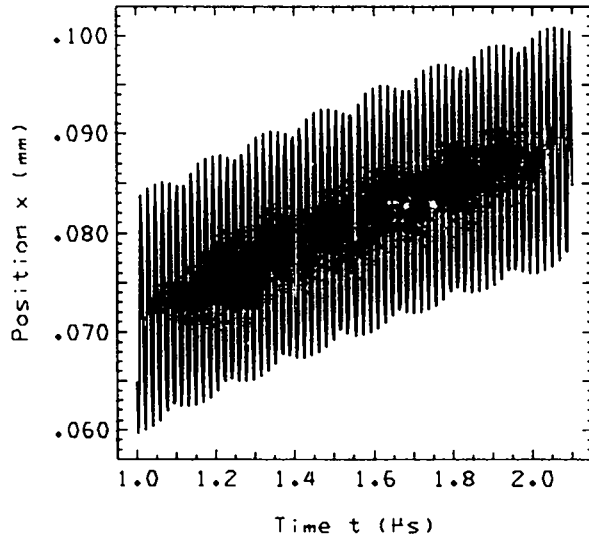


Fig. 18 (cont)

10. STEADY DETONATION, Q = 0. 1.414 / DIFFERENCE / LEAD SHOCK

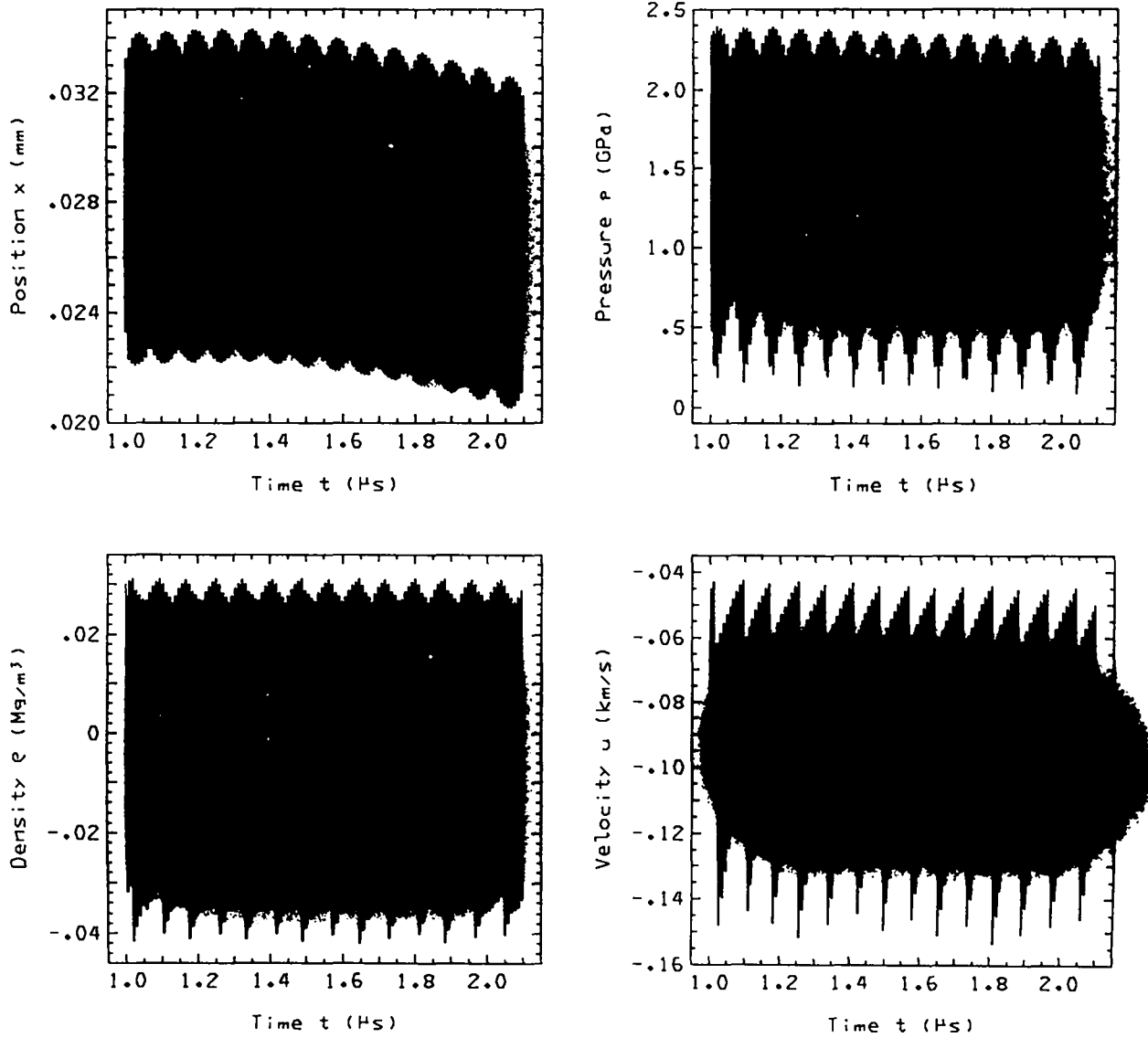


Fig. 18 (cont)

AL, P=30 / Q = 0.3, 1, 0 / TIME= 6.8500E+01

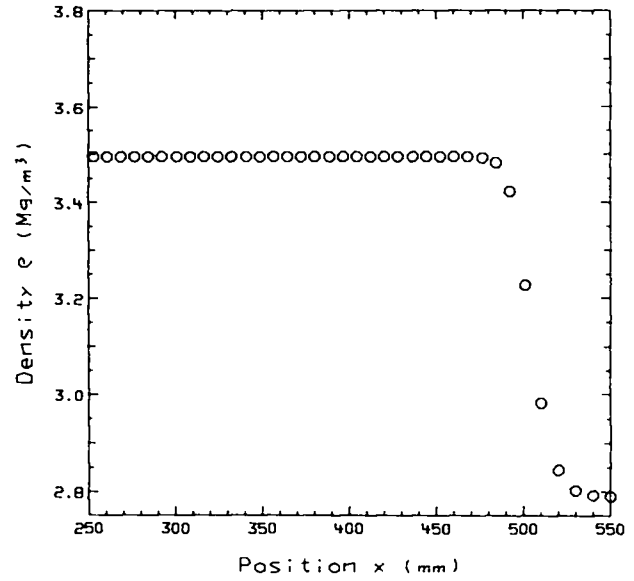
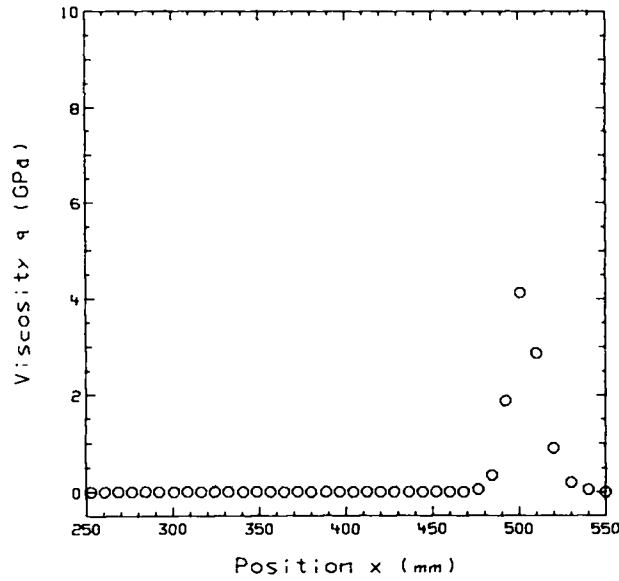
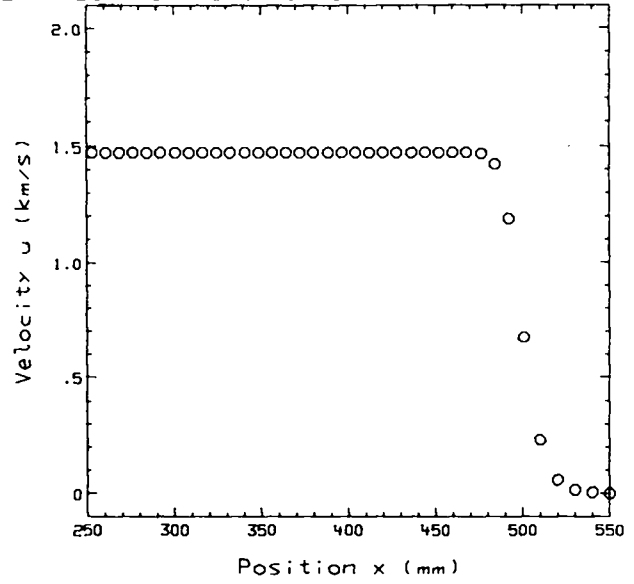
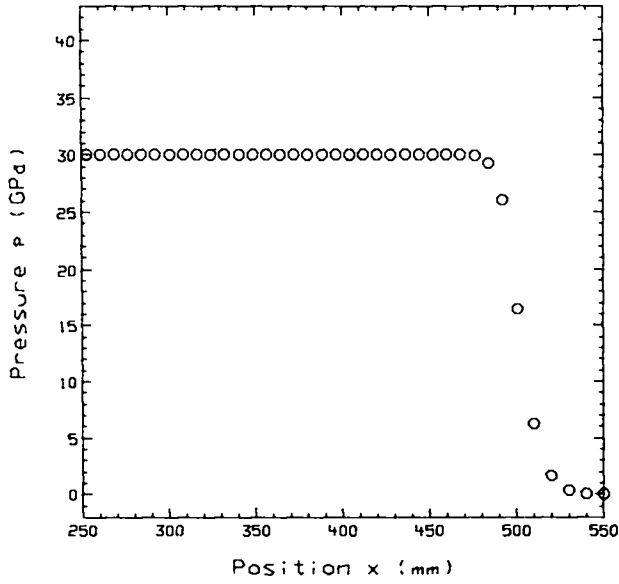


Fig. B-1.
Snapshots and particle histories for all optimum and one quadratic viscosity.

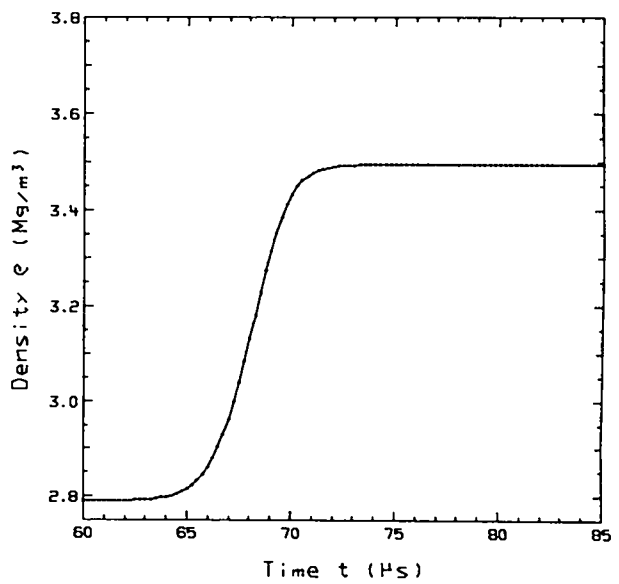
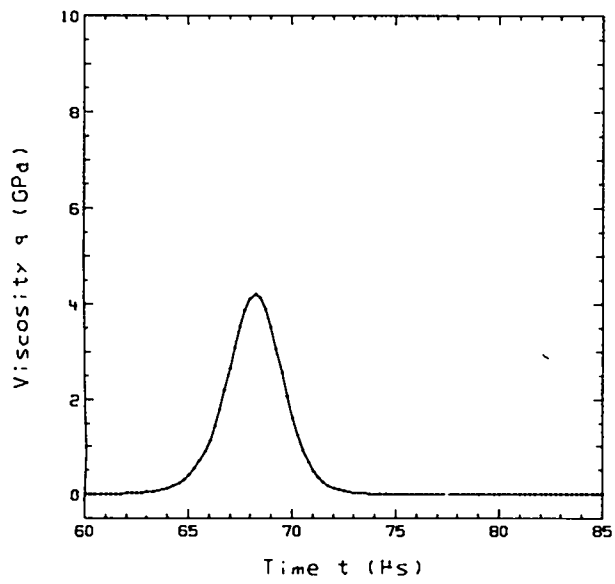
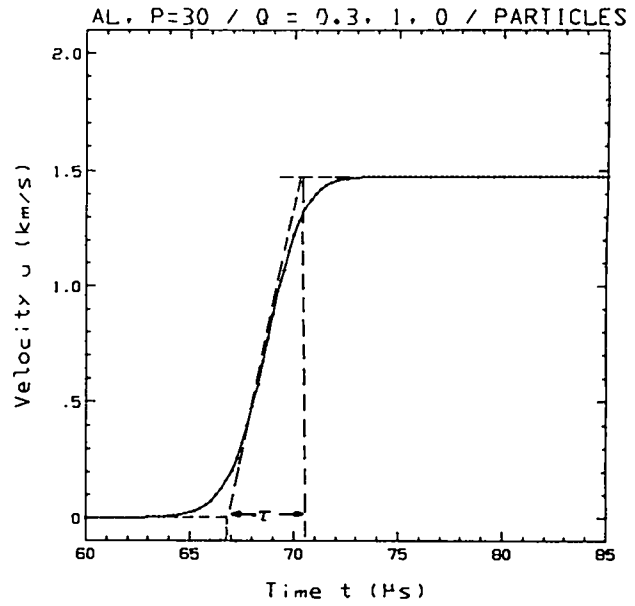
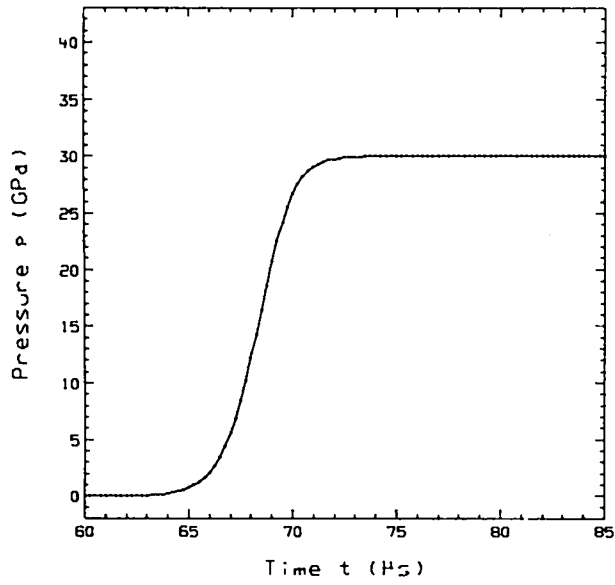


Fig. B-1 (cont)

PMMA, P=15 / Q = 0, 1.414, 0 / TIME = 8.5000E+01

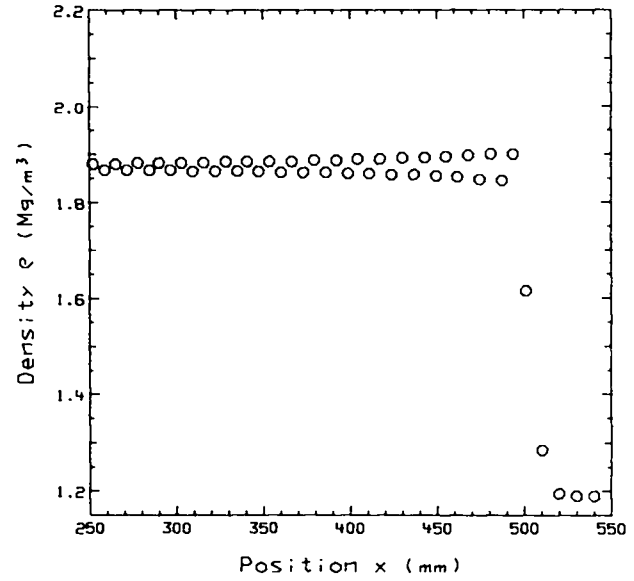
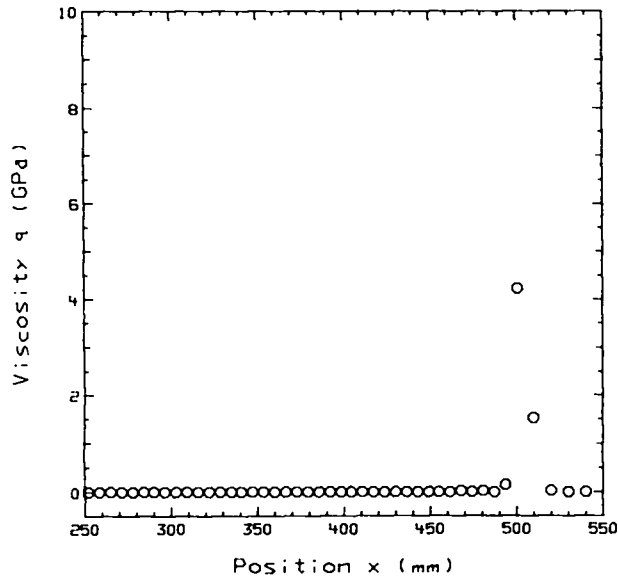
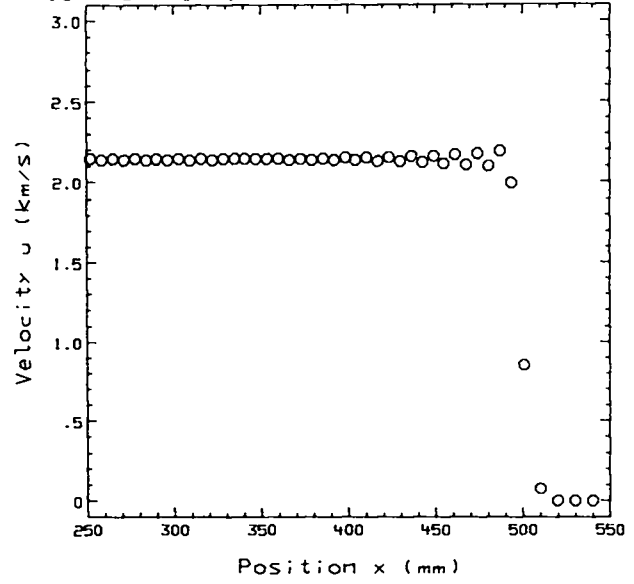
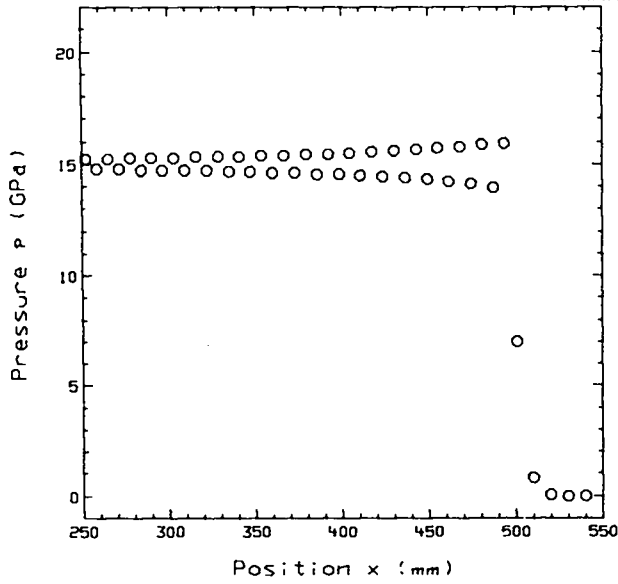


Fig. B-1 (cont)

PMMA, P=15 / 0 = 0, 1.414, 0 / PARTICLES

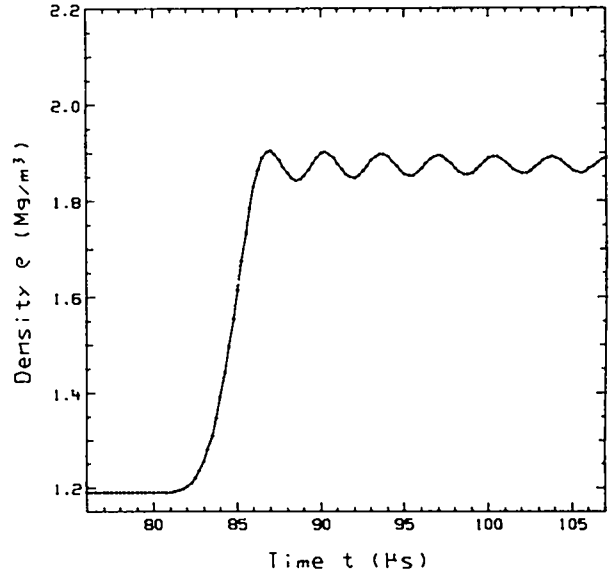
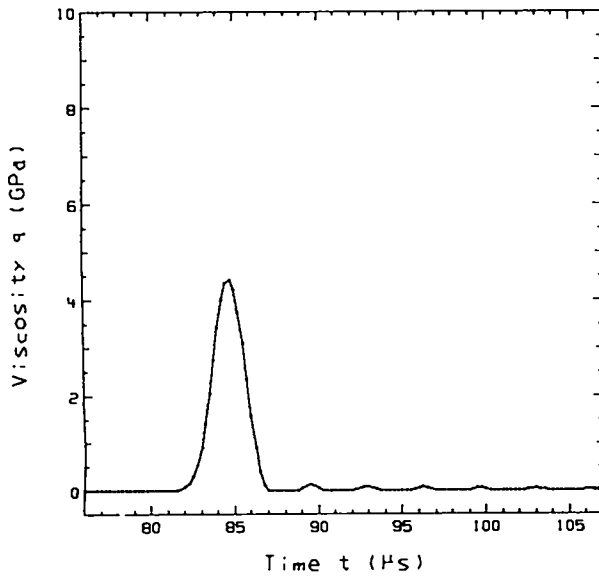
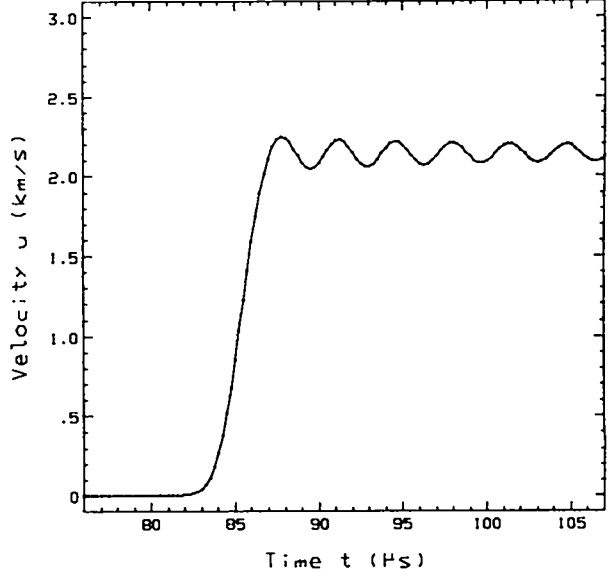
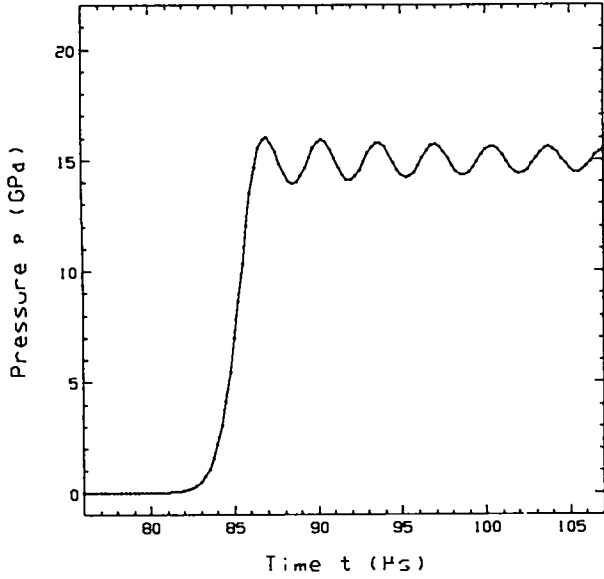


Fig. B-1 (cont)

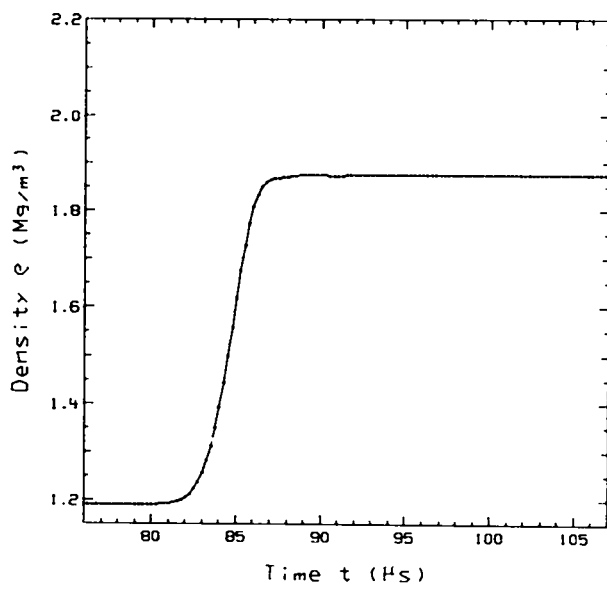
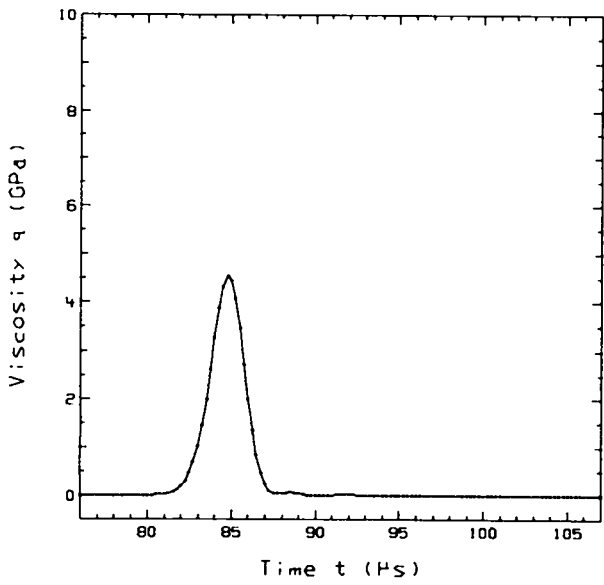
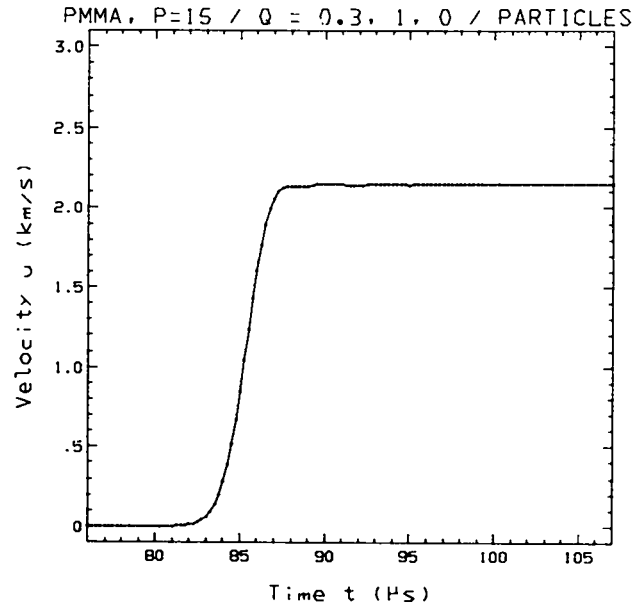
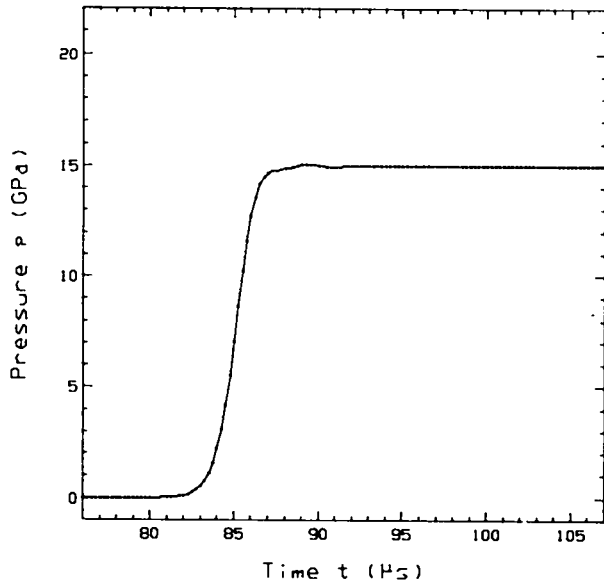


Fig. B-1 (cont)

PG, G=7, P=15 / Q= 0.2, 2.0 / PARTICLES

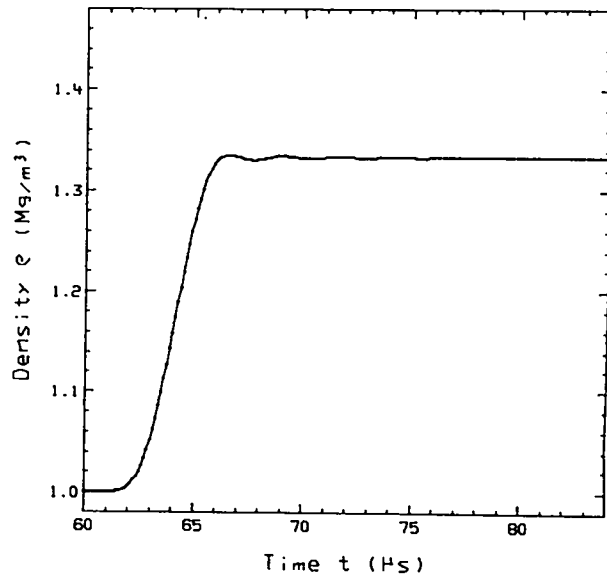
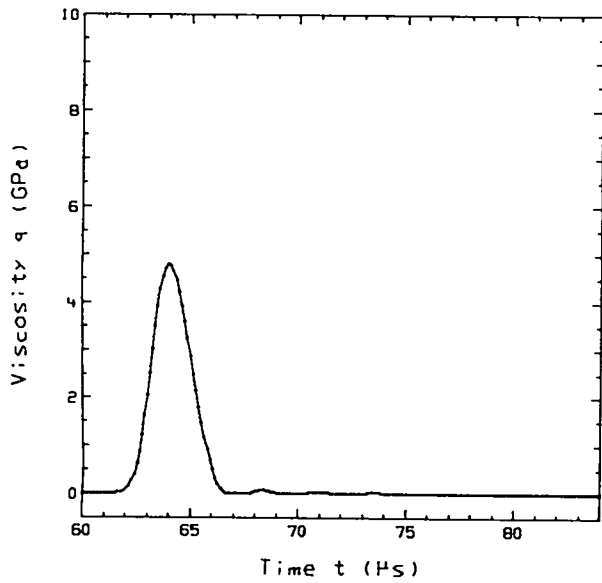
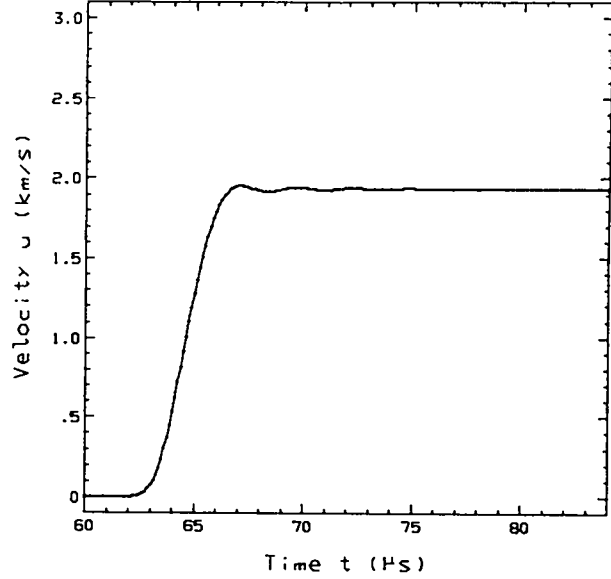
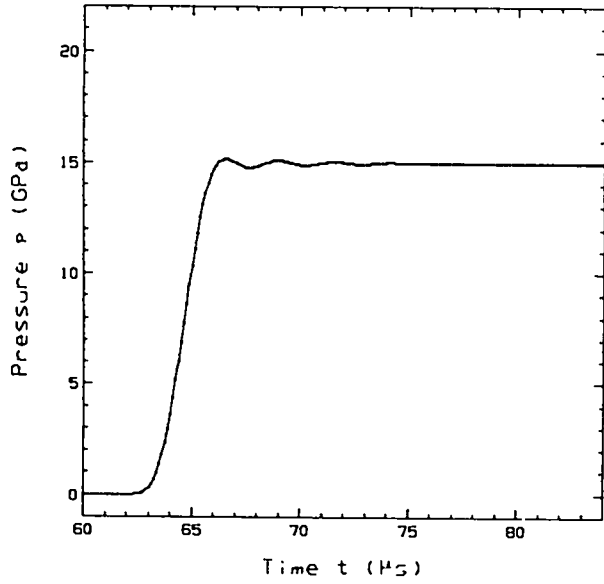


Fig. B-1 (cont)

PG, G=3, P=60 / Q = 0.3, 1.0 / PARTICLES

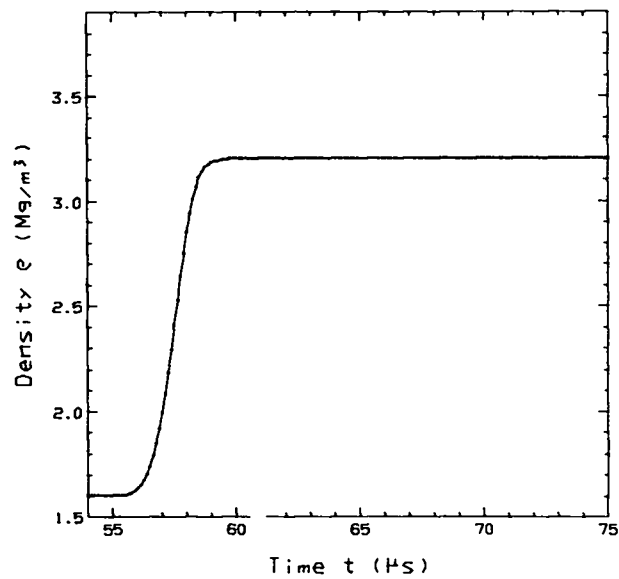
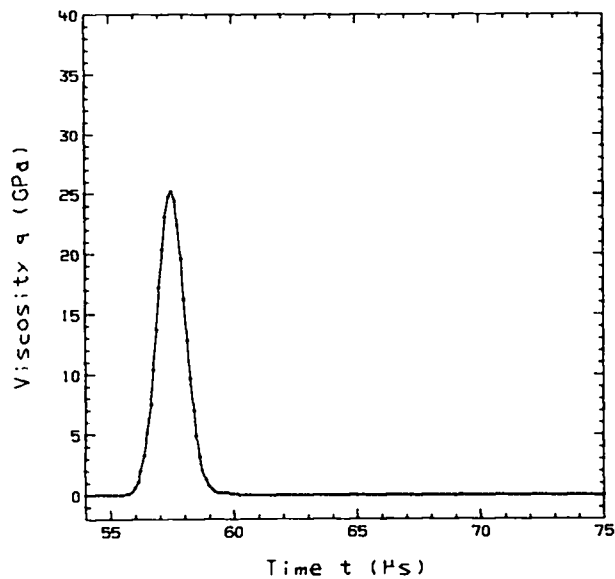
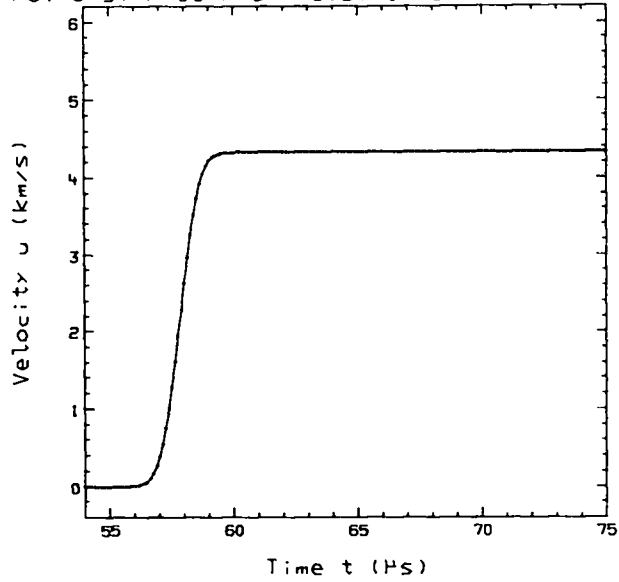
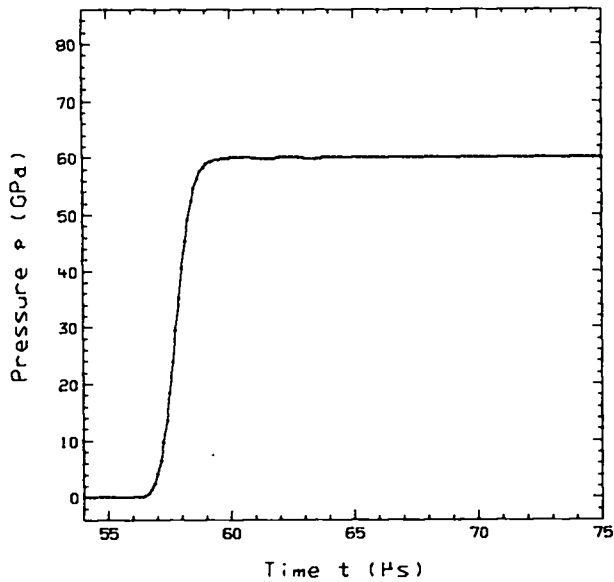


Fig. B-1 (cont)

$Q = 0.1, 0.0$ / PARTICLES

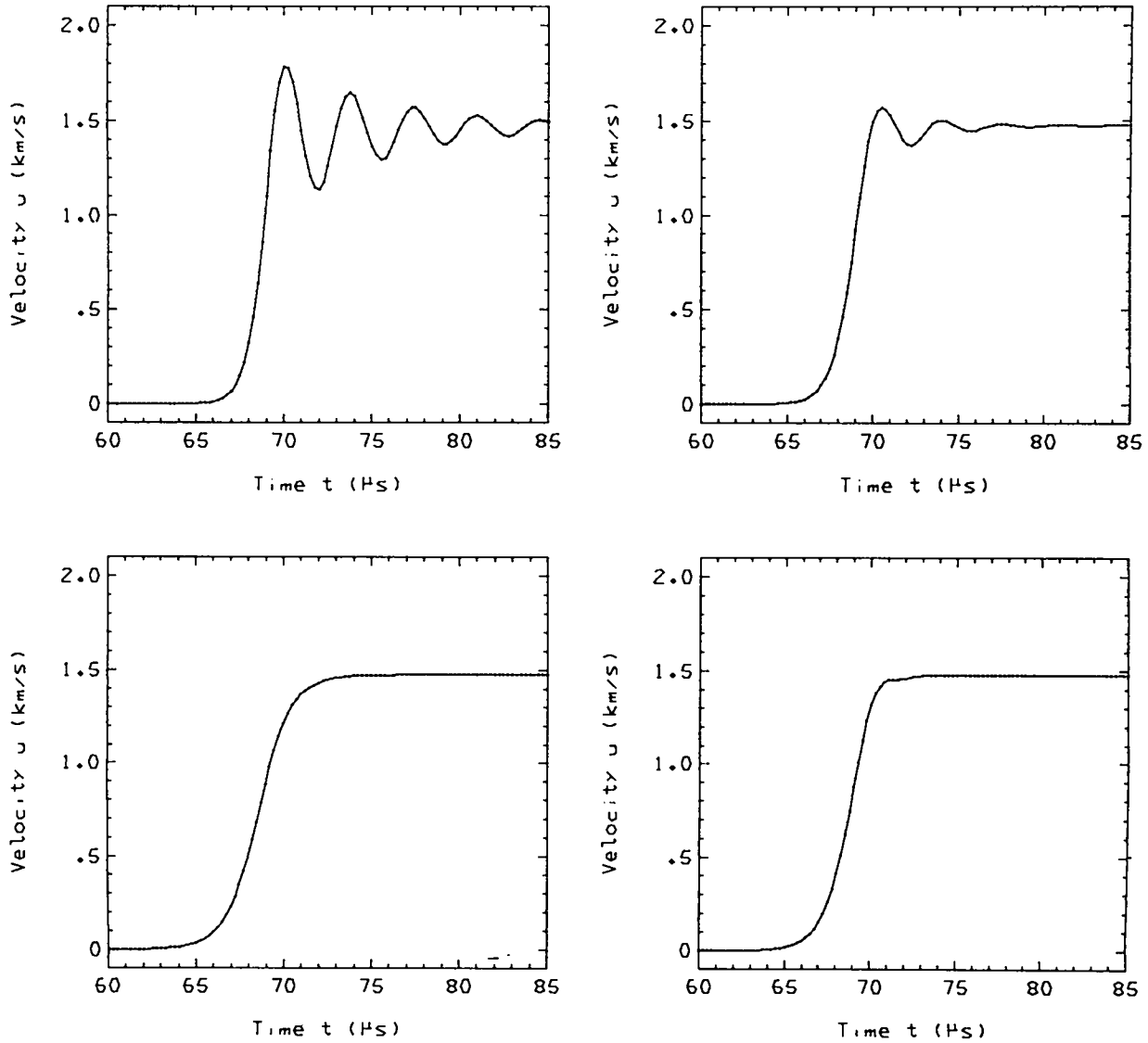


Fig. B-2.

Particle velocity histories for all cases in Table B-II. The frames are arranged in the same order as the table. The label at the upper right gives the viscosity value for the topmost left frame, and the frames are in clockwise order—upper left, upper right, lower right, lower left.

Q = 0, 1.414, 0 / PARTICLES

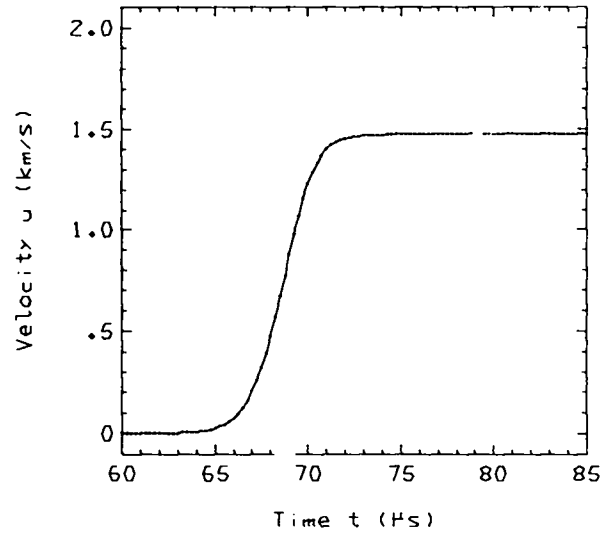
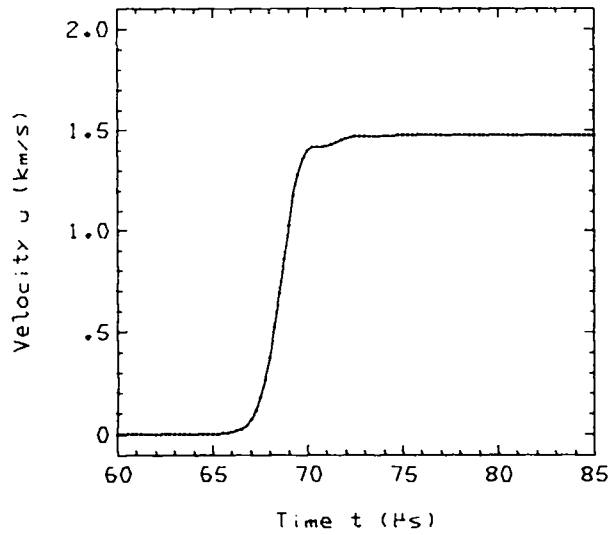
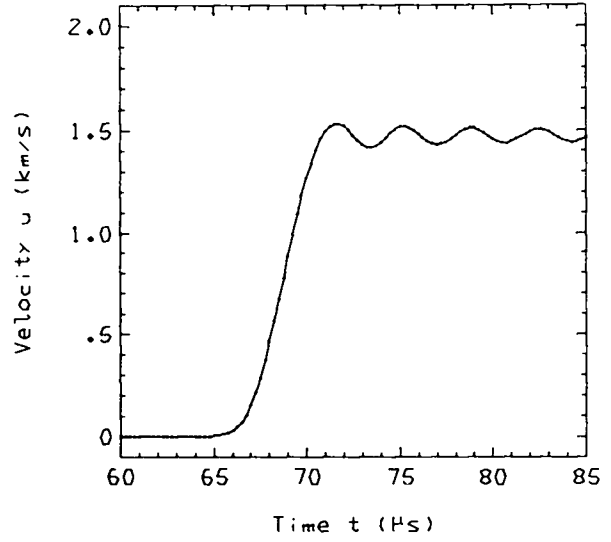
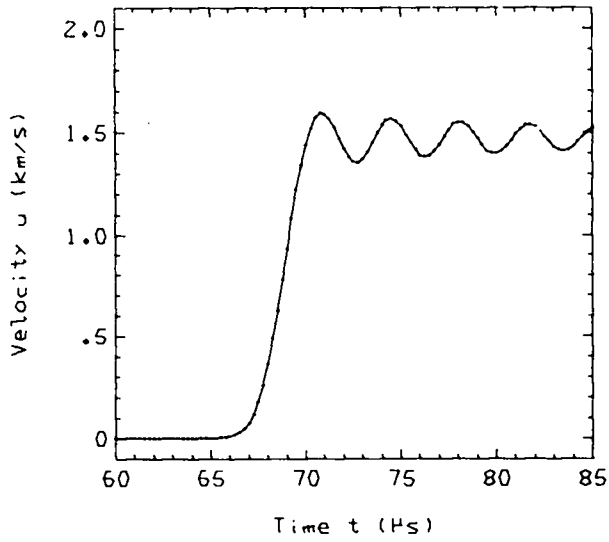


Fig. B-2 (cont)

Q = 0.3, 0. 0 / PARTICLES

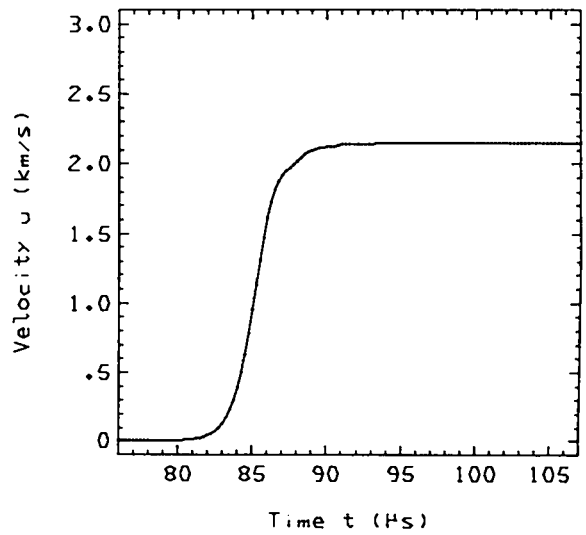
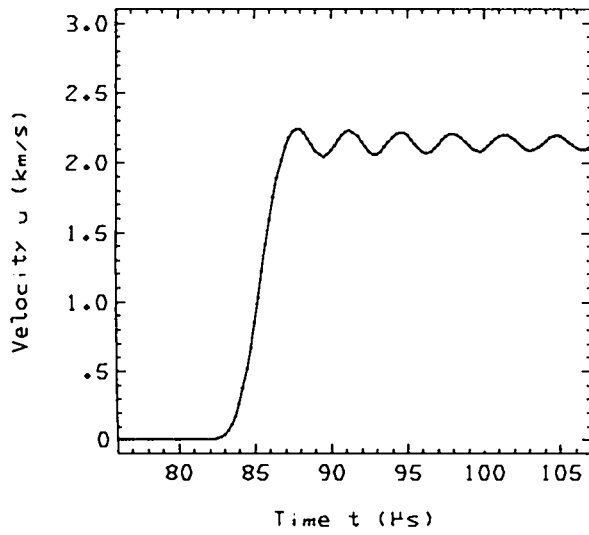
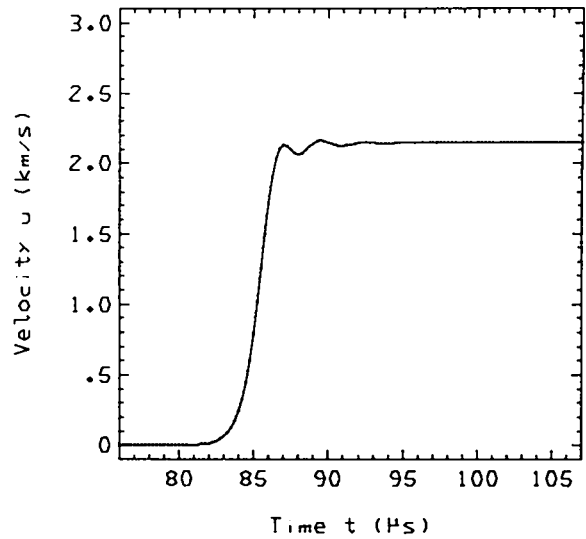
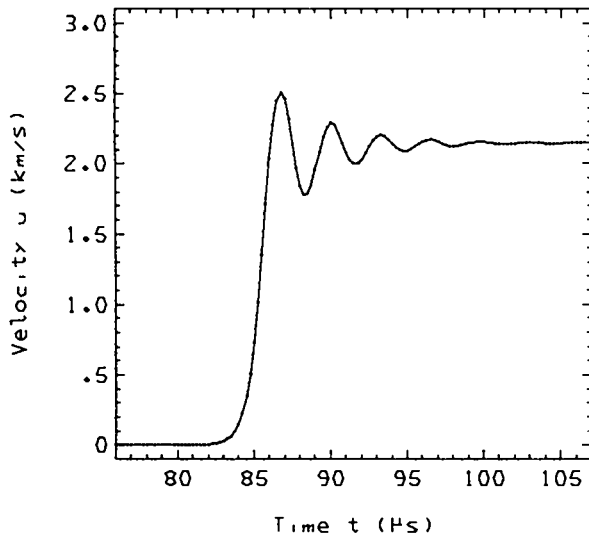


Fig. B-2 (cont)

Q = 0.3, 1.0 / PARTICLES

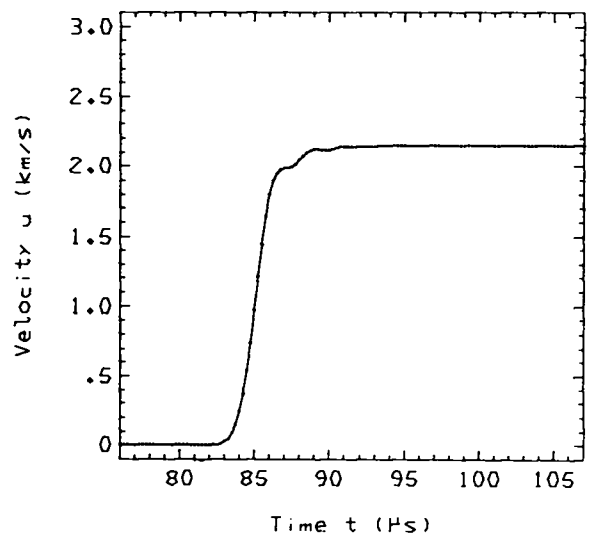
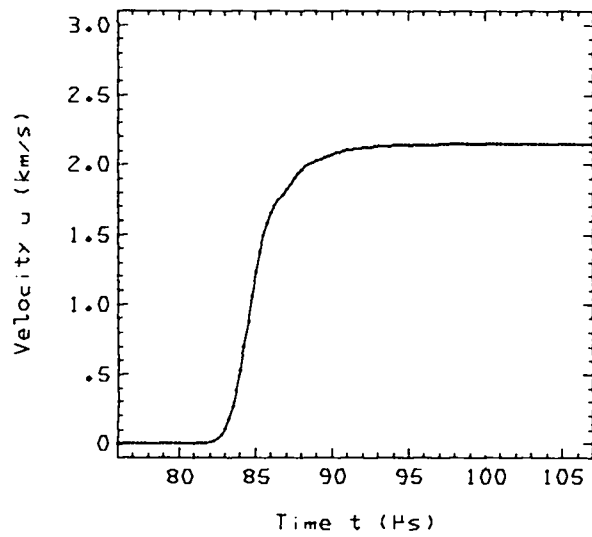
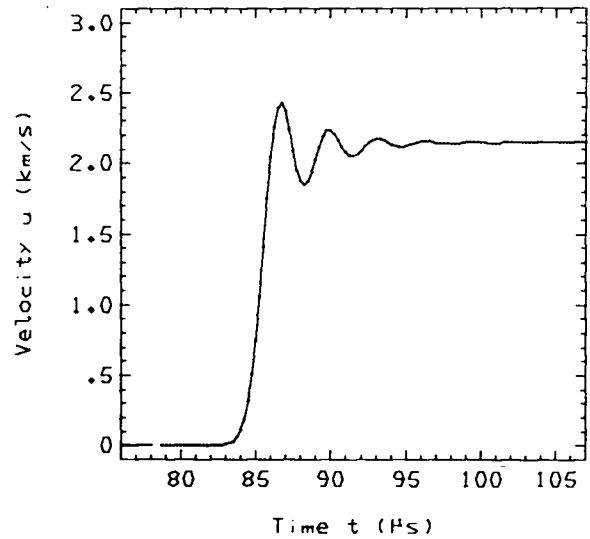
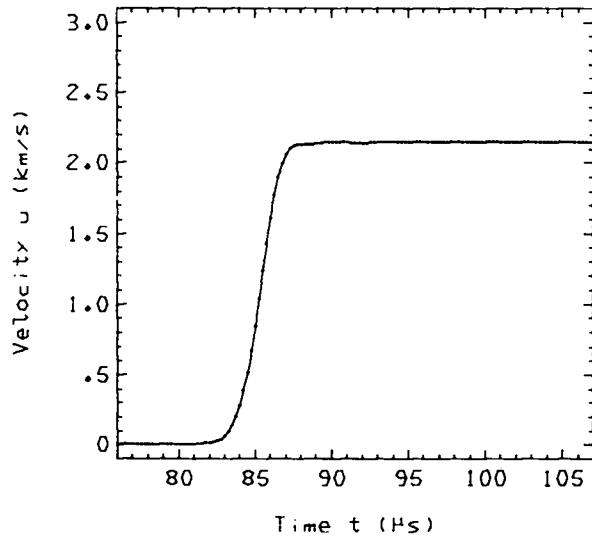


Fig. B-2 (cont)

Q= 1, 0.125, 0 / PARTICLES

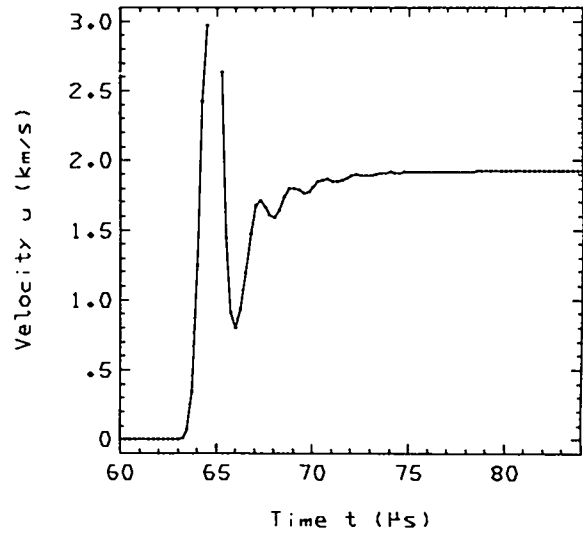
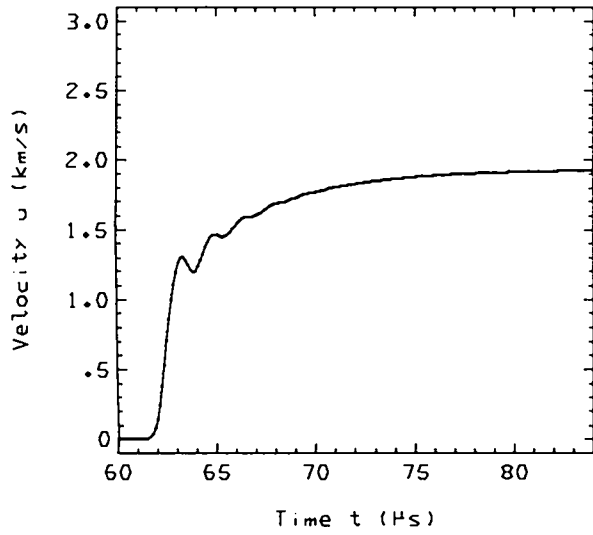
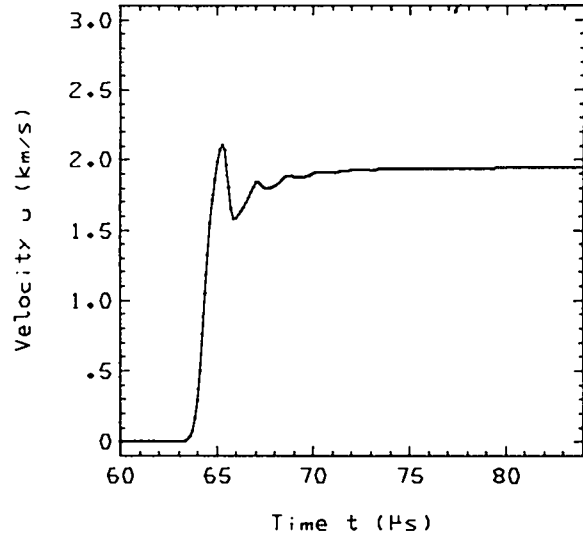
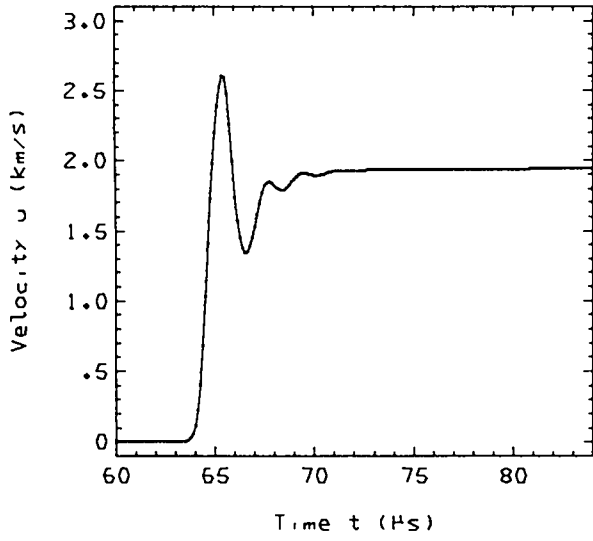


Fig. B-2 (cont)

Q= 5, 0.125, 0 / PARTICLES

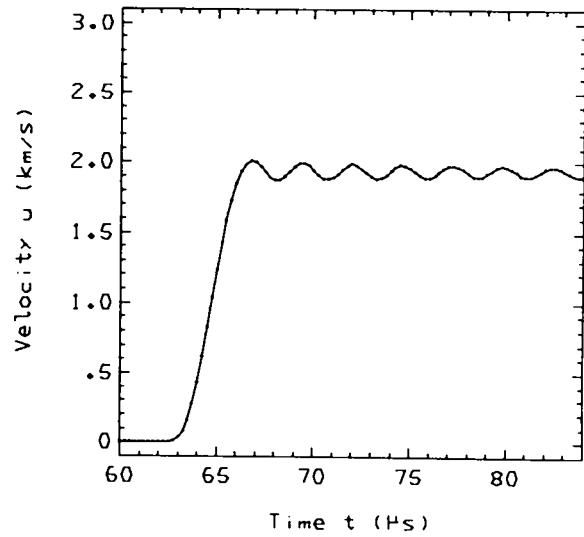
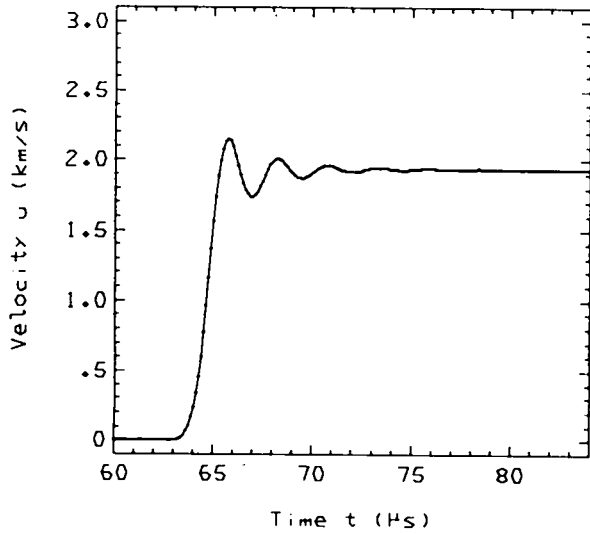
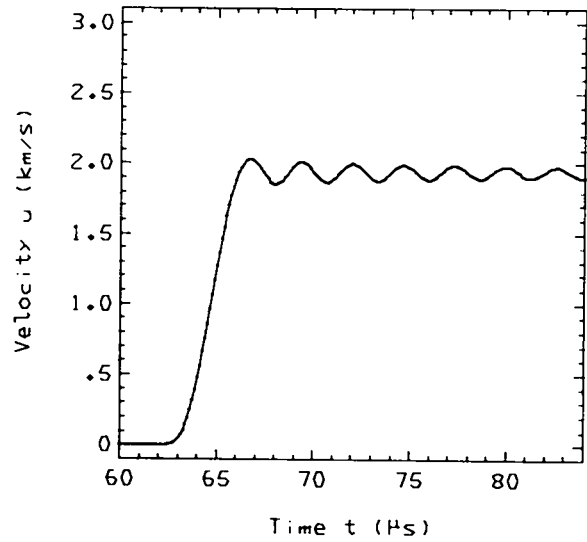
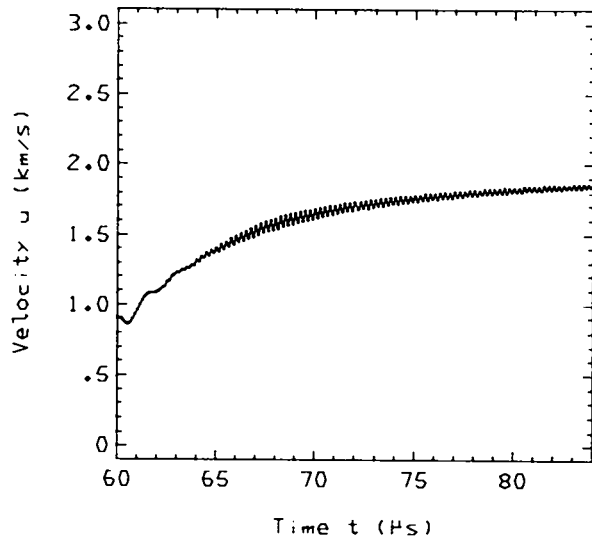


Fig. B-2 (cont)

$\theta = 0.5, 1, 0$ / PARTICLES

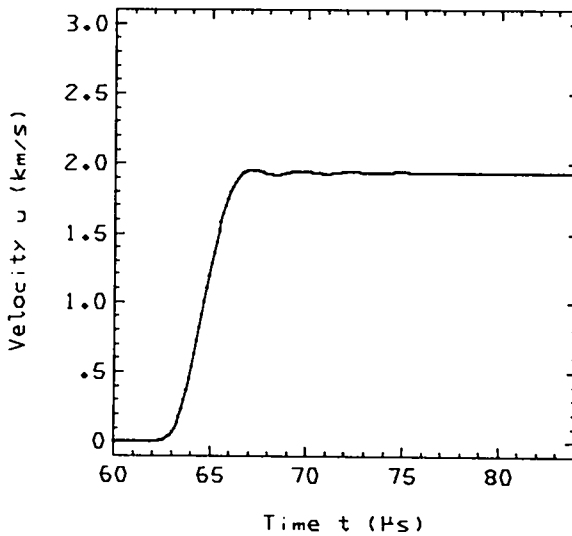
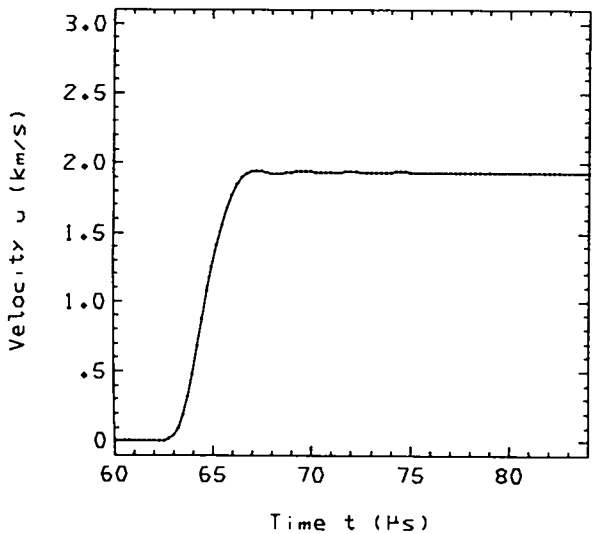
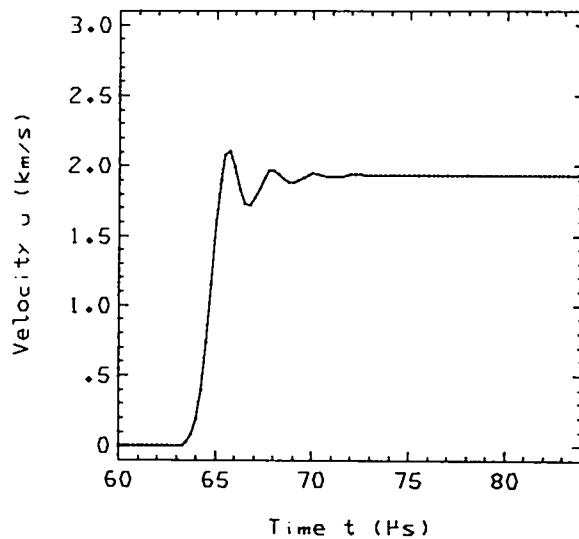
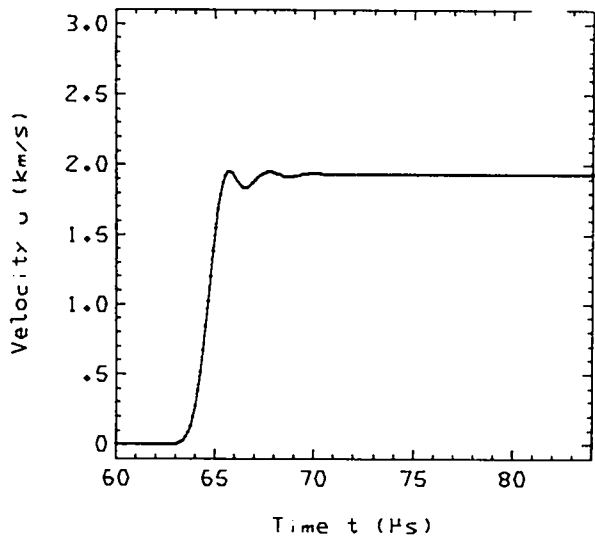


Fig. B-2 (cont)

Q= 0, 0, 2 / PARTICLES

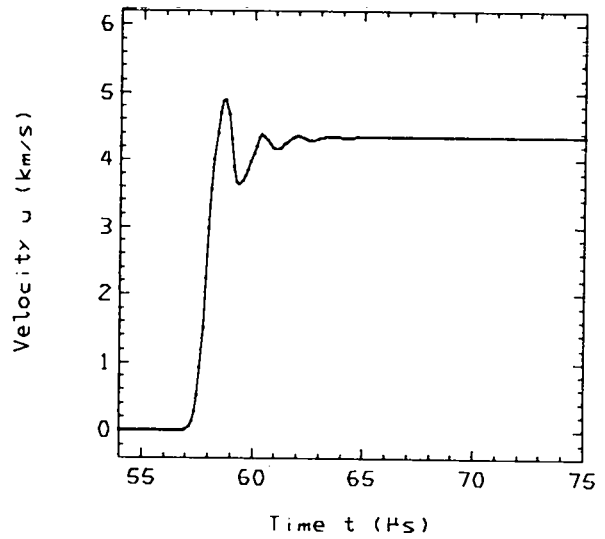
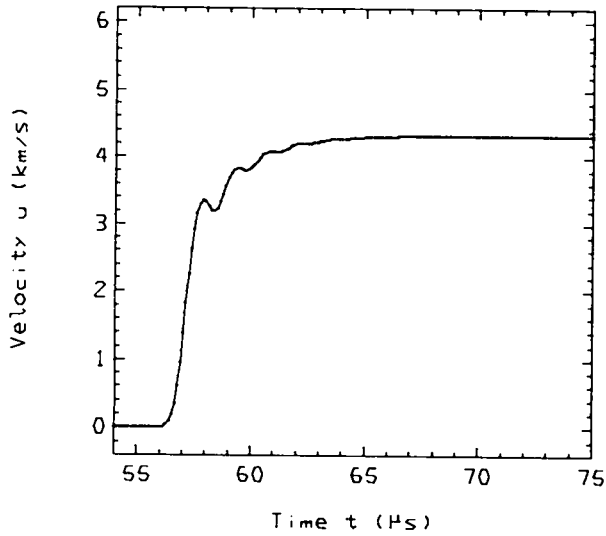
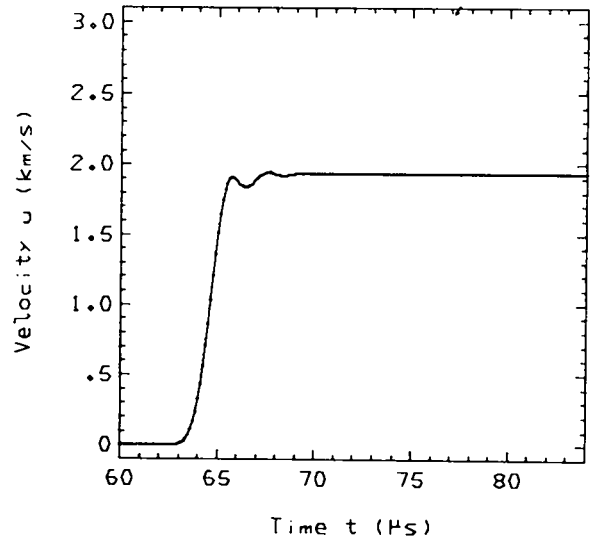
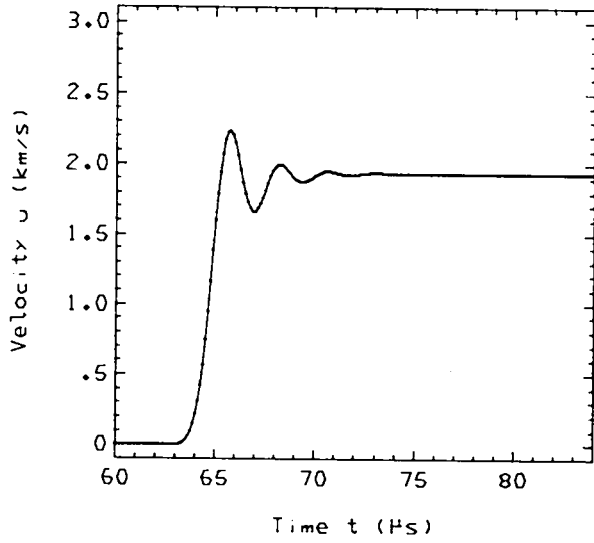


Fig. B-2 (cont)

$Q = 4, 0.125, 0$ / PARTICLES

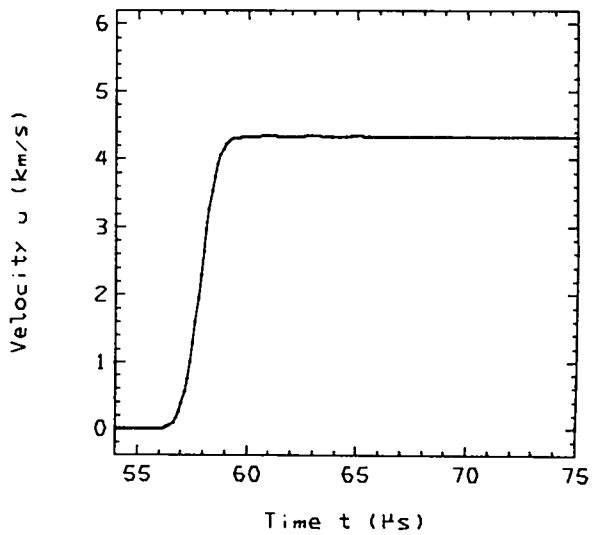
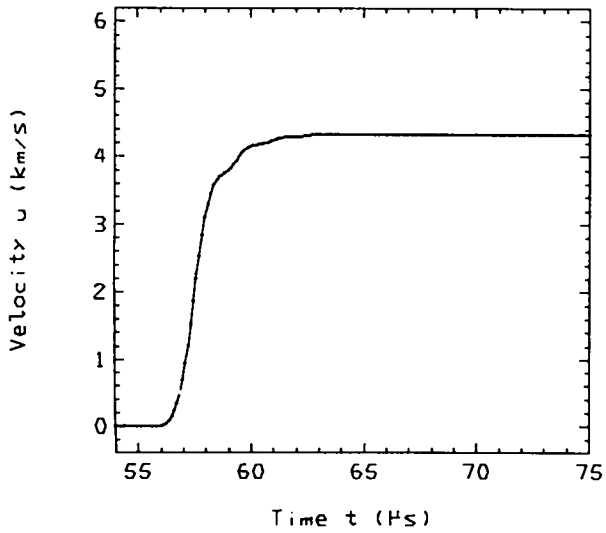
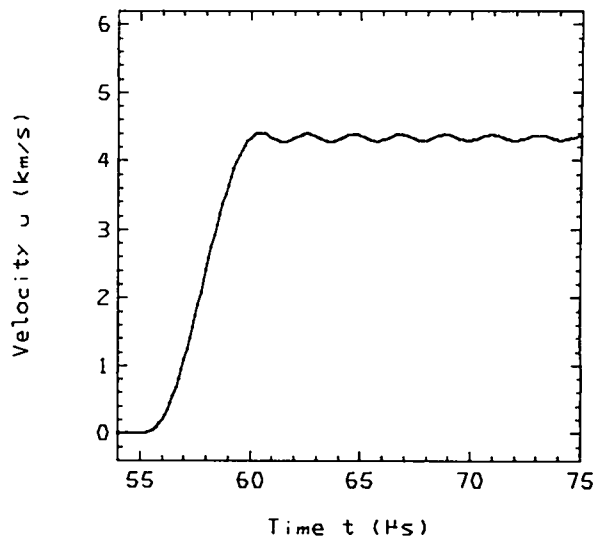
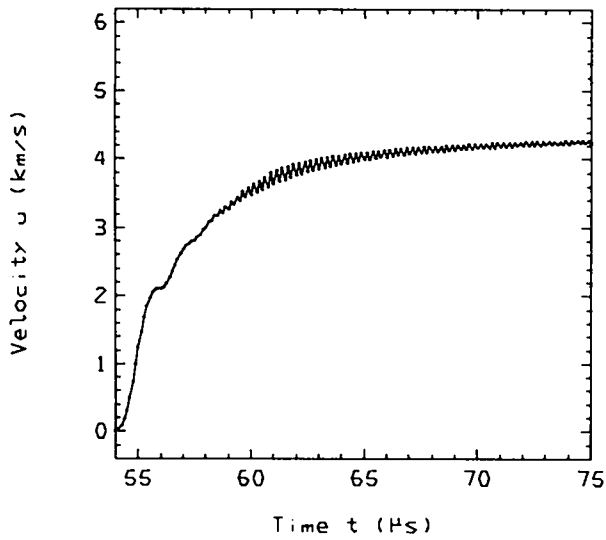


Fig. B-2 (cont)

RECEIVED

DEC 27 '76

LASL LIBRARIES